Application of a plug & play connection as a beam-to-column connection in a steel frame

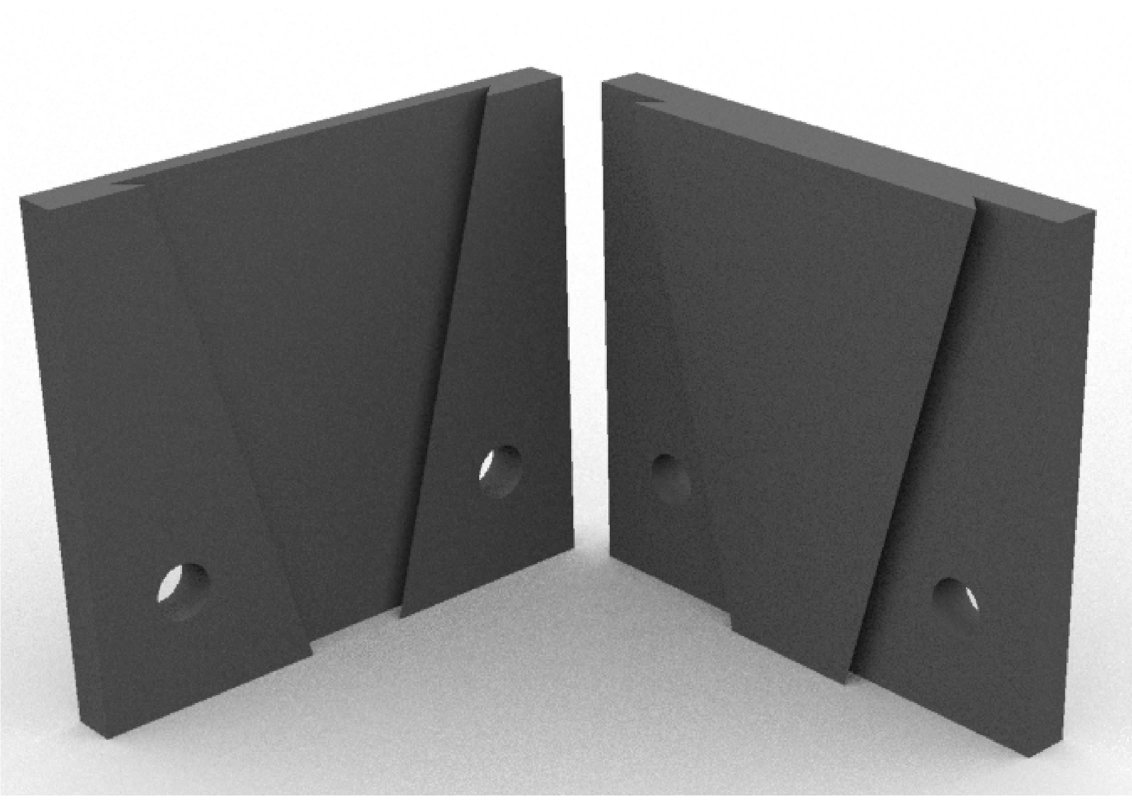

L.P. Bogers
MSc thesis
August 2021

Delft
University of
Technology

The Dutch Steel Company

Application of a plug & play connection as a beam-to-column connection in a steel frame

Master Thesis
Structural Engineering - Faculty of Civil Engineering at TU Delft
In cooperation with De Kok Staalbouw

August 2021

Author

L.P. (Lars) Bogers

Thesis committee

TU Delft:

Prof.dr. M. Veljkovic	Department of steel structures
Dr. F. Kavoura	Department of steel structures
Dr. ir. P.C.J. Hoogenboom	Department of structural mechanics

De Kok Staalbouw:

A.J. Boogaard	Lead structural engineer

Preface

This thesis is the last part of my master in structural engineering at the TU Delft. Before the start of my thesis I have never heard of plug & play connections and did not know better then that steel connections are either welded or bolted. A few months later I have gained more experience in the structural performance of plug & play connections. Another thing I have learned is that joint assumptions, with regards to the stiffness and resistance, made in the first step of the design can create difficulties in the later joint design step, as the joints have to be designed according to these assumptions. During chats with colleagues at De Kok I found out that this is not only the case for my thesis, but is happening in the industry as well. With this thesis I hoped to show what possibilities and problem plug & play connections offer over traditional steel connections.

I would like to thank everyone who helped me during my thesis. Thanks to all my committee members for their feedback and guidance. Special thanks to Florentia who was always willing to answer my questions and for her remarks which helped me to improve my report. I also want to thank Nico-Jan for the discussions regarding the design considerations and De Kok to offer me a place where I could work on my thesis.

At last I want to thank my parents for their support during my complete period at the TU Delft.

Lars Bogers
Heerle 2021

Abstract

A steel frame is designed which is expandable and reducible at any time. In order to reduce the assembly and disassembly time of the frame a new type of beam-to-column connection is proposed, a so-called plug & play connection. The design codes cannot be used for the estimation of the structural performance of this connection. Therefor the following objective is defined:

What is the structural performance of the plug & play connection and how can the connection be reusable?

In the state of art the benefits and problems plug & play connections offer over traditional steel connections is given. A case study of a steel frame, which consists of stacked units with fixed dimensions, is described. For this case study a global analysis is performed to investigate the possible internal forces on the plug & play connection.

With the results obtained from the state of art and the global analysis an initial design is made. This initial design assumes a perfect fitted connection. Both the stiffness of a column major and minor axis joint is investigated for a hogging, sagging and out-of-plane bending moment. For all cases the joint is classified as semi-rigid. The inclined parts of both socket and plug will yield for all cases and the highest plastic strain will occur in the inclined parts of the connection. The thin base plate of the socket causes that the socket shows a bending deformation for all displacement cases, this bending deformation makes that the plug will be easier to pull the plug out of the socket, which reduces the stiffness.

So an optimized design is checked for the minor axis case. For this optimized design the base plate thickness of the socket is increased in order to prevent the bending deformation of the socket. This optimized design also includes tolerances. The optimized design has removed the bending deformation of the socket. For a downwards displacement slip will occur, as a consequence of the tolerances, before contact between plug and socket is initiated. No slip will occur for an upwards or out-of-plane displacement as the bolt will be immediately in tension. So for the downwards case the initial stiffness is depending on the contact between plug and socket, while for the upwards and out-of-plane displacement the initial stiffness is provided by only the bolts. For all cases the stiffness is increased compared to the initial design.

The final step is to evaluate the re-usability of the connection. The plastic de-

formation has to be limited in order to be able to reuse the connection. For the upwards and out-of-plane case, in the optimized design, no plastic strain occurs in the inclined parts of the connection when the moment is below the elastic moment resistance. This is because the elastic moment resistance is only provided by the bolts. For the downwards case there is plastic deformation in the inclined parts. However, increasing the thickness of the plug has reduced the maximum plastic strain compared to the initial design. So when the moments on the connection are below the elastic moment resistance the connection should be reusable. A visual inspection should prove whether the plug still fits in the socket.

A real test should prove whether the plug & play connection reduces the assembly and disassembly time. If this is the case, then the moments on the joint should below the elastic moment resistance, so the connection could be reused. The joints will not be classified as rigid, so their semi-rigid behaviour should be taken into account in the global analysis.

Contents

List of Figures

List of Tables

Introduction

1

1.1 Thesis Background

An idea for a temporary steel frame is designed as shown in figure 1.1a. With columns and beams of a fixed size, a frame can be constructed which can be expanded or reduced at any time and when the structure is not needed anymore it can be disassembled and the parts can be reused. A new type of connection is proposed which should make assembly and disassembly of the structure easier and also reduce the time for assembly and disassembly.

The proposed connection is a so-called plug & play connection as shown in figure 1.1b. The structural performance of this new type of connection cannot be obtained with the current design codes. The stiffness, resistance and ductility of the connection are unknown and need to be investigated. This thesis investigates the application of a plug & play connection as a beam-to-column connection and other applications of the plug & play connection are not investigated in this thesis.

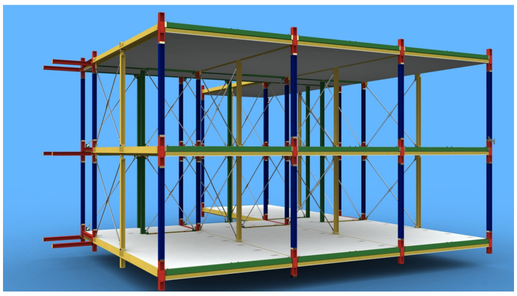

(a) Temporary unit

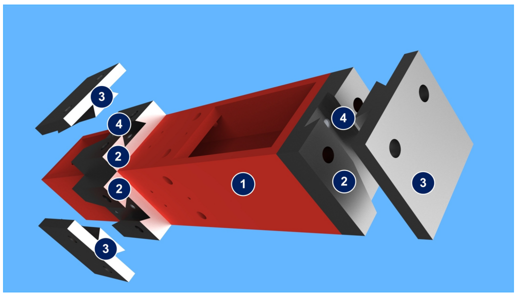

(b) plug & play connection

Figure 1.1: Temporary structure and proposed connection

The plug & play connection which will be investigated consists of two parts: a socket and a plug. In figure 1.2 both parts are shown. The socket has a tapered shaped slot which acts as a guide for the plug. The wedge shape of the plug matches the slot shape of the socket. The connection is locked with two bolts.

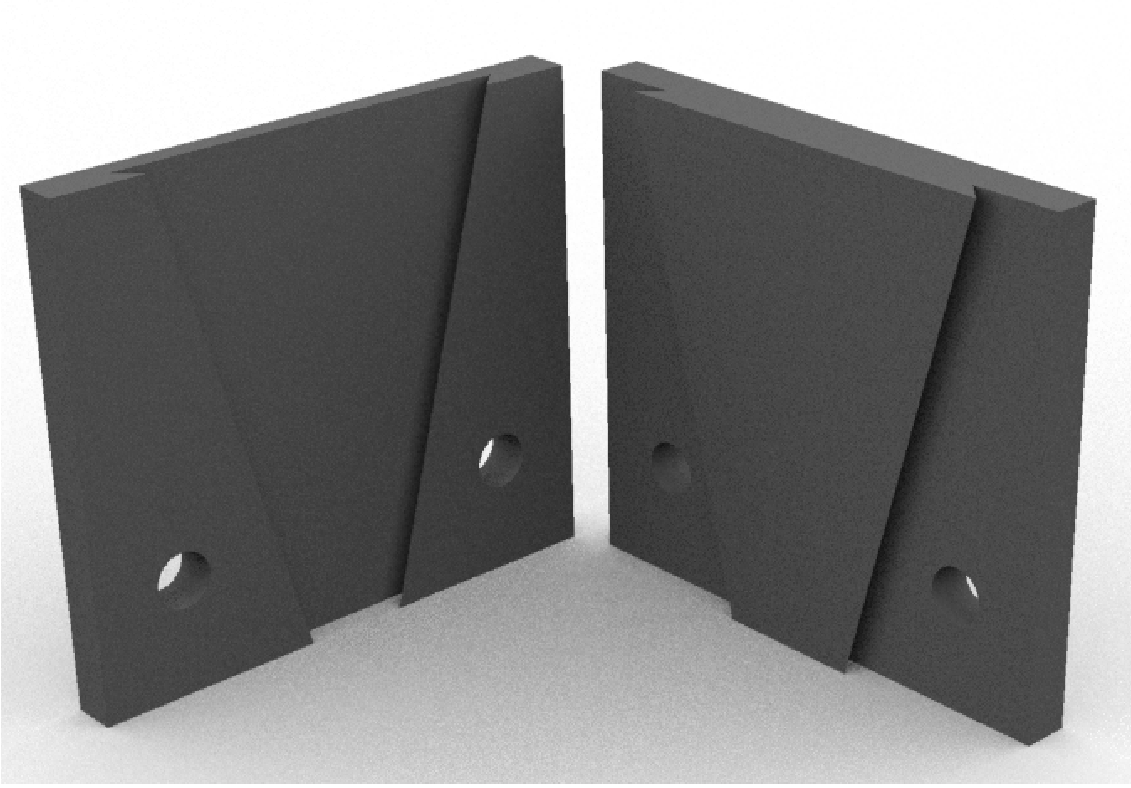

Figure 1.2: plug & play connection, socket (left) and plug (right)

1.2 Objective and Research Questions

The aim of this thesis is to investigate if a plug & play connection can be used as a beam-to-column connection in a steel frame, which leads to the objective:

What is the structural performance of the plug & play connection and how can the connection be reusable?

The following research questions are relevant with regard to the objective:

- How are the stiffness, resistance and ductility of a joint determined?
- What are the possible forces that needs to be transmitted by the plug & play connection?
- What is the structural performance of the joint for both a column major and minor axis joint?
- How can the stiffness and resistance of the joint be increased?

- What is the critical part of the connection?
- What is the criteria for re-usability

1.3 Thesis Structure

The first part of the thesis is a theoretical part, which provides information about the determination of the structural performance of connections and the current research on plug & play connections. The second part gives the global design and analysis of the frame and the last part is the analysis of the plug & play connection.

Besides the research questions defined in the previous section several other questions per chapter are defined. The structure of the thesis including the research questions for each chapter is given here.

Chapter 2: Steel joint characterisation
In order to evaluate the plug & play connection the structural properties of connections and how to obtain these properties is explained in this chapter. Besides the evaluation of the connections structural properties the requirements for joint classification are described as well. The research questions addressed in this chapter are:

- How are the stiffness, resistance and ductility of a joint determined?
- How are the joint properties implemented in the global analysis?

Chapter 3: State of art
In the state of art research on other plug & play connections is evaluated and discussed. The following questions are answered regarding the plug & play connections in the state of art:

- How is the load transferred in the plug & play connections?
- What difficulties and problems do plug & play connections face over traditional steel connections?
- What are the benefits of plug & play connections offer over traditional steel connections?

Chapter 4: Finite element analysis This chapter is used to give a short explanation of the fundamentals of the finite element method, which is used to analyse the connection.

Chapter 5: Case study
In this chapter the case study is explained together with the frame configuration used for the global analysis.

Chapter 6: Global analysis
For the defined case study a global analysis is performed, and the sections

of the columns and beams are determined. For this chapter one question is defined:

- What are the design considerations made in the global analysis with regard to the design of the plug & Play connection?
- What forces need to be transmitted by the plug & play connection?
- What is the consequence of the assumptions made for the joint stiffness?

Chapter 7: plug & play connection
This chapter involves the analysis of the joints and the plug & play connection. The research question which are answered in this chapter are:

- What is the design of the plug & play connection and what design considerations need to be taken into account?
- What is the structural performance of the joint for a column major and minor axis joint?
- What is the effect of a connection on all sides compared to only on one side?
- Which is the critical part of the connection?
- How can the stiffness and resistance of the joint be increased?
- Which are the criteria for re-usability of the connection?

Conclusion and Recommendations
In the last chapter the information and results obtained in the previous chapter is used to answer the objective.

1.4 Methodology

The previous section shows already a part of the methodology which will be used to obtain the design of the connection.

First the theory on how to obtain the joint properties and how to model them is given, the second part of the theory investigates and discusses other plug & play connections.

A case study is defined and a global analysis is performed for this case study. The purpose of the case study is to see what internal forces on the plug & play connection will act. The behaviour of the joints is unknown and in the first step all connections are assumed rigid, when the real joint behaviour is known it will be checked whether this assumption is correct.

Based on the results obtained from the research on other plug & play connections and the global analysis an initial design is made. The structural performance of the joint is checked, using numerical models, for the possible internal forces obtained in the global analysis. The structural performance of the joint is evaluated and the design of the plug & play connection is evaluated for the critical parts. Based on the results of the initial design an optimized model is created to improve the structural performance of the connection, this optimized joint will be analysed and evaluated to check if the optimized design lead to improvements.

1.5 Scope and Limitations

The thesis focuses only on the structural performance of the connection for the purpose as beam-to-column connection and the structural performance is based on finite element results. Experimental tests of the connection are not within the scope of this thesis. A real model should also show whether that a plug & play connection decrease the assembly and disassembly time.

Last, for the global structural analysis only open hot rolled sections are taken into consideration. This is done because it is wanted to use bolts in the connection, which cannot be used when hollow sections are used.

Steel joint characterisation 2

The joint behaviour is defined by its stiffness, resistance and ductility. This chapter explains how these properties are obtained and how these properties are used in the global analysis.

2.1 Joint Modelling

The response of the joint is taken into account in the global structural analysis in terms of stiffness and/or resistance. In terms of stiffness joints can be regarded as: rigid, semi-rigid or pinned and in terms of resistance a joint can be regarded as full-strength, partial-strength or pinned. The meaning of each term is explained in the next section. Table 2.1 shows the possible types of joint modelling.

Table 2.1: Types of joint modelling [1]

Stiffness	Resistance		
	Full-strength	Partial-strength	pinned
Rigid	Continuous	Semi-continuous	
Semi-rigid	Semi-continuous	Semi-continuous	
Pinned			Simple

The interpretation of the joint modelling depends on the performed type of global structural analysis. In table 2.2 the relevant joint properties for each type of global structural analysis are shown. So for an elastic analysis only the stiffness is of interest and for a rigid-plastic analysis only the resistance is of interest for all other types of analysis both stiffness and resistance need to be taken into account.

In table 2.3 the simplification for beam-to-column joints in the global frame analysis is given.

Normally joints are designed in a later design stage and the stiffness and resistance of the joint are therefore unknown. So in global frame analysis joints are modelled as either rigid or pinned and the joints have to be designed according to the assumptions made in the global structural analysis.

Table 2.2: Joint modelling and frame analysis [1]

Modelling	Type of global structural analysis		
	Elastic analysis	Rigid-plastic analysis	Elastic-perfectly plastic and elasto-plastic analysis
Continuous	Rigid	Full-strength	Rigid/full-strength
Semi-continuous	Semi-rigid	Partial-strength	Rigid/partial-strength Semi-rigid/full-strength Semi-rigid/partial-strength
Simple	Pinned	Pinned	Pinned

Table 2.3: Simplification of joint in global structural analysis [1]

Joint modelling	Modelling in global structural analysis
Simple	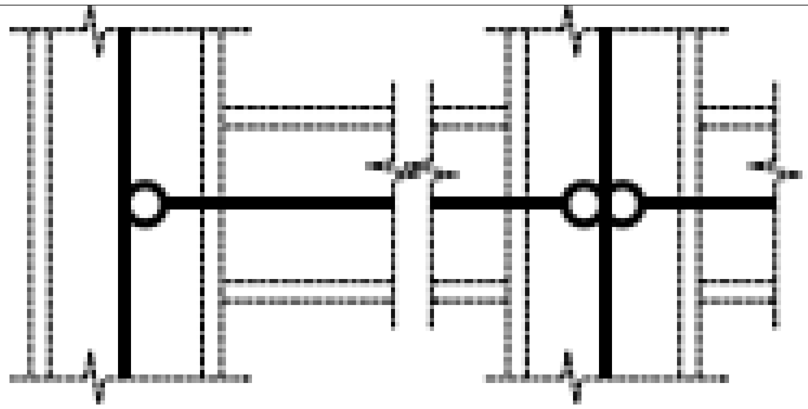
Semi-continuous	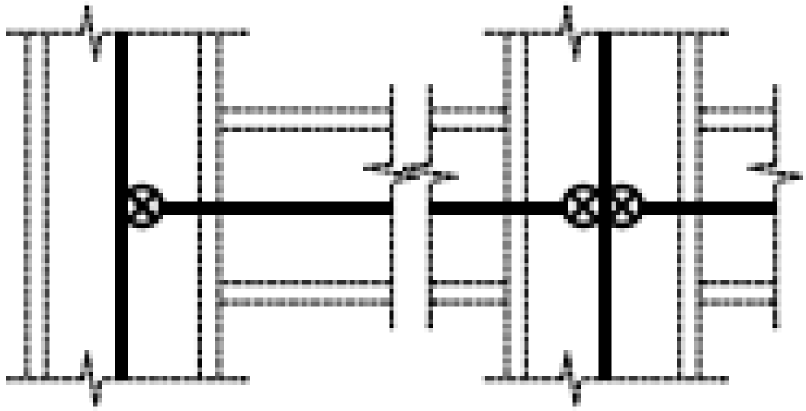
Continuous	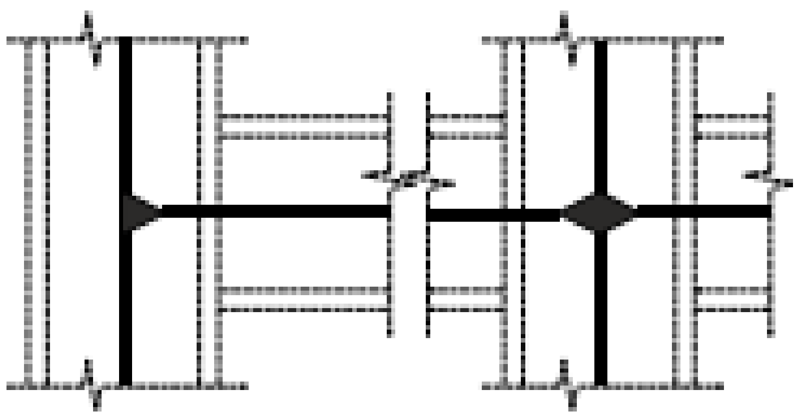

2.2 Joint Classification

The values for the resistance, stiffness and ductility are obtained from the M-ϕ curve of the joint. In figure 2.1 an example of a M-ϕ curve is given. Classification criteria for each joint property define how the joint should be modelled in the global structural analysis. This section explains these classification criteria.

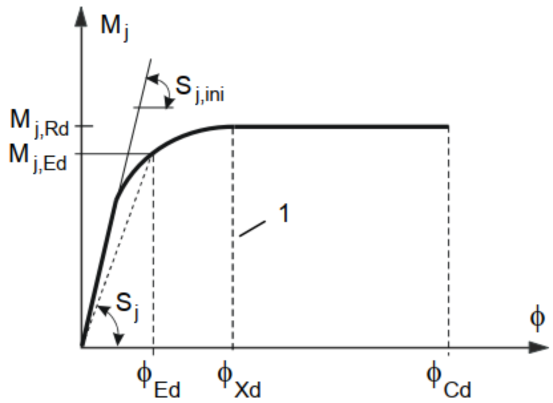

Figure 2.1: M-ϕ curve [1]

2.2.1 Resistance

The resistance of a joint is defined as the design moment resistance $M_{j,Rd}$. The value for the design moment resistance is obtained from M-ϕ curve as the value of the yield plateau. For the resistance classification the resistance of the joint is compared with the resistance of the attached sections. According to the EC 1993-1-8 (2011)[2] in terms of resistance a joint can be classified as:

- *Full-strength:*

  A joint is full-strength when the joint resistance is higher than the weakest of the connected members.

- *Partial-strength:*

  A joint is partial-strength when its resistance is between the boundaries of full-strength and pinned.

- *Pinned:*

  A joint is pinned when its design resistance is 25% lower than the full-strength resistance. (So when the resistance is lower than 25% of the resistance of the weakest member.)

In figure 2.2 the resistance classification boundaries are shown. The values of these boundaries depend on the used sections.

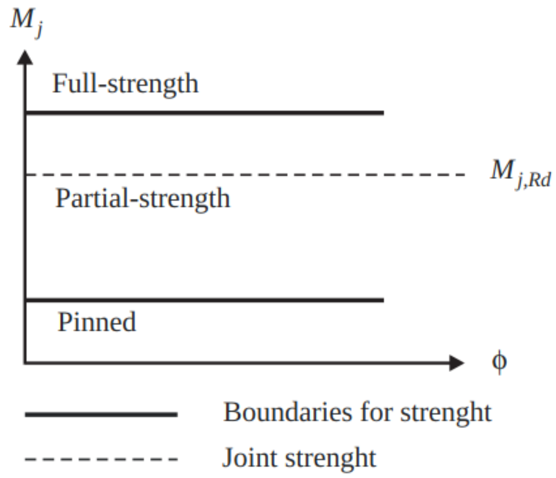

Figure 2.2: Resistance classification boundaries [1]

2.2.2 Stiffness

The stiffness or rotational stiffness of a joint is defined as the slope of the M-ϕ curve. There are two types of stiffness the initial stiffness $S_{j,ini}$ and the secant stiffness S_j (both shown in figure 2.1). The secant stiffness is calculated with the formula as shown in equation 2.1, where η is a correction factor depending on the type of joint and the joint typology. The secant stiffness is to simplify the real structural behaviour of the joint in a global structural analysis.

$$S_j = \frac{S_{j,ini}}{\eta} \tag{2.1}$$

If the moment-rotation curve is known instead of approximated with the component method, the secant stiffness can be derived from the $M - \phi$ curve, instead of using the formula. The secant stiffness is used for the moments which are beyond the elastic part of the $M - \phi$ curve. For each moment the stiffness is determined as the slope of a linear line between the origin and the intersection point on the $M - \phi$ curve related to the moment on the connection.

The initial stiffness is determined from the slope of the elastic part of the M-ϕ curve. For the stiffness classification the initial stiffness is used and the joint classification given in the Eurocode [2] is as follows:

- *Rigid*
- *Semi-rigid*
- *Pinned*

In EC 1993-1-8 (2011) the classification boundaries for the stiffness of a joint are given. The classification boundaries depends on the type of joint (beam-to-column, beam-splice or column base and whether the frame is braced or unbraced). In figure 2.3 the stiffness boundaries for all type of connections, except column base connections, are given.

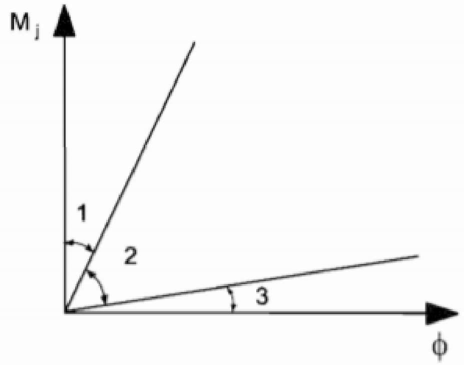

Zone 1: rigid, if $S_{j,ini} \geq k_b EI_b / L_b$

where:

$k_b = 8$ for frames where the bracing system reduces the horizontal displacement by at least 80 %

$k_b = 25$ for other frames, provided that in every storey $K_b/K_c \geq 0,1$ *)

Zone 2: semi-rigid

All joints in zone 2 should be classified as semi-rigid. Joints in zones 1 or 3 may optionally also be treated as semi-rigid.

Zone 3: nominally pinned, if $S_{j,ini} \leq 0,5 EI_b / L_b$

*) For frames where $K_b/K_c < 0,1$ the joints should be classified as semi-rigid.

Figure 2.3: Stiffness classification boundaries [2]

2.2.3 Ductility

The last property is the ductility of the joint. Ductility is the behaviour of the joint after reaching the yield strength. The ductility of the joint is of importance for the rotational capacity. A long yield plateau is necessary to allow for internal force distribution and development of plastic hinges [1].

After reaching the value of $M_{j,Rd}$ a post-limit behaviour develops. This behaviour is the effect of strain-hardening and possibly membrane effects. This post-limit behaviour is the ductility of the joint and there are three types of ductile behaviour. The first is infinitely ductile behaviour which is shown in figure 2.4. The value of $M_{j,u}$, which is the ultimate resistance capacity of the joint, is not reached because of too high deformations [1].

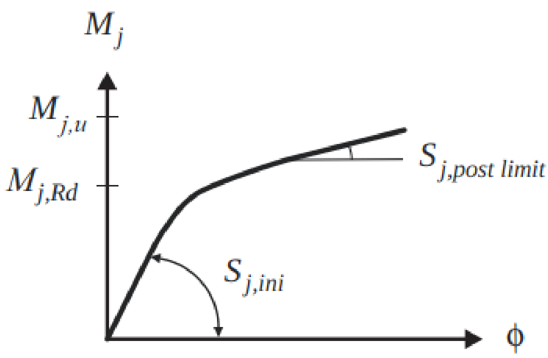

Figure 2.4: Infinitely ductile behaviour [1]

The second is limited ductile behaviour, shown in figure 2.5. The value of $M_{j,u}$ is reached. At this point collapse of the joint occurs, material failure or instability of a component, and the capacity is degrading.

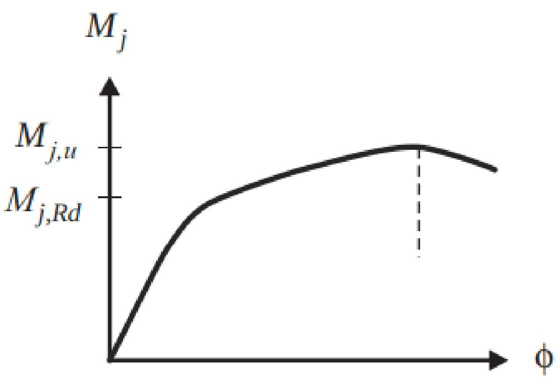

Figure 2.5: Limited ductile behaviour [1]

The last type is non-ductile behaviour or brittle behaviour, shown in figure 2.6. Collapse of the joint occurs before a high rotation capacity of high resistance capacity is developed.

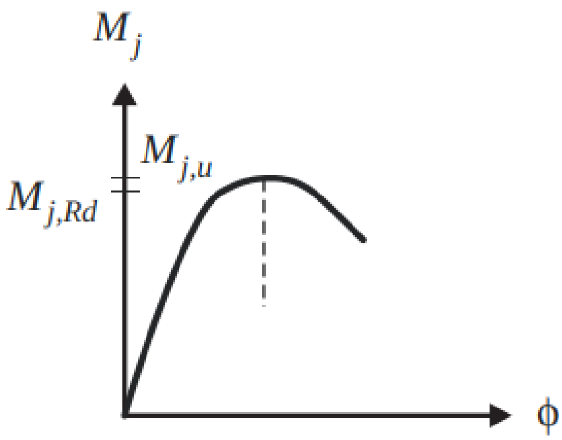

Figure 2.6: Non-ductile behaviour [1]

Exceedance of the design moment resistance is not taken into account in the global analysis. Figure 2.7 shows some examples on how the non linear behaviour of joints is idealised in the global structural analysis.

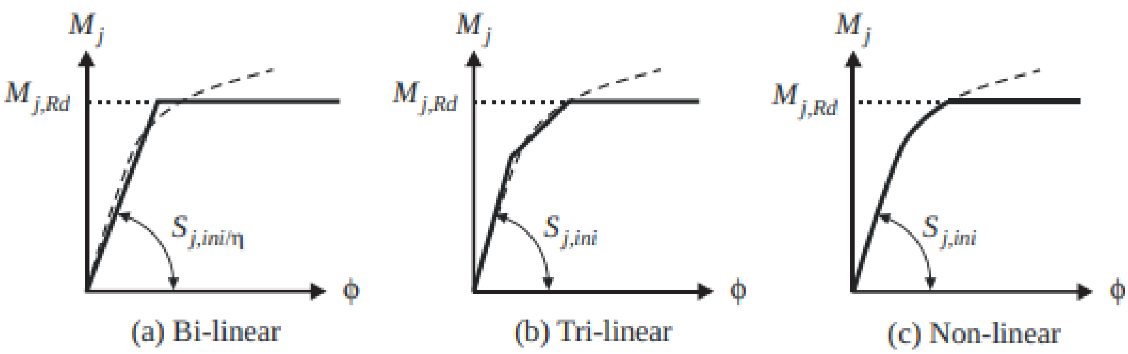

Figure 2.7: Non-linear idealisation of joint response [1]

2.3 Analysis Methods

In the previous sections the classification of the structural properties and how to obtain them from the M-ϕ curve is explained. This last section explains the possible methods to obtain these M-ϕ curve.

There are three possible types of analysis methods possible [1]:

- *Experimental*:

  This approach involves testing of real specimens in laboratories under controlled conditions. This approach provides the most accurate results for the joint characterisation. However, it is also the most expensive approach and is only valid for the specific type of joint which is tested.

- *Numerical*:

  This approaches involves numerical methods such as the finite element method. There are several finite element programs/packages, the user should look which is the most suitable. A benefit is that with finite element analysis several designs can be analysed in a short amount of time. However, the finite element method should not be used as a blackbox and the results should be validated to prove that the results are accurate.

- *Analytical*:

  The easiest method for calculation of the joints stiffness and resistance is an analytical method. The Eurocode provides an analytical method called the component method for the calculation of the stiffness and resistance of the joint. In the Eurocode 1993-1-8 (2011) a list of basic components is defined together with formula to obtain the the stiffness and resistance of each component, a disadvantage is that for joints which are not composed of these basic components the structural properties cannot be estimated with the component method.

2.4 Obtaining joint characterisation

The previous sections described how steel joints are modelled and how steel joints are classified according to stiffness, resistance and ductility. At last the analysis methods to obtain the $M-\phi$ curve are given. The figure below shows the relation between the $M-\phi$ curve and the modelling of the joint in the global analysis.

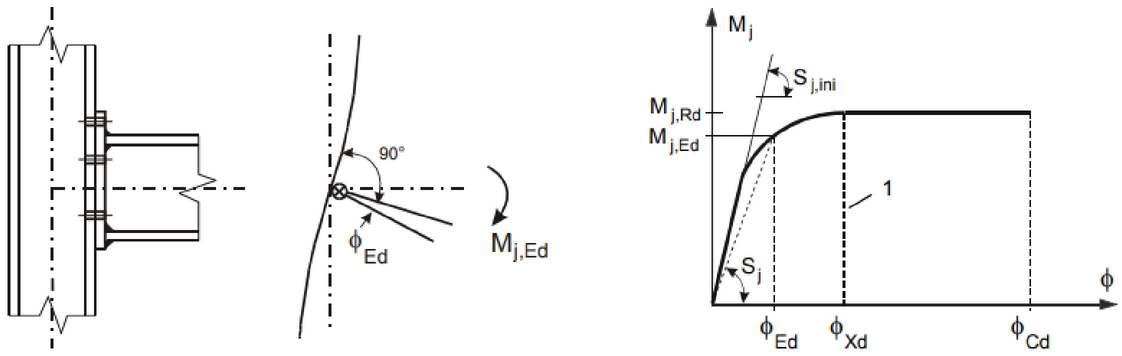

Figure 2.8: Relation moment rotation curve and the connection

The $M-\phi$ curve gives the relation between the relative rotation of the connection and the moment on the connection. From this curve the joint stiffness and resistance used in the global analysis are obtained.

2.5 Conclusion

The research question for this chapter are:

- How are the stiffness, resistance and ductility of a joint determined?
- How are the joint properties implemented in the global analysis?

The joint properties which are implemented in the global analysis depend on the type of the global analysis. The intention of the plug & play connection is that it can be reused, so an elastic global analysis is performed. For an elastic analysis the stiffness of the connection is of importance. The stiffness of the joint is determined as the slope of the $M-\phi$ curve. For the elastic part of the $M-\phi$ curve the initial stiffness is used, for moments which are not in the elastic part of the joint the secant stiffness needs to be used. The secant stiffness can be obtained by calculating the slope at the corresponding moment on the connection.

State of Art 3

This chapter describes and evaluates examples of plug & play connections.

3.1 plug & play connections

3.1.1 Lock Key connection

Szlendak and Szpyrka have developed a non welded plug & play connection for N type joints in trusses, with square or rectangular hollow section [3]. The connection is called a ”lock - key” connection. The ”lock” in this connection is the chord member. With aid of automated laser cutting special slots are cut in the chord member. The ”key” is the brace member and it is slide in these slots as can be seen in Figure 3.1. To keep the chord and brace together two parts are used: the first part is the anchor block which is connected to both chord and brace (the red parts in figure 3.1), the anchor block has ”teeth” which slide into the special cut slots in the brace and chord. The second part has a cylindrical surface which allows load transfer from different inclination angles to the anchor block and it acts as a support for nut and washer (the grey part in figure 3.1). Due to the cylindrical surface different angles of the diagonal are possible, the diagonal is a threaded rod which goes through the chord member and is used to clamp the anchor blocks on both sides together.

The lock - key connection has as an advantage that both bottom and top flange can be used for load transfer while with welded connections only the top flange will be used. A disadvantage is that the slots decrease the resistance due to reduction of the section. At last, the connection allows temporary frames with hollow sections.

Although this connection is not a beam-to-column connection it is mentioned as it is a plug & play connection.

The benefit of the connection is that no welding is needed. However, although no installation time is mentioned it is unknown whether it is fast and easy to use this connection for all joints in the truss.

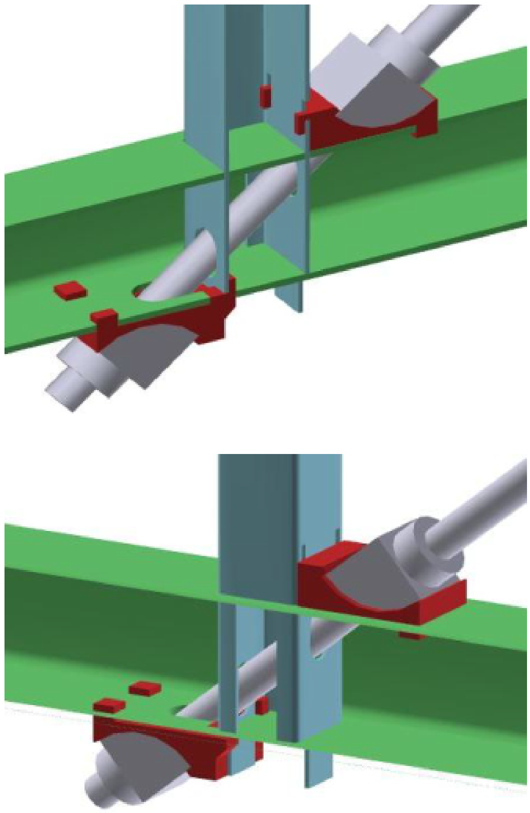

Figure 3.1: Lock - Key connection [3]

3.1.2 plug & play - INNO3DJOINTS

This plug & play connections is developed within the INNO3DJOINTS project and combines coldformed lightweight steel and tubular members [12, 13]. The sections are made of coldformed hollow sections. The plug & play connection consists of a socket which is welded on the column face and a plug which is connected to the truss with a lapjoint connection and is reinforced with stiffeners. The socket consists of two s-shaped parts and the plug is combination of a T-shape part, which is locked in the socket, and a U-shape part, which is connected to the horizontal truss. The plug is connected to the socket with 2 bolts and the connection is regarded as a shear connection. The top and bottom member of the truss are both connected to the column, this results in an equivalent moment. The two connections per column provide the lateral stability of the system.

The use of coldformed lightweight steel can improve the safety and erection time on site. A disadvantage of the connection is that it cannot be used as a beam-to-column connection on itself. This connection needs to be used in combination with a truss. So if a truss is not possible or wanted in a structure for any reason, then this connection is not useful.

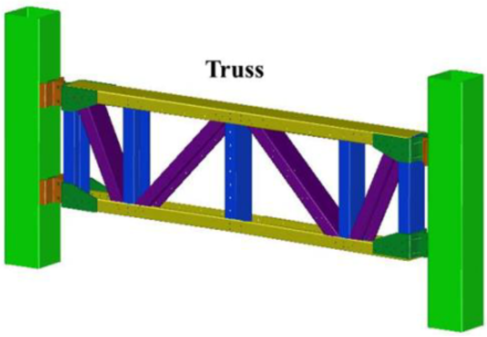

(a) structural system [12]

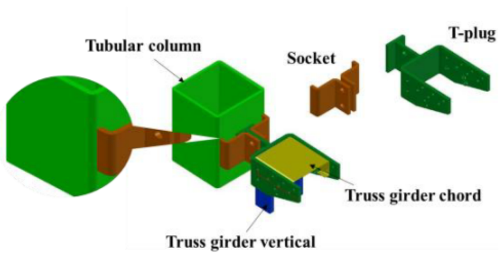

(b) plug & play connection [12]

3.1.3 ConXTech connections

ConXtech is a company which has developed and commercialized a few types of plug & play connections [4]. The structural configuration consist of: square hollow sections which are filled with concrete for the columns and open I sections for the beams. For each connection type a limited range of sections and spans can be used. Within these limits a desired structural configuration can be made.

The different connections are the following:

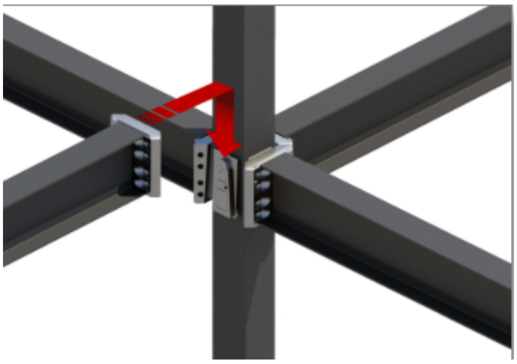

Figure 3.3: ConXR connection [4]

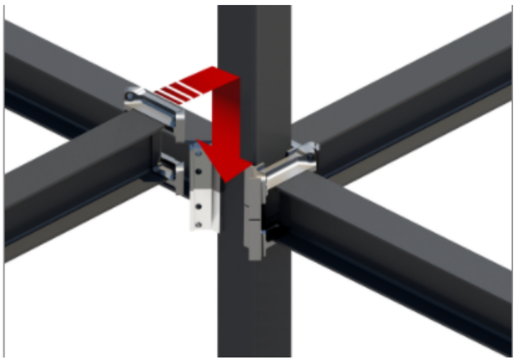

Figure 3.4: ConXl connection [4]

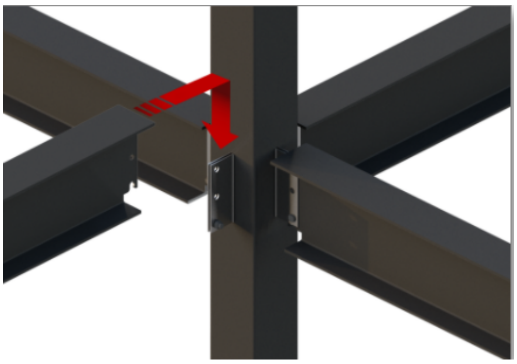

Figure 3.5: ConX gravity connection [4]

The ConXR connection is a moment resistant connection when fully bolted. The full connection is made out of four tapered collar plates. Each collar plate is connected with 4 bolts to the adjacent collar plate and the bolts are pretensioned. The ConXR connection also has a three dimensional tapered ”shear key” which is welded to the column face. The beam part of the connection has a slot which matches the shape of the shear key on the column face. 4 Collar plates are necessary at each joint even when there are less then 4 beams connected to the column. The collar consist of a one- sized solid cast connection. Only one beam section is possible with this connection.

The ConXL connection allows for larger bay size then the ConXR connection and has a limited set of possible beam sections. Instead of one solid collar piece two parts are attached to the beam, this make it possible to use different beam sizes. The connection has no shear key, but uses 4 pretensioned bolts at each side, which makes that the connection is also moment resistant.

The ConX gravity connection is a secondary connection and can be regarded as a shear connection which is for beam-to-beam connections.

A benefit of the ConXtech is that it is easy and quick to install. The connection without bolts is strong enough to bear the loads during installation of the building. The bolts can be installed when the floors are placed. There are no boltholes in the column as the bolts are connected diagonal between the collar plates. The disadvantage of the ConXtech connections is the restricted choice for sections; however, with the limited set of sections a lot of structural configurations is possible. At the end of use stage of the structure, the structure can be easily disassembled and the connections or whole structural configuration can be reused. A disadvantage is that the collar working of the connection requires that a collar plate is installed at all sides of the column, even when there is no beam attached to that side of the column.

3.1.4 ATLSS connection

ATLSS (advanced technology for large structural systems) is a project which has a goal to ease fabrication and installation of steel structures [14, 15]. The fundamental principle of the developed design is a self-guiding installation feature and initial placement with reduced human assistance (only a crane operator needed) in order to assemble the structure quicker, cheaper and safer. The idea of the connection is that a tenon which is connected to the beam slides into a mortise guide which is welded to the column. (see figure 3.6a)

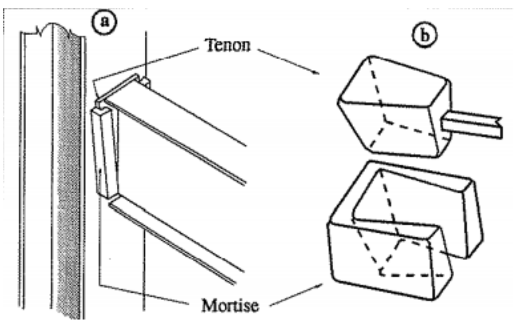

(a) principle idea ATLSS connection [14]

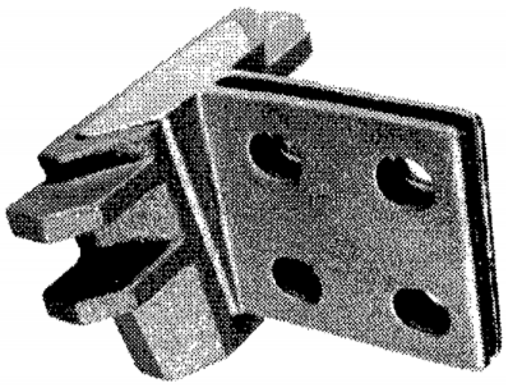

(b) ATLASS prototype [14]

Figure 3.6: ATLSS connection

Several features were defined regarding the purpose of the connection:

- Self-alignment: the beam must be able to guide to the proper location without jamming. Also it must not be able to pull out the beam horizontal once engaged.
- Tolerances: the tenon piece must always be able to enter the mortise piece.
- Adjustment: easy adjustment must be possible.

- Strength and Stability: the connection must be strong and stable to carry the erection loads until the final fastening is done.
- Modularity: limited set of mass produced connections.

The classification of the connection depends on the design of the connection. Is the connection only needed for erection purposes then tolerances can be larger compared with when the connection is needed for load transfer as well. Is the connection pinned, partial-moment resistant or fully moment resistant.

For this type of connections tolerances are the most important to account for. High tolerances within the connection itself, for example a loose fitting of the connection due to an oversize mortise part of the connection, would reduce the strength. A tight fitting connection would require strict tolerances to the misalignment of the columns and the beams should be installed horizontal without to large inclinations.

3.1.5 ISC

The ISC (Intermeshed Steel Connection) [5] is a gravity-resisting connection, which uses digital manufacturing. Special interlocking parts are made with the aid of digital manufacturing and automated cutting techniques. The force is transferred by bearing between the surfaces. The connection is suitable for column splices, beam splices and column rafter connections.

There are two types of ISC, the front intermeshed and the side intermeshed. The biggest difference is that for the side intermeshed option the flanges are meshed to create a connection for extra slotted side plates.

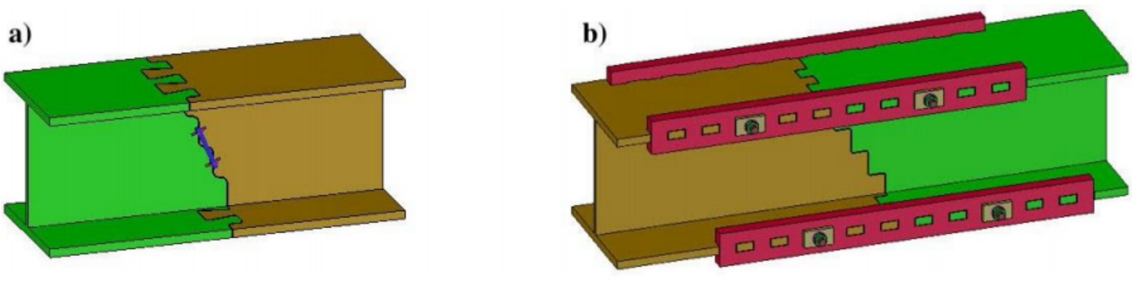

Figure 3.7: ISC a) front intermeshed, b) side intermeshed [5]

The front intermeshed connection need not only precise cutting of the connected members, also the the connection is not much adjustable for possible misalignments of the structure. The front intermeshed connection was tested and shows a low moment resistance and a linear load drop almost immediately after the peak load. The side intermeshed connection shows a larger initial displacement/slip as a consequence of lower tolerances. The peak load of the connection is larger than the load needed to reach the plastic resistance of the section. The connection shows some rotational capacity.

The connection proved to be easy and quick to install. however, the fabrication of the front intermeshed connection needs to be done precise, small tolerances are excepted as the load is transferred by the wedge action. The side intermeshed connection allows for larger tolerances as the side plates uses multiple bearing faces to carry the load. Another variation of the side intermeshed connection is to replace the side plates for full depth side plates connecting both top and bottom flange as well. A direct beam-to-column is not possible with this type of connections, so first a meshed beam part needs to be bolted to the column in order to create a frame. So although the installation of the ISC connection itself will be quicker and easier than a standard bolted connection, an extra connection must be made to use this connection as a beam-to-column connection (see figure 3.8. However an advantage of the intermeshed connections is that they are applicable for all steel sections and sizes and can be used for several connection types instead of only a beam-to-column connection.

Figure 3.8: Installation of ISC [5]

3.1.6 Summary and evaluation

Several plug & play connections were discussed in this chapter. The INNO3DJOINT and the Lock - Key connection are described to give a complete image of the available plug & play connections, but cannot be used as a beam-to-column connection. The research questions are answered for the following categories: fabrication, installation, load transfer and design flexibility.

Fabrication

The ConXTech connections and the ATLSS connection both propose to cast the parts, which will be mass produced.. The ConXTech offers two type of connections, a one piece collar plate over the full height of the beam (ConXR) and two pieces collar plates which are connected to the top and bottom flange of the beam (ConXL), the ConX gravity connection is fabricated by plasma cutting of the beam. The ATLSS connection was also fabricated by casting and mass production. The ISC uses modern cutting techniques to create the intermeshed surfaces on the sections.

Installation

One of the aims of the plug & play connection is that it should lead to an easy and quick installation of the structure. The ConXTech connection needs one person at each side of the beam who guides the plug part into the socket part of the connection, the shear key aligns the connection to the correct position. The idea behind the ATLSS connection is that it is self-guiding. Only a crane operator is needed to move the beam to its position, the design of the connection is in such a way that the beam is guided to its final position by aid of gravity, the condition is that no jamming or catch occurs. The ISC needs a person who guides the beam to its final position, for the front ISC no further actions are necessary, for the side ISC the side plates need to be installed when the beam is on its final location. A test proved that the ISC is easy and quick to install.

Load Transfer

In the ConXR and ConXL the collar plates are connected to each other with pretensioned bolts to create a moment resisting connection. The connection without the pretensioned bolts is enough to carry the loads during installation. The ATLSS has two types of load transfer. The tennon is connected with bolts to the beam, the forces are transferred as shear force from the beam to the connection. The second type is the load between tennon and mortise which is based on bearing (surface contact). The ATLSS connections can be regarded as a shear connection, and angle cleats are used to increase the moment resistance of the connection. The ISC transfers its loads fully by bearing between the materials. In order to increase the resistance and stiffness of the connection the total bearing surface is increased.

Design Flexibility

With the design flexibility is meant the freedom to use any section. For the ConXTech connections this design freedom is limited. The columns are executed in square hollow section, for the ConXR connection only one type of beams is possible. The ConXL connection offers some flexibility in section size, a limited number of different sections is possible. The ConX gravity connection is used for secondary elements and the sizes are depending on the primary beams. The ATLSS connection offers good design flexibility, the connection is attached with bolts to the web of the beam. The ISC offers good design flexibility as well. The intermeshed pattern can be applied on all sections. Even the pattern of the intermeshed connection is flexible.

Final evaluation

The research questions for this chapter are:

- How is the load transferred in the plug & play connections?

- What difficulties and problems do plug & play connections face over traditional steel connections?
- What are the benefits of plug & play connections offer over traditional steel connections?

The answer regarding the load transfer in the connections is already discussed in the previous section.

The difficulties and problems of the plug & play connections face over traditional steel connections are:

- If the load is transferred by bearing then a large contact area is required.
- Tolerances should be taken into consideration as they will lower the stiffness and resistance of the connection and strict tolerances of the connection will also require strict tolerances for the alignment of the columns.
- The plug & play connections require extra adjustments to create a connection with moment resistance (ConXtech: pretensioned bolts , ATLSS: angle cleats and ISC: side plates).
- The conXtech moment resistant connections requires a collar plate at all sides of the column, even when there is no beam attached to that side.

What are the benefits of plug & play connections offer over traditional steel connections?

- The self-guiding feature which helps to quickly install the beams to the correct location.
- The shear key in the ConXR connection which does already provide resistance for shear forces during installation, the bolts can be installed when the floors are placed which improves the safety.

3.2 Snap-fit connection

The last connection which will be discussed is called snap-fit connection, a special section is devoted to this connection as a lot of research is available on this connection and also real experiments are performed on this type of connection. The information in this section is derived from the thesis of S. Quesada. [6]

An example of the snap-fit principle is shown in figure 3.9a. The snap-fit realised in the connection is done by position pins which are used to lock the connection. When the plug slides in the socket part the pins in the socket are pushed back and when the pins are aligned with the holes in the plug then the pins would snap into place and the connection is locked, see figure 3.9b.

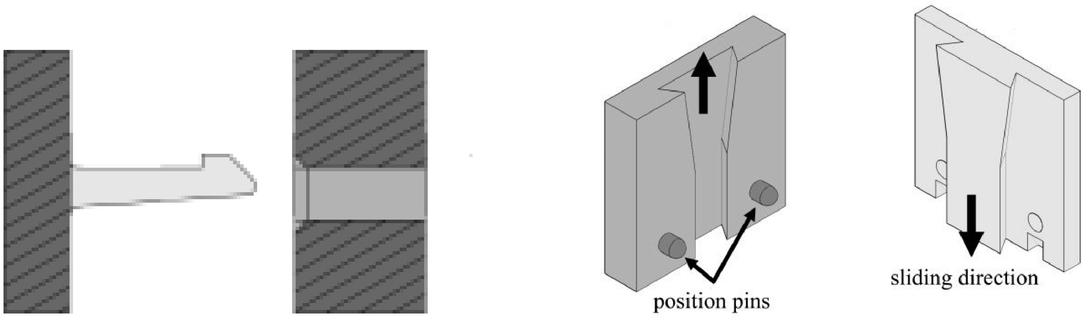

(a) Snap Fit principle (b) Snap-Fit connection

Figure 3.9: Snap-fit connection [6]

3.2.1 Experimental tests

The connection has been tested for a beam-to-column connection. In total 3 tests on different geometries are performed and the results of the tests are shown below. From the material of test 1, a coupon test is performed which resulted in the following material properties: an E-modulus of 195000 MPa and a yield stress of 500MPa.

Experimental test 1

The first test is performed for a connection without the position pins and the contact areas of the connection are lubricated. The geometry of the tested connection is shown in figure 3.10, the connection is welded to a HEB140 section of material class S235. The used test setup is shown in figure 3.11. The obtained moment-rotation curve is shown in figure 3.12 and the failure mechanism is shown in figure 3.13. The failure mechanism shows that the plug part was lifted out of the socket and the uplift caused a slip in the moment rotation curve. The use of pins should prevent this upwards movement. The resistance of the connection is lower than the resistance of the beam (57.5 kNm). The use of a lubricant lowers the frictional forces between the parts of the connection, so the use of the lubricant makes it easier for the plug to be pulled out of the socket.

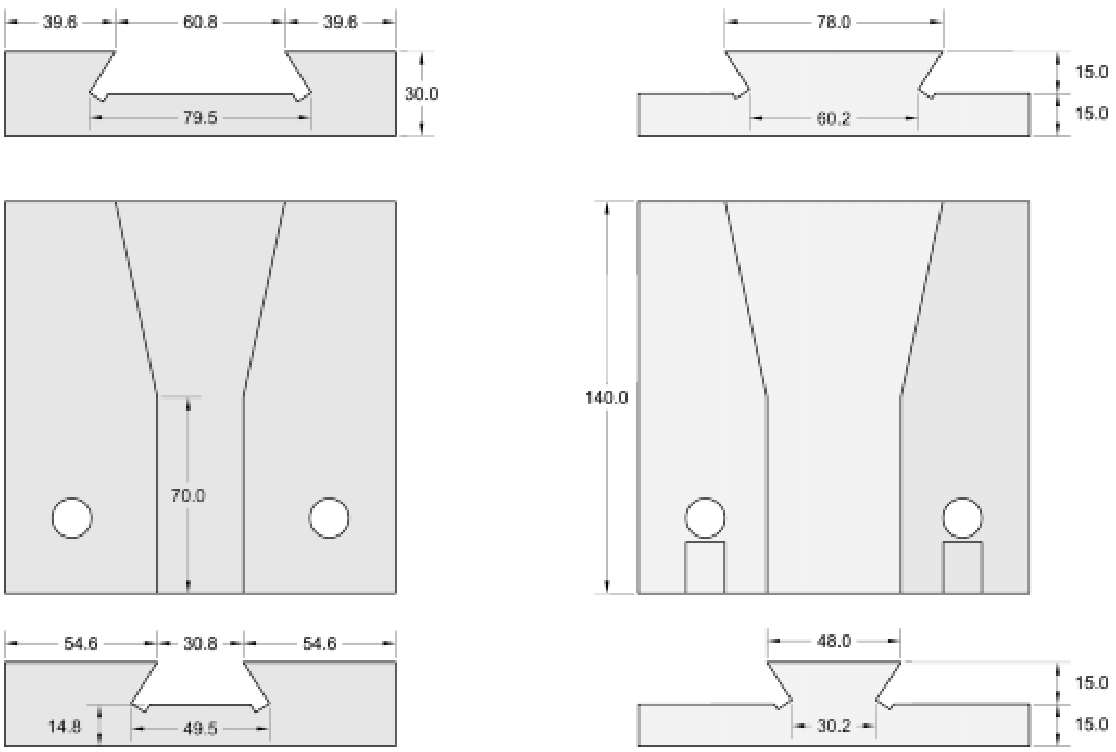

Figure 3.10: Geometry of the snap-fit connection test 1 [6]

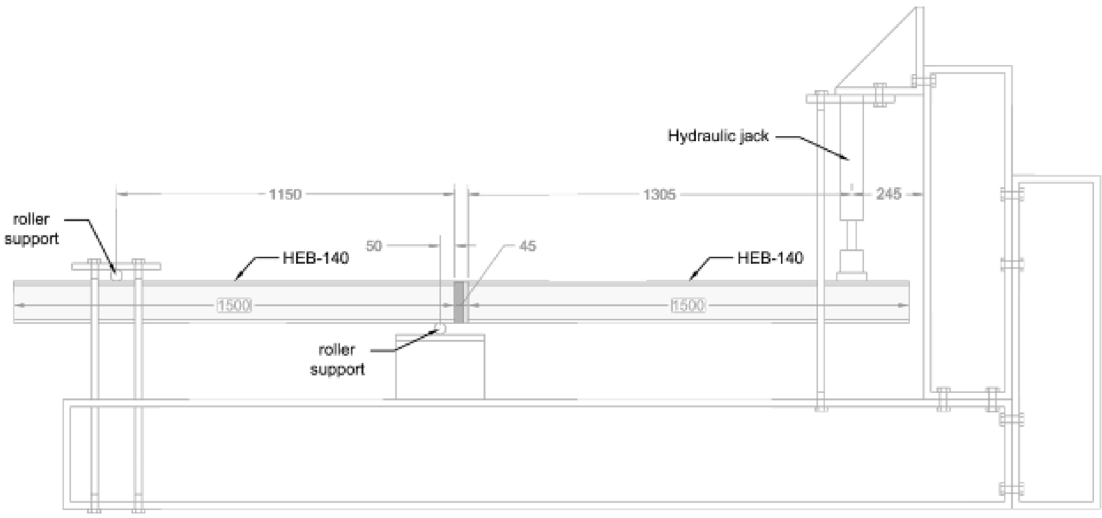

Figure 3.11: Setup test 1 [6]

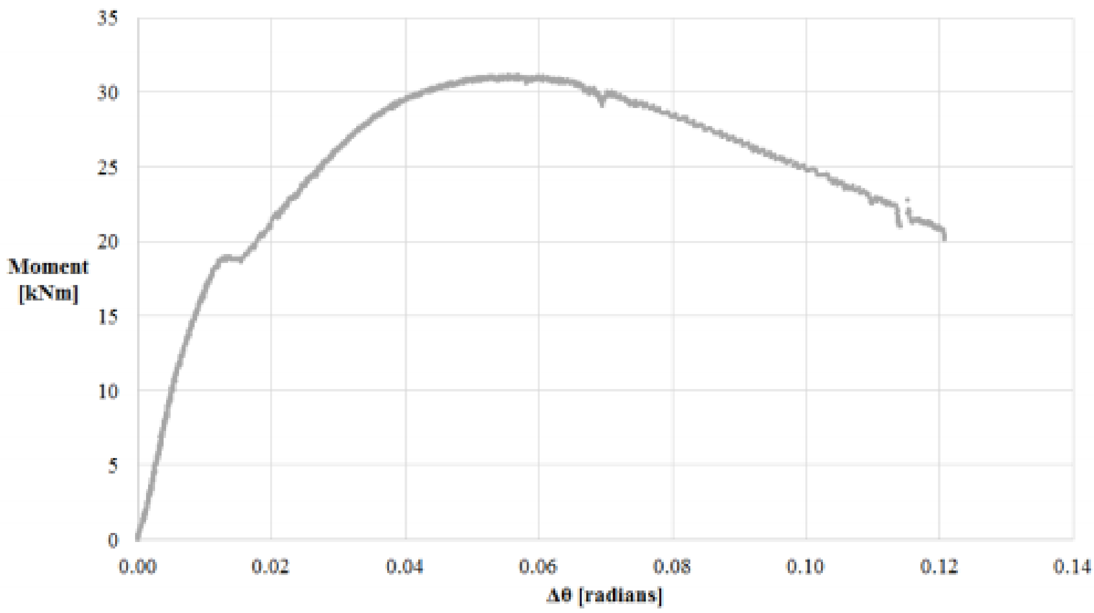

Figure 3.12: Moment rotation curve test 1 [6]

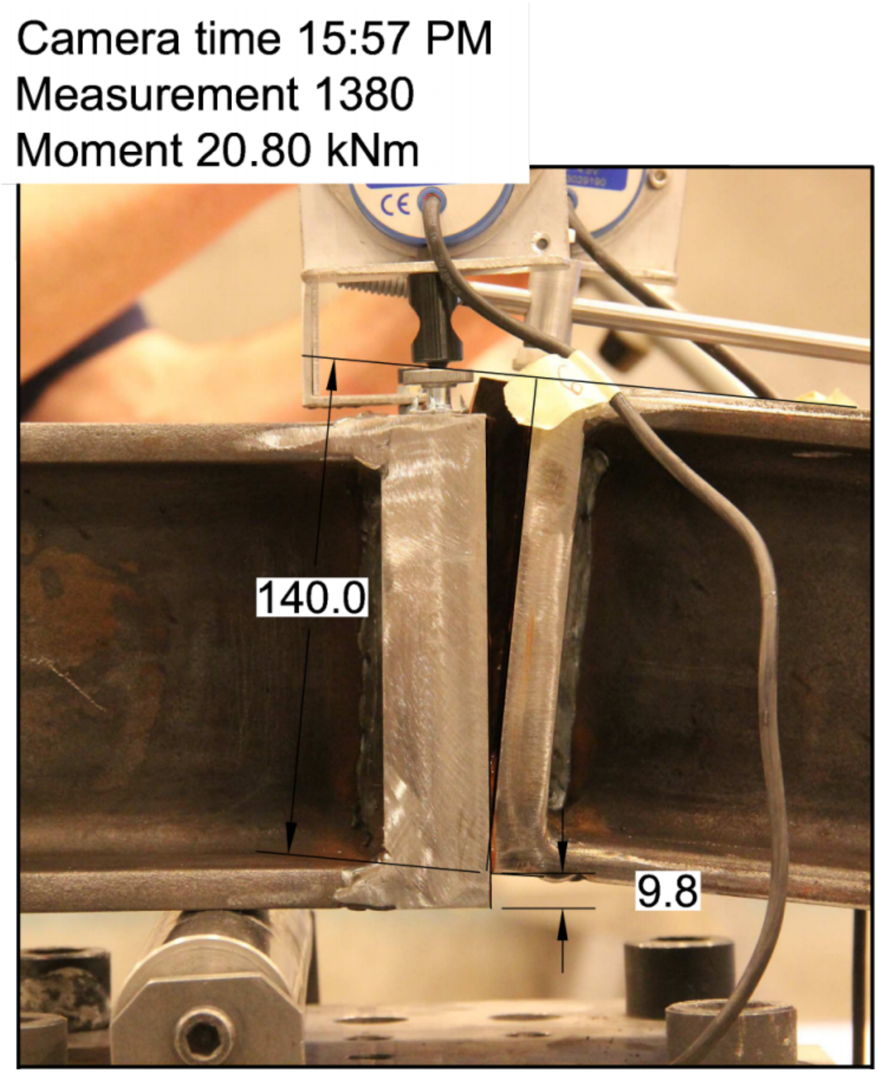

Figure 3.13: Failure mechanism test 1 [6]

Experimental test 2

The second test was performed with the position pins, the section of the beams was changed to HEB300 and the connection was welded to an endplate, which width and height is equal to that of the beam. An extra hole at the back of the endplate was made for an extra weld with the connection and this is shown in figure 3.15. The geometry of the connection changed as well and is shown in figure 3.14. This time no lubrication was used and a force of 250 kN was needed to push the plug into the socket. The used test setup for test 2 is shown in figure 3.16. In figure 3.17 the results of the test are shown. In the moment-rotation a drop in resistance is shown. This drop was caused by cracking of the socket as shown in figure 3.18.

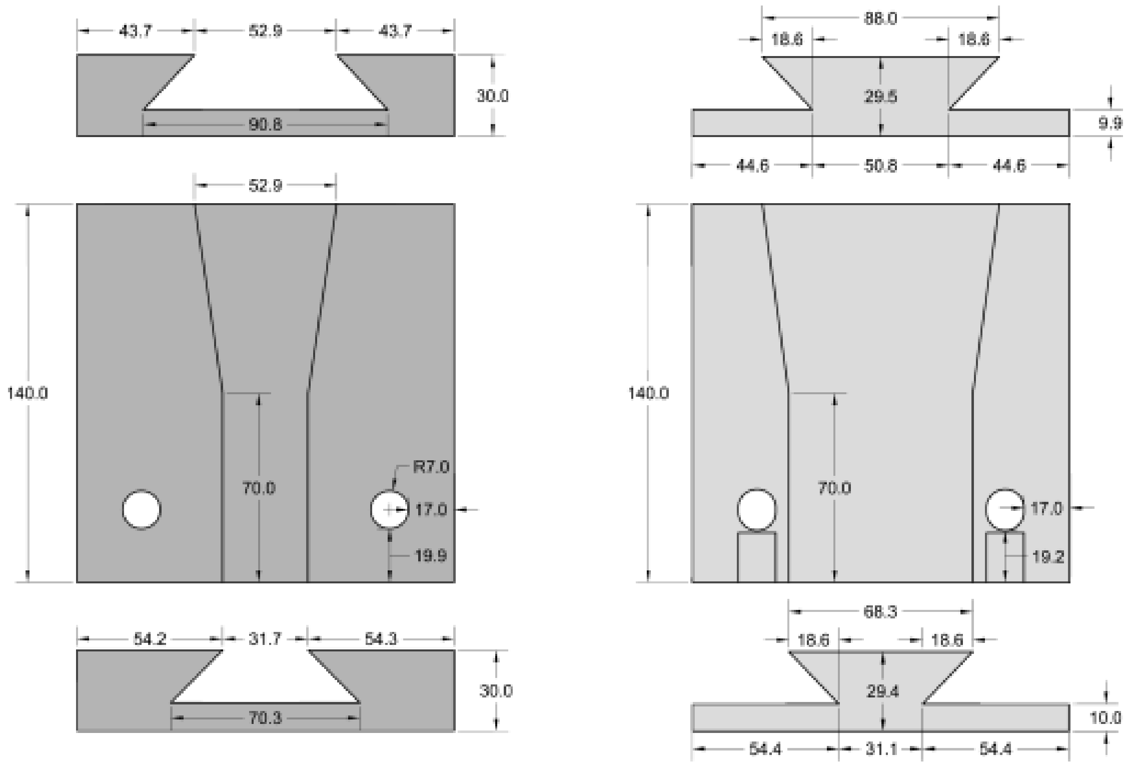

Figure 3.14: Geometry of the snap-fit connection test 2 [6]

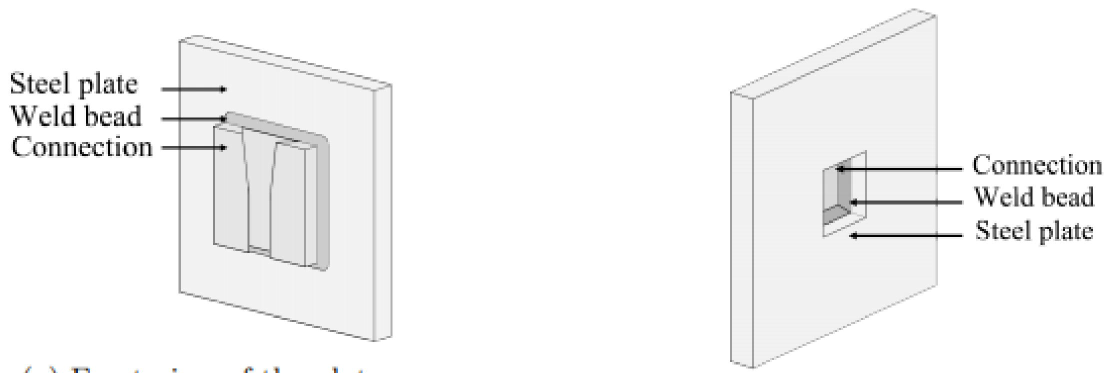

(a) Front view of the plate

(b) Back view of the plate

Figure 3.15: Weld connection test 2 [6]

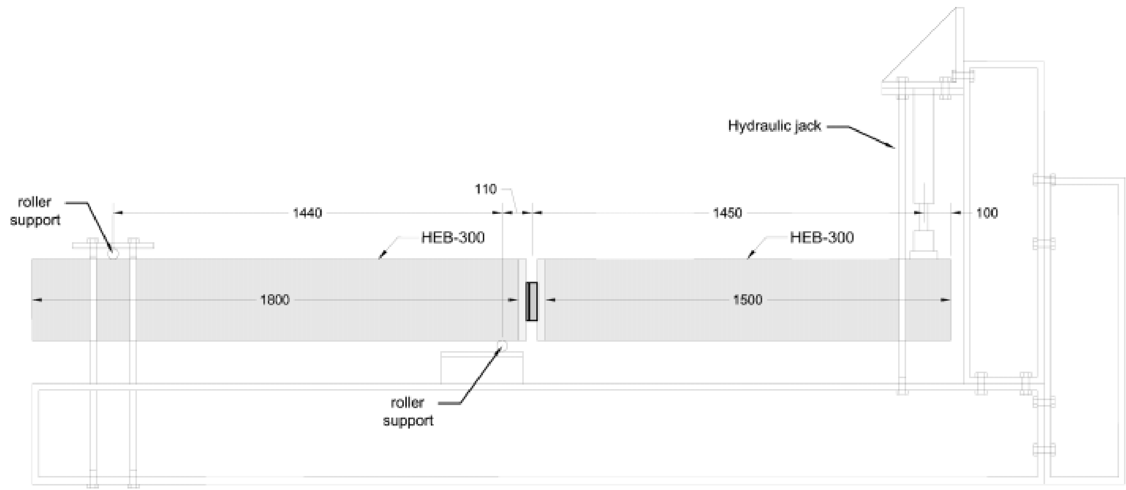

Figure 3.16: Setup test 2 [6]

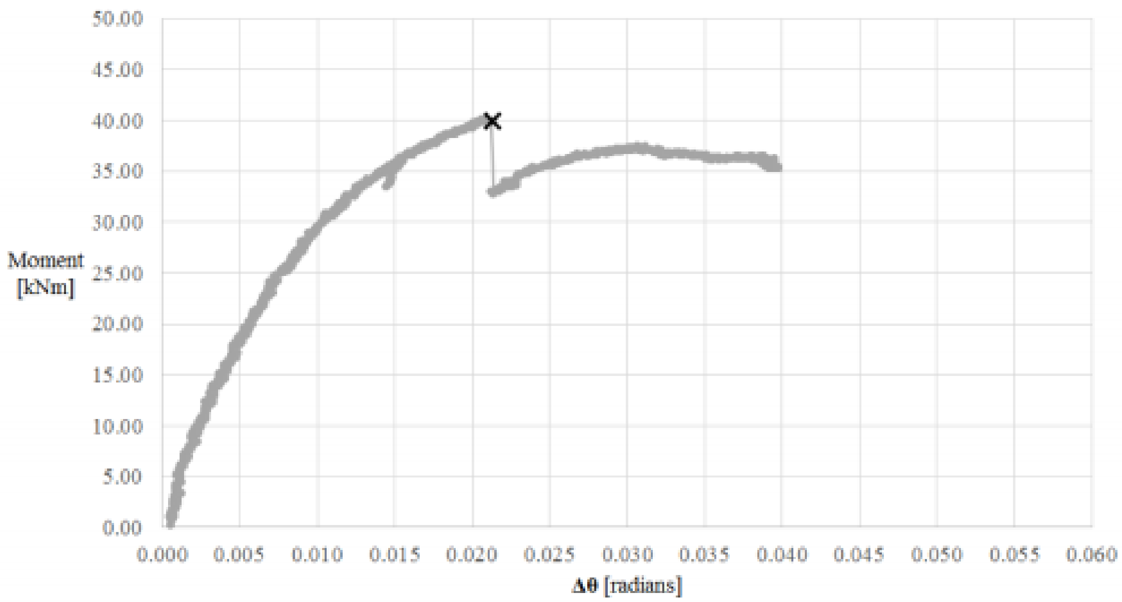

Figure 3.17: Moment rotation curve test 2 [6]

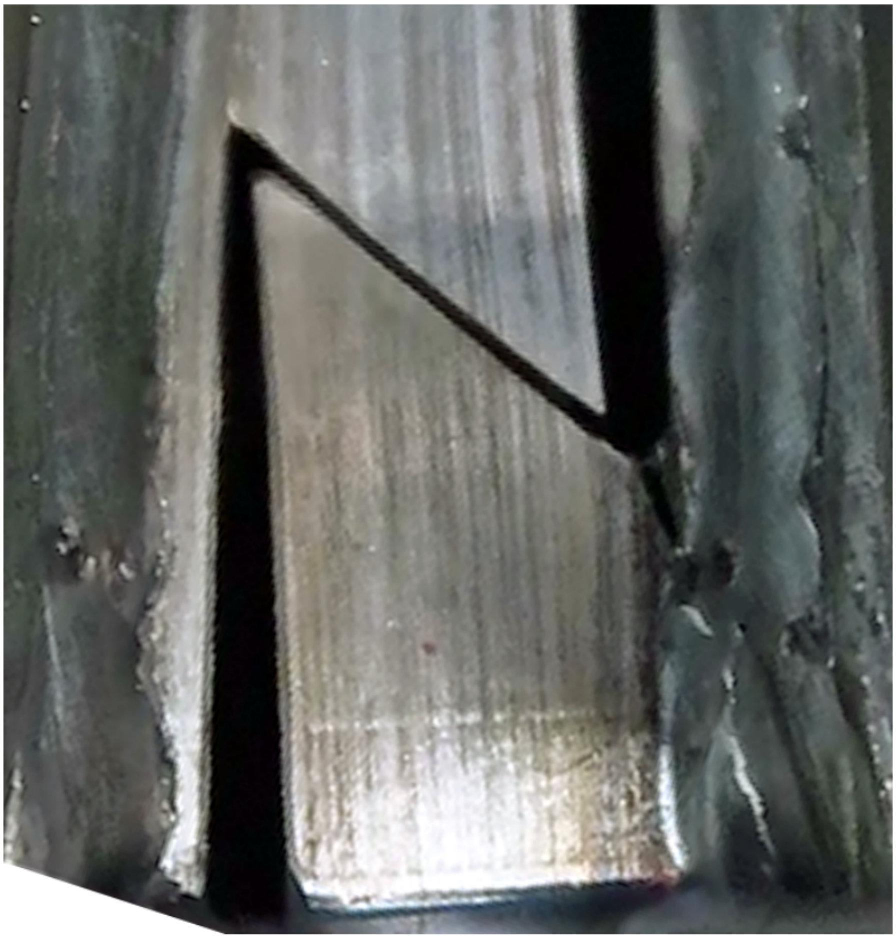

Figure 3.18: Failure mechanism test 2 [6]

Experimental test 3

The last test which was performed was for a connection with pins and a new geometry. The new geometry is shown in figure 3.19, where it can be observed that the inclination angle of the plug is made smaller. No lubrication was used and no force was required to put the connection together. The test setup is shown in figure 3.20. The corresponding moment-rotation curve is shown in figure 3.21. The maximum resistance of the connection is even lower compared to first test which was without pins. The small inclination angle made it easier for the plug to be pulled out of the socket. There was no crack developed in the connection.

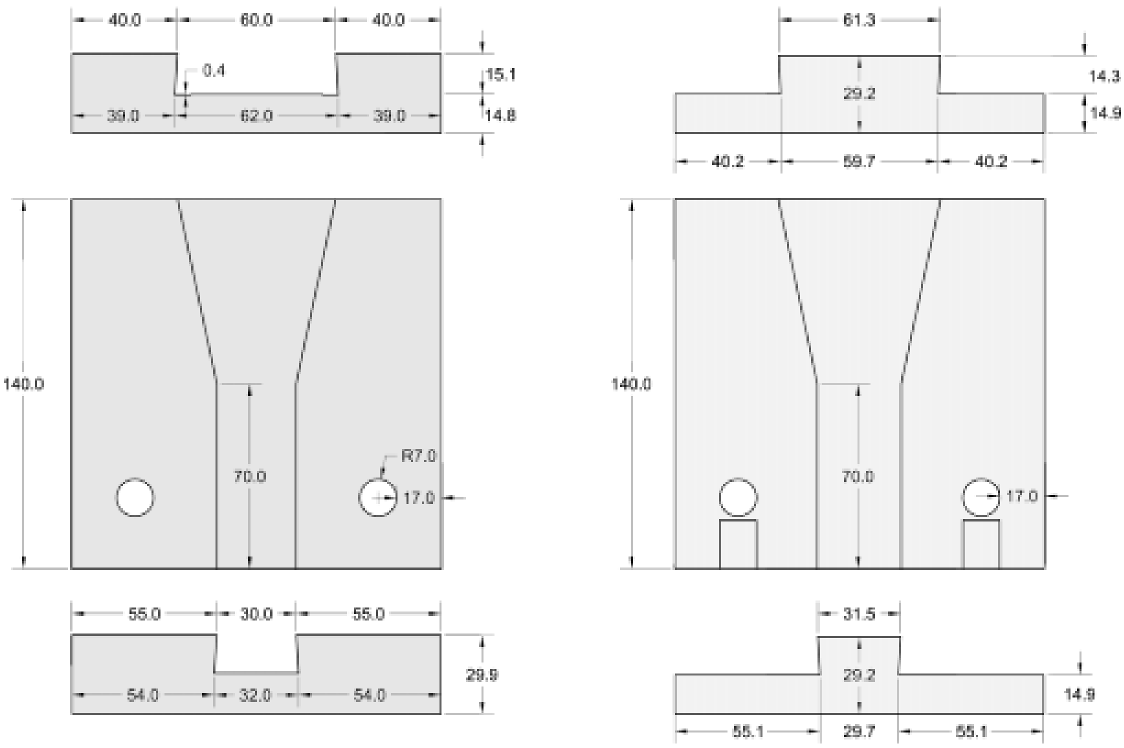

Figure 3.19: Geometry of the snap-fit connection test 3 [6]

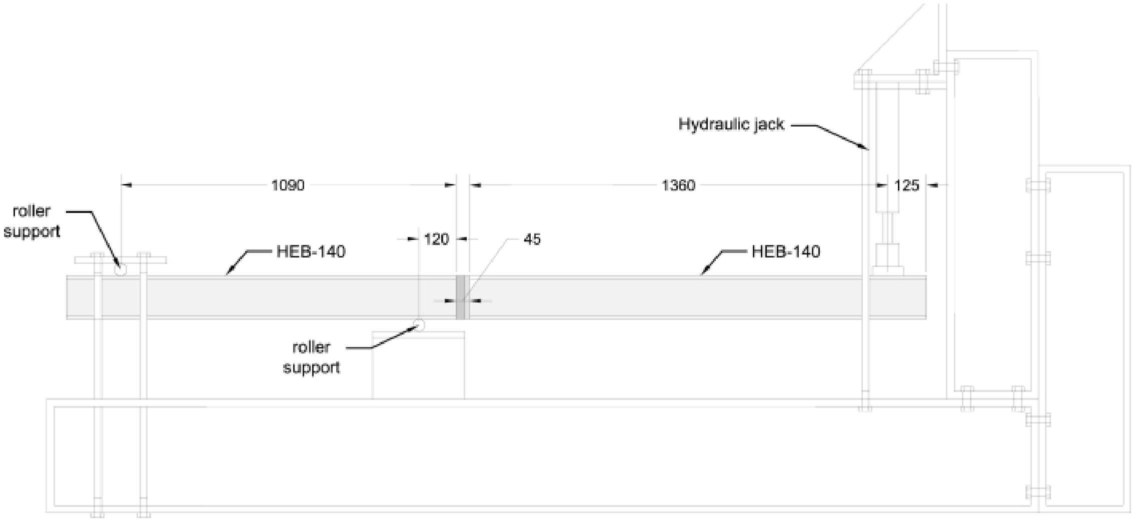

Figure 3.20: Setup test 3 [6]

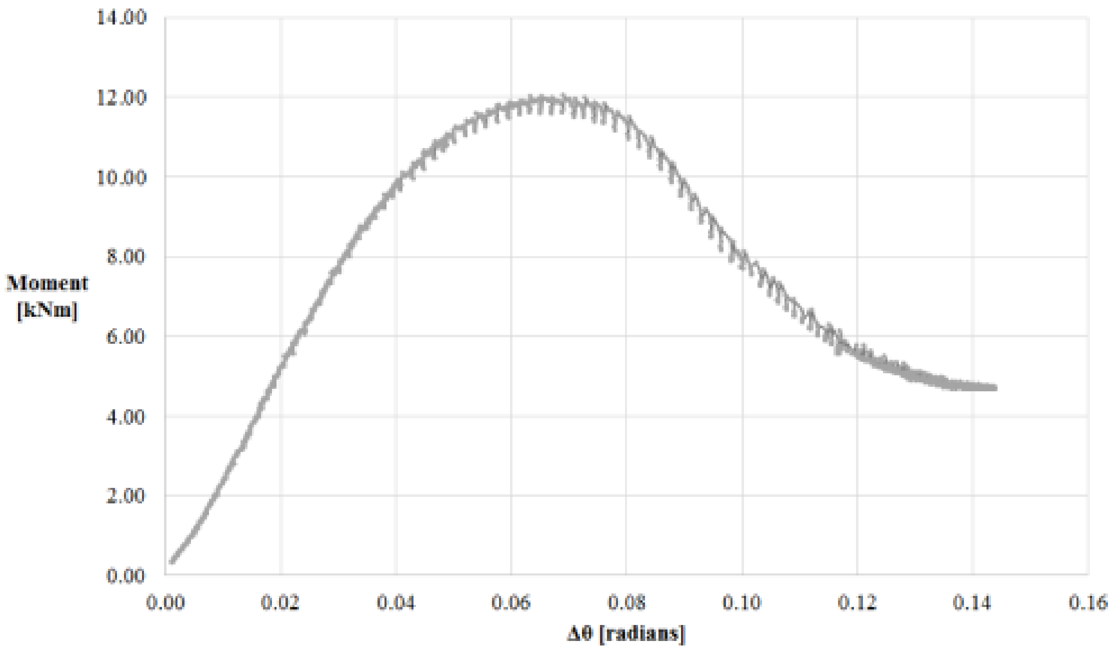

Figure 3.21: Moment rotation curve test 3 [6]

3.2.2 Parameters Study

After these tests a numerical study was performed by Sergio Moriche Quesada [6]. He investigated the influence of several parameters on the stiffness, resistance and ductility of the connection, by showing the $M - \phi$ curves. The investigated parameters are:

- Influence of frictional coefficient
- Influence of tolerances
- Influence of shear force
- Influence of welt configuration
- Influence of rounded corners
- Influence of inclination angle
- Influence of geometry changes

Experimental test 2 showed that a crack can develop in the corner. A cross in the $M - \phi$ indicates that the ultimate strain of the material is reached and the material would crack. The experimental tests results in the graphs are from the results of experiment 1. Numerical simulations for both a connection with and without pins are performed.

Besides the model which regards tolerances all numerical models assume a perfect fit connection.

Description and validation numerical model

The numerical model used by Quesada [6] to investigate the influence of the parameters is shown in figure 3.22. Due to symmetry only half of the connection is modelled to reduce computational times. The beam is modeled as a rigid body element with a kinematic constraint. The connection is modelled using solid elements and the pins are modelled with solid elements as well. The numerical models only consider that the top part will be in tension, and the cases for the bottom in tension are not analysed.
The results of the experimental tests are compared with the corresponding numerical results and are used to validate the model. The figures below show the results for validation for each test.

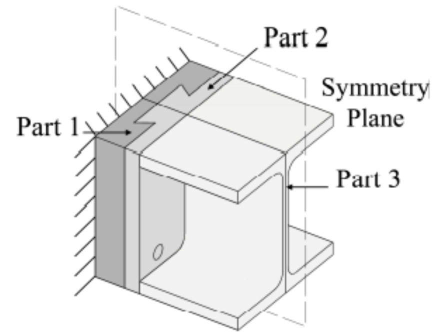

Figure 3.22: Numerical model snap-fit

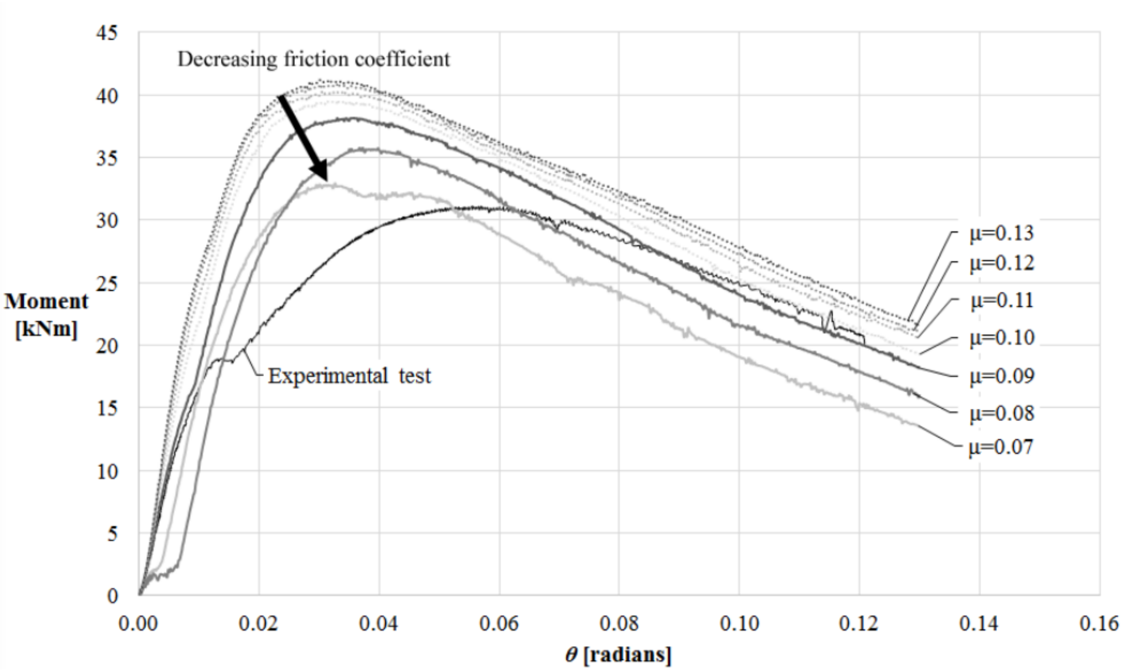

Figure 3.23: Validation test 1

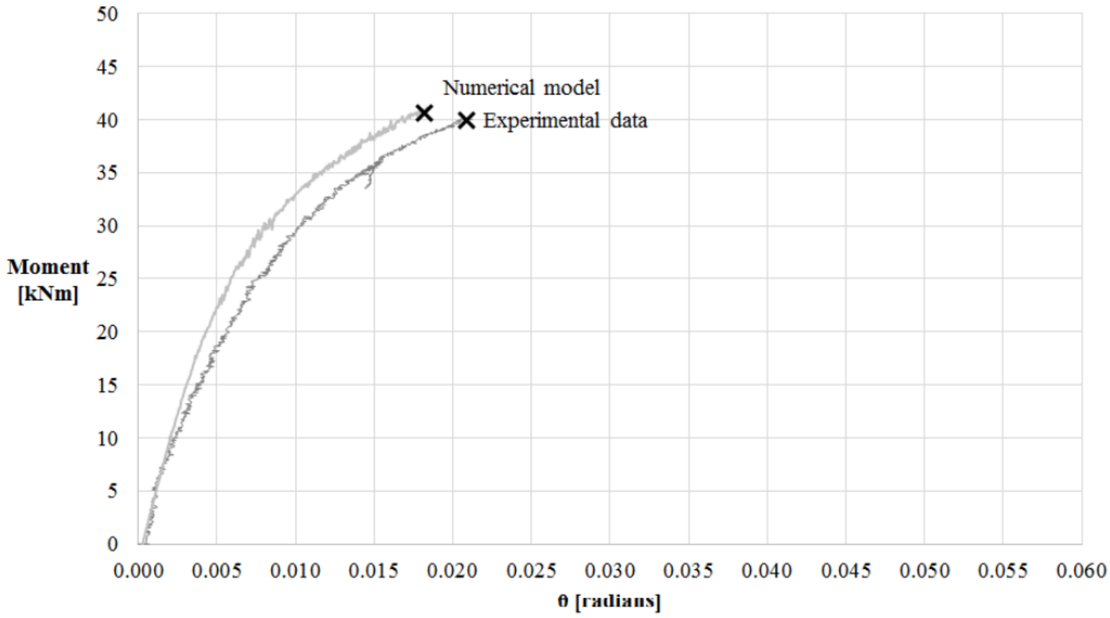

Figure 3.24: Validation test 2

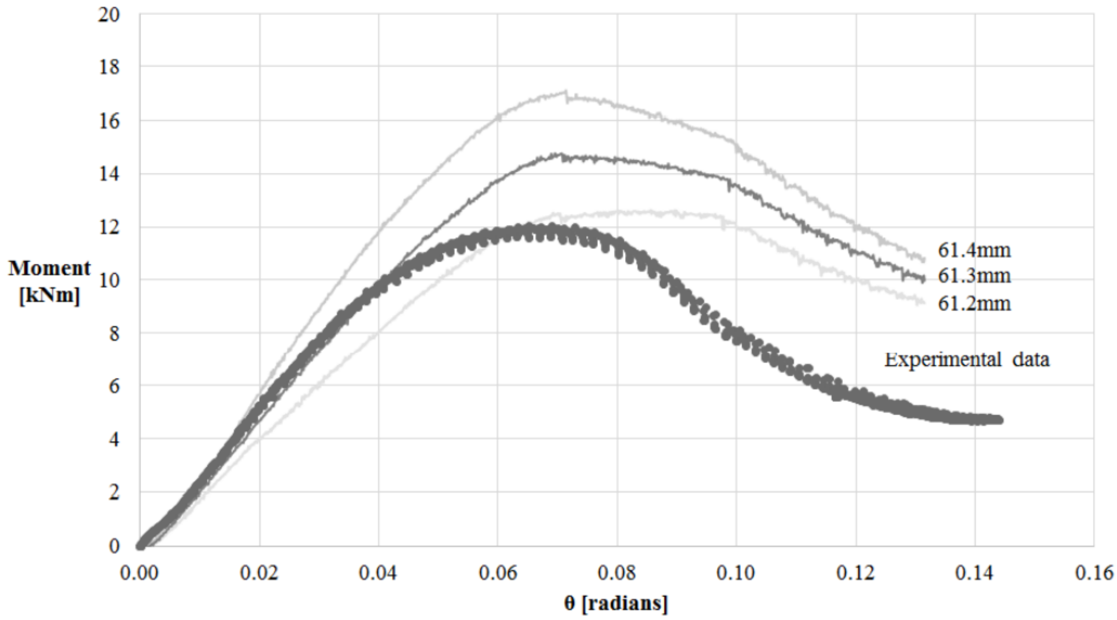

Figure 3.25: Validation test 3

In the figures 3.23, 3.24 and 3.25 the results for the validation of the numerical model is shown. The numerical results do not exactly match the experimental results. In table **??** the difference with the experimental results is given.

Frictional coefficient

The frictional coefficient depends on the used materials for the connection and on actions taken during installation of the frame, such as whether a lubricant is used.

Table 3.1: Validation results of snap-fit connection

Test	Difference stiffness	Difference resistance
1	range(-80% - +120%)	range(+5% - +30%)
2	+50%	+2.5%
3	range(-20% - +20%)	range(+5% - +40%)

In figures 3.26 and 3.27 the moment rotation curve for different frictional coefficients is compared with the experimental results of test 1. The Eurocode 1993-1-8 (2011) provides a table (Table 3.7) with the frictional coefficients for steel to steel contact in slip connections, without the use of lubricant. The range of the frictional coefficient in the EC gives values between 0.2 - 0.5 depending on the surface treatment, this is larger then the frictional coefficients evaluated in the numerical tests.

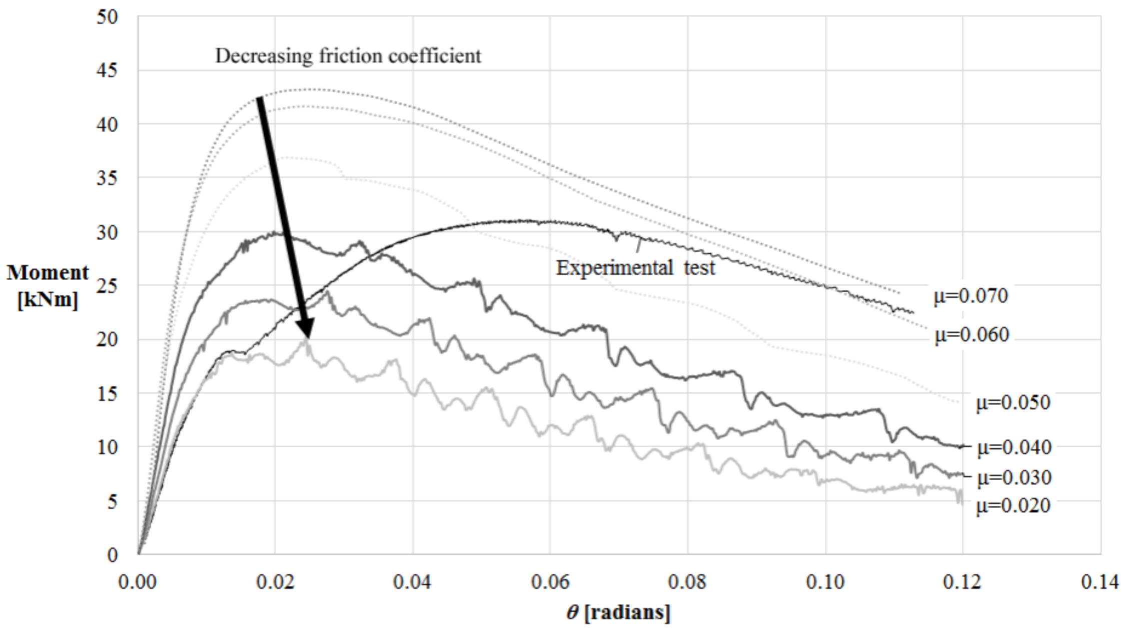

Figure 3.26: Moment rotation curve for different frictional coefficients without pins [6]

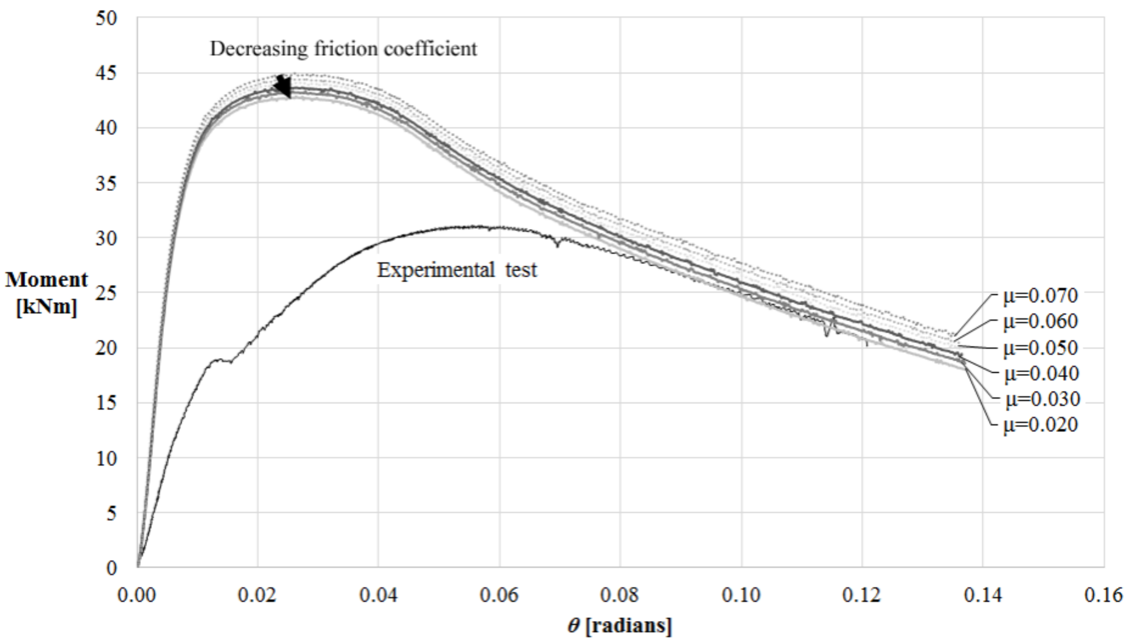

Figure 3.27: Moment rotation curve for different frictional coefficients with pins [6]

From figures 3.26 and 3.27 can be concluded that the pins make the connection more stable and less depended on the frictional coefficient. The friction coefficient does not have influence on the stiffness of the connection when it contains pins. The investigated friction coefficients are all for lubricated surfaces. The effect of friction coefficients for non lubricated surfaces with a friction coefficient between 0.2 and 0.5 is not investigated, it is unknown how much the use of a lubricant effects the results compared with a non-lubricated surface.

Tolerances

Tolerances between the socket and plug will occur, these tolerances cause gaps between the socket and plug. In figure 3.28 it is shown which tolerances are investigated. In this paragraph the influence of these gaps is shown.

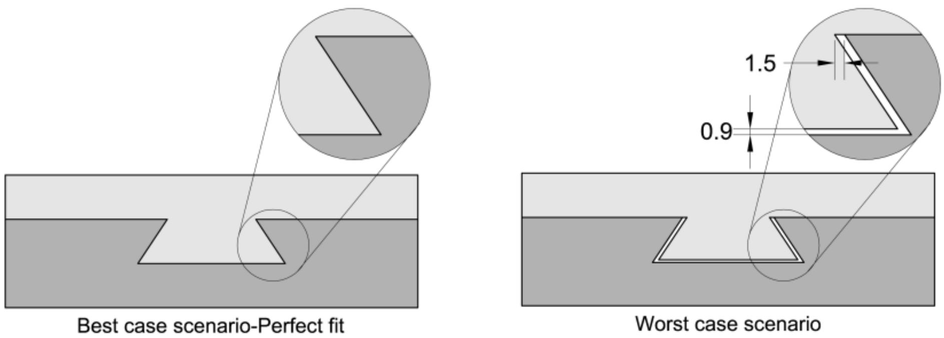

Figure 3.28: Tolerances in connection [6]

Similar to the frictional coefficient the horizontal and vertical tolerance is investigated for the situation with and without pins. The results are shown in figures 3.29 and 3.30. H200 means a horizontal gap of 2mm, similar V25 means a vertical gap of 0.25mm and the used value for the friction coefficient is 0.05 [6].

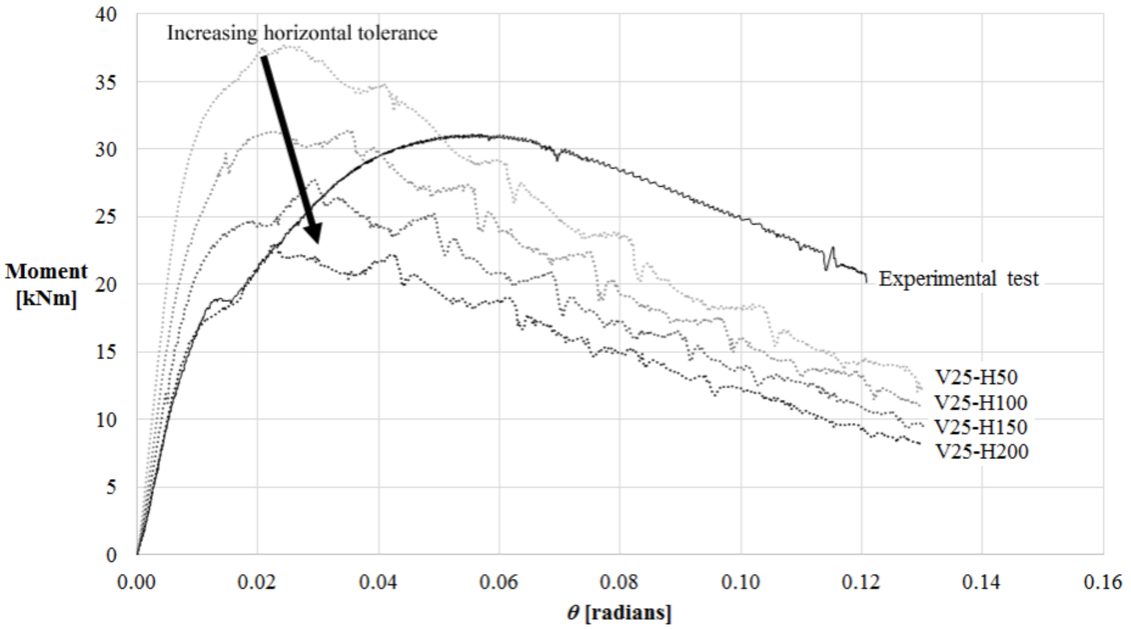

Figure 3.29: Moment rotation curve for different horizontal tolerances without pins [6]

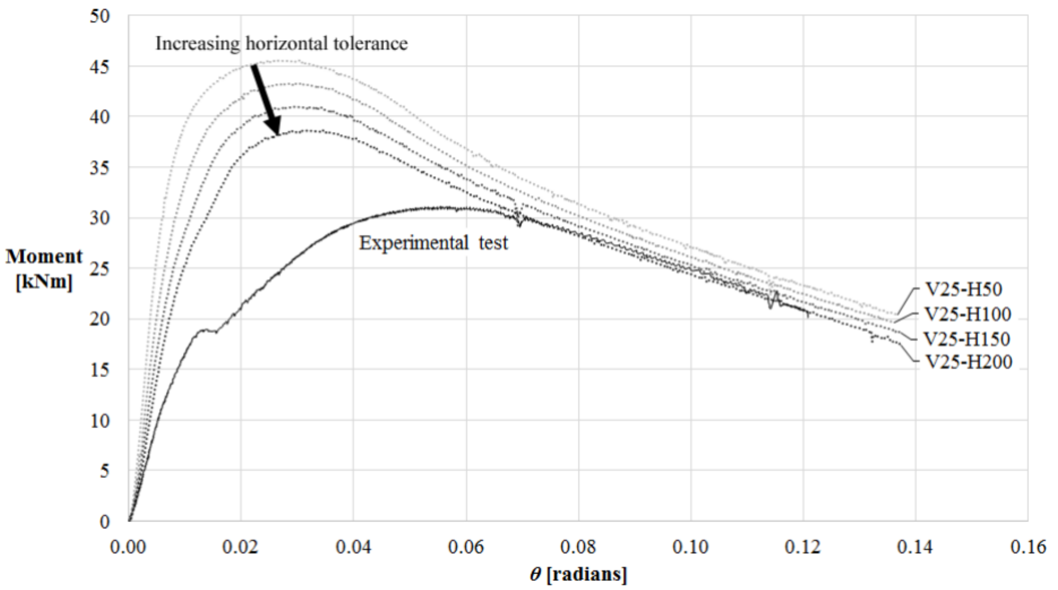

Figure 3.30: Moment rotation curve for different horizontal tolerances with pins [6]

The use of pins increased the resistance of the connection and also stabilized the behaviour of the connection. From both graphs can be concluded that a horizontal gap decreases both the resistance and stiffness of the connection.

Figures 3.31 and 3.32 show the results for the vertical tolerances. Similar to the horizontal tolerances the resistance was increased when pins were used. For the case without pins it can be seen that vertical tolerances have less influence on the resistance than the horizontal tolerances. When pins are used then the resistance decreases slightly for an increasing vertical gap and the stiffness seemed to be independent of the vertical gap.

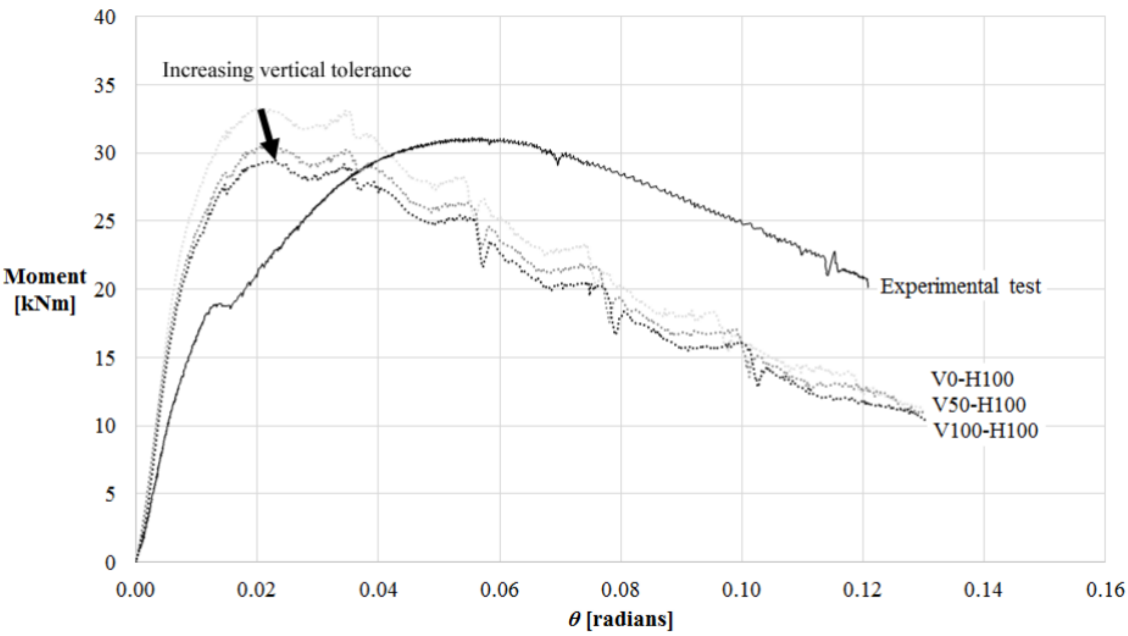

Figure 3.31: Moment rotation curve for different vertical tolerances without pins [6]

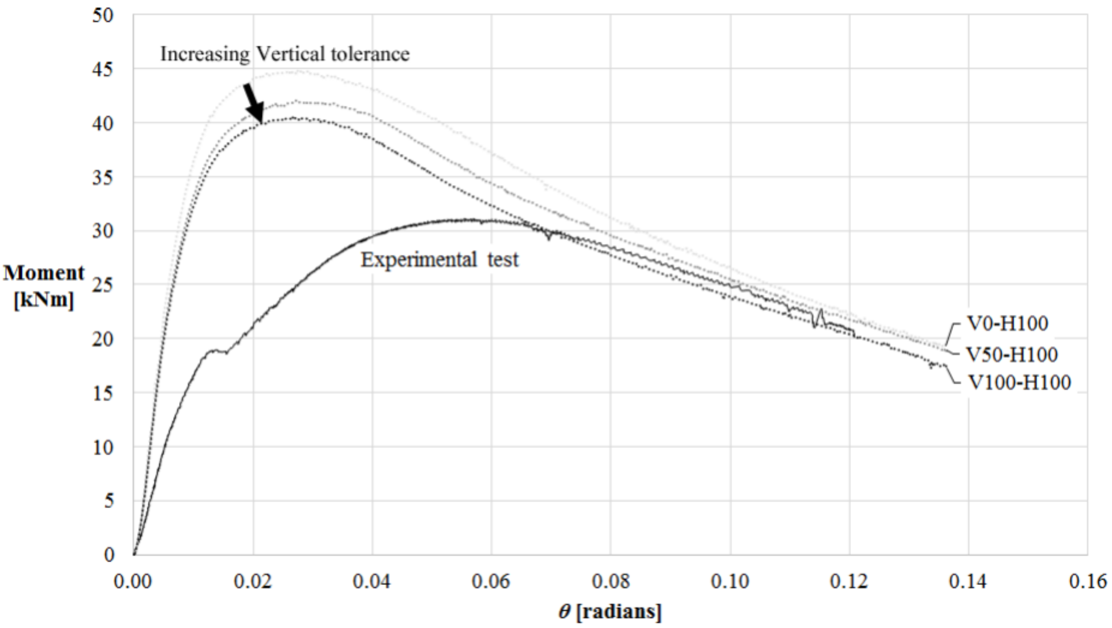

Figure 3.32: Moment rotation curve for different vertical tolerances with pins [6]

The relative difference between the resistances for different tolerances for the vertical gap was the same for both situations, while for the horizontal gap the relative difference was also decreasing when pins were used. Both tolerances influence the maximum resistance and stiffness of the connection, but the effect of horizontal tolerances were the largest.

Shape of corners

Experimental test 2 showed a crack in the socket, this is caused by the strain reaching the ultimate strain at that place. This localised high strain limits the maximum resistance of the connection. A possible option to reduce the stress concentration is to replace the sharp angular corner for a more "smooth" rounded corner and so better distribute the strains in the corner of the socket. The geometry of the connection with rounded corners is shown in figure 3.33.

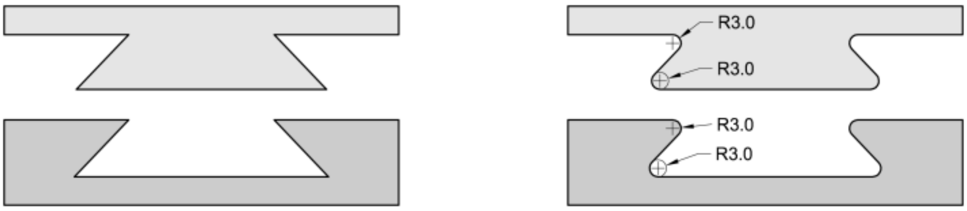

Figure 3.33: Geometry with sharp and rounded corner [6]

The results of the rounded corners on the structural performance of the connection is shown in figure 3.34. The original line represents the numerical result of the validation model for experimental test 2.

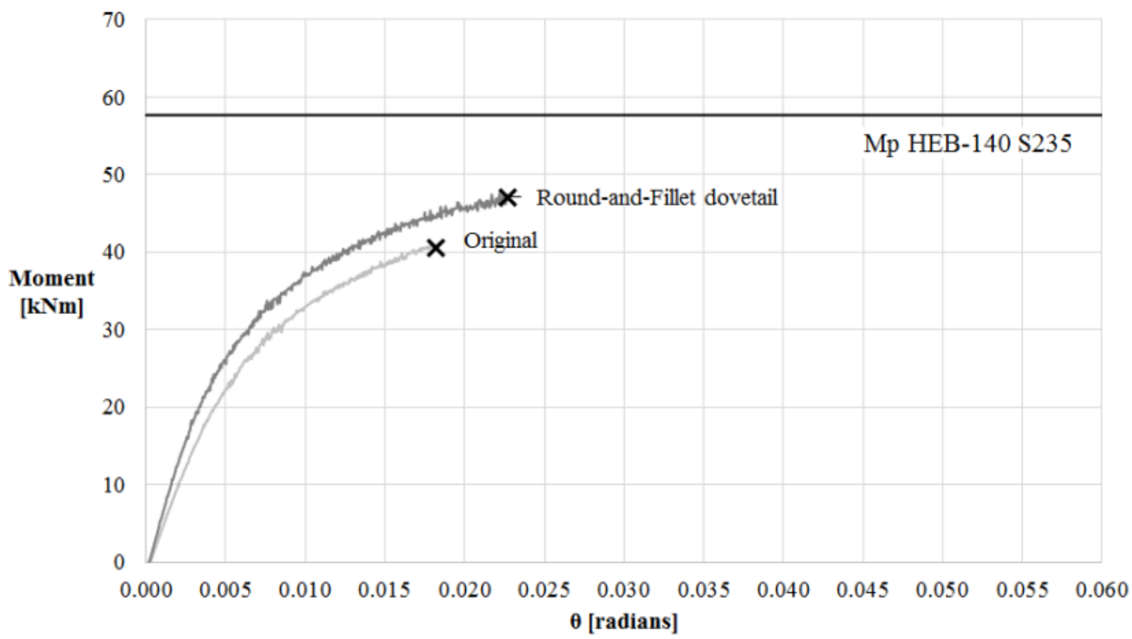

Figure 3.34: Moment rotation curve with rounded corners [6]

The maximum resistance has increased 17.5% compared to the original design and the stiffness is increased with 33%. Also the maximum rotation has increased with 25%. However, the problem of the localised ultimate strain in the corner is not solved.

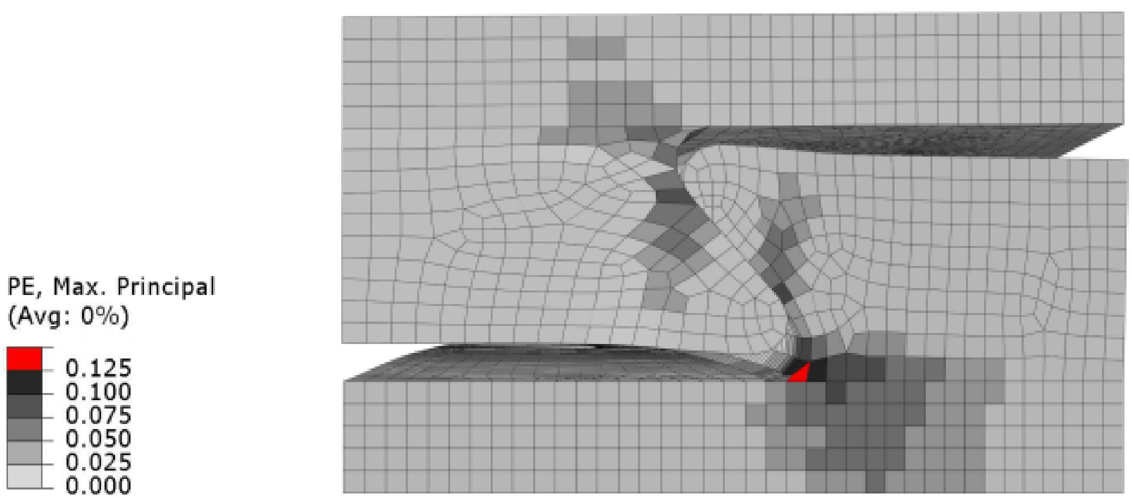

Figure 3.35: Principal strain rounded corner [6]

Inclination angle

It is checked whether changing the inclination angle can reduce the maximum strain. An increasing inclination angle will lead to a reduced surface contact area. Figure 3.36 shows the geometries with different inclination angle which are tested.

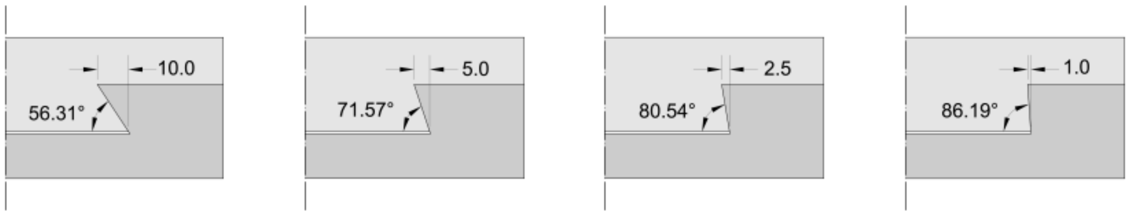

(a) Alternative 1 (b) Alternative 2 (c) Alternative 3 (d) Alternative 4

Figure 3.36: Geometry with different inclination angles [6]

For the test a frictional coefficient of 0.42 is used. Figure 3.37 shows the moment rotation curves for different inclination angles. The cross indicates that the maximum strain of the material is reached. In figure 3.38 the location of the maximum strain is indicated.

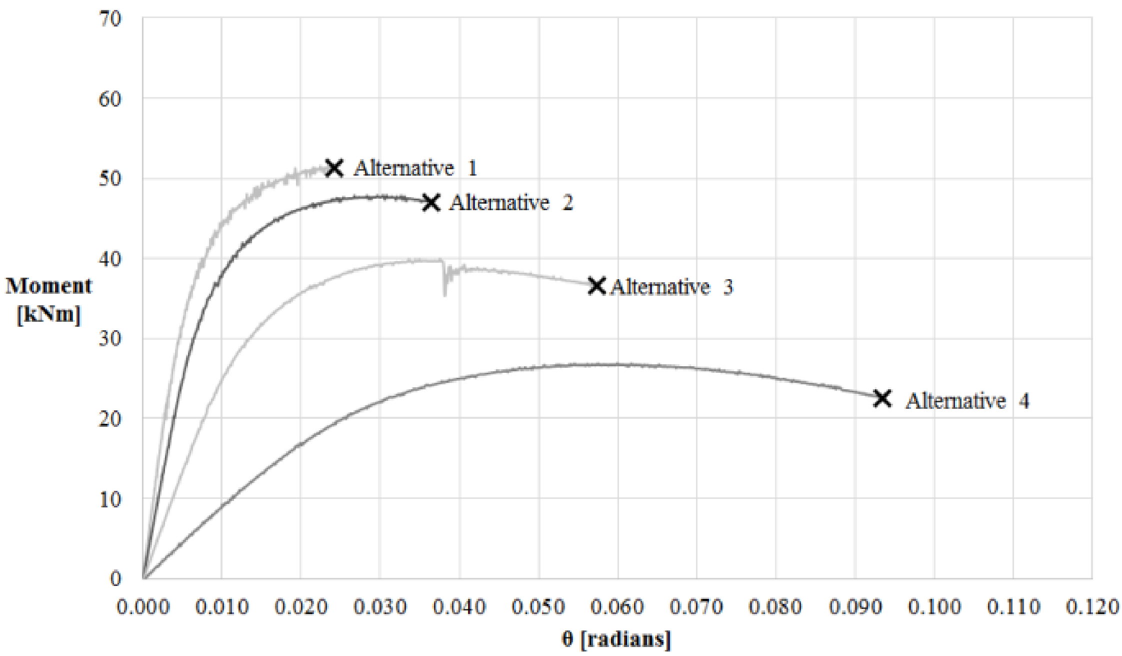

Figure 3.37: Moment rotation curve for different inclination angles [6]

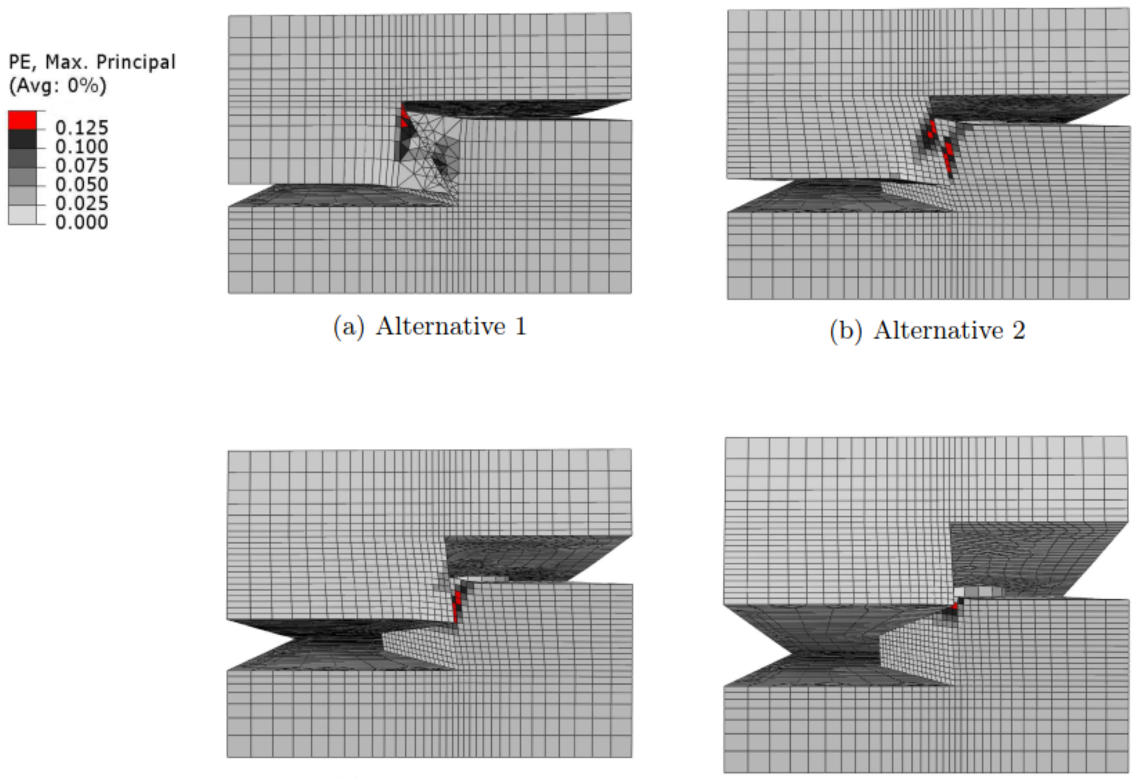

(a) Alternative 1

(b) Alternative 2

(c) Alternative 3

(d) Alternative 4

Figure 3.38: Principal strain inclination angle [6]

Figure 3.38 shows that by changing the inclination angle the location where the maximum strain occurs is changed. Changing the inclination angle has a big impact on the stiffness, resistance and ductility of the connection. A large inclination angle will remove the strain concentration from the corner to the tip of the plug. The large inclination will result in a lower stiffness and resistance but a higher ductility. The large inclination makes it easier to pull the plug out of the socket.

This increase of ductility is caused by the large displacement of the connection. As can be seen in figure 3.38 the gap between the socket and plug increases for an increasing value of the inclination angle.

The reduced contact area results in a lower stiffness and resistance of the connection, but in a higher maximum rotation. In table 3.2 the differences in stiffness, resistance and maximum rotation compared to alternative 1 is given.

Table 3.2: Comparison results for different inclination angles

Alternative	Diff stiffness	Diff resistance	Diff ductility
1	7500 kNm/rad	51 kNm	0.024 rad
2	-17%	-8%	+50%
3	-60%	-29%	+140%
4	-85%	-56%	+290%

Geometric Parameters

In figure 3.39 the parameters for the geometry study are given. All parameters are discussed below. For the simulation a frictional coefficient of 0.07 is used.

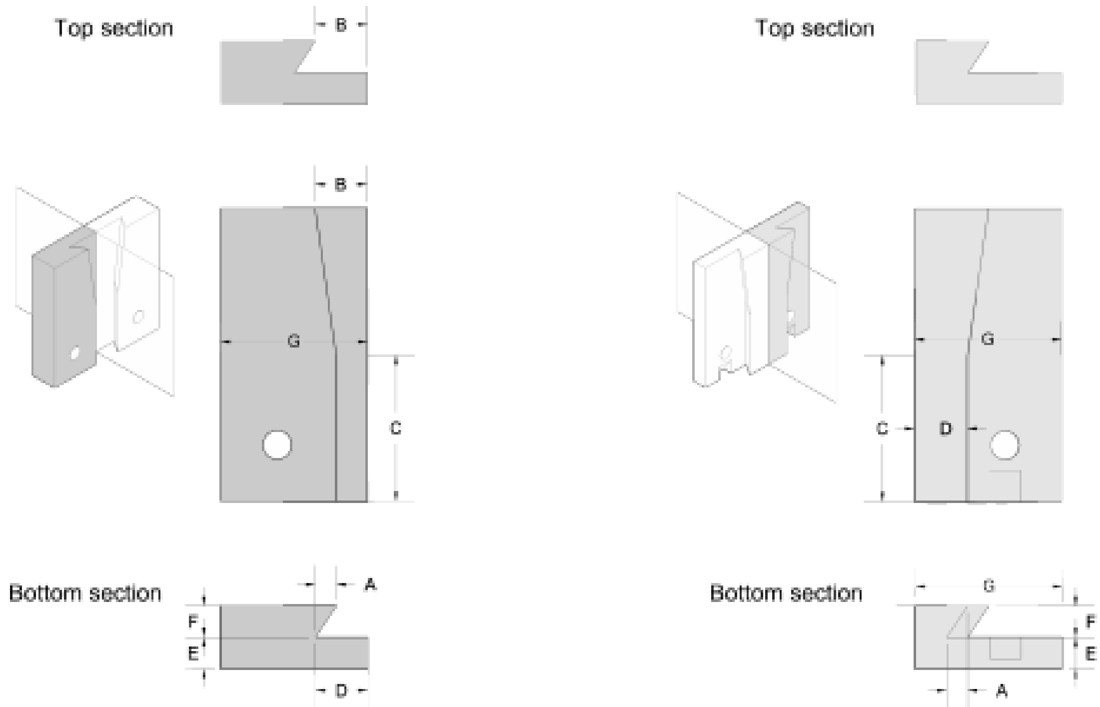

Figure 3.39: Parameters for geometry study [6]

A - offset plug

A change of the offset has a direct effect on the inclination angle, for an increasing value of A the inclination angle will decrease. In figure 3.40 the moment rotation curves for different values of parameter A are given. The value of A is in mm. It can be seen that an increasing the value of A, which increases the surface contact area, leads to an increase in resistance.

Parameter A also involves the inclination angle, but the difference in ductility is not as large as is observed in figure 3.37. A lower friction coefficient used for the geometry study which could cause the small difference in ductility.

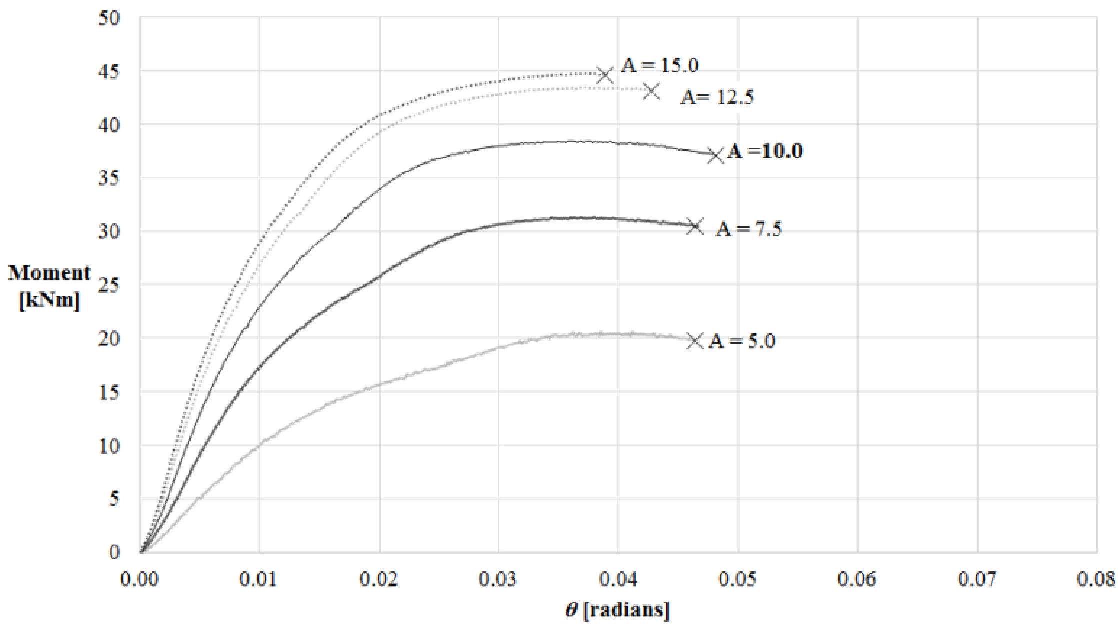

Figure 3.40: Moment rotation curve parameter A [6]

In table 3.3 the difference in results is compared to the reference value for the offset of 5mm.

Table 3.3: Comparison results offset plug

Offset plug	Diff stiffness	Diff resistance	Diff ductility
5 mm	1000 kNm/rad	20 kNm	0.046 rad
7.5 mm	+70%	+55%	0%
10 mm	+130%	+90%	+5%
12.5 mm	+160%	+120%	-10%
15 mm	+190%	+125%	-15%

B,C & D

The parameters B (offset tapered part of the inclination), C (length straight part of the inclination) and D (width straight part of the inclination) are combined to one paragraph as the effect of changes in these parameters have little effect on the structural performance of the connection. Figures 3.41, 3.42 and 3.43 show the moment rotation curves for the different values of parameter B, C and D. The figures show that for different values of the parameters the structural behaviour would be almost the same. This can be explained as the changes of the parameters do not change the surface contact area and therefor the frictional force will be constant to.

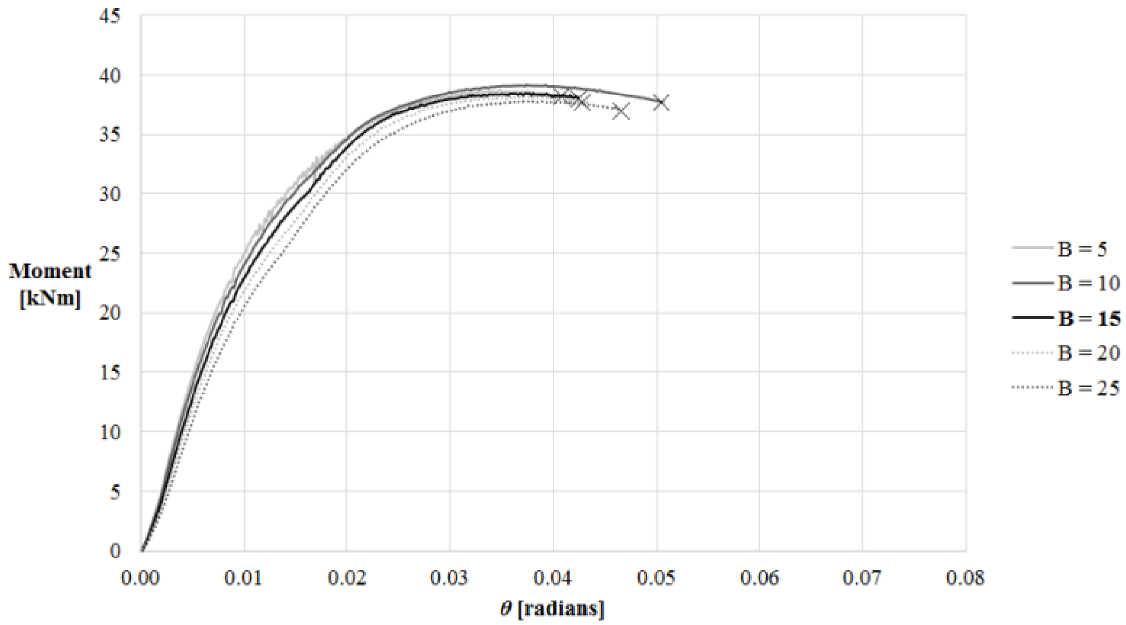

Figure 3.41: Moment rotation curve parameter B [6]

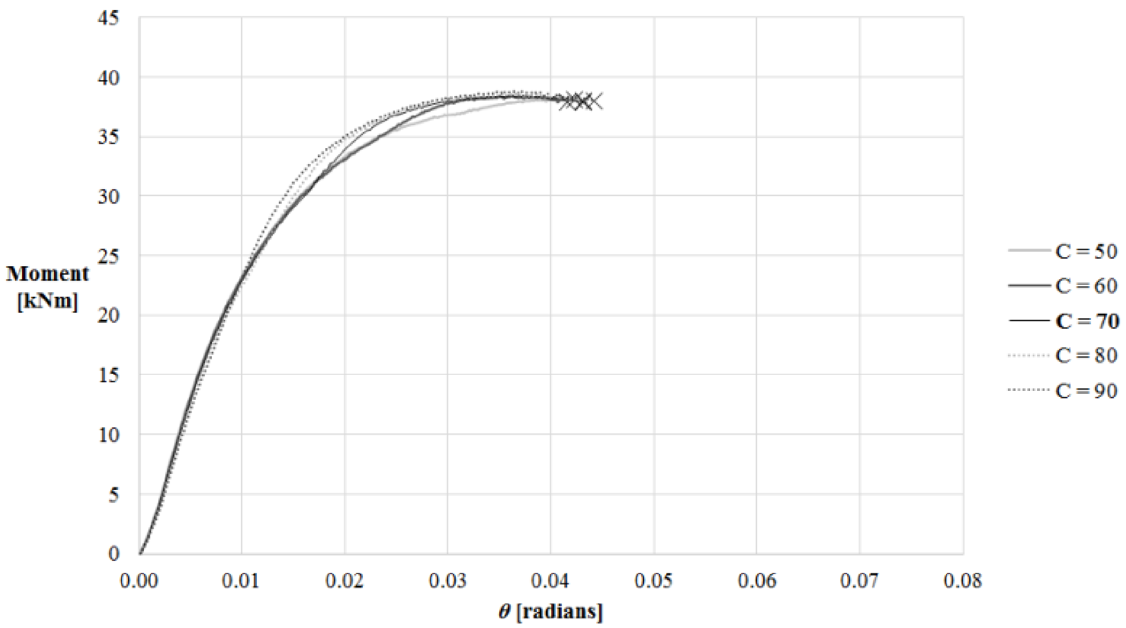

Figure 3.42: Moment rotation curve parameter C [6]

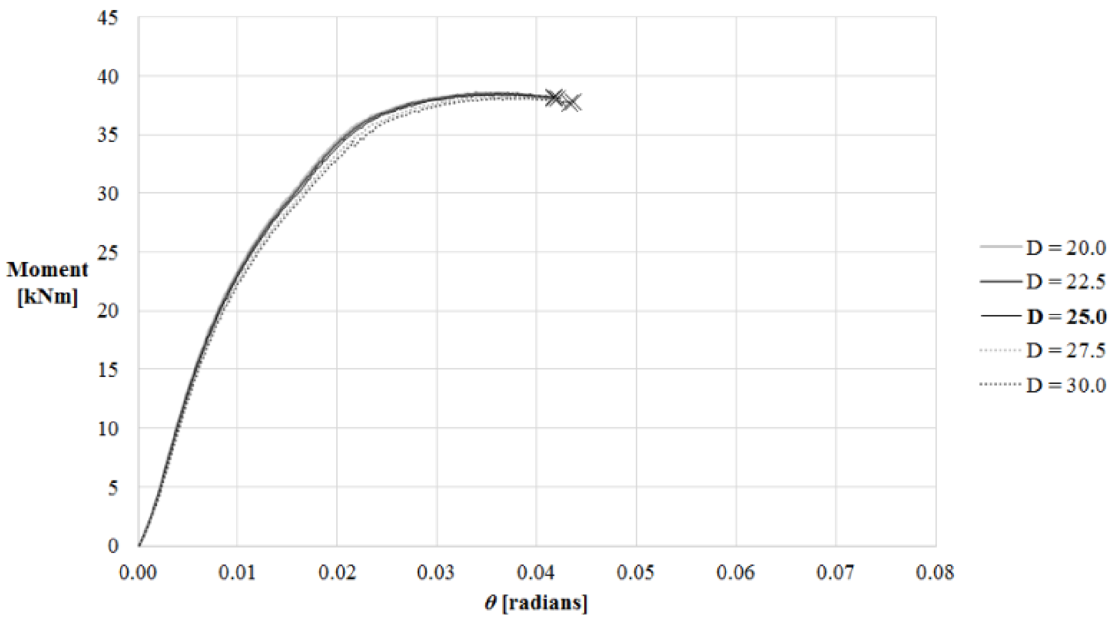

Figure 3.43: Moment rotation curve parameter D [6]

E - thickness base plate

The following parameter is the thickness of the base plate(s). The thickness of the base plate for the socket and plug is the same. The moment rotation curve is shown in figure 3.44.

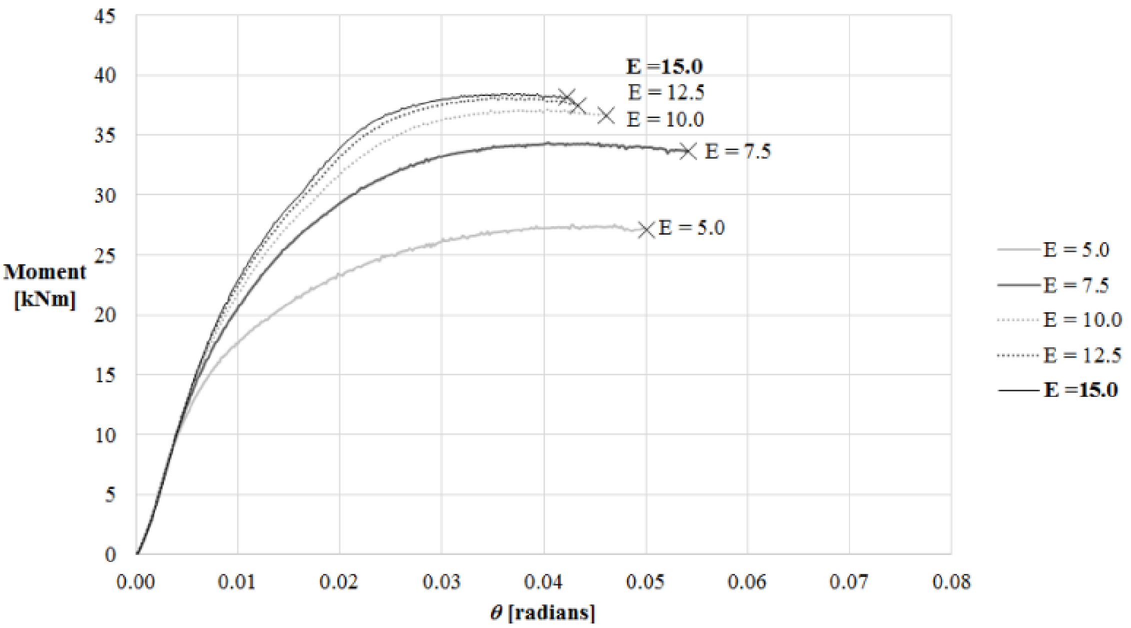

Figure 3.44: Moment rotation curve parameter E [6]

The resistance for a base plate thickness of 10mm is 5% lower then the resistance for a base plate thickness of 15mm and the difference in ductility is also 5%, the initial stiffness for a thickness of 10mm, 12.5mm and 15mm is the same. Figure 3.45 shows the Von Mises stresses in the connection for a base plate thickness of 5mm, 7.5mm and 15mm. As can be seen in this figure increasing the thickness of the base plate reduces the yielded area of the base plate.

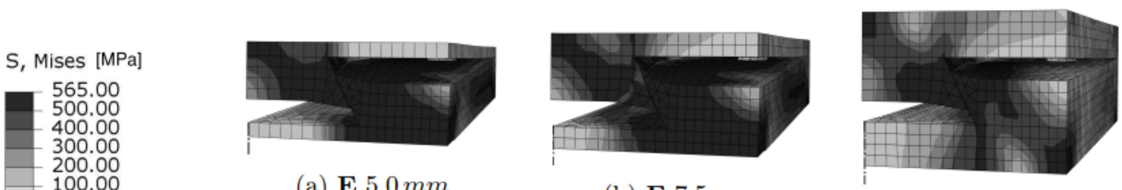

(a) **E** 5.0 mm (b) **E** 7.5 mm (c) **E** 15.0 mm

Figure 3.45: Stress due to parameter E [6]

F - thickness plug and socket

Parameter F involves the change in thickness of the plug and the thickness of the slot in the socket. The moment rotation curves for different values of F are shown in figure 3.46.

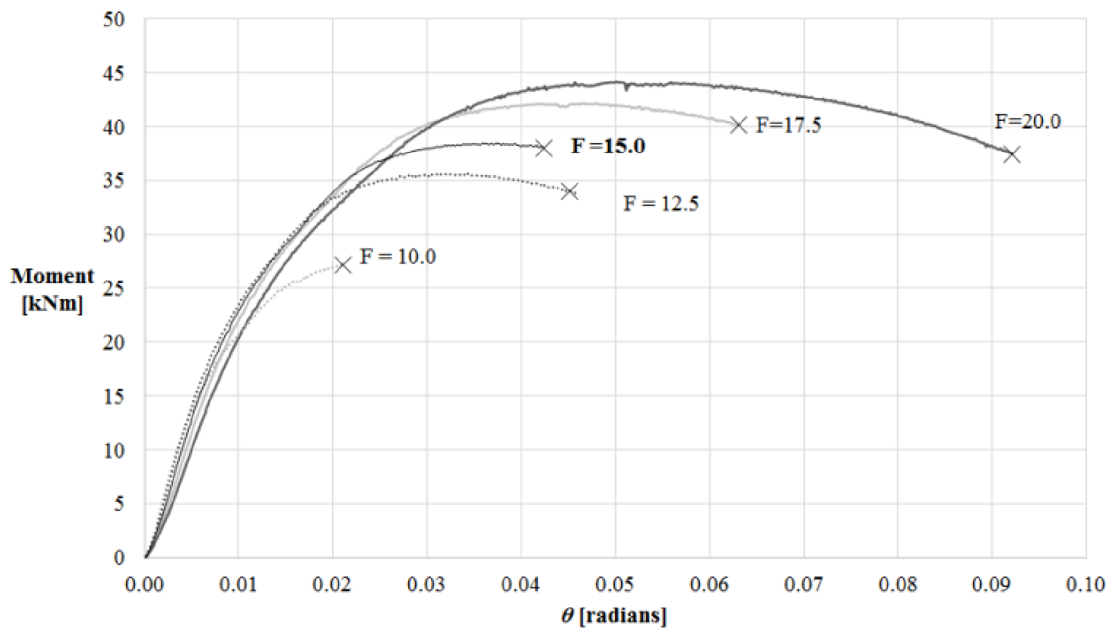

Figure 3.46: Moment rotation curve parameter F [6]

Similar to parameter A, parameter F does effect the inclination angle as well. An increasing value of F leads to an increasing value of the inclination angle. Earlier was shown that for an increasing value of the inclination angle the structural performance would decrease, the opposite can be seen in figure 3.46. This can be explained that in figure 3.37 the increasing inclination angle resulted in a reduced contact area. When parameter F is increased not only the inclination angle increases but also the contact area. So the resistance of the connection is more depended on the contact area then on the inclination angle.

In table 3.4 the comparison between the results is given in which a thickness of 10mm is taken as the reference for comparison.

Table 3.4: Comparison results thickness plug and socket

Thickness	Diff stiffness	Diff resistance	Diff ductility
10 mm	2000 kNm/rad	27.5 kNm	0.021 rad
12.5 mm	0%	+30%	+115%
15 mm	-5%	+35%	+100%
17.5 mm	-10%	+50%	+195%
20 mm	-20%	+ 60%	+340%

The increasing ductility is caused by the decreased inclination angle. The higher resistance can be explained by the increased contact area. The reduction of the stiffness is a consequence of the increased inclination angle.

The structural behaviour for the value of 12.5mm is remarkable as it shows better ductility than the geometry with value 15mm. No explanation is given.

G - width connection

The last parameter which is investigated is the width of the connection. The contact area remains constant for all analyses. The moment rotation curves are shown in figure 3.47. This parameter does show what the effect is of the area between the edge of the plate and the start of the inclination.

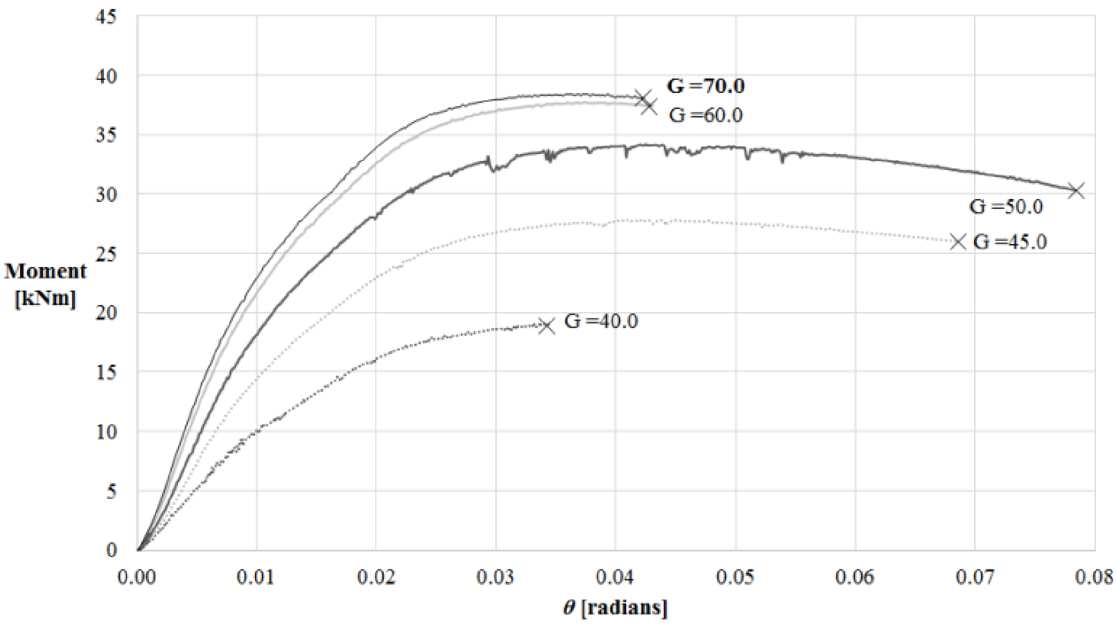

Figure 3.47: Moment rotation curve parameter G [6]

In table 3.5 the results are compared to the reference width of 40mm. The lower increase in ductility for a thickness of 60mm and 70mm, compared with the ductility increase for 45mm and 50mm, is because of full yielding of the area between the edge and the start of the inclination for the 45mm and 50mm case. For the case of 60mm and 70mm this area is not fully yielded.

Table 3.5: Comparison results for width

Width	Diff stiffness	Diff resistance	Diff ductility
40 mm	1000 kNm/rad	19 kNm	0.034 rad
45 mm	+40%	+45%	+100%
50 mm	+80%	+80%	+130%
60 mm	+110%	+90%	+25%
70 mm	+130%	+195%	+20%

Figure 3.48 shows the Von Mises stress distribution in the connection for the top part of the connection. For increasing G it can be seen that the distance between the start of the inclination and the edge of the plate increases. For G=40mm this distance is zero at the top. So increasing this distance between inclination and edge of the plate results in a stiffer and stronger connection.The higher ductility for G=45mm and G=50mm is caused by the area

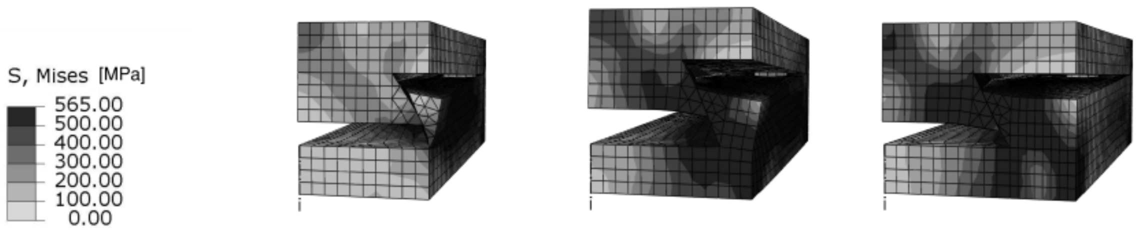

(a) **G** 40.0 mm (b) **G** 50.0 mm (c) **G** 60.0 mm

Figure 3.48: Stress due to parameter G [6]

between the edge and inclination which completely yields. For G=60mm and G=70mm the area between the edge and inclination is partly yielding and the connection is stiffer and stronger.

3.2.3 Summary and evaluation

The snap-fit connection is discussed elaborated in this section. This summary provides a quick overview of the most important parts of the connection discussed in this section.

- **Friction coefficient:** the friction coefficient has the most influence on the connection without pins. The plug will show an uplift from the socket if the upward forces are higher than the friction forces. To prevent this uplift pins are used to keep the socket in its place and these pins make the solution less friction depended. However, the investigated frictional coefficients only considered the use of a lubricant, the effect of a non-lubricated surface is not investigated.

- **Tolerances:** due to tolerances the connection will not be a perfect fit connection and gaps between the socket and plug occur. Horizontal gaps, the gaps with the tapered part of the connection, seems to have a larger impact on the stiffness and resistance of the connection than the vertical gaps. Again the pins reduce the effect of the gaps in the connection.

- **Local stress concentration:** the connection seems to fail because the maximum strain of the material is reached in the corner of the inclination of the socket. Rounded corners slightly increase the resistance and stiffness of the connection, but the will not remove the stress concentration.

- **Inclination angle:** increasing the inclination angle reduces the stiffness of the connection and increases the ductility of the connection. The maximum resistance of the connection is more depend of the contact area then on the inclination angle.

- **Thickness base plate:** the thickness of the base plate of both socket and plug only effects the structural performance of the connection if it is too small then yielding of the base plate will occur. The thickness needs to be at least 10mm to prevent the base plate from yielding.

- **Distance between edge of plate and inclination:** the distance between the edge of the plate and the inclination effects the ductility, resistance and stiffness of the connection. If the area between the edge and the inclination is 45mm or 50mm the area will completely yield resulting in a doubling of the ductility compared to the case in which it is 40mm. If the area is large enough, 60mm or 70mm, then only a part of the area will yield resulting in a increase of ductility of 20%. The minimum distances between the edge and the start of the inclination needs to be 20mm and increasing it to 30mm does not have much effect on the results.

The best way to increase the resistance of the connection is to increase the contact area, to increase the stiffness of the connection the inclination angle needs to be reduced. Increasing the ductility will result in a loss of stiffness and resistance.

For all geometric changes the failure mechanism remains the same, which is the ultimate strain of the material that is reached..

Finite Element Modelling of Connections 4

For the analysis of the connection a finite element analysis will be performed. This chapter gives a short description of finite element modeling. The finite element program ABAQUS / CAE is used for the analysis of the connection.

4.1 Finite Element Analysis

The finite element method is a powerful tool to solve differential equations. The finite element method allows to calculate complex problems which cannot be solved with analytical calculations. The finite element analysis is an estimation of reality; however, a good model can approximate reality.

Figure 4.1 shows the steps involved for a finite element analysis and indicates that the finite element analysis is an iterative method. The iterations will lead to a more adequate solution. The 3 steps for a finite element analysis are:

Pre-process

The pre-process stage involves all the input of the finite element model. The following steps needs to be defined in the pre-processing stage:

- *Define geometry:* the geometry is created outside ABAQUS with the CAD program rhino/grasshopper and is then important into ABAQUS.
- *Define physical model / material properties*
- *Define the loads*
- *Define the boundary conditions*
- *Create mesh*

Numerical Analysis

In the numerical analysis stage the type of analysis is defined, a linear or non-linear analysis. In this step the matrices of the model are generated and all equations are solved.

Post-processing

The last step in the finite element analysis is the post-processing stage. In this stage the visualisation of the results is created.

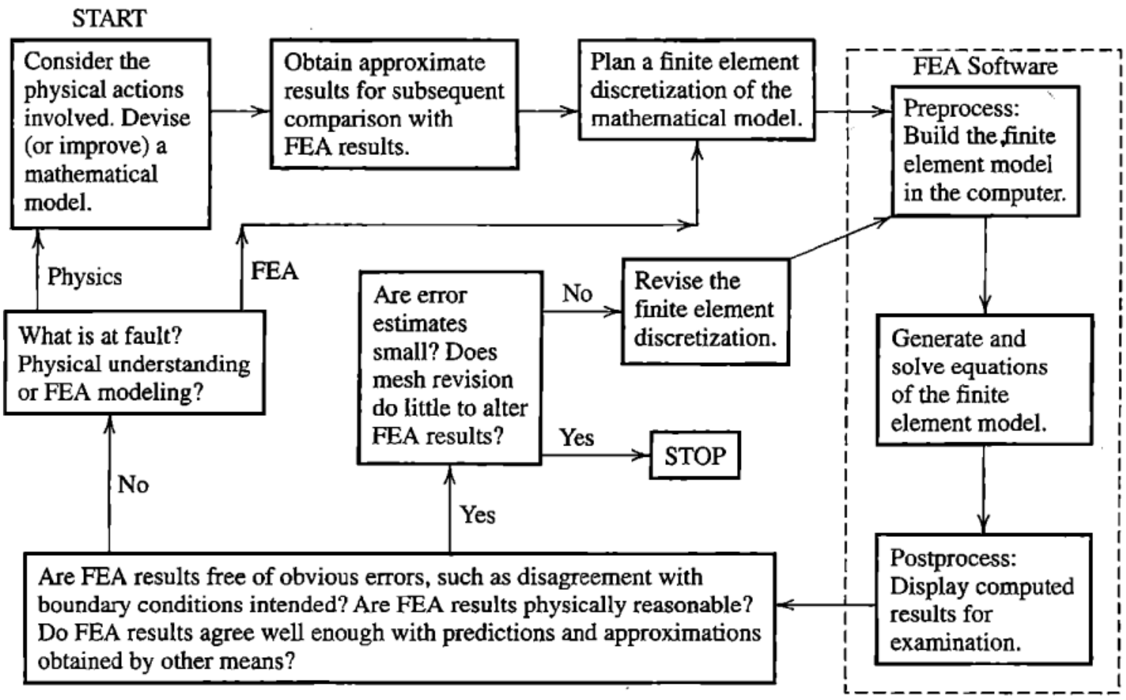

Figure 4.1: Outline finite element analysis [7]

Case Study 5

5.1 Project Description

The principle of the project is that the structure can be expanded or reduced at any time of its life. In order to achieve this principle, a unit is developed with fixed dimensions. These units can be stacked vertically and horizontally to increase the dimensions of the building. Figure 5.1 shows an example of a structural configuration composed of units and a hallway.

Figure 5.1: Example structural configuration

5.1.1 Structural elements

In the initial design in order to construct a unit, 3 elements are used: beams, columns and connection pieces. In figure 5.1 the connection pieces are indicated as the "red" parts. The column splice connection and the beam-to-column connection are both constructed with the plug & play connection. The plug & play connection should ease the assembly and disassembly of the frame and also decrease the time for assembly and disassembly.

All structural elements are made of hot rolled open sections in order to allow the use of normal threaded bolts.

Several changes have been made regarding the initial design. The first is that the column splices are performed with a normal flush endplate connection instead of the plug & play connection. The second is that the "red" connection parts are removed and the plug & play connection is directly attached to the column. These changes are done to reduce the number of connections in the structure.

5.1.2 Non structural elements

With the non structural elements the facade and floors are meant.

These project uses special designed floor elements, which consists of 3 sheets of metal with are separated by a layer of isolation material. The isolation material and metal sheets which are connected by a glued connection. These floor panels are tested by TNO for a floor load of $2.5kN/m^2$ results in a maximum span of $3.9m$ (No reference available, taken from internal available information). The benefit of this floor panels is that the self-weight of the panels is $0.58kN/m^2$. The floors span in 1 direction with a length of $3.6m$. Half of the floor element is placed on top. This is done to reduce the height of a unit. In figure 5.2 the cross section of a panel is shown. There is no direct connection between the floor panels and the beams and do not provide restraints for lateral stability.

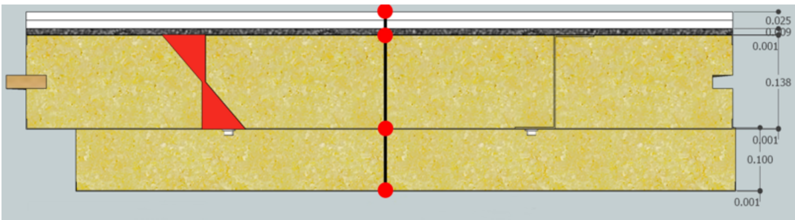

Figure 5.2: Cross-section floor panel

For the facade panels glass elements or an isolated sandwich panel can be used. The panels span in the vertical direction and transfer their loads to the beams.

5.1.3 Dimensions of one unit

The dimensions of the frame are determined taken into account the regulations by the Bouwbesluit 2012[16]

The minimum height according to the Bouwbesluit 2012[16] is 2.6m, from the top of the floor to the bottom of the ceiling. As mentioned earlier a part of the floor elements is on top of the beams, 173mm is the floor height above the beam. For the beams HE sections will be used because of their limited height compared to I sections. The exact size of the beams is yet unknown. For the center-to-center distance of the beams 3.2m is taken, this leaves a height of 427mm to be used for beam height and ceiling (and some possible room for installations).

The building is used for residential purposes and according to the Bouwbesluit 2012 a minimal area required for residential purposes (including bathroom, toilet and cooking area) is $21.46m^2$. Taken into account the minimum sizes the center-to-center distances of the ground floor of a unit will be $6.48m$ x $3.6m$ resulting in an area of $23.33m^2$, the placement of inner walls will result is some loss of area. The side of $6.48m$ is split in two equal sized bays of $3.24m$.

The dimensions are shown in figure 5.3

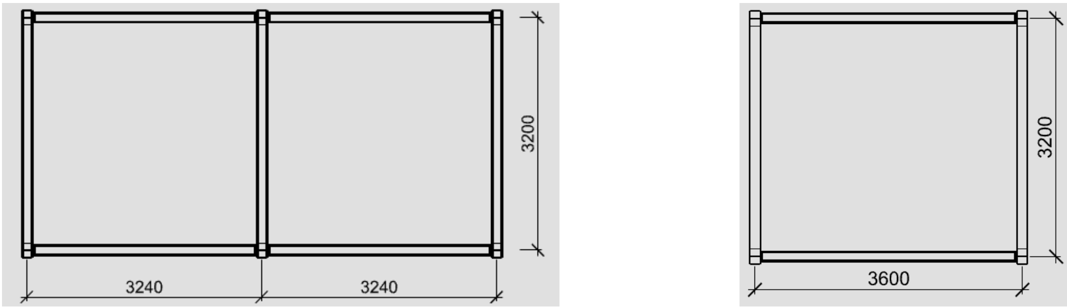

(a) Dimensions front view (b) Dimensions side view

Figure 5.3: Dimensions unit

5.2 Case study

The case study is used to determine the possible forces on the connection. Another reason for the case study is that the width and height of the plug & play connection depend on the size of the beam. A global structural analysis is performed of the case study in order to determine the beam sizes.

The case study is of a building consisting of a total of 60 units. The dimensions of the frame are given below. At each floor one unit is used as staircase.

- Depth: 5 units in depth, total depth 5 x 3.6m (18m)
- Width: 2 units + hallway in width, total width 2 x 6.48m + 1.5m (14.46m)
- Height: 6 units in height, total height 6 x 3.2m (19.2m)

6 Structural Analysis

The global analysis is used to determine the internal forces which would need to be resisted by the connection. The size of the connection is limited by the used sections, the sections are determined in the global analysis.

6.1 Introduction

The structure is evaluated according to EN 1990, EN 1991 and EN 1993. For the structure it is assumed that it is located in the Netherlands and therefore the Dutch national annexes will be used as addition to the Eurocodes. The building will be used as a residential building and according to EN 1990 the building is assigned to CC2. The used material properties of steel are according to EN 1993.

The beams and columns are made of hot-rolled HE sections of class S235. Open sections are chosen in order to allow the use of bolts to lock the connection.

The software of SCIA Engineer version 20.0 is used to perform the global structural analysis and evaluate the internal forces and displacements of the structural frame.

6.2 Loads

The loads in the global analysis can be divided in:

- Permanent loads (G): self weight of the structure and building elements
- Variable loads (Q): loads on floors, roof and facade elements due to different actions.

The loads which are covered for the analysis are shown in table 6.1. One unit at each floor is used as staircase, in order to allow the staircase to be used in any unit a higher variable floor load is used. According to Dutch national annex of EN 1991-1-1 (2019) [17] for not publicly accessible floors a distributed load of $1.75kN/m^2$ has to be used. The staircase and hallway are publicly accessible and according to the national annex a distributed load of $3kN/m^2$ has to be used. The floors are tested for a distributed load of $2.5kN/m^2$. A distributed floor load of $2.5kN/m^2$ will be used instead of $3kN/m^2$ the assumption of larger floor loads on non publicly accessible floors compensates the lower floor load on the publicly accessible floors.

Seismic and fire actions are not taken into consideration in the global analysis.

Tag	**Load case**	**Load**
G1	Self weight steel frame[18]	$0.785\ kN/m^3$
G2	Floor panels + Fermacell cover	$0.84\ kN/m^2$
G3	Finishing/ interior walls	$0.5\ kN/m^2$
G4	Facade	$0.25\ kN/m^2$
Q1	Variable loads Category A stairs [18]	$2.5\ kN/m^2$
Q2	Variable loads Category H roofs (non accessible) [18]	$1.0\ kN/m^2$
Q3	Snow load for flat roofs [19]	$0.56\ kN/m^2$
Q4	Wind load according to EN 1991-1-4 (2020)	see 6.2.1

Table 6.1: Loads

6.2.1 Wind

The building can be placed at any location in the Netherlands, therefore the most unfavourable wind conditions need to be taken into account. The Netherlands is divided into 3 different wind areas. Used for the analysis is rural conditions and wind area 1, coastal area is not considered resulting in a v_b of $29.5m/s$ [20]. The wind pressure at a height of 19.2m is $1.26kN/m^2$

Because the building is symmetric two wind directions need to be taken into account instead of four. Wind direction $0°$ and $90°$ are taken into consideration.

6.3 Load Combinations

The serviceability limit state and the ultimate limit state combinations are analysed.

6.3.1 Serviceability limit state

The serviceability limit state regards the functionality, appearance and comfort of the building. The checks in the global structural analysis, regarding the serviceability limit state, will only involve deformation of the structure. The characteristic load combination is used for the serviceability limit state and the expression is given below.

$$\sum_{j\geq 1} G_{k,j} + Q_{k,1} + \sum_{i>1} \psi_{0,i} Q_{k,i} \tag{6.1}$$

The requirements regarding the displacement in the serviceability limit state are according to the national annex of EN1990[21].

- $u_i = h_i/300$ where h_i is the storey height
- $u = h/500$ where h is the building height
- $w_{max} = l_{rep}/250$ where l_{rep} is the length of the span

Where u are the horizontal displacements and w is the vertical deflection.

6.3.2 Ultimate limit state

The ultimate limit state regards the strength of the building. The expressions below show the load combinations for the analysis in the ultimate limit state. The equations are according to the Dutch national annex of EN 1990[21].

$$1.35G_{k,j,sup} + 0.9G_{k,j,inf} + 1.5\psi_{0,1}Q_{k,1} + 1.5\psi_{0,i}Q_{k,i} \quad (6.2)$$
$$1.2G_{k,j,sup} + 0.9G_{k,j,inf} + 1.5Q_{k,1} + 1.5\psi_{0,i}Q_{k,i} \quad (6.3)$$

The decisive combinations are as follows:

- For the variable load on the floor only one floor is set as decisive and all other floors are implemented with a ψ value. The variable load is placed on the most unfavourable floor, which is the highest floor.
- For the wind load in each direction 4 wind load combinations are checked, positive and negative values for the pressure coefficients and the positive and negative effect of the permanent loads is taken into account.
- Snow is decisive
- Variable load on the roof is decisive

6.3.3 ψ values

The ψ values given in table 6.2 are according to the Dutch national annex of EN 1990 [21].

Load	ψ_0	ψ_1	ψ_2
Category A: residential rooms and spaces	0.4	0.5	0.3
Category H: roofs	0	0	0
Snow load	0	0.2	0
Wind	0	0.2	0

Table 6.2: ψ values

6.4 Global Analysis

For the global analysis the structural behaviour of the joints should be properly modelled. The modelling of steel joints is described in EN 1993-1-8. The structural behaviour of the plug & play connection is unknown, one of the objectives of this thesis is to obtain the structural behaviour of the plug & play connection. The plug & play connection is assumed to be rigid, initially the effect of the column splices is neglected for the design of the frame and the assumption is made that the columns are continuous.

A global elastic analysis is performed as the non-linear behaviour of the plug & play connections is unknown as well. All connections are assumed to be rigid, this assumption results in the maximum moments in the connections. When the real stiffness of the connection is known a global analysis with the real stiffness have to be performed and see whether it still met the requirements of the serviceability limit state and the ultimate limit state. For the verification of the members the possible plastic resistance of the members is taken into account.

In figure 6.1 an 3D image of the frame is given. in figure 6.2 the side and top views of the frame are given, together with the load panels and the direction in which they transmit the load.

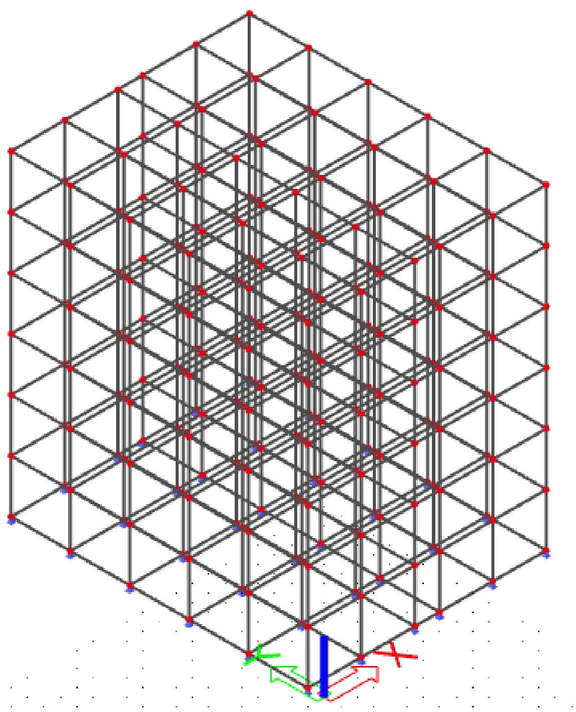

Figure 6.1: Frame model for global analysis

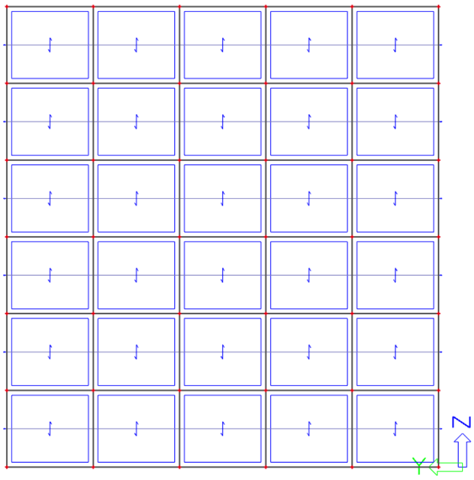

(a) Side view X direction

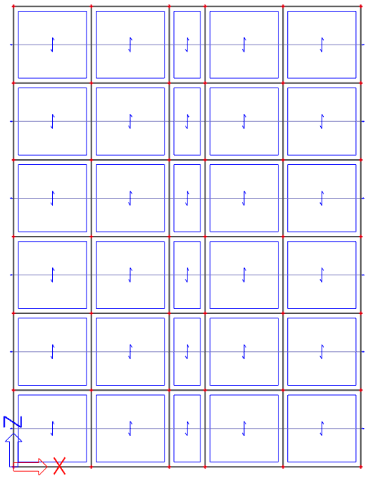

(b) Side view Y direction

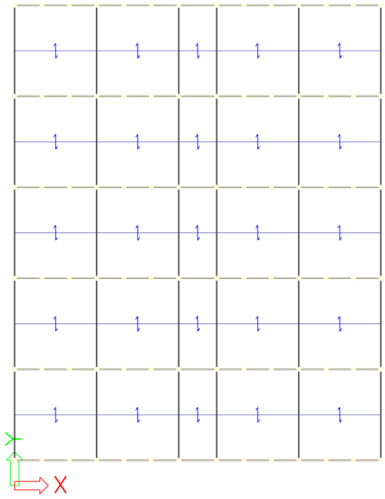

(c) Top view

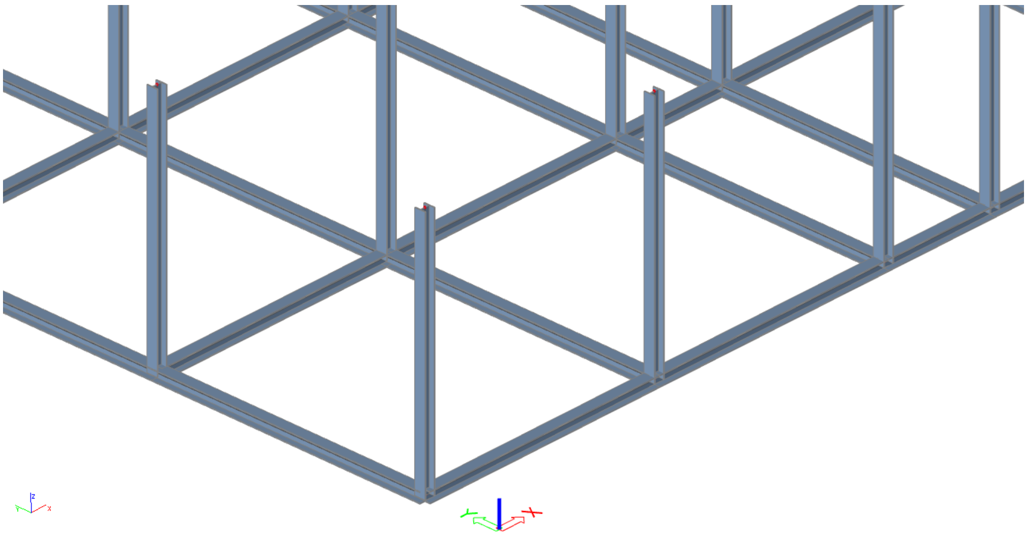

(d) Column orientation

Figure 6.2: Frame configuration

The load transfer in the construction is as follows:

- The facade elements span vertically and are connected to the beams. Half of the load is transferred to the top beam and the other half is transferred to the bottom beam. This load transfer is for both vertical (self weight facade elements) and horizontal loads (wind pressure or suction).
- The floors span in one direction with a span of 3.6m, and are placed partly on top of the beams.
- The roofs span in the same direction as the floors, in the analysis is assumed that for both roof and floors the same panels are used.
- The local Z direction of the sections is in the global X direction.
- The column base connections are assumed as hinged connections, so the column bases do not carry bending moments.

The first structural analysis is performed for a frame consisting of HEB140 sections for both beams and columns and all connections are assumed rigid. HEB sections for both columns and beams are chosen because up to HEB300 sections the width and height of the sections are the same, this means that the same connection can be used for the minor and major axis. The connections are assumed rigid for both in-plane and out-of-plane bending, this provides the stability of the frame without using a bracing system. EC 1993-1-1 (2016) equation (5.1) [9] provides a requirement to see whether a second order analysis has to be performed. Equation 6.4 is the equation according to the EC. SCIA Engineer can calculated the α_{cr} values for each load combination. For each load combination the first 10 critical load factors are calculated, as it is possible that buckling modes other than the first mode can occur. For some load combinations the values of α_{cr} are below 5, therefor a second order analysis will be performed. The lowest α_{cr} value is 5.89 for the loadcase where the variable load at the top floor is decisive.

$$\alpha_{cr} = \frac{F_{cr}}{F_{Ed}} \geq 10 \tag{6.4}$$

SCIA provides a flowchart on the different paths for steel design check, the used path for second order analysis is shown in figure 6.3. The accuracy of the paths is increasing were the left path is the least accurate and the right path is the most accurate. However the lower paths will result in faster calculations. The chosen path takes into account both global and local imperfections, the EC 1993-1-1 (2016) 5.2.2 (7a) states that by taken into account global and local imperfections in the frame analysis no individual in plane member stability checks are required. At the end only stability out of plane need to be checked.

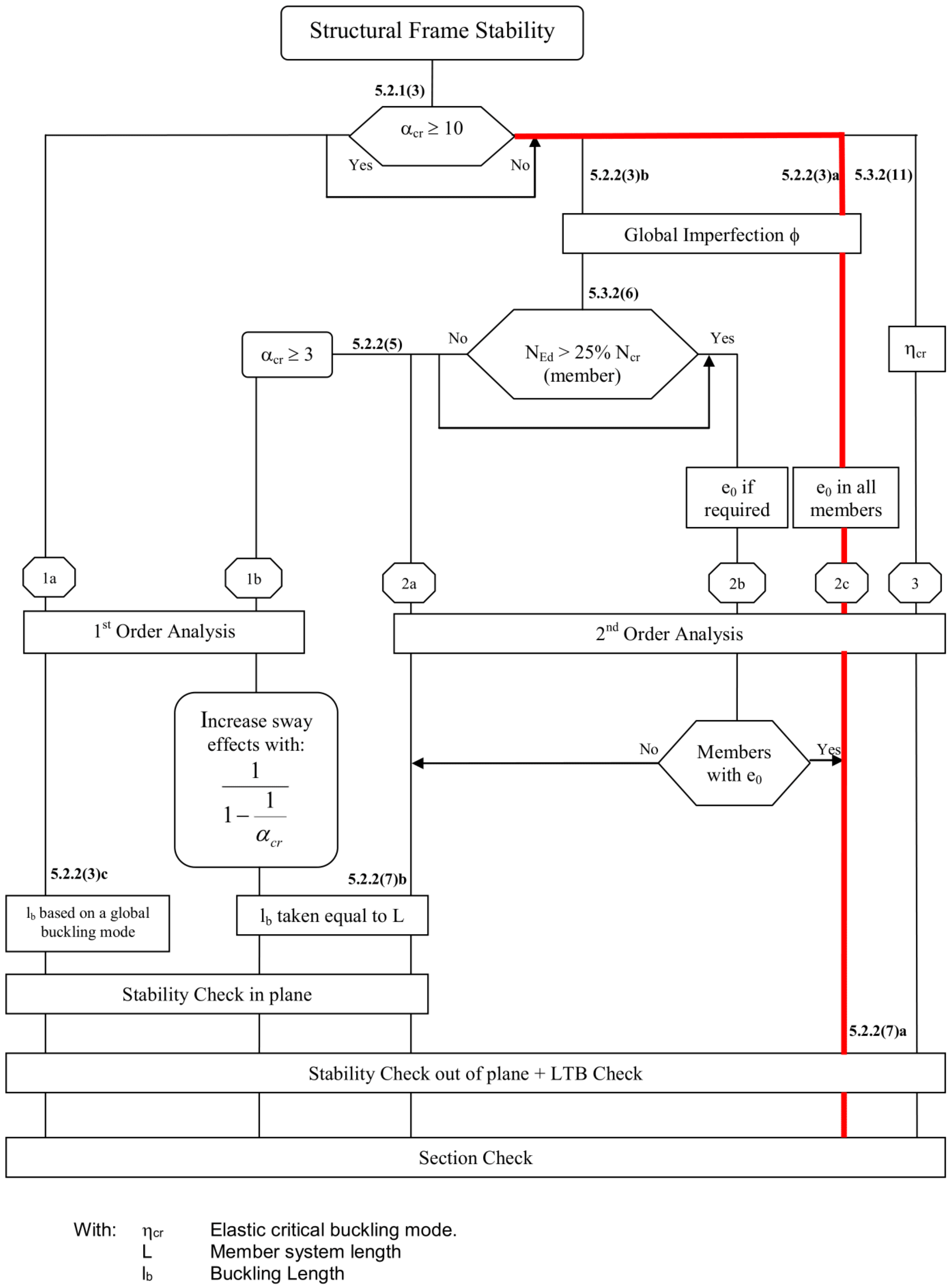

Figure 6.3: Flowchart for steel design [8]

Global Imperfections

The global imperfections are taken into account by using sway imperfection defined by the EC 1993-1-1 (2016). In figure 6.4 is shown how the sway imperfection is taken into account.

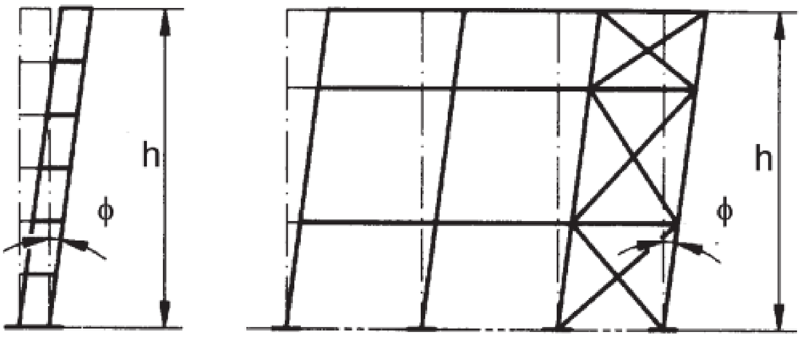

Figure 6.4: Sway imperfections [9]

The value for the inclination of the is calculated with the following formula:

$$\phi = \phi_0 \; \alpha_h \; \alpha_m \tag{6.5}$$

In which:

$$\phi_0 = 1/200$$
$$\alpha_h = \frac{2}{\sqrt{h}} \text{ but } \frac{2}{3} \leq \alpha_h \leq 1$$
$$\alpha_m = \sqrt{0.5(1 + \frac{1}{m})}$$

where m is the number of columns in a row which caries a normal force not lower that 50% of the average of the vertical force in the considered vertical plane

The height of the building is $19.2m$ therefor α_h is equal to $\frac{2}{3}$. The value of m is set to 4 in x direction and to 5 in y direction which takes into account the lowered compressive forces as consequence of the load combinations in which wind is decisive.

Local Imperfections

The global imperfections take into account sway of the whole frame. The local imperfections take into account the local member imperfections. The local member imperfections are taken into account as shown in figure 6.5. The value of e_0 is depended on the type of analysis (elastic or plastic) and the buckling curve of the members. Table 6.3 gives the values for e_0/L where L is the length of the element. This initial imperfections is only used for the columns as the beams are primarily subjected to bending.

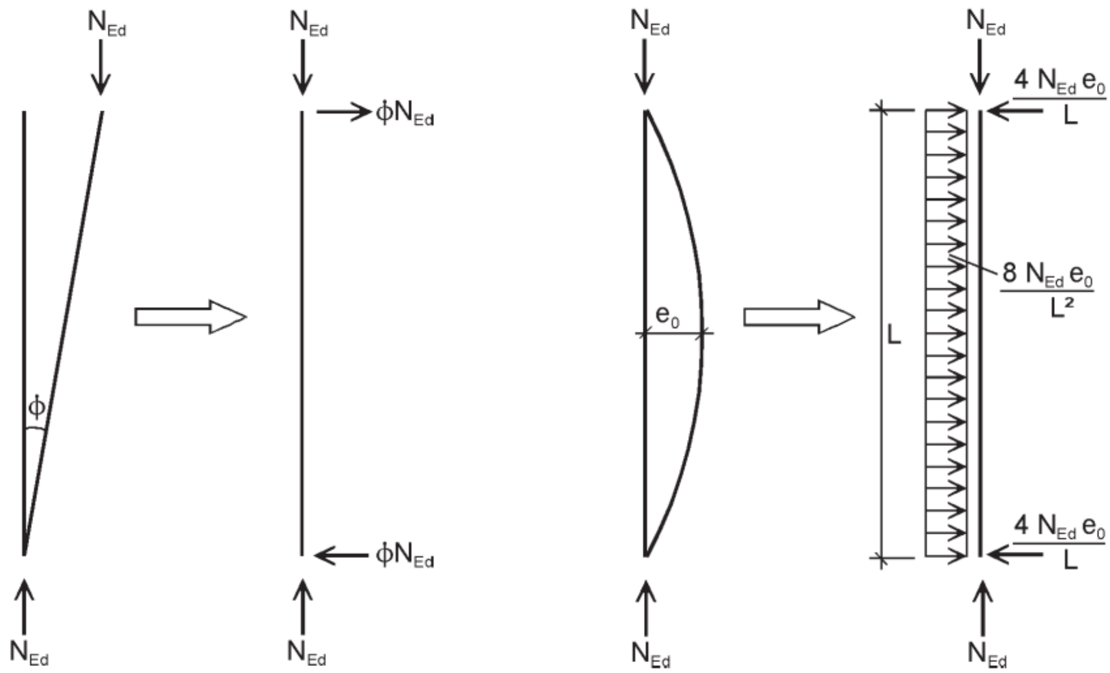

Figure 6.5: Initial imperfections [9]

Table 6.3: Member bow imperfections

Buckling Curve	Elastic e_0/L
a_0	1/350
a	1/300
b	1/250
c	1/200
d	1/150

6.4.1 Results initial frame

In this section the results of the initial frame will be discussed.

In figure (fig 6.6) the normal force distribution in case of wind blowing in X direction with a partial factor of 0.9 for the contribution of the self-weight is shown. As can be seen in the figure tension forces (blue) will develop in the in the structure due to the low self-weight of the structure. These tension forces occur in the corner columns and the tension forces and edge columns at bottom level, the foundation need to be able to carry these tension forces. On the top level tension forces occur as well, the splice connection need to take these tension forces.
The distribution of the moments when the wind is blowing in X direction is shown in figure 6.7. Wind from this direction causes bending around the major axis of the columns, the bending moments around the minor axis are not low.

When the wind is blowing in Y direction moments around the minor axis are significant and the bending moments around the major axis are low, an indication of the moment distributions is shown in figure 6.8.

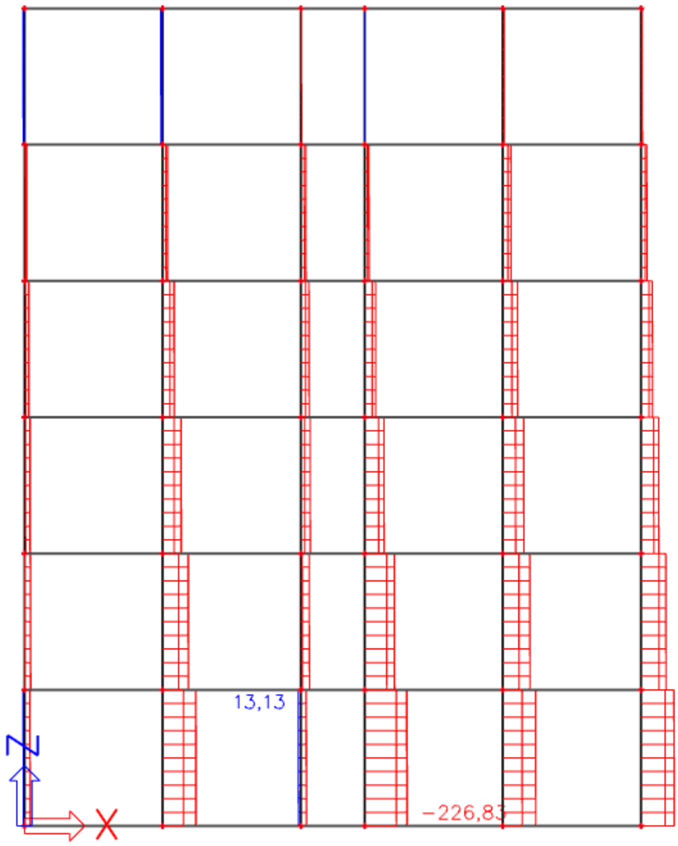

Figure 6.6: Internal normal forces for wind in X direction and permanent load partial factor is 0.9

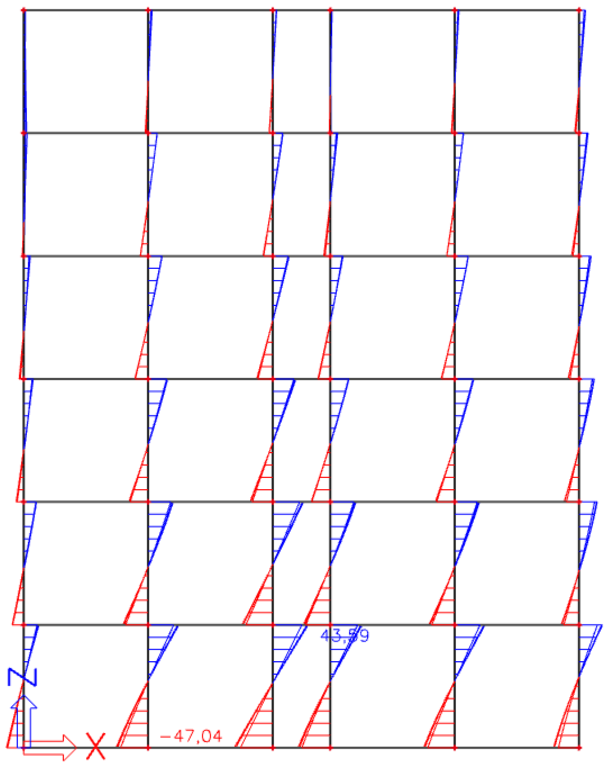

(a) Column major axis bending

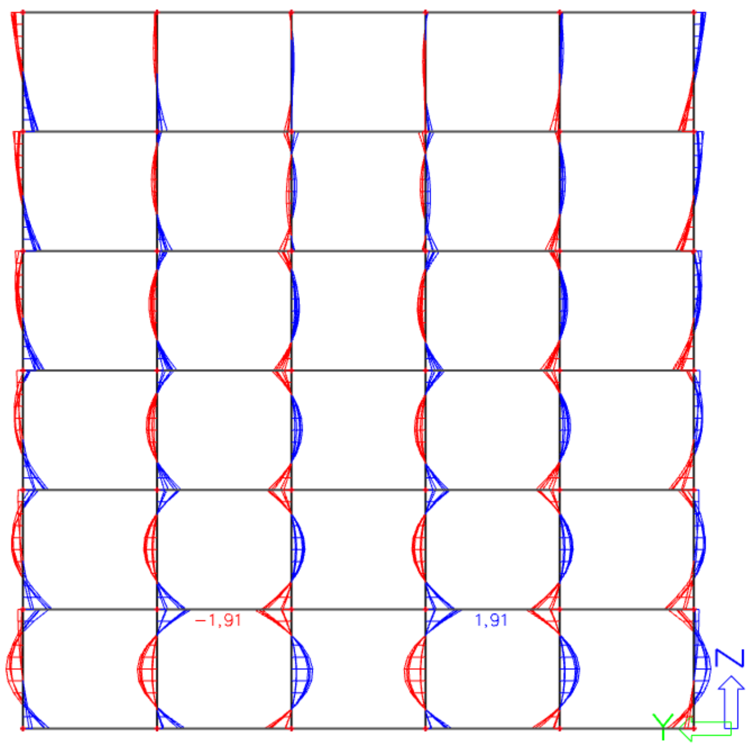

(b) Column minor axis bending

Figure 6.7: Wind in positive X direction as fundamental load

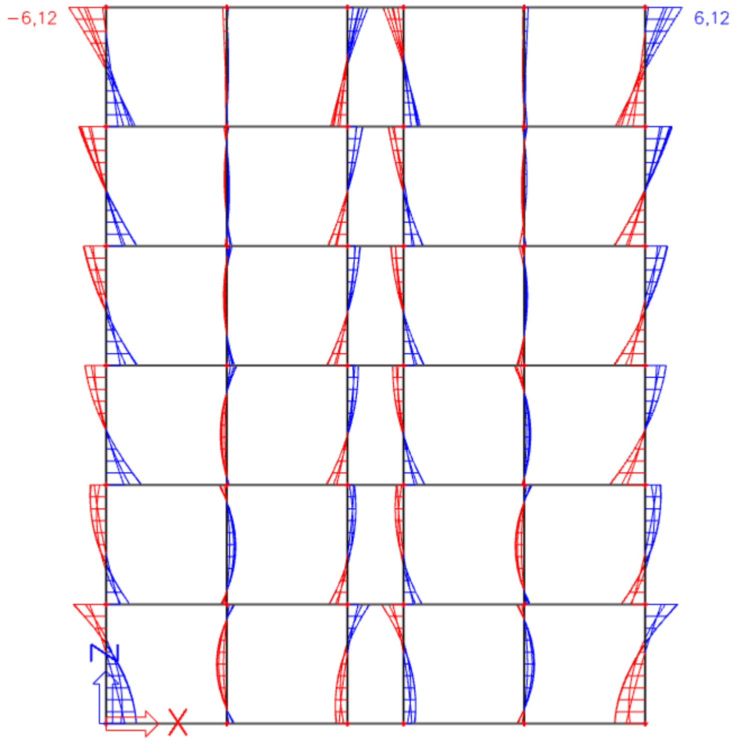

(a) Column major axis bending

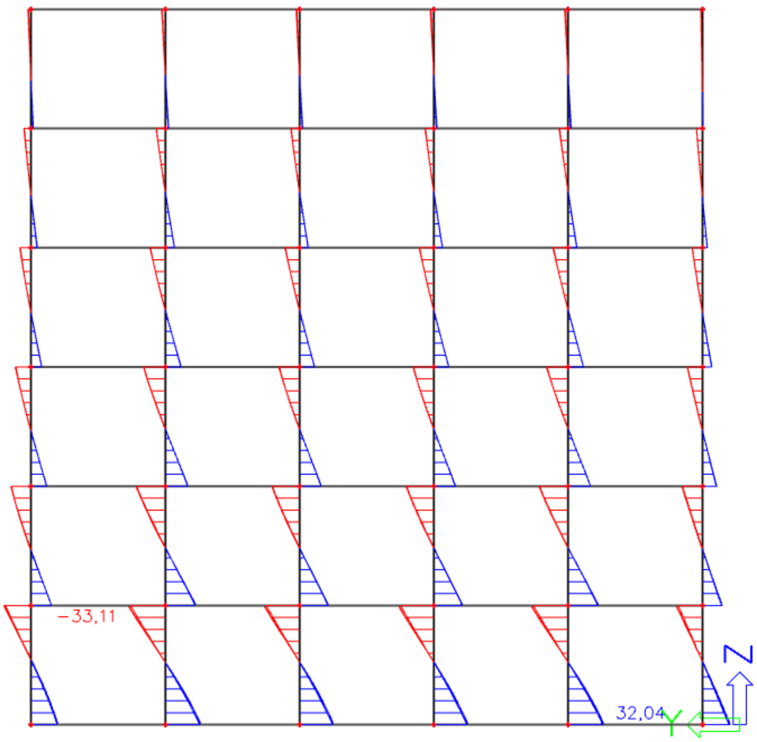

(b) Column minor axis bending

Figure 6.8: Wind in positive Y direction as fundamental load

As mentioned earlier a second order analysis is performed to check the ULS conditions. The SLS conditions are checked with a first order analysis where all partial safety factors are equal to 1.

The internal forces are defined according to the local coordinate system of the sections. The local coordinate system for the sections is shown in figure 6.9

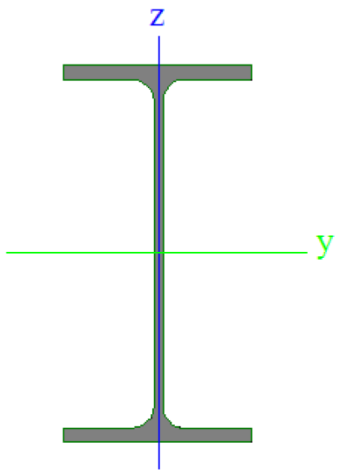

Figure 6.9: Local coordinate system scia [8]

The bottom columns are subjected to the largest internal forces and are decisive regarding the ULS requirements. The range of the internal forces in the bottom columns within the considered load cases is:

- Normal Force $-254kN\ (compression) < N < 13kN\ (tension)$
- Column Major Axis Bending $-47kNm < M_y < 44kNm$
- Column Minor Axis Bending $-33kNm < M_z < 33kNm$

The wind load causes large bending moments in the structure. When the wind is blowing in X direction the bending moments around the major axis are large and the bending moments around the minor axis are low. The opposite applies when the wind is blowing in Y direction, then the bending moments around the minor axis are large and the bending moments around the major axis are low. These moments are below the plastic moment capacity of the section, $M_{y,Pl,Rd}$ = 86.98 kNm and $M_{z,Pl,Rd}$ = 42.6 kNm, without reduction for axial force.

The internal forces at the beam ends are the forces which are the relevant for the plug & play connections. The second order effect is included in the analysis therefor no individual member stability checks need to be performed as the effects are included in the internal forces. The columns are checked for axial force and bending.

In figures 6.10 and 6.11 the bending moments around the major axis of the beams is given. For vertical loads only the connections should only withstand hogging bending moments. The horizontal wind loads introduce sagging bending moments in the connection. The horizontal loads also cause bending moments around the minor axis of the beams, which is shown in figure 6.14 for wind blowing in Y direction.

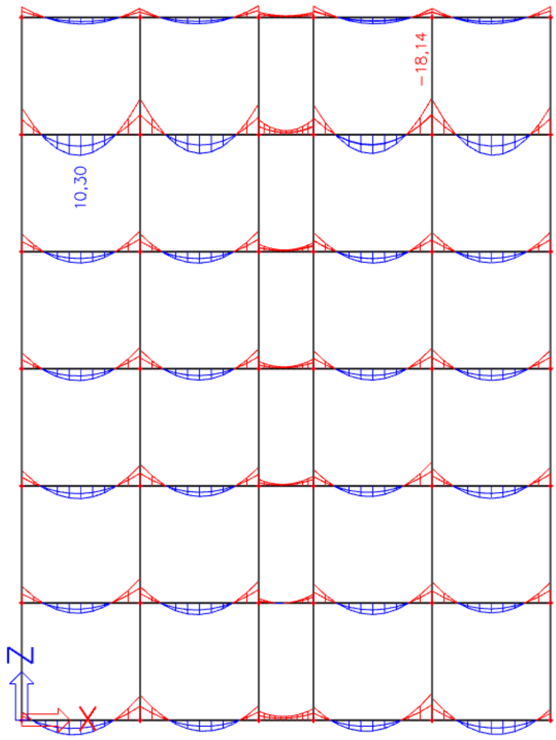

Figure 6.10: Beam major axis bending moments due to vertical load

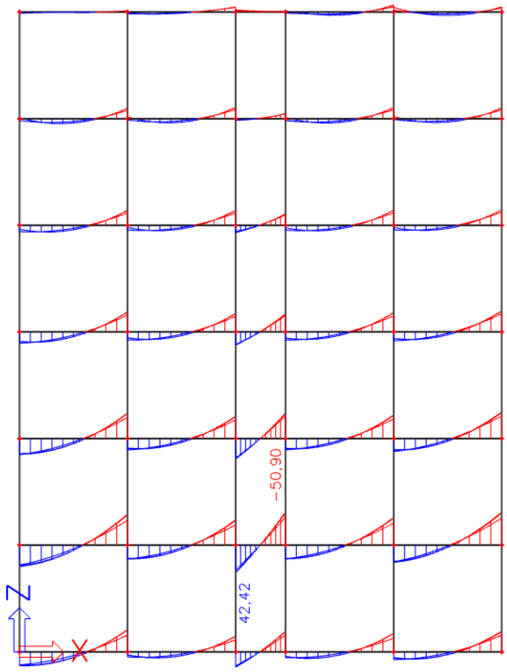

Figure 6.11: Beam major axis bending moments due to wind load in X direction (top view)

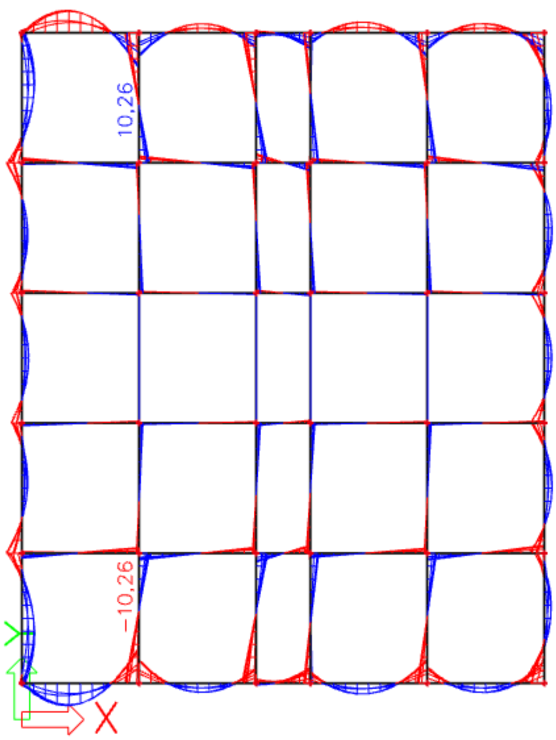

Figure 6.12: Beam minor axis bending moments due to wind load in X direction

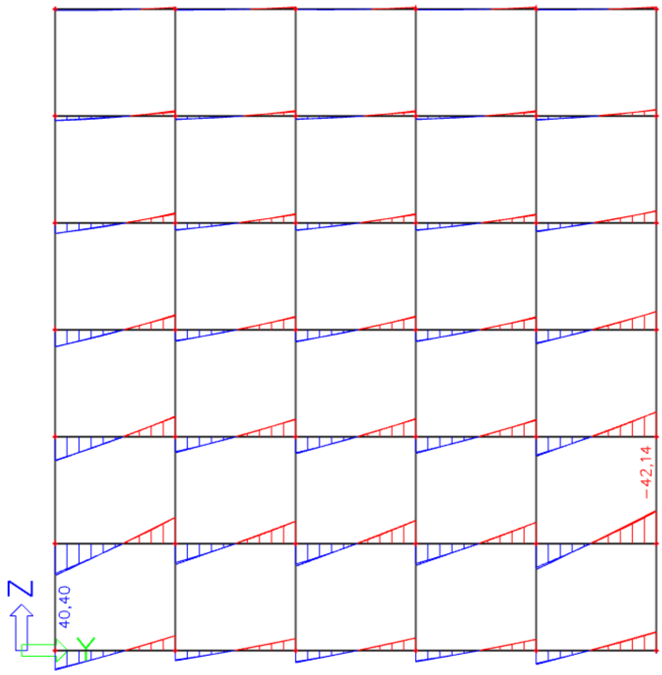

Figure 6.13: Beam major axis bending moments due to wind load in Y direction

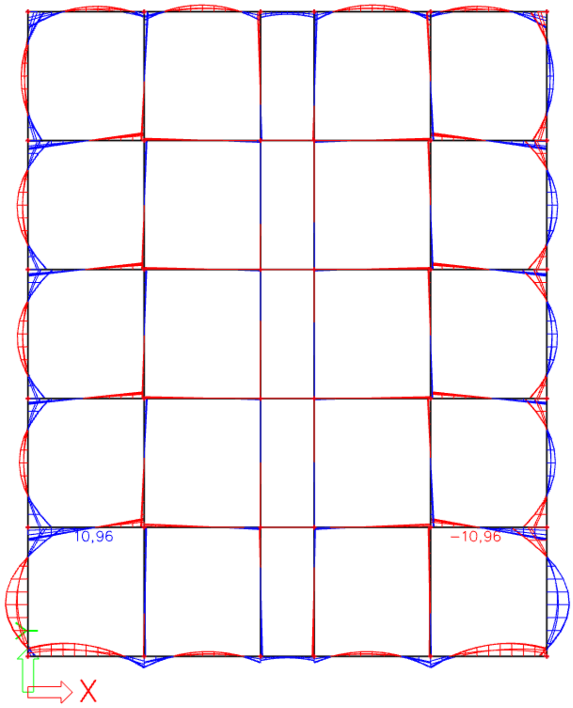

Figure 6.14: Beam minor axis bending moments due to wind load in Y direction (top view)

The internal forces in the beams at beam ends are:

- Beam Major Axis Bending $-50kNm\ (hogging) < M_y < 42kNm\ (sagging)$
- Beam Minor Axis Bending $-10kNm < M_z < 10kNm$
- Shear Force Vertical $-70kN\ (upwards) < V_z < 33kN\ (downwards)$
- Shear Force Horizontal $-17kN < V_y < 17kN$
- Maximum Tension Force $28kN$

Because a second order analysis is performed which includes global and local imperfections, it is not required to perform a local member stability check, besides possible lateral torsional buckling. The resistance check for the sections is done for bi-axial bending with the following formula:

$$\left[\frac{M_{y,Ed}}{M_{N,y,Rd}}\right]^{\alpha} + \left[\frac{M_{z,Ed}}{M_{N,z,Rd}}\right]^{\beta} \leq 1 \tag{6.6}$$

In which:

$$\begin{aligned}
\alpha &= 2 \\
\beta &= 5n \text{ but } \beta \geq 1 \\
n &= N_{Ed}/N_{pl,Rd} \\
M_{N,y,Rd} &= \text{reduced bending moment resistance due to axial load} \\
M_{N,z,Rd} &= \text{reduced bending moment resistance due to axial load}
\end{aligned}$$

The check of equation 6.6 results in a maximum unity check of 0.78 (detailed calculation in appendix A)

Besides this check the elements should be checked for lateral torsional buckling as the floor panels do not provide stability regarding lateral torsional buckling. A check for lateral torsional buckling is provided in Appendix B, there is no risk for lateral torsional buckling in the structure.

So the frame fulfill the ULS conditions and the SLS conditions should be checked. Figure 6.15 shows the displacements due to wind in X and Y direction. According to the EC the maximum allowed displacement at the top is $19.2m/500 = 38.4mm$. The displacement at the top is 79.2mm when the wind blows in the X direction and the displacement at the top is 115.4mm when the wind blows in the Y direction. The maximum vertical displacement of the beams is 4.8mm were the maximum allowed is $3.24m/250 = 12.96mm$.

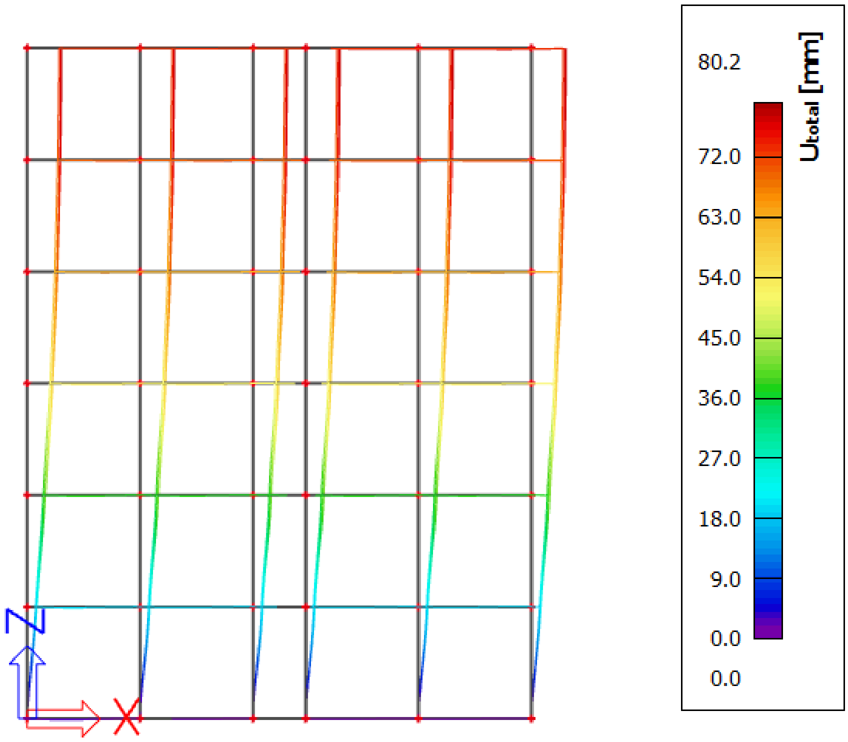

(a) Wind in X direction

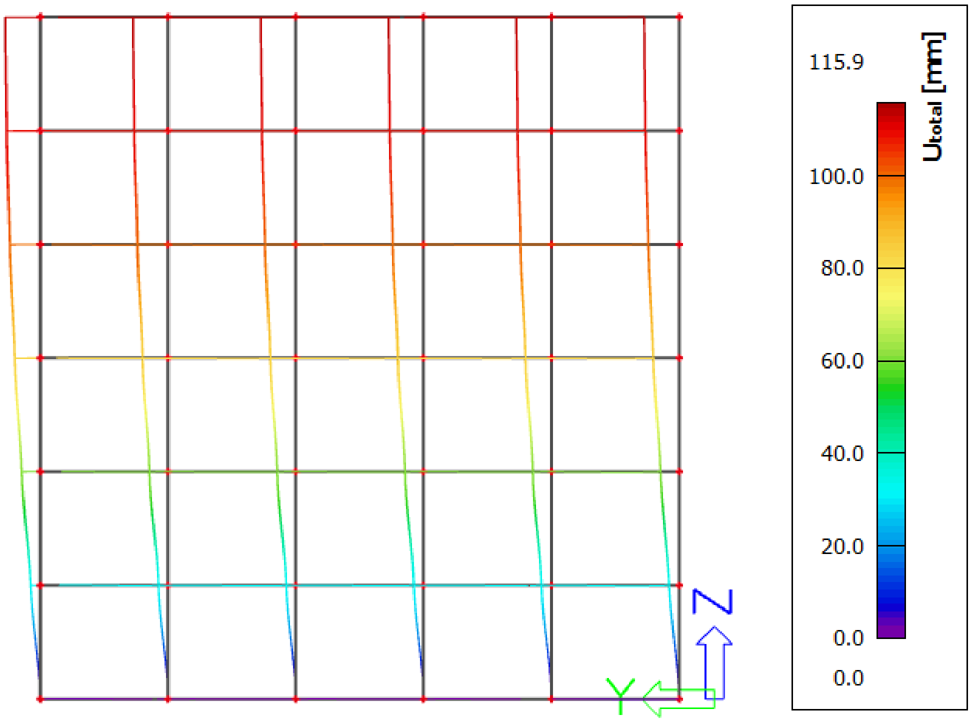

(b) Wind in Y direction

Figure 6.15: Horizontal displacements due to wind load

The displacements are not within the SLS limits. Their are two options two decrease the horizontal displacements: the first is to increase the sections and increase the stiffness of the frame or by applying a bracing system in the frame. For a braced frame it is usual to use hinged connections as the stability does not need to be provided by rigid connections.

The configuration of the frame with a bracing system is not considered because of the following reasons:

- The plug & play connection would be an expensive solution for a hinged connection.
- A bracing system would limit the design freedom of the frame, for example it is not possible to have large windows in walls where a bracing system is present.
- One of the principles to use the plug & play connection is that it would decrease installation time, installing a bracing system in each unit would increase the installation time.

So in order to reduce the horizontal displacements of the frame it is chosen to increase the section size.

6.4.2 Results modified frame

In order to decrease the horizontal displacements of the frame the columns and beams are increased to sections of HEB200. Although increasing the beam sections that much is not necessary to reduce the horizontal displacements of the frame it is chosen to keep the same section for both beam and columns. This is done because the stability of the unbraced frame relies on the stiffness and strength of the connections. Based on the results of the snap-fit connection in chapter 3 it is expected that an increase in the dimensions of the connection would also increase the stiffness and resistance of the connection. Therefore HEB200 will be used for the beams as well. Another reason to keep the beams and columns the same dimension is that the connection is also applied in the minor direction of the column. The connection is attached to the flanges and not to the web, a HEB section has the same width and height so the plug & play connection can be attached to both the major and minor column axis.

Similar to the initial design a second order analysis is performed, this is done to have the same type of analysis and be able to compare the results.

An example of a unit in the modified frame is shown in figure 6.16.

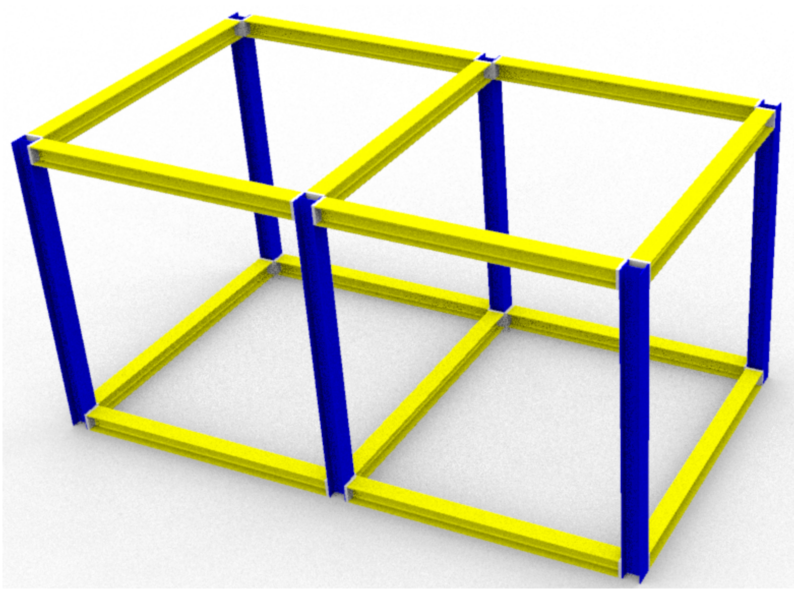

Figure 6.16: Modified frame

The internal forces in the columns for the design with HEB200 sections is given below:

- Normal Force $-268kN(compression) < N < 10kN(tension)$
- Column Major Axis Bending $-44kNm < M_y < 40kNm$
- Column Minor Axis Bending $-29kNm < M_z < 29kNm$

The internal forces have changed a little compared to the internal forces of the initial design, a large difference was not expected as well as the forces remained the same except from the self-weight of the structure. The initial design resulted in an unity check of 0.78 an increased section would result in an even lower unity check, with the same steel quality. Therefor the steel quality is changed from S355 to S235. The maximum U.C. is 0.40, the same check as given in equation 6.6 is done.

The internal forces at the beam ends become:

- Beam Major Axis Bending $-49kNm\ (hogging) < M_y < 36kNm\ (sagging)$
- Beam Minor Axis Bending $-11kNm < M_z < 11kNm$
- Shear Force Vertical $-62kN\ (upwards) < V_z < 33kN\ (downwards)$
- Shear Force Horizontal $-17kN < V_y < 17kN$
- Maximum Tension Force $28kN$

The increase section results in an increase of M_{cr} and a larger $M_{b,Rd}$, the bending moment on the beams is the same therefore the risk of lateral torsional buckling is lower compared to the initial design. As in the initial design there was no risk of lateral torsional buckling the new situation with increased sections will also fulfill the stability condition regarding lateral stability.

The horizontal displacements of the frame are shown in figure 6.17. The maximum top displacements are now: 22.5mm when the wind is in X direction and 31.9mm when the wind is in Y direction. The maximum allowed displacement is 38.4mm, so the displacements are now within the SLS limits for the deflection. The deflection for the X direction has been reduced with 71.5% and for the Y direction with 72.5%.

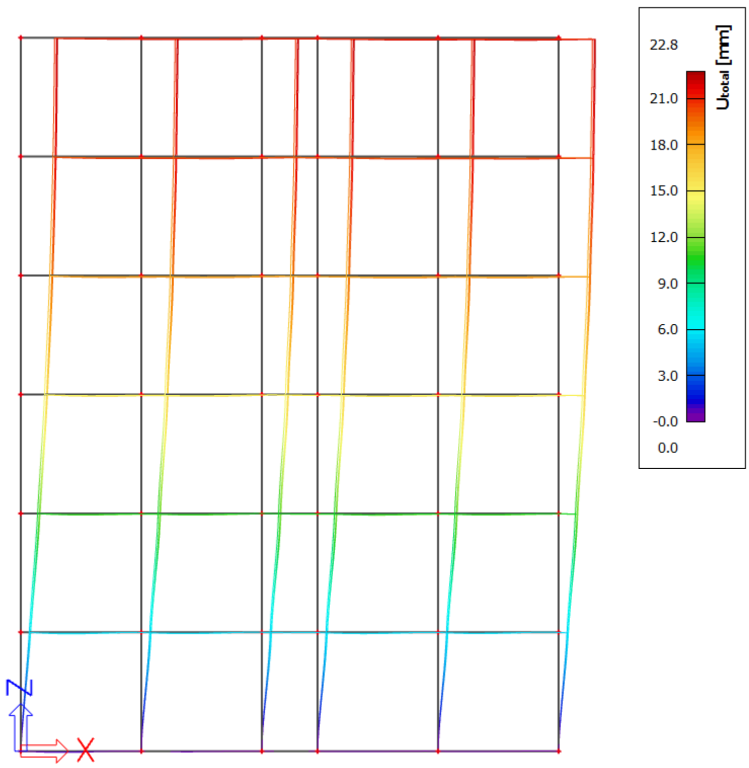

(a) Wind in X direction

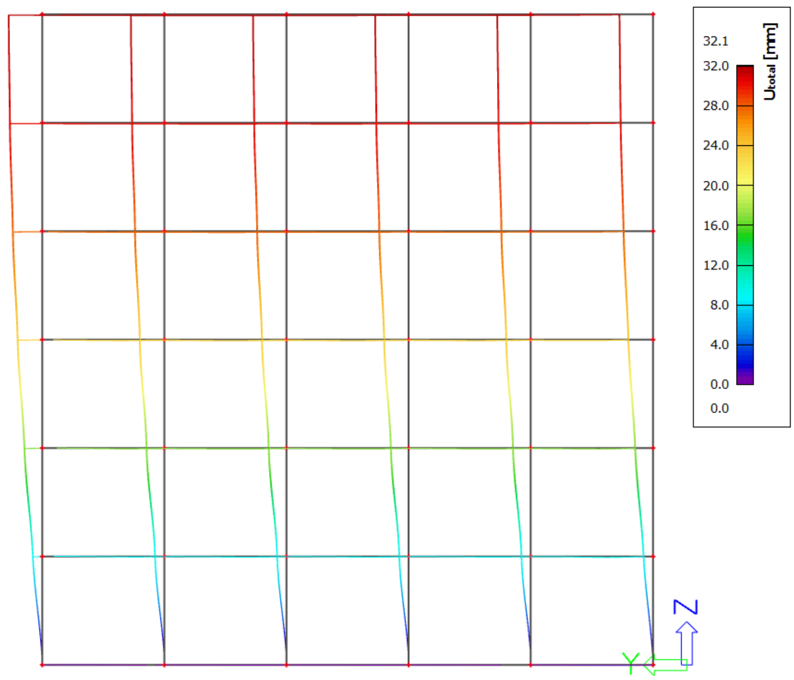

(b) Wind in Y direction

Figure 6.17: Horizontal displacements

Including Column Splices and plug & play Connection

In reality the columns are not continuous but are connected with columns splices. The locations of the column splices is shown in figure 6.18 with circles.

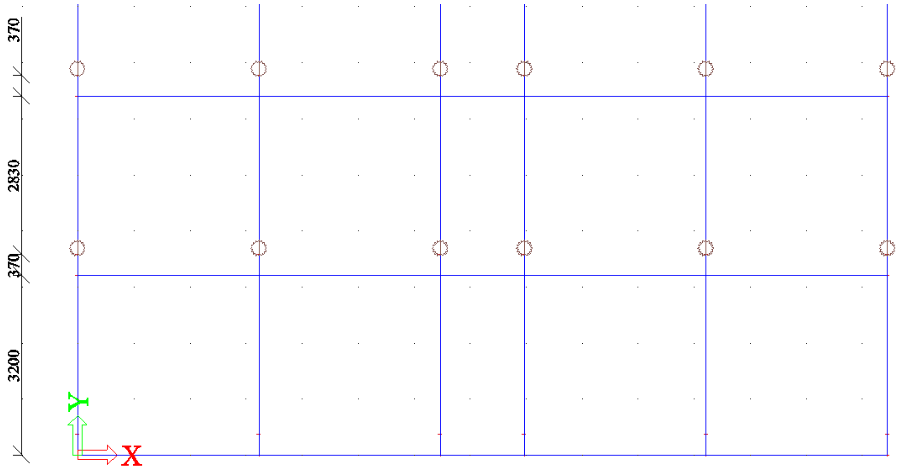

Figure 6.18: Location column splices

The columns on the ground floor span the whole storey height. The columns on the higher floors are connected with a splice which is located 100mm above the top of the floor, and 370mm above the centroidal axis of the beams. The ground floor columns has a height of 3570mm because there is no splice connection on the ground floor, and all the other columns have a height of 3200mm. An extended plate is not possible as it would cause problems with hoisting the beams into place. Therefore a flush endplate is used as column splices. The stiffness of the connection should be checked whether it can be regarded as rigid otherwise the joint stiffness should be taken into account in the analysis. In figure 6.19 a sketch of the column splice connection is shown.

Because the frame is subjected to both major and minor axis bending, the stiffness around the major and the minor axis is needed. In appendix C the calculation of both the resistance and stiffness of the column splice is given for both the major and minor axis.

The stiffness of the plug & play connection should be checked whether it meets the rigid classification boundary. If the beam-to-column joint cannot be classified as rigid, then the stiffness of the joint should be taken into account in the frame analysis.

The rigid classification boundary for the column is $25\frac{EI}{L_c}$ for a HEB200 of length 3200 the major axis stiffness boundary is 93.45 MNm/rad and for the minor axis the stiffness boundary is 32.86 MNm/rad. The initial stiffness of the joint is 23.18 MNm/rad for the major axis and 7.33 MNm/rad for the minor axis. The stiffness of the column is for the major axis 3.738 MNm/rad and for the minor axis 1.31 MNm/rad. The stiffness of the joints is above half the beam stiffness, so the joints are classified as semi-rigid.
A frame with the actual stiffness for both the columns splices and beam-to-column connections will be checked if it met the SLS requirements regarding

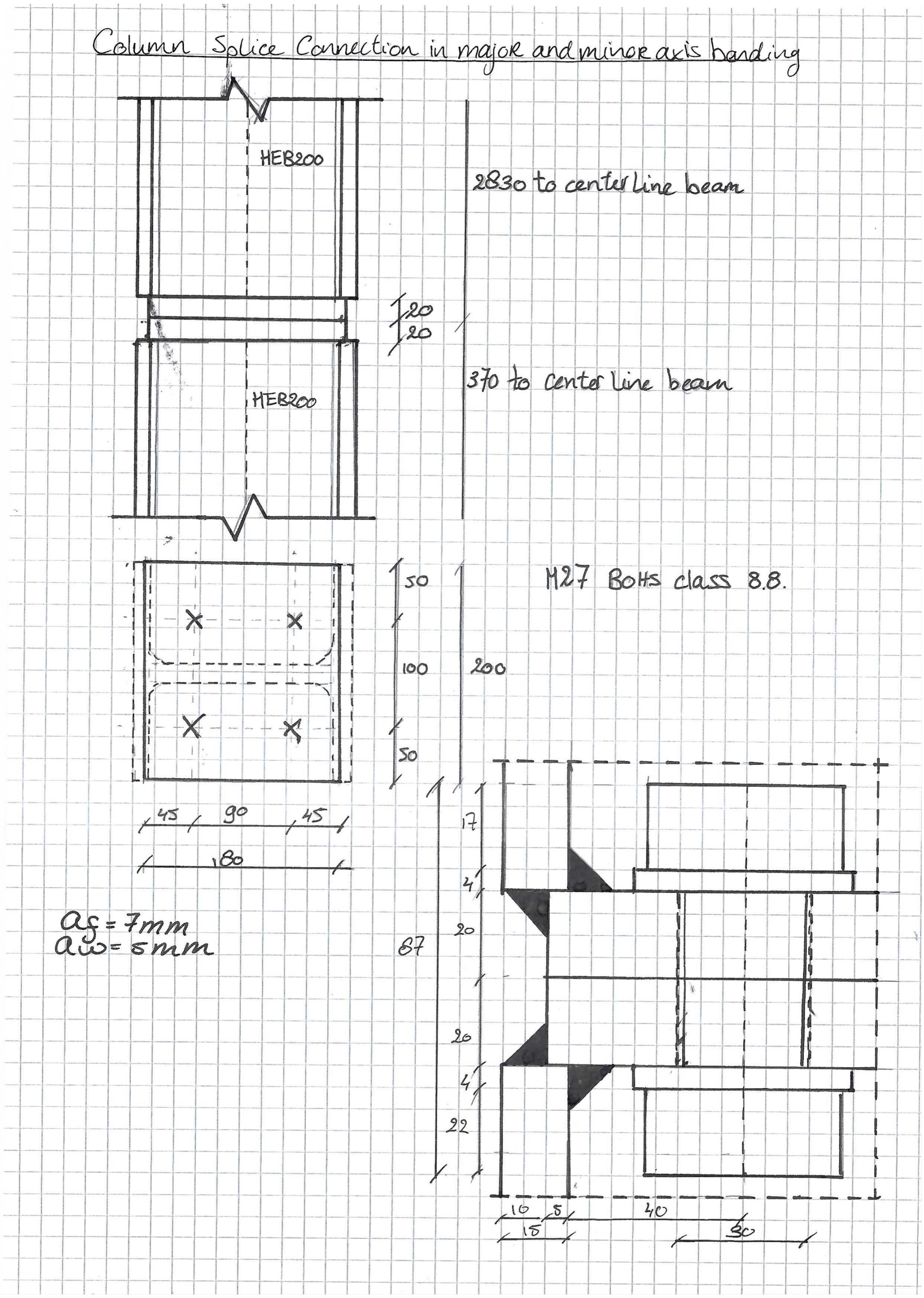

Figure 6.19: Column splice

the displacements. If the moments will change significantly compared with the model in which all connections are rigid, then the ULS model will be also recalculated with the actual stiffness of the joints to see whether all sections do meet the strength requirement. The actual stiffness of the plug & play connections is derived from the $M-\phi$ curves. The derivation of the $M-\phi$ curves is given in chapter 7. For each joint the stiffness should be derived based on the acting moment on the joint. The maximum bending moments on the beams in the SLS are given in appendix D.

The maximum possible moments in the column are $28.57kNm$ around the major axis and $18.20kNm$ around the minor axis (see appendix D), for respectively wind in X direction and wind in Y direction. This is at the bottom row columns, these columns do not contain a splice. In the column splices the moments would be lower. If the moments are lower than $\frac{2}{3}M_{j,Rd}$, then the initial stiffness of the joint can be used. The elastic moments are $\frac{2}{3}74.09kNm = 49.4kNm$ for the major axis and and $\frac{2}{3}36.66kNm = 24.44kNm$. The maximum moments are already below the elastic moments, so for the column splices the initial stiffness can be used for both the major and minor axis.

The largest bending moments and displacement in the frame are caused by the wind loads. The frame is checked with the actual joint stiffness for wind in X direction and wind in Y direction. The maximum possible major axis bending moment for wind in X direction is $30.98kNm$, for this moment the initial stiffness is taken although mentioned in chapter 7 that the maximum elastic moment capacity is $30kNm$. The $M - \phi$ curve for beam major axis downwards displacement shows that $30.98kNm$ is close to the elastic stiffness, so the difference in stiffness would be small. For all other cases the bending moments for beam major and minor axis bending for hogging, sagging and out-of-plane bending moments are in the elastic range of the joint, so for all joints the stiffness is equal to the initial stiffness.

The displacement of the frame with taking into account the joint stiffness is shown in figure 6.20. The maximum displacement for wind in X direction is 37.6 mm, which is an increase of 65% compared with the frame with all rigid joints. The maximum displacement for wind in Y direction is 56.0 mm, which is an increase of 74.5% compared with the frame with all rigid joints. The maximum allowed displacement is 38.4 mm, so the frame in which the joint stiffness is taken into account will not meet the SLS requirements, for wind in the Y direction. For wind in the X direction the frame still fulfill the SLS requirements. The new internal forces are shown in appendix D. The bending moments around the major and minor axis are reduced. The forces in the columns are increased but are still below the elastic moment capacity of the joint. So the initial stiffness can still be used for the column splices. For the beam-to-column joints the bending moments are still within the elastic moment capacity as well, so the initial stiffness can still be used and no new iteration is needed. The forces on the columns has changed but no new check of the members is done as already the SLS requirements are not met.

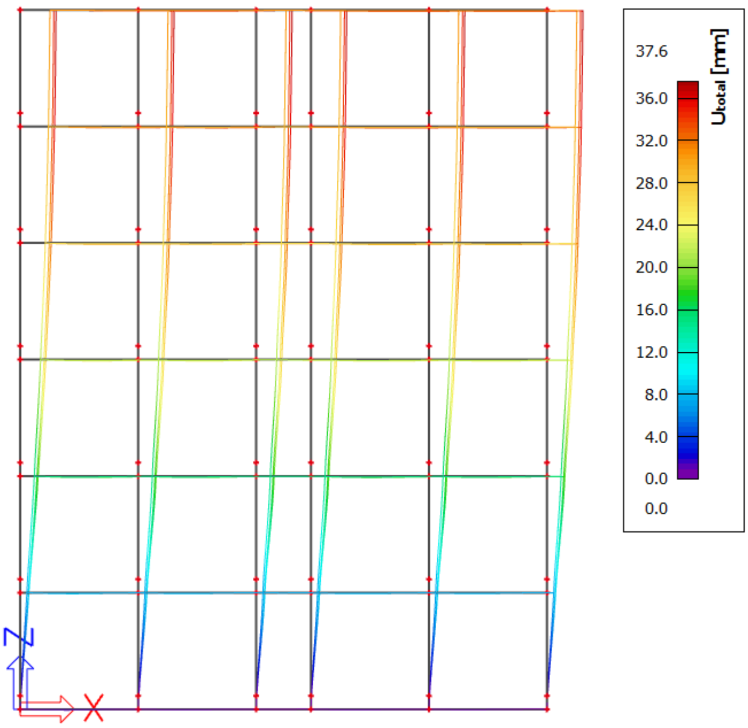

(a) Wind in X direction

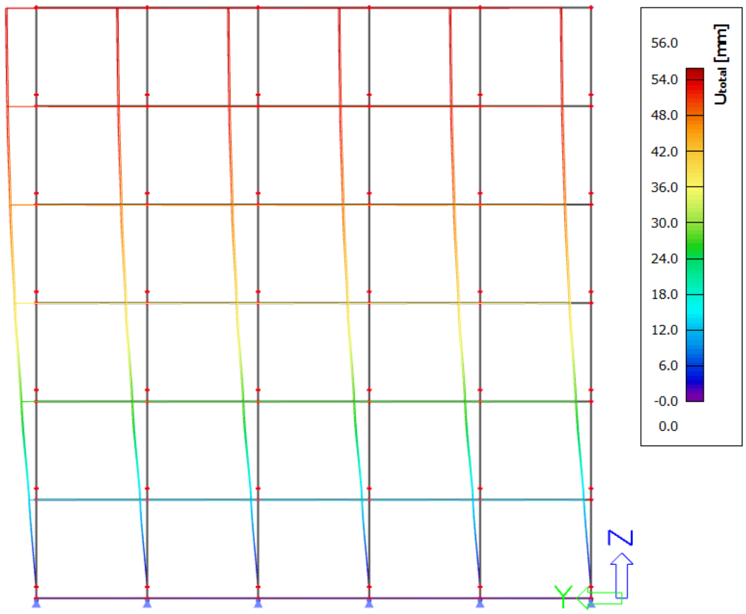

(b) Wind in Y direction

Figure 6.20: Horizontal displacements

6.5 Conclusion

The research questions for this chapter are:

- What are the design considerations made in the global analysis with regard to the design of the plug & Play connection?
- What forces need to be transmitted by the plug & play connection?
- What is the consequence of the assumptions made for the joint stiffness?

The initial frame is made of all HEB140 sections of class S355 in which all joints are assumed to be rigid. An stability check to determine the critical load factor shows that a second order analysis needs to be performed on the frame. The frame is checked with second order effects and the results show that the frame has sufficient strength. However, the stiffness of the frame is too low, with as a consequence that the SLS requirements are not met.

In order to reduce the lateral displacements the sections of both the beams and columns are increased to a HEB200 section. The same section for beam and column is chosen as the width and height of the beams and columns are equal and therefor the plug & play connection can be designed with equal dimensions as the sections. The HEB sections make it possible that the same connection can be used for both the major and minor axis of the column. The initial design already satisfied the ULS requirements, an increased section would result in a reduced unity check. Therefor the steel class of the sections is changed from S355 to S235. The frame is checked and both the ULS requirements regarding the strength and the SLS requirements regarding the displacements are met. All connections are still assumed to be rigid. The forces that need to be transmitted by the connection are tension forces, hogging and sagging bending moments and out-of-plane bending moments caused by the wind loads on the facade.

A column splice connection is designed, as the plug & play connections will be directly attached to the column it is not possible to use extended endplates for the column splice. The designed column splice is classified as semi-rigid, which means that the actual stiffness of the joint has to be taken into account. The plug & play connection is also classified as semi-rigid, which means that all joints in the frame are semi-rigid instead of rigid. A new analysis shows that the frame with all semi-rigid joints has deformations which are not within the SLS requirements.

Finally a global analysis is performed with the actual stiffness of the column splices and the stiffness of the plug & play connection. Both connections are not classified as rigid which was made as an assumption in the start. This results in an increase of the lateral displacements of the frame. The lateral displacements are now not within the SLS boundaries. If it is wanted to use the plug & play connection and column splices for such frame, then the maximum number of units in height should be investigated for which it meets the

SLS requirements regarding the displacement. Another option to reduce the lateral displacements, for a frame with 6 units in height, is to use a bracing system. However, in this chapter is already mentioned that this does not apply as it would limit the design flexibility of the frame. Also in a braced frame it is usual to design the joints as pinned, but the plug & play connections is classified as a semi-rigid joint. So the plug & play connection would be an expensive solution for a hinged connection. The last possibility could be to use the obtained stiffness in a new frame design, this would result in heavier sections. This heavier sections would also lead to increased dimensions of the plug & play connection.

plug & play Connection 7

7.1 Geometry

7.1.1 Geometry of the connection

Based on the results of the Snap-fit connection mentioned in chapter 3 and the sections and internal forces obtained in chapter 6, an initial design has been made.

For investigating purpose a perfect fitted connection is analysed. In the research of the snap-fit connection in chapter 3 is mentioned that gaps in the connection are possible and these gaps have a negative effect on the performance of the connection.

The width and height of the connection result from the HEB200 section which is used in the frame. The dimensions of the connection are kept equal to the dimensions of the HEB200 section. For the determination of the bolt size the following things were taken into account:

- The upwards shear forces will fully be resisted by the bolts.
- The hogging bending moment causes tension in the bottom of the connection. Because the contribution of the inclination of the connection is unknown, the tension forces caused by this moment should be taken for a large part by the bolts.
- The axial tension has to be taken by the bolts.

From the results of the snap-fit connection of chapter 3 the following parameters were used:

- **Thickness base material:** the thickness of the base material should be at least 10mm, any increasing value would not result in a significant increase in stiffness, resistance or ductility (see figure 3.44).
- **Thickness plug:** the plug is taken as 15mm, increasing the thickness of the Plug would not result in a significant increase of the stiffness of the connection (see table 3.4).

- **Inclination angle:** the inclination angle is taken as 45°, an inclination angle closer to 90°results in ductile behaviour and low stress and an inclination closer to 45°angle results in a connection with higher stiffness and resistance, but less ductility. A high stiffness is wanted and therefore an inclination angle of 45°is used (see table 3.2).

The results of the global analysis lead to the following design choices:

- **Dimensions:** as mentioned earlier the width and height of the connection are kept equal to the width and height of the beam section. The width and height are both 200mm.

- **Bolts:** the bolts should be able to resist the the upwards shear force and the tension force in the bottom. A simplified approach is used to estimate the tension force in the bolts. The lever arm is taken as the distance between the top of the connection, which is assumed as the center of compression, and the centerline of the bolts. So the tension at the bolt height is $\frac{49kNm}{0.155m} = 316.1kN$. This force should be taken by two bolts, so each bolt should be able to resist $158.1kN$. The tension resistance of the M20 bolts is $141.1kN$. The vertical shear capacity of the bolts is $94.1kN$, the upwards shear force is $62kN$, so one bolt could already carry the upwards shear forces. Although the tension forces are higher than the tension capacity of the bolts, it is not chosen to increase the bolt size as the plug also has some tension resistance. The analysis would show whether it is necessary to increase the bolt size.

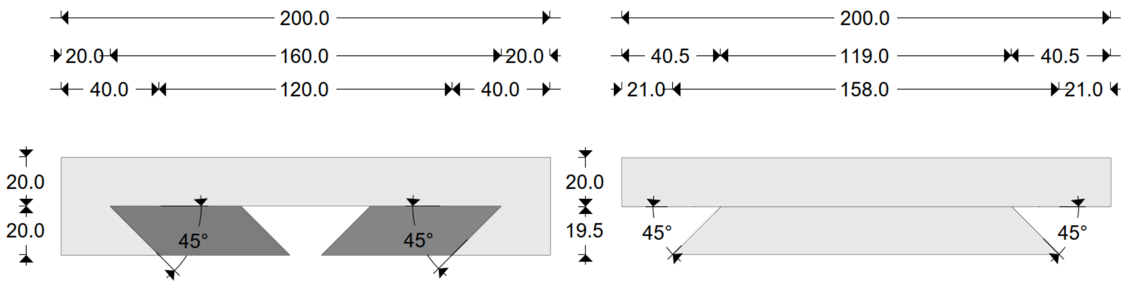

(a) Top view

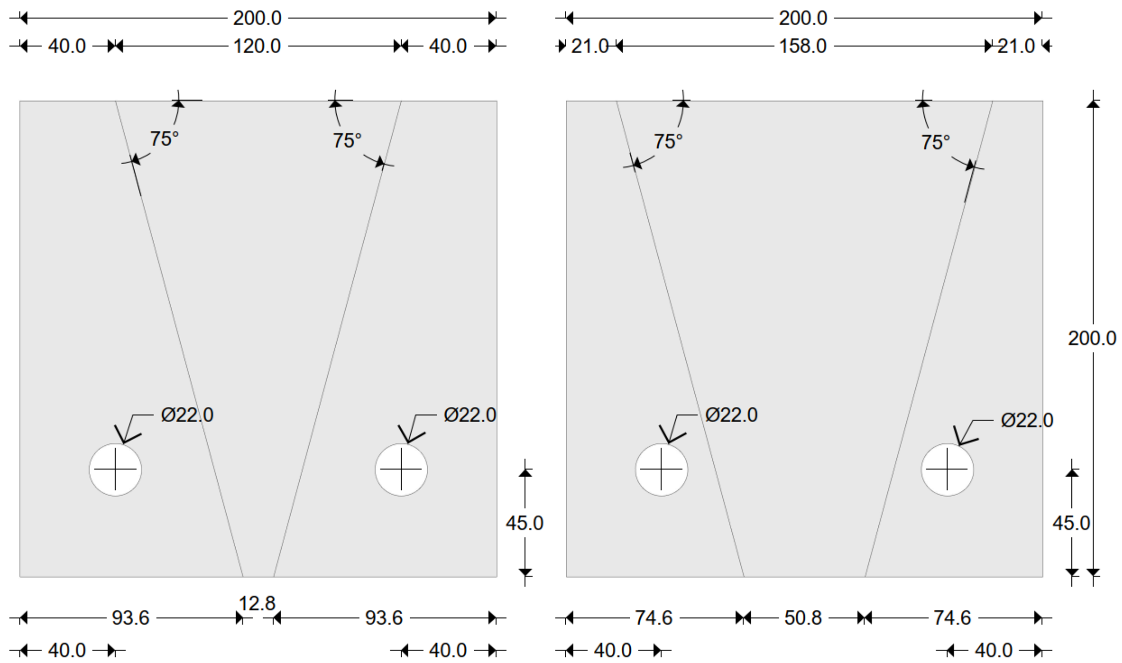

(b) Front view

Figure 7.1: Dimensions initial design

7.1.2 Geometry of the numerical model

In figure 7.2 the dimensions of the numerical model is shown. The part of the column above the beam is equal to the distance to the top of the column splice. The part of the column below the beam is the distance to the middle of the storage height. The modelled length of the beam is equal to half the real beam length.

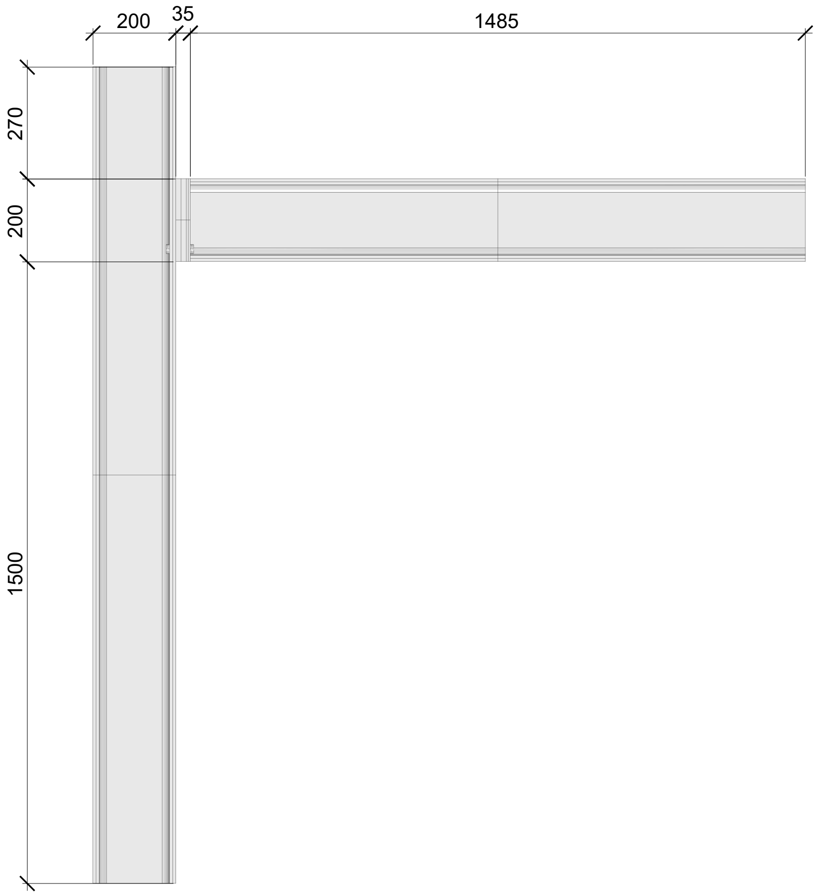

Figure 7.2: Dimensions numerical model

7.2 Modelling settings

These section describes the settings used for the finite element model.

7.2.1 Material properties

For all materials the same density, elastic modulus and Poisson ratio is used respectively: $7850 kg/m^3$, $210000 MPa$ and 0.3. The material properties regarding plasticity for the different parts is given below. The used properties for the S355 and the bolts class 8.8 are obtained from coupon test unrelated to this project and are the results for a true stress-strain relation.

plug & play:

For the modelling of the plug & play connection is assumed that the connection is made of structural steel of class S355. The hardening of the material is included in the model and failure of the material is included as a low stress at the ultimate plastic strain. The table below shows the plasticity material properties:

Table 7.1: Plasticity S355

f_y	ϵ_p
355.60	0
359.90	0.012
492.27	0.045
540.50	0.138
0.1	0.262

Bolts material:

For the bolts normal threaded bolts of class 8.8 are used. The hardening of the material is included as well. The table below shows the plasticity material properties used:

Table 7.2: Plasticity Boltclass 8.8

f_y	ϵ_p
778.8	0
888.0	0.011
944.5	0.021
985.8	0.031
1011.7	0.040
1018.5	0.045

Beam and column material:

For the beams and columns the structural steel class S235 is used. The internal stress in the column and beam is of less interest compared to the stress in the connection. Therefore it is chosen to use a bi-linear material model for the beams and columns, to decrease the complexity of the model and reduce computational time. So plasticity is defined as the nominal yield strength and no strain hardening is taken into account.

7.2.2 Interaction properties

Abaqus allows to define interaction properties for surfaces which are in contact. In Abaqus the tangential behaviour (friction) and normal behaviour is defined. The normal behaviour is defined as ”hard” contact, so the surfaces would not penetrate each other, and separation between surfaces is allowed.

Friction coefficient

In chapter 3 is shown that for the snap-fit connections with pins, the frictional coefficient has less influence on the results. The real frictional behaviour could be obtained from results, but based on the results of the snap-fit connection it is expected that it is of little influence on the performance of the connection. In the NEN-EN 1090-2 [22] some values for frictional coefficients with structural steel are given. The lowest friction coefficient given by NEN-EN 1090-2 for structural steels is used, which is $\mu = 0.20$. This is implemented in Abaqus by defining a penalty for the tangential behaviour equal to the friction coefficient.

Constraints

In reality the socket would be welded to the column flange(s) and the plug would be welded to the beam face. The welds are not explicitly modelled but are taken into account by using a tie constraint. This means no relative displacement between the parts which are tied together will occur.

7.2.3 Boundary conditions and loads

Boundary conditions

The bottom of the column is restricted for displacements in any direction and rotation along the columns axis. The wind is the decisive load combination, this load combination results in zero bending moment in the middle of the columns, therefore only displacements are prevented. The top of the column is restricted for only horizontal displacements and rotation along the column axis, the top part is at the location of the column splice, the moments are not zero in this location; however, the column splice is not rigid, so only displacements are prevented. The boundary conditions are applied on a reference point, which is connected with a rigid body constraints to the section.

Loads

A displacement controlled test is done. A displacement is defined at the beam end. The displacement is applied on a reference point, which is connected with a rigid body constraint to the section. Torsional rotation of the beam end and displacement perpendicular to the loading direction are prevented.

7.2.4 Type of elements, mesh and analysis

The model is simulated with 8 node hexahedral solid elements with reduced integration (C3D8R).

A fine mesh is used for the parts of the plug & play connection, the bolts and around the bolt holes in the column, for the remaining part of the column and the beam a coarse mesh is used.

A general static analysis is performed in ABAQUS which uses an implicit solving technique.

7.3 Design criteria

For the evaluation of the connection the following criteria need to be taken into consideration and their influence on the structural behaviour.

7.3.1 Failure criteria

The following criteria are used to check whether the plug & play connection can be used. The aim of the project is that the construction is reusable. Therefor failure of the connection is when it cannot be reused. The connection cannot be reused when:

The connection is too much permanently deformed

Expected is that yielding of the inclined parts of the socket will occur. As a consequence of yielding the inclination angle will decrease and this would effect the structural performance of the connection. If the permanent deformation of the connection is too large reuse is not possible.

The second failure criteria is that the connection cannot be reused if:

A crack develops in the connection

In chapter 3 the results of experimental tests on a similar connection are shown. The results showed that a crack appears in the connection. As a consequence of local stress concentrations the material could crack. When a crack occurs in the connection the connection is regarded as unsafe. The connection cannot be reused and therefor the connection is regarded as failed.

Using the first criteria to evaluate the plug & play connection in the ULS would be too strict as the ULS gives the maximum possible forces, which are not likely to occur often during the lifetime of the structure. Therefor the first criteria is evaluated using the internal forces of the SLS as these forces are the most likely to occur during the lifetime of the structure. For the ULS the plug & play connection is allowed to plasticly deform and yield, but the connection should still be safe in the ULS conditions. So the second failure criteria is used to evaluate the plug & play connection in the ULS.

7.3.2 Tolerances

In the NEN-EN 1090-2 [22] the tolerance limits in steel constructions are given. Table B.6 in the NEN-EN 1090-2 shows the fabrication tolerances for construction parts. The relevant tolerances used for the design of the plug & play connection is the tolerances for surfaces in contact pressure. The code provides two classes with the following tolerances limits:

- Class 1) $\Delta = 0.50mm$
- Class 2) $\Delta = 0.25mm$

Figure 7.3 shows the definition of the tolerance.

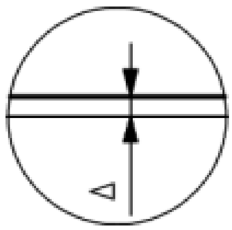

Figure 7.3: Tolerance definition

In chapter 3 it is already shown that the tolerances decrease the stiffness and the resistance of the connection. For the derivation of the $M - \phi$ curves the tolerances are not taken into account and only perfect fit connections are analysed.

7.4 Validation of numerical model

It has to be checked whether the results of the numerical model are reliable, this is done by creating a validation model with the same assumptions made as for the numerical models of the plug & play model. A validation model is made of test 3 mentioned in chapter 3 and the geometry of figure 3.19 is used. A validation model is made with the available information on this test and the numerical results is compared with the experimental results.

The principles that are used are the same:

- The way the load/displacement is applied, so displacement applied on the whole section. With a reference point using tied with rigid body constraints. Also boundary conditions are applied in the same way.

- The definition of interaction, the interaction is defined the same way and with the same values as in the models of the plug & play connection.
- The same type of analysis.
- The model is fully meshed with solid elements.

7.4.1 Geometry

The test setup used to test the connection is shown in figure 7.4 and the model used for the numerical analysis is shown in figure 7.5

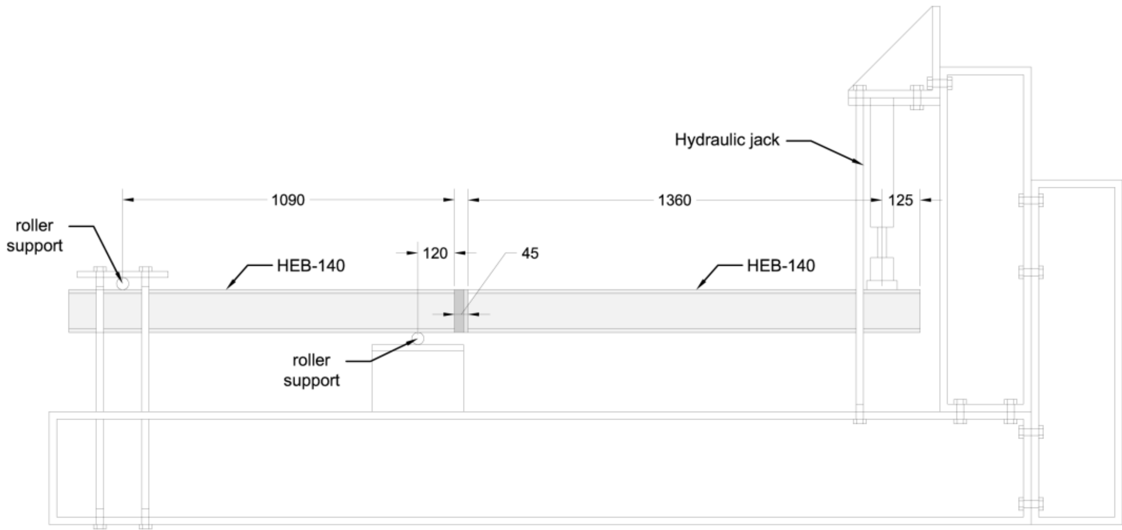

Figure 7.4: Test setup [6]

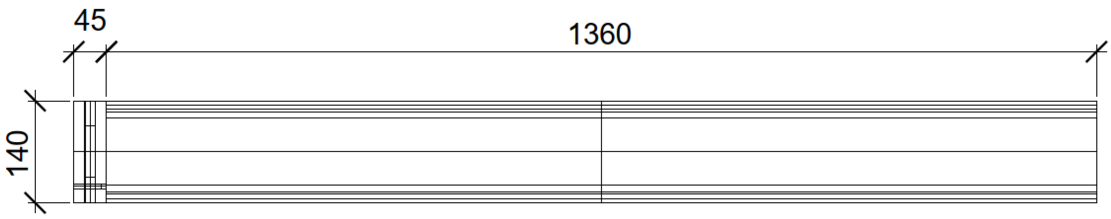

Figure 7.5: Model for numerical analysis

7.4.2 Modelling settings

Material properties

A tensile test is performed on the material used in the test and this resulted in the following properties used for modelling. The density is the same $7850kg/m^3$, the elastic modulus is a little lower and is $195000MPa$, the Poisson ratio is kept at 0.3. Plasticity is implemented with a simplified approach and includes hardening and softening of the material. Hardening of the material starts directly after the yield stress is reached. The material properties show the true stress-strain relation.

Table 7.3: Plasticity Snap-fit

f_y	ϵ_p
500	0
600	0.06
470	0.15

The material properties are used for both the Snap-fit connection and the steel pins in the connection. The steel class of the beam is unknown therefor no plasticity is included in the material properties of the beam and only elasticity is modelled. The experimental results showed that the connection was the critical part, so the connection would fail before yielding of the beam could occur.

Interaction properties

The same interaction properties are used as for the numerical models of the plug & play connection.

The pins are tied with a tied constraint to the plug so the pins move with the same displacement as the plug.

Boundary conditions and loads

A displacement is applied at the beam end on the whole section. The boundary condition is applied at the socket and both displacements and rotations in all directions are restricted. The boundary conditions and loads are applied on a reference point which is tied with rigid body constraint to the section.

Type of elements and analysis

In the validation model 8 node hexahedral solid elements with reduced integration (C3D8R) are used. An implicit static general analysis is done with Abaqus/standard.

7.4.3 Evaluation of results

The results of the numerical analysis have to be compared with the experimental results, when the results are similar it means that the numerical model is reliable and the same settings can be used to analyse the plug & play connection.

The easiest result which can be compared is the force displacement at the point of the load/displacement, as this requires no further post-processing of the numerical results. In the experiment a load-cell is used to measure the applied load and a sensor measure the displacement of the beam at the section where the load is applied. In figure 7.6 the results of the experimental test and the numerical results is shown.

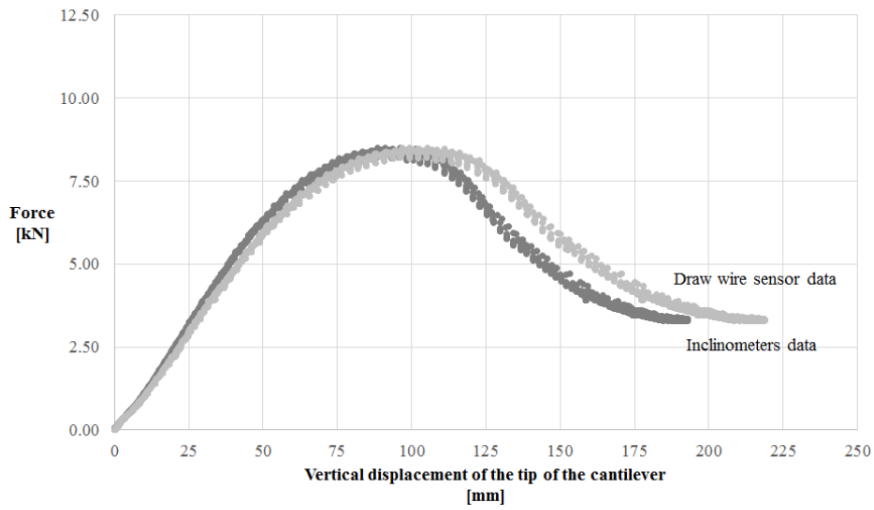

(a) Experimental results [6]

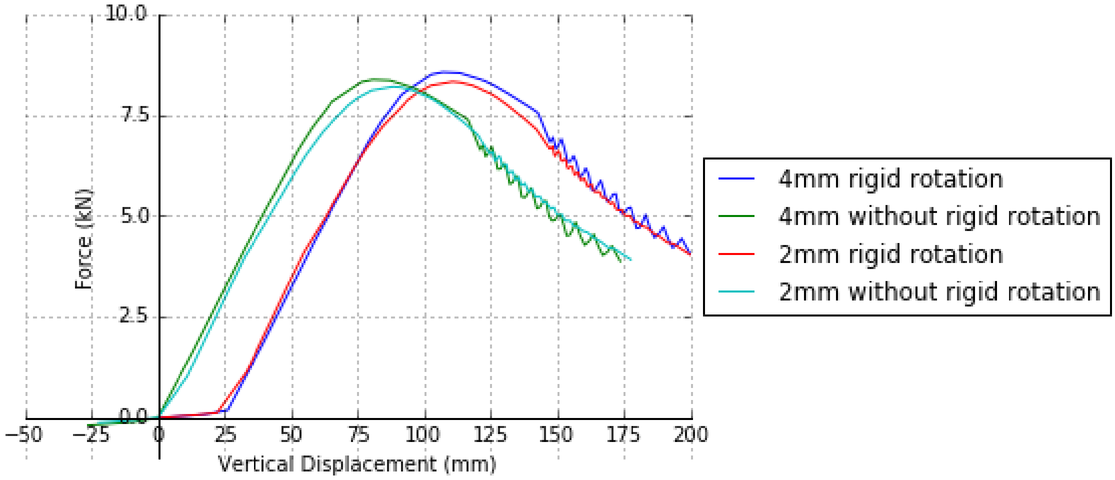

(b) Numerical results

Figure 7.6: Force-displacement curve at load point

The 4mm mesh showed some load drops and therefor an analysis with a finer mesh of 2mm is used, this results in a smoother curve.

The connection is not perfect fitted, the plug is a little smaller than the shape of the socket, this causes a rigid body rotation. In figure 7.6b this is shown as a increase in the vertical displacement without a significant increase in the force. In the experimental results the selfweight of the beam, removes this rigid body rotation and immediately establish contact between the plug and socket. In the numerical results the rigid body rotation is removed by shifting the graph to the point where the load starts to increase.

A second check is made for the $M - \phi$ curve. The $M - \phi$ curve is given for the relative rotation of the connection. The socket and plug will have both a different rotation, the rotation of the socket is also measured in the rotation of the plug. The relative rotation of the connection is obtained by subtracting the rotation of the socket from the rotation of the plug. The location of the inclinometers where the rotation of the connection is measured for the $M - \phi$ curve is given in figure 7.7.

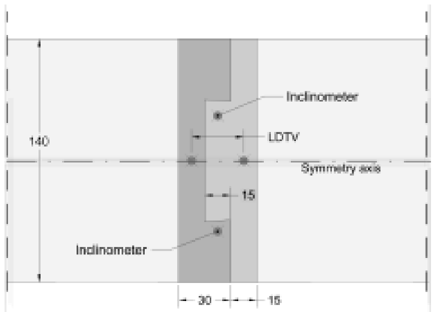

(a) Upper view

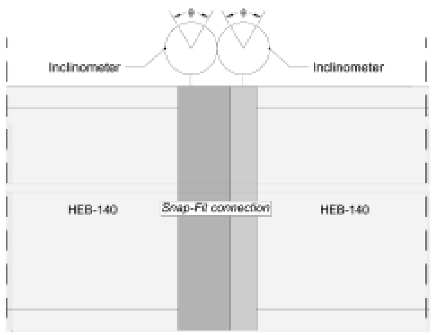

(b) Side view

Figure 7.7: Location inclinometers [6]

The $M - \phi$ curve is given in figure

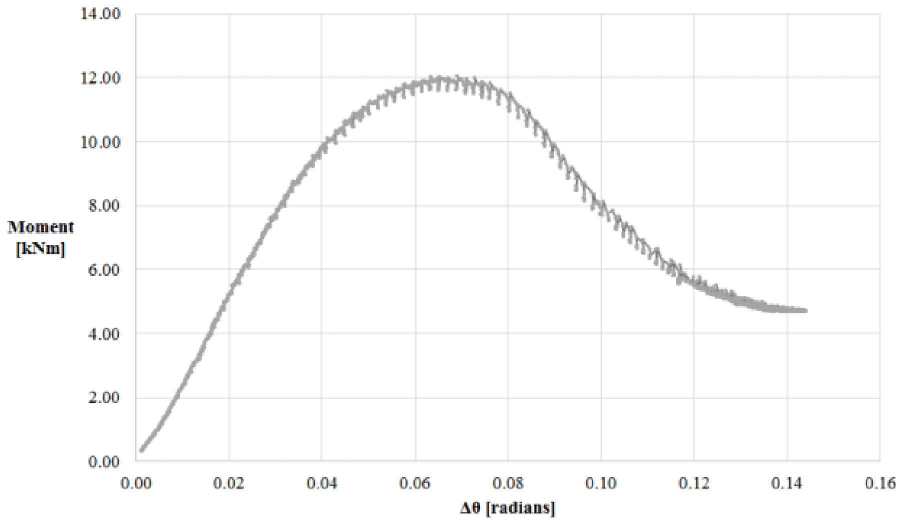

(a) Experimental results [6]

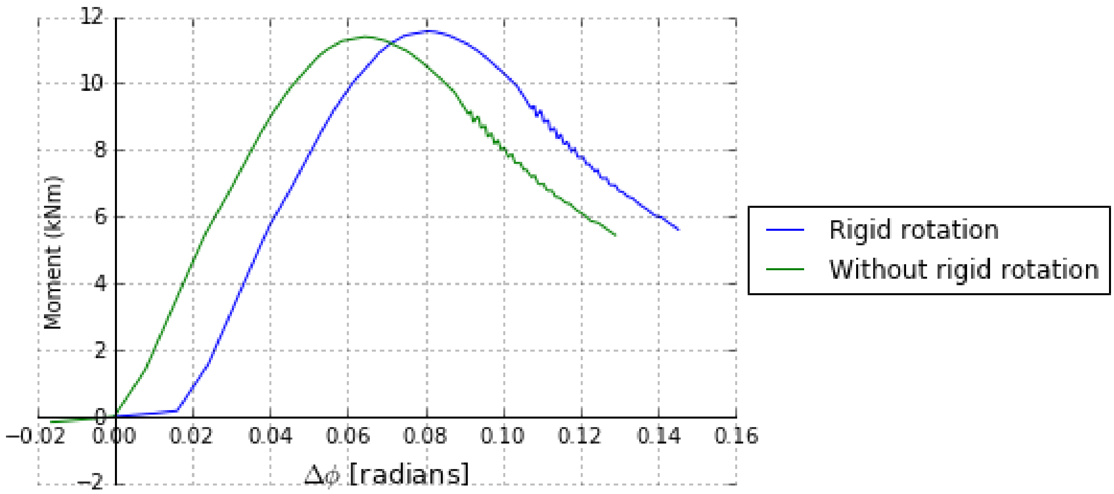

(b) Numerical results

Figure 7.8: $M - \phi$ curve at connection

Again the graph is shifted to remove the rigid body rotation of the connection.

The shape of the curve of the numerical results for both the force-displacement curve and the $M - \phi$ curve correspond to the shape of the experimental test curve. The values of numerical results match the experimental results. So the numerical method is validated.

7.5 Results Numerical Models

7.5.1 Derivation moment-rotation curve

Figure 7.9 shows the nodes which are used for the derivation of the $M - \phi$ curve. The vertical and horizontal displacements are taken at 4 points on the column and at 2 points on the beam. The forces on the structure are taken from the reference point on the beam end. As the intersection point of the centerlines of the beam and column is not on a node this point needs to be calculated. The two data points on the beam are used to calculated a point which is on the centerline of the beam. The location of the intersection point is calculated from the two inner data points on the column. In the global coordinate system used the location of the intersection point would be x=-100, y=100, z=100. The initial coordinates of the two used points on the column to calculate the intersection point are: (-100,100,119.23) and (-100,100,90). The distance between the the bottom point and the intersection point is assumed to be constant during loading. A linear interpolation is used to calculate the location of the intersection point. The same method is used for the calculation for the point on the centerline of the beam.

For the minor axis bending the same method is done with only different points. This method is only suitable for the downwards and upwards case, for the out-of-plane displacement another method has to be used.

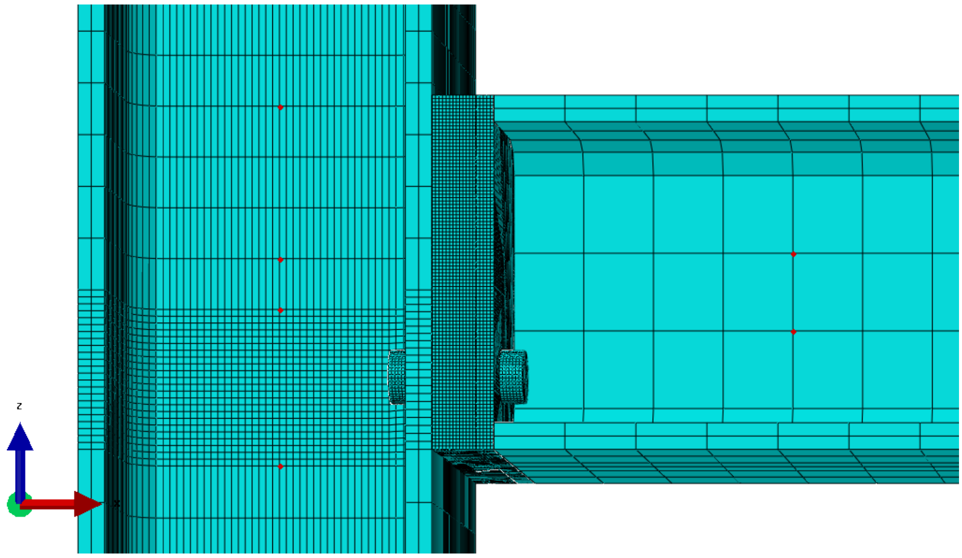

(a) With mesh

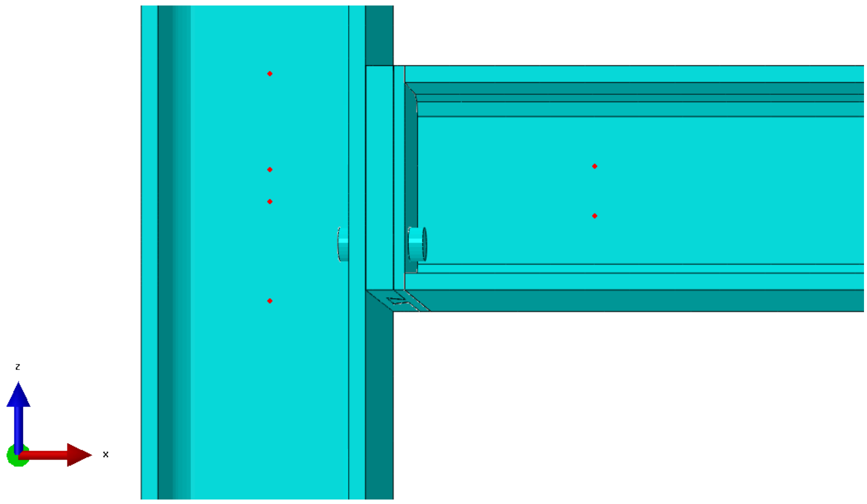

(b) Without mesh

Figure 7.9: Location data points

In total 3 rotations are calculated:

- **Rotation column top:** is the angle between the intersection point and the top data point on the column.
- **Rotation column bottom:** is the angle between the intersection point and the bottom data point on the column.
- **Rotation beam:** is the angle between the intersection point and the calculated point on the beam centerline.

The moment is calculated the same for all cases and is calculated by multiplying the reaction forces with the leverarm. In which the leverarm is the distance between the intersection point and the beam end.

In the article by Gil and Roñi [10] the test and results for a joint subjected to out-of-plane bending is described. The used test setup for a joint modelled to out-of-plane bending is given in figure 7.10. The test setup uses inclinometers to measure the rotations, for the numerical models the displacements at points shown in figure 7.11, all these points are at the centerline of the beam.

The following rotations are calculated:

- **Rotation web:** is the rotation between the points O and 1.
- **Rotation flange:** is the rotation between the points 1 and 2.
- **Rotation beam:** is the rotation between the points 1 and 3

The relative rotation of the joint is the rotation of the beam minus the rotation of the web.

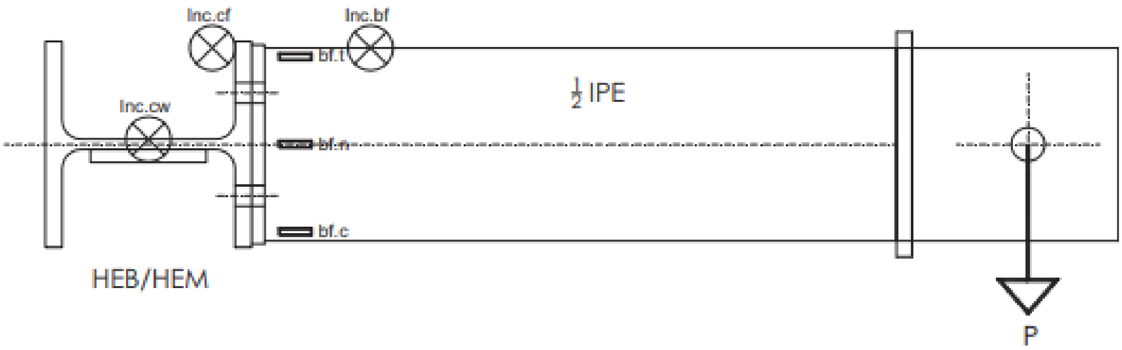

Figure 7.10: Test setup out-of-plane bending [10]

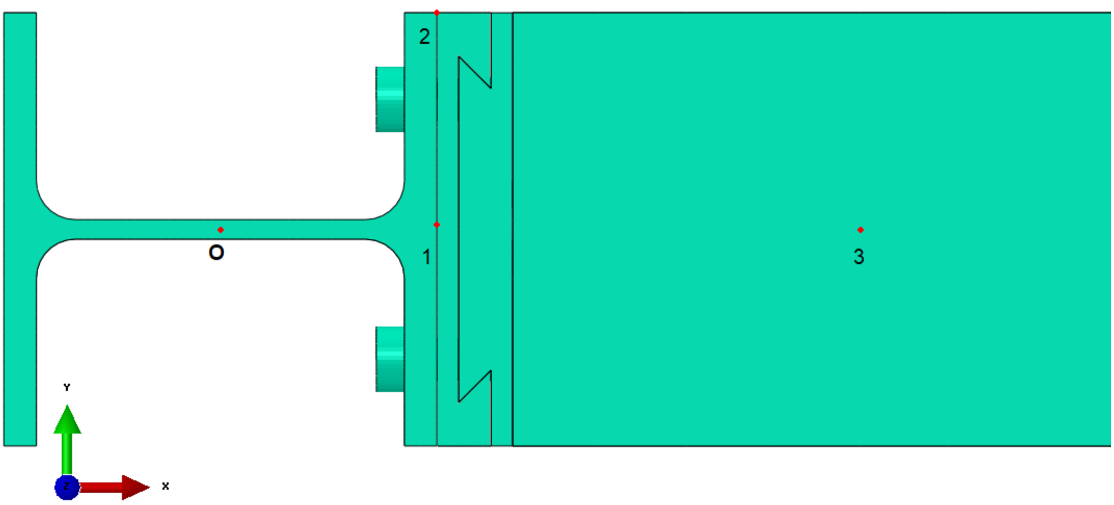

Figure 7.11: Location data point for out-of-plane bending

7.5.2 Column major axis analysis

For the major axis behaviour two models are analysed:

1. Model with only 1 plug & play connection attached to the flange of the column
2. Model with 3 plug & play connections where the plug & play connections on the sides are modelled as a solid plate.

These two models are made to see the effect of the connection on the sides. The $M - \phi$ curves are determined for both configurations for downwards, upwards and sideways displacement.

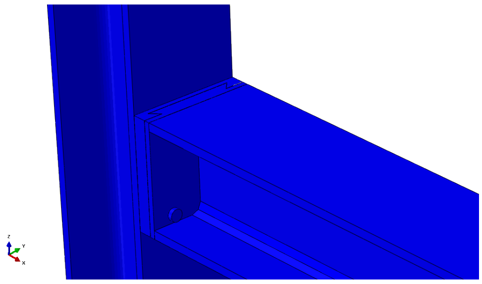

(a) Without connection on sides

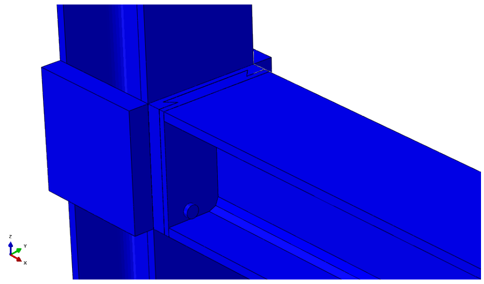

(b) With connection on sides

Figure 7.12: Analysed models

In the frame the connection will be attached to 3 or 4 sides of the column. The results are compared with when there is only 1 connection, to see what the effect is of the side connections on the joint stiffness and resistance.

Downwards displacement

The first model for downwards displacement was run using a static general analysis in ABAQUS. When on the models models an upwards or horizontal displacement was applied convergence problems occurred. The bolt head and nut were tied to their contact surface in order to improve the convergence of the solution. The effect of this model change on the results in shown in figure 7.13. It can be seen that the tie constraint for the bolts has no effect on the results. Using the tie constraint improves the convergence of the models.

The initial model is run up to a vertical displacement of 100mm at the beam end. The tied bolts model is run to a vertical displacement of 50mm at beam end. It is chosen to not run the model with a displacement above 50mm as the curve already is beyond the bending moments acting on the joints and to save computational time.

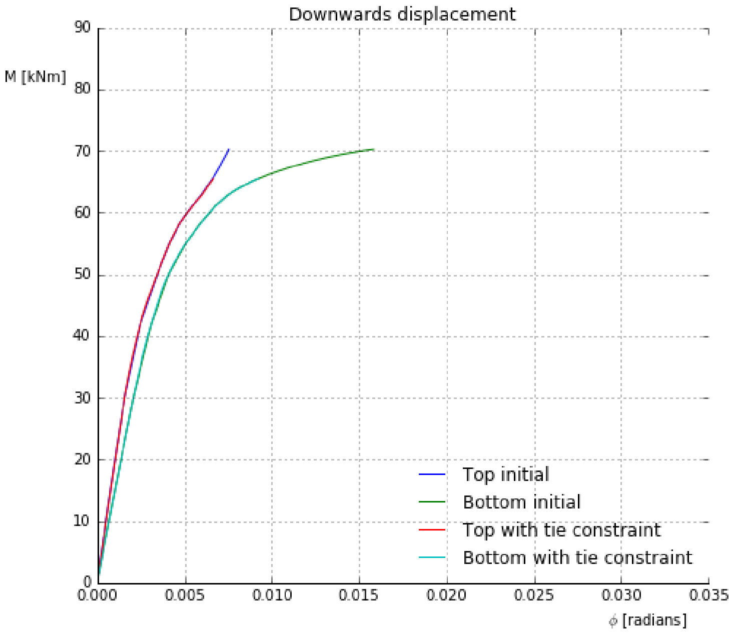

Figure 7.13: $M - \phi$ curve for model with and without bolt tie constraint

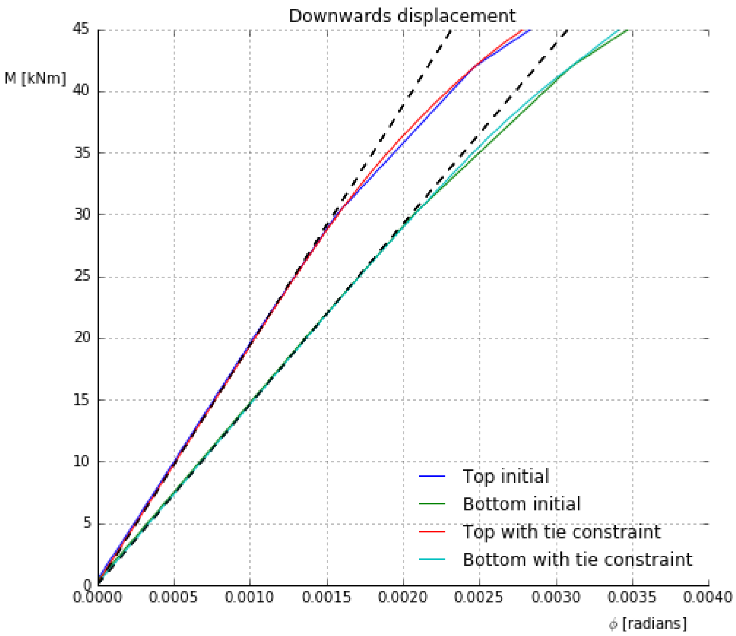

Figure 7.14: ZOOM of the $M - \phi$ curve for model with and without bolt tie constraint

In figure 7.14 the tangent line for the elastic part of the joint is shown. The tangent line is calculated using a least-square curve fit which starts at the origin. The figure shows that the tangent lines are equal for both curves. Therefor it is assumed that the tie constraint for the bolts does not effect the results. The top part of the column has a smaller span than the bottom part, see figure 7.2. The top part will rotate less then the bottom part and therefor the top part will result in a higher stiffness.

Figure 7.15 shows the $M-\phi$ curves for the model with and without the connections on the sides. The models with and without side connections are shown in figure 7.12. It can be seen that taking into account the connections on the sides increases both the resistance and stiffness of the connection, when subjected to the same displacement. Both test are performed for a beam-end displacement of 50mm. The maximum possible moment on the connection is -49 kNM.

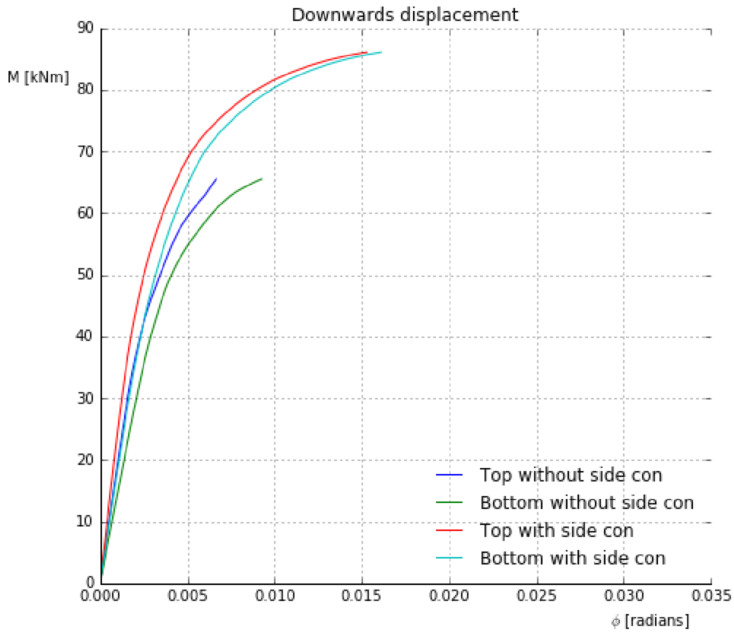

Figure 7.15: $M-\phi$ curve for model with and without side con

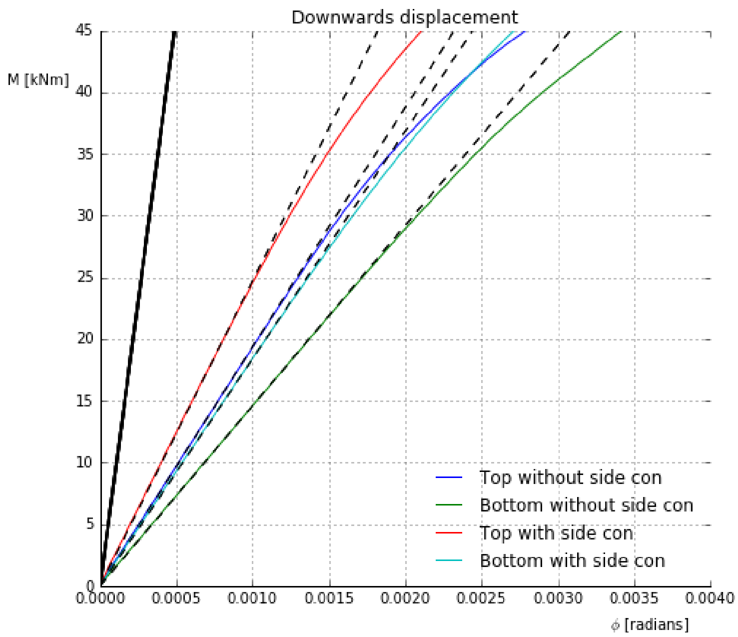

Figure 7.16: ZOOM of the $M-\phi$ curve for model with and without side con

The stiffness derived from figure 7.16 for the several graphs is:

- Top without side connections: $S_{j,ini}$ = 19400 kNm/rad
- Bottom without side connections: $S_{j,ini}$ = 14600 kNm/rad
- Top with side connections: $S_{j,ini}$ = 24700 kNm/rad
- Bottom with side connections: $S_{j,ini}$ = 18400 kNm/rad

Taking the side connections into account results in an increase of the stiffness of 27% for the top and 26% for the bottom. The elastic moment capacity is for both models at 30 kNm, for moments beyond 30 kNm the secant stiffness should be taken into account. The stiffness of the beam is $\frac{EI_B}{L_B} = 3692kNm/rad$ for a HEB200 with a length of 3240mm. The rigid classification boundary for an unbraced frame is 25 times the beam stiffness, the rigid classification boundary is shown in figure 7.16. The pinned classification boundary is 0.5 time the beam stiffness, the joint stiffness is above the beam stiffness. The joint can be classified as semi-rigid.

In figure 7.17 the final deformation of the model is shown. A scale factor of 20 is used to clearly show the deformation of the model. It can be seen that the connection on the sides prevents the column flange from local bending. In the model without connections on the side the column flange is the part which shows the largest deformation. For the model with connections on the side the plug & play connection is the critical part which deforms the most.

The von Mises stress at the final displacement of 50mm for the two models is shown in figure 7.18. The von Mises stress shows which parts of the connection will yield. The equivalent plastic strain at the displacement of 50mm is given in figure 7.19. From this figure can be seen that the connections on the side prevent that a plastic strain will occur in the column web.

The figures 7.20 and 7.21 show the decomposition of the von Mises stress in the global directions, it is shown for both the model with and without connections on the sides. The legend is for all figures between -355MPa and 355MPa. The figures show that the connections on the sides reduce the stress in the column, mainly the shear stress in the column web. The side connections result in an increased stress and deformation in the loaded plug & play connection. All what is grey or black in the figures means exceedance of the yield stress.

For both models it is shown that the inclined part of the socket is moving outwards and the inclined part of the plug is moving inwards. This causes that the plug will be pulled out of the socket. The tensile stress in the socket is a consequence of this outwards bending of the inclined part, in the middle of the plug compressive forces will occur due to the inwards movement of the inclined part. The excessive bending of the plug causes also normal compressive forces in the z direction, this is especially for the model with the side connections. For the model with side connections the plug is yielding at the location of the bolts, in the model without side connections the plug is not deforming at the bolts as the column flange is deforming. The pull out motion of the plug causes xy shear stress in the top of the connection.

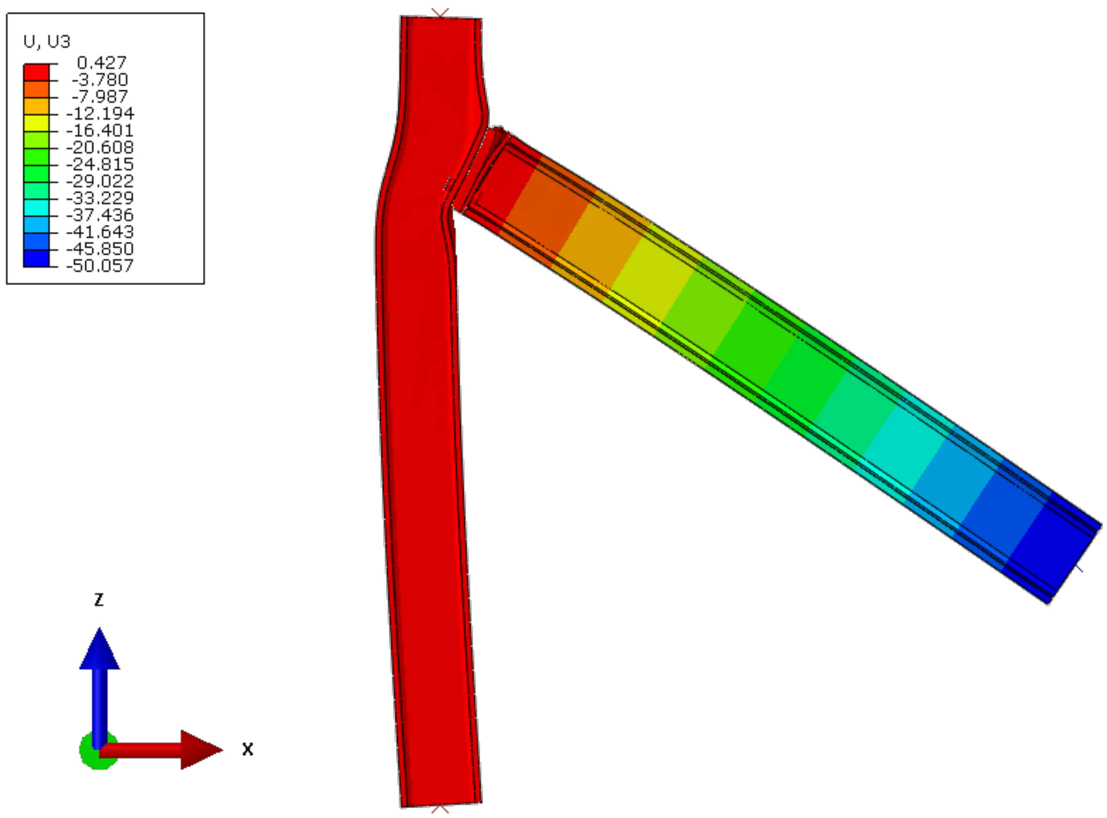

(a) Without connections on the sides

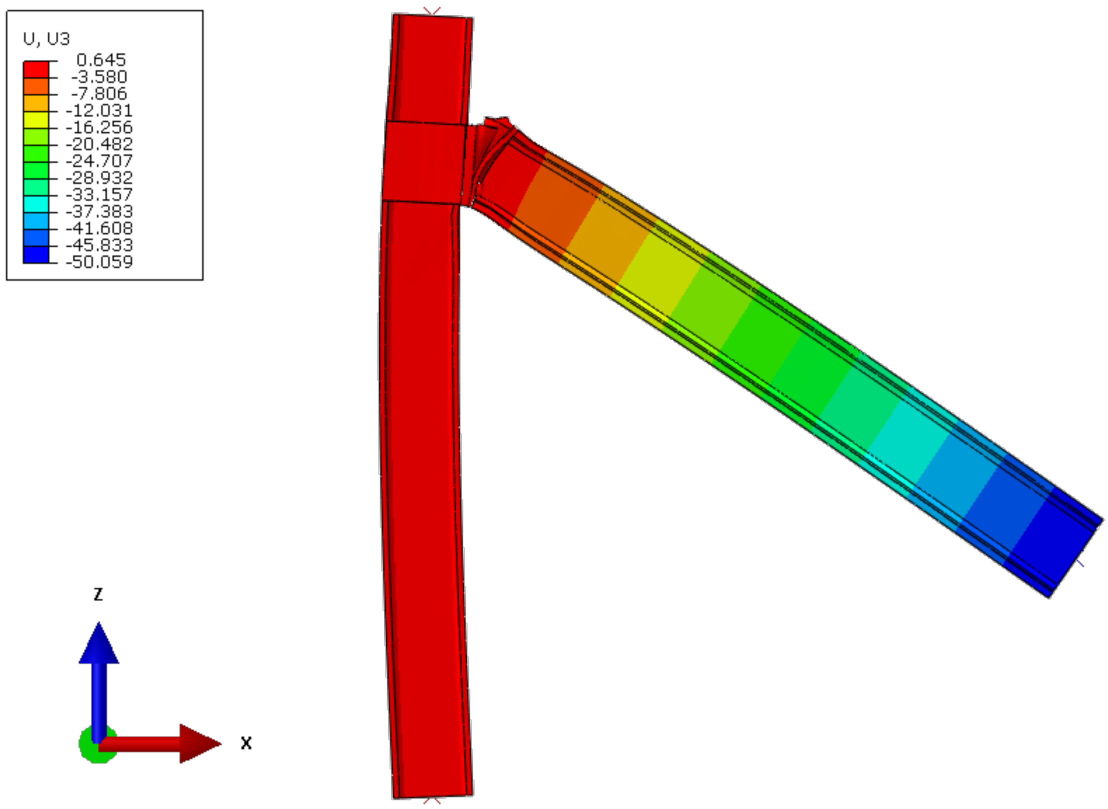

(b) With connections on the sides

Figure 7.17: Deformed model (scale factor 20) for downwards displacement

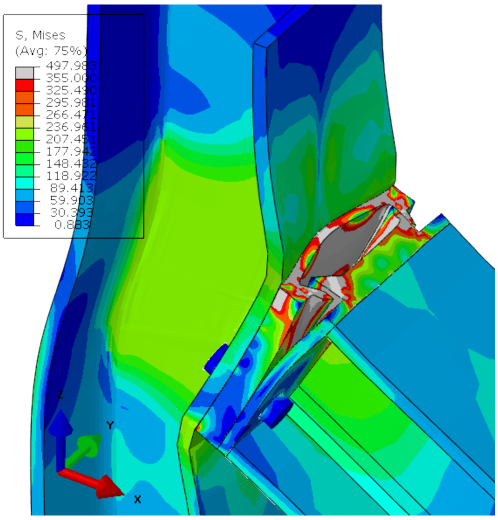

(a) Von Mises

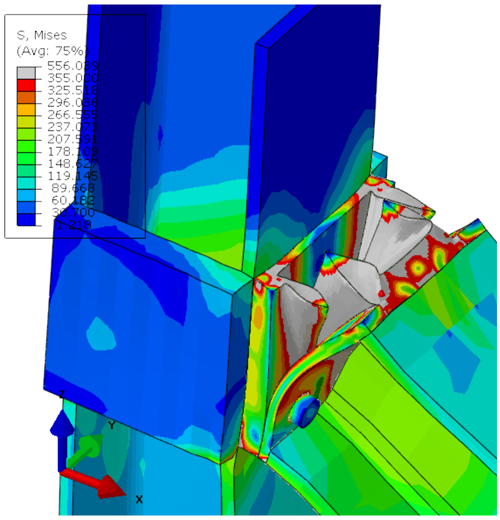

(b) Von Mises

Figure 7.18: Von Mises stress (scale factor 20)

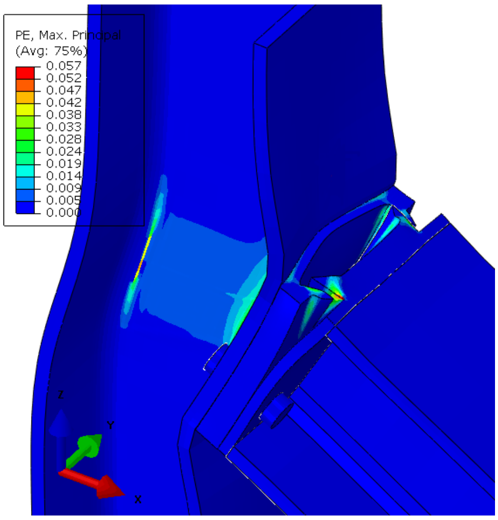

(a) Plastic strain

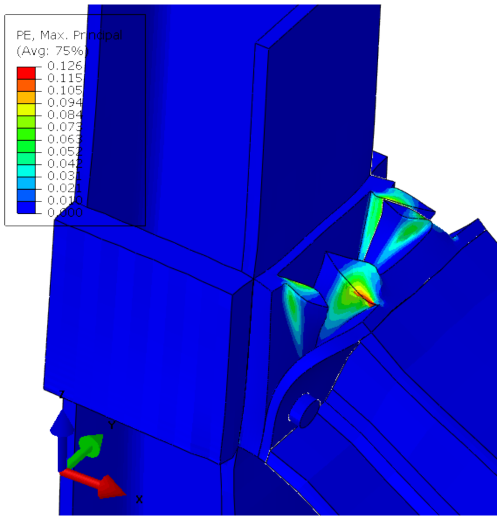

(b) Plastic strain

Figure 7.19: Plastic strain (scale factor 20)

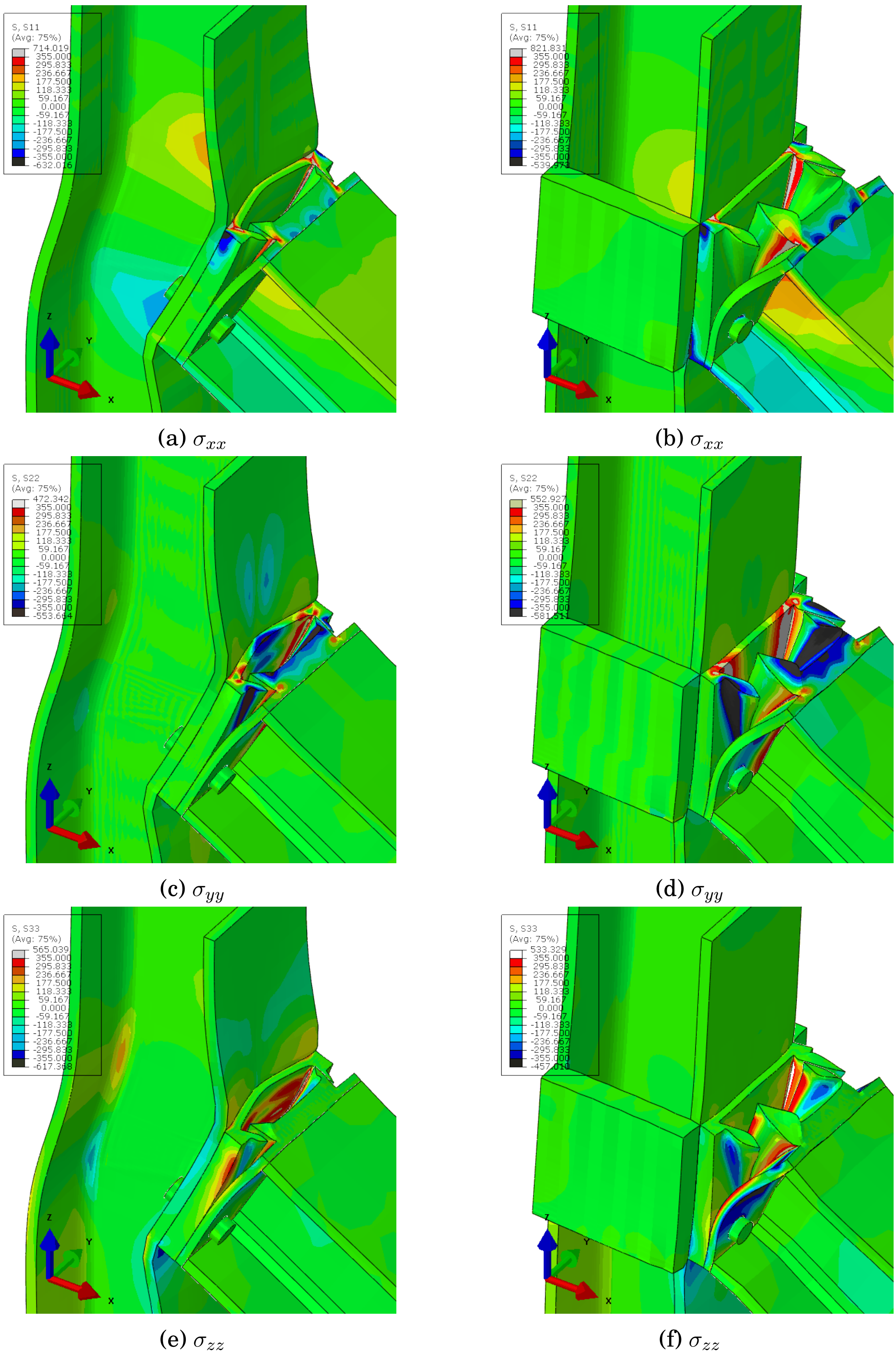

(a) σ_{xx} (b) σ_{xx}

(c) σ_{yy} (d) σ_{yy}

(e) σ_{zz} (f) σ_{zz}

Figure 7.20: Normal stress (scale factor 20)

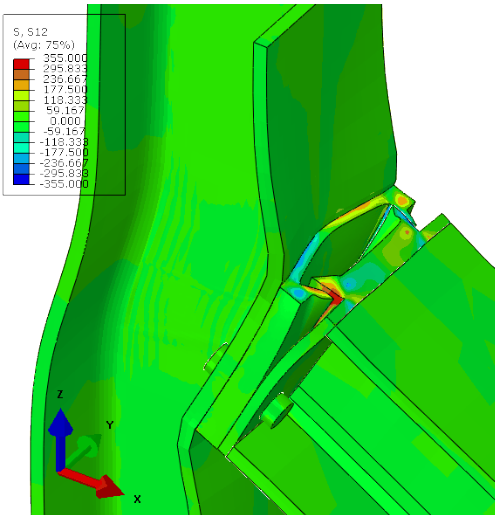

(a) σ_{xy}

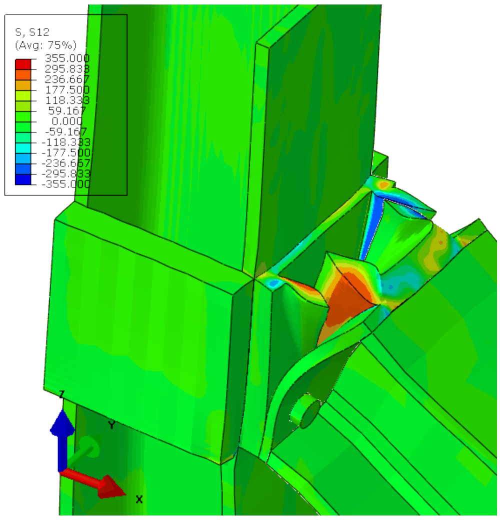

(b) σ_{xy}

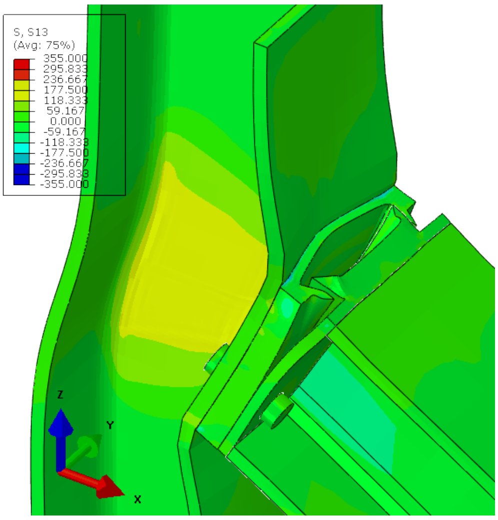

(c) σ_{xz}

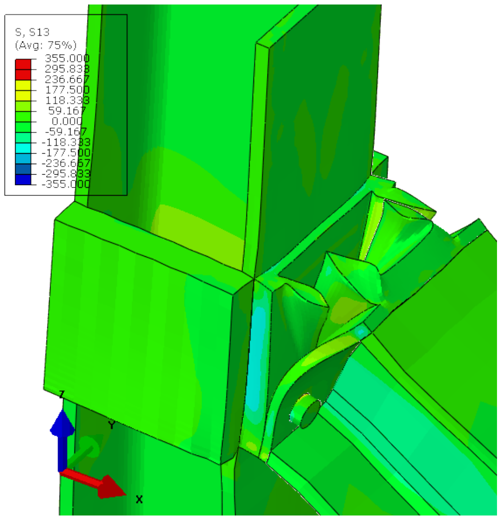

(d) σ_{xz}

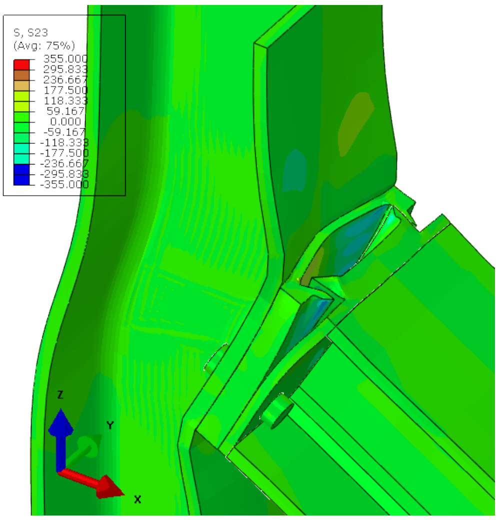

(e) σ_{yz}

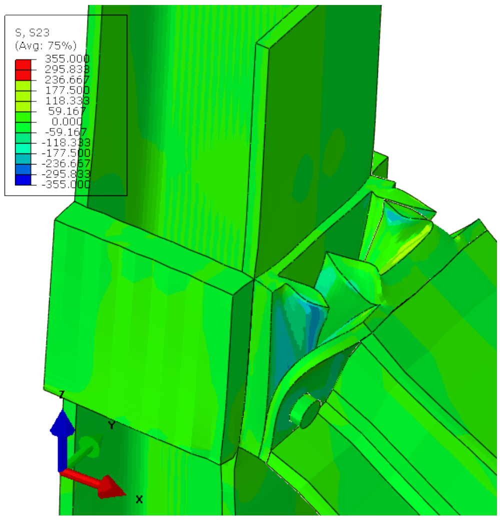

(f) σ_{yz}

Figure 7.21: Shear stress (scale factor 20)

Upwards displacement

The connections can have both positive and negative bending moments. The model without connection on the side is run up to a displacement of 50mm. The model with connections on the side is stopped at a maximum displacement of 15mm. Again both models are analysed to see what the effect of the connections on the side is on the joint properties. The maximum possible positive moment (sagging) is 36 kNm, this is lower then the maximum negative moment (hogging) of 49 kNm.

The $M - \phi$ curve is shown in figure 7.22 and in figure 7.23 is zoomed in on the elastic part of the $M - \phi$ curve.

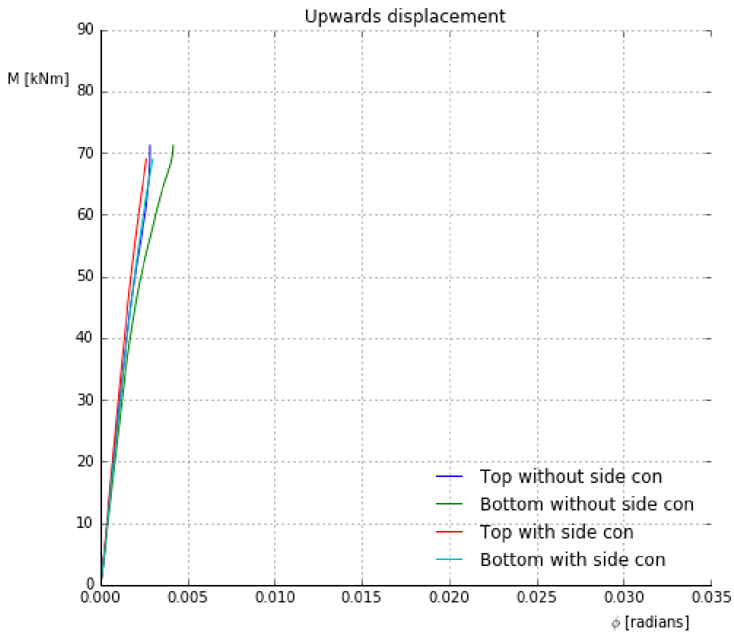

Figure 7.22: $M - \phi$ curve for upwards displacement

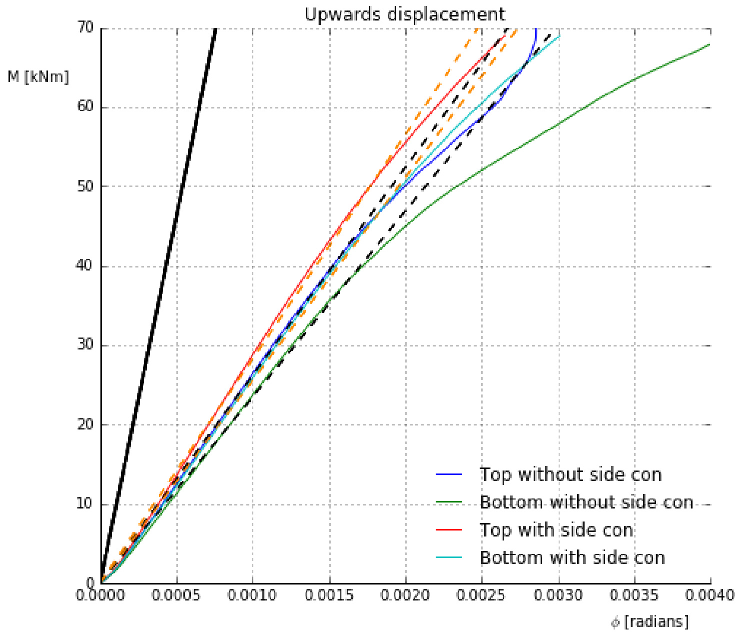

Figure 7.23: ZOOM $M - \phi$ curve for upwards displacement

The stiffness derived from figure 7.23 for the several graphs is:

- Top without side connections: $S_{j,ini}$ = 26165 kNm/rad
- Bottom without side connections: $S_{j,ini}$ = 23425 kNm/rad
- Top with side connections: $S_{j,ini}$ = 28230 kNm/rad
- Bottom with side connection: $S_{j,ini}$ = 25530 kNm/rad

The side connections result in an increase of the stiffness of 8% for the top and 9% for the bottom. The rigid classification boundary is also shown in figure 7.23, the stiffness of the joint is higher than half the beam stiffness and the joint can be classified as semi-rigid. The actual stiffness of the joint needs to be taken into account in the frame analysis. The elastic moment capacity of the joint without connections on the sides is 40 kNm and for the joint with connections on the side the elastic moment capacity is 50 kNm. The maximum possible sagging moment is 36 kNm, so for all joint which have a saggging moment the initial stiffness can be taken into account in the frame analysis.

In figure 7.24 the final deformation of the models is shown. Similar to the downwards displacement mode, without connections on the sides, the column flange is deforming at the location of the connection. The connections on the side prevent the local deformation of the column flange, the deformation is now the largest in the connection itself. In the figures 7.25, 7.26, 7.27 and 7.28 the model is rotated to show the tension side of the connection. In figure 7.25 the deformation of the connection can be better observed. The plug is yielding at the inclination and the plug plate is bending at the location of the bolts. The connections on the side prevent that plastic strains will occur in the column as can be seen in figure 7.26.

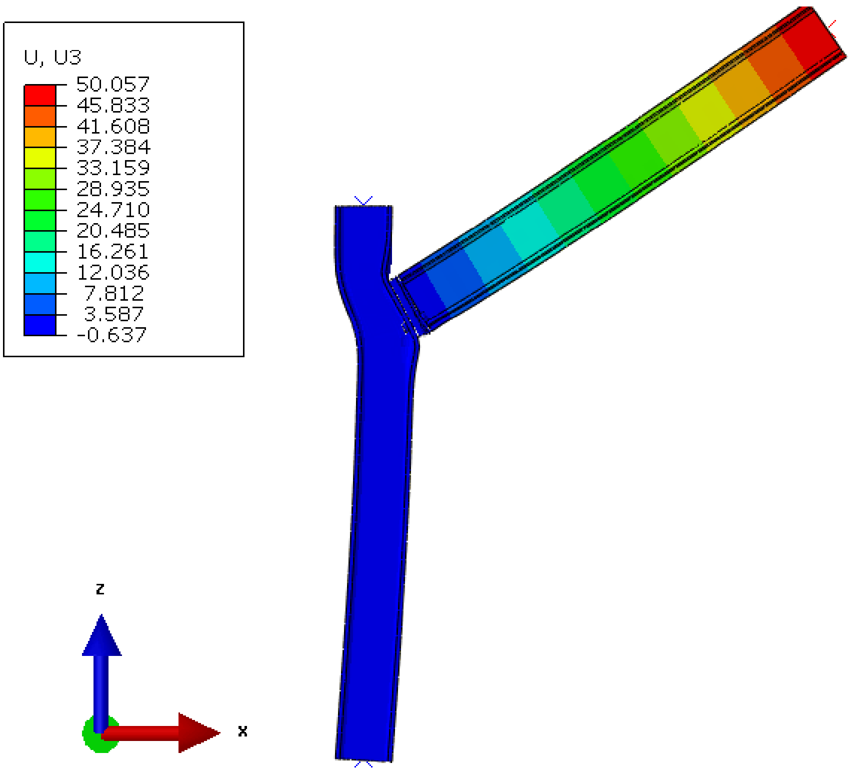

(a) Without connections on the sides

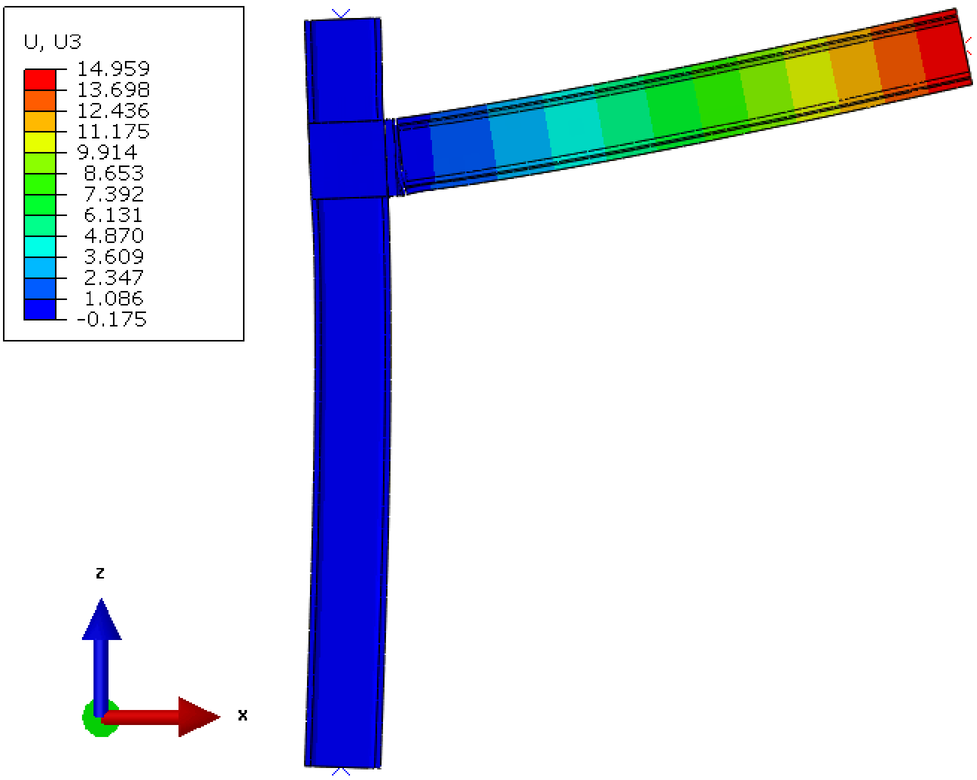

(b) With connections on the sides

Figure 7.24: Deformed model (scale factor 20) for upwards displacement

The figures 7.27 and 7.28 show the decomposition of the Von Mises stress in the global directions. The stresses for the joint with connections on the sides occur for a lower displacement compared to the stresses for the joint without side connections. But the figures already show where the largest stress will develop. The connections on the sides reduce the stresses in the column and at the contact area between the socket and column. The bending of the plug plate cause large normal stress in the Z direction around the bolt holes. The tension force caused by the bending moment in the connection makes the plug wants to pull out of the socket. The pull out causes large normal stress in the Y direction and causes the inclined parts of the socket and plug to bend. From the $M - \phi$ curves can be observed that the joint is stronger for upwards displacement then for downwards displacement. For both causes the plug plate is bending at the location of the bolts, for the upwards displacement case the distance from the tension side of the connection to the bolts is smaller compared with the downwards displacement case. A smaller area of the plug plate is deforming for the upwards case then for the downwards case, this results in a stiffer and stronger connection. The bolts have a higher strength and when the plug plate has yielded at the bolts, then the bolts will carry the load.

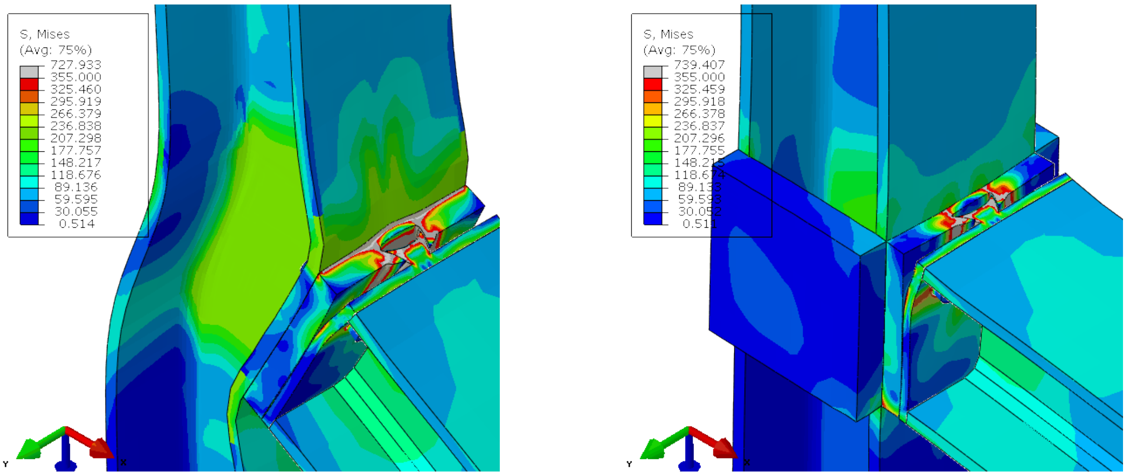

(a) Von Mises (b) Von Mises

Figure 7.25: Von Mises stress (scale factor 20)

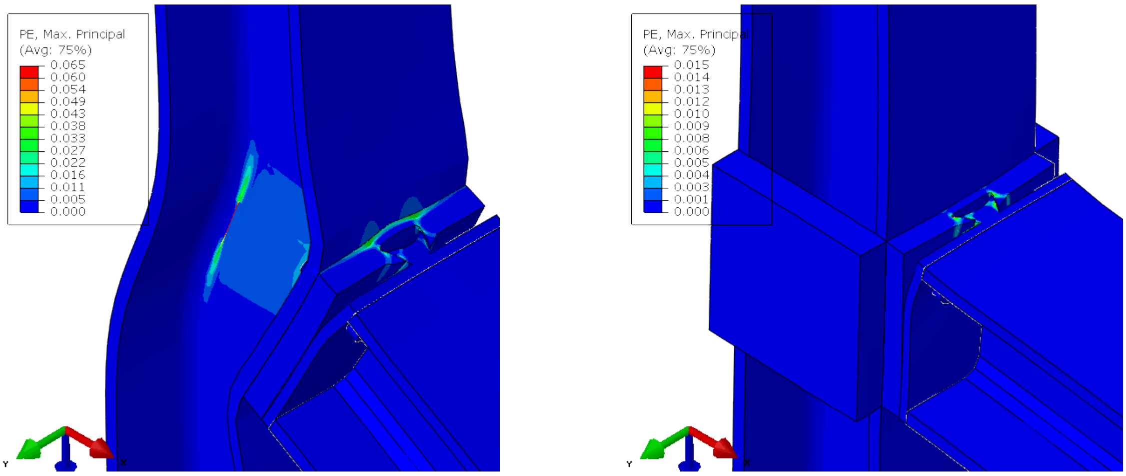

(a) Plastic strain (b) Plastic strain

Figure 7.26: Plastic strain (scale factor 20)

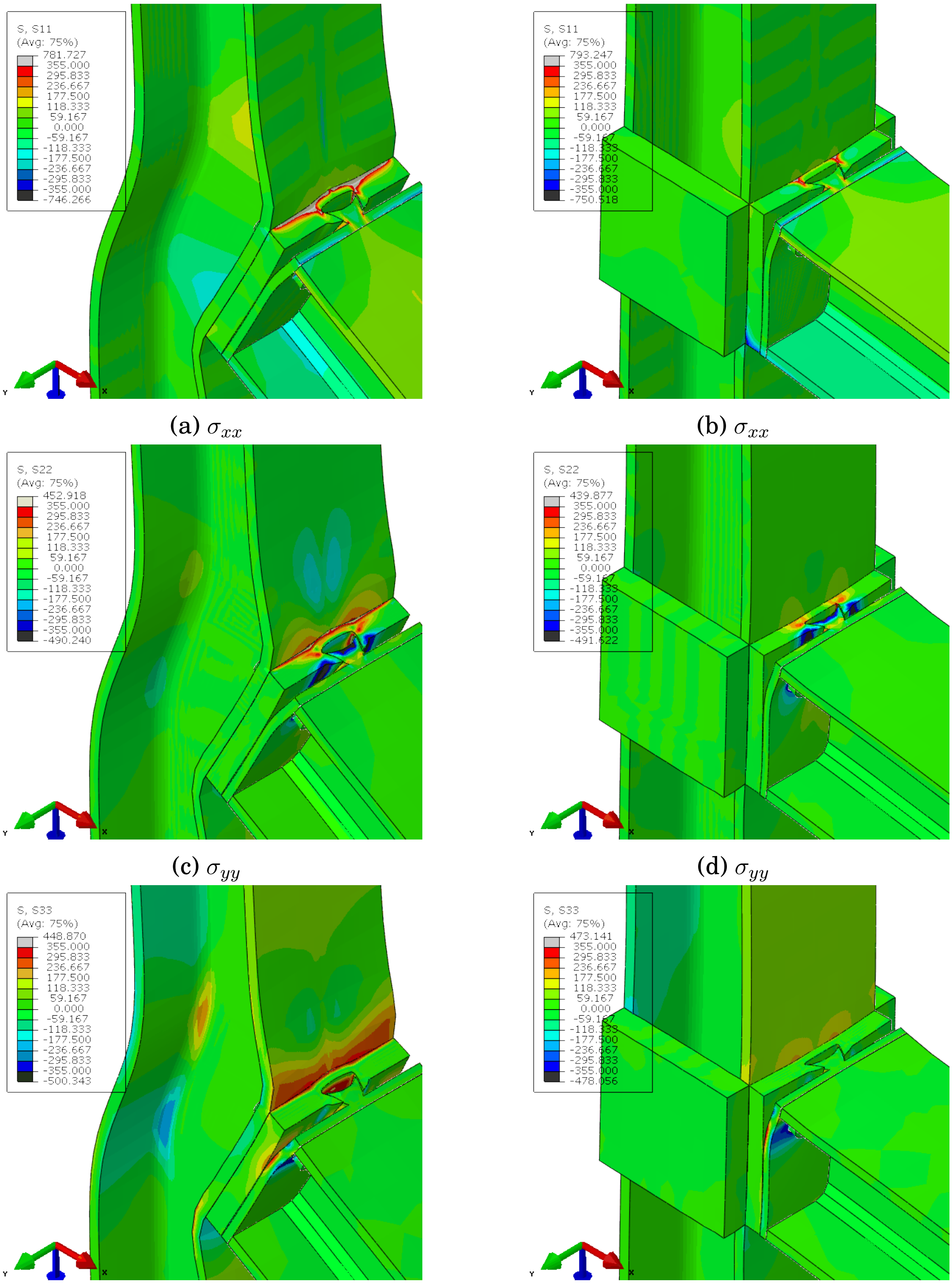

(a) σ_{xx} (b) σ_{xx}

(c) σ_{yy} (d) σ_{yy}

(e) σ_{zz} (f) σ_{zz}

Figure 7.27: Normal stress (scale factor 20)

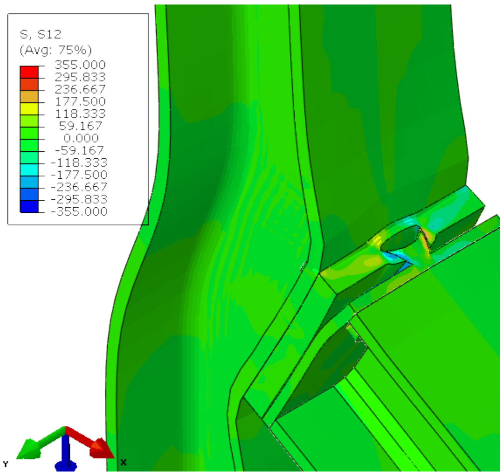

(a) σ_{xy}

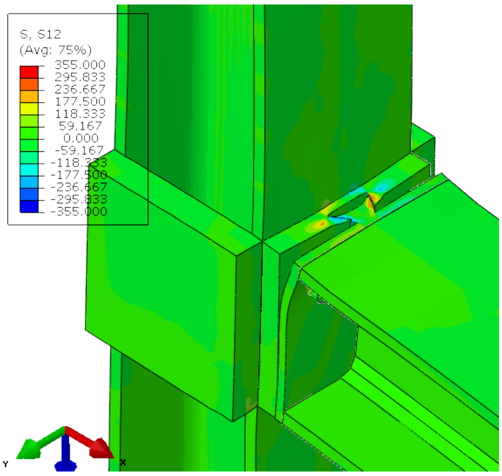

(b) σ_{xy}

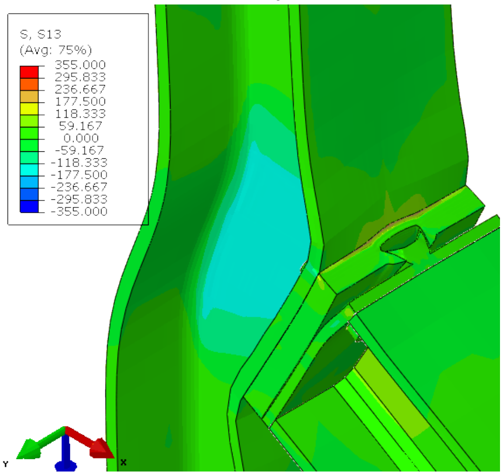

(c) σ_{xz}

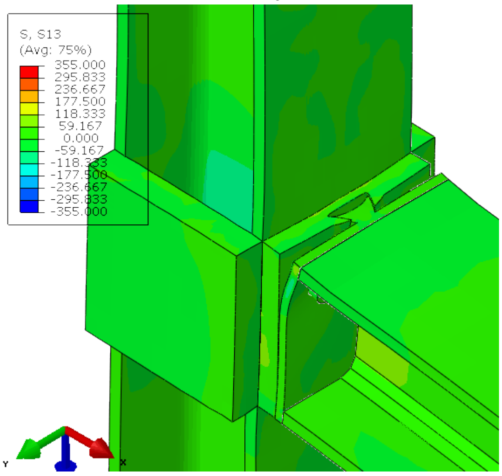

(d) σ_{xz}

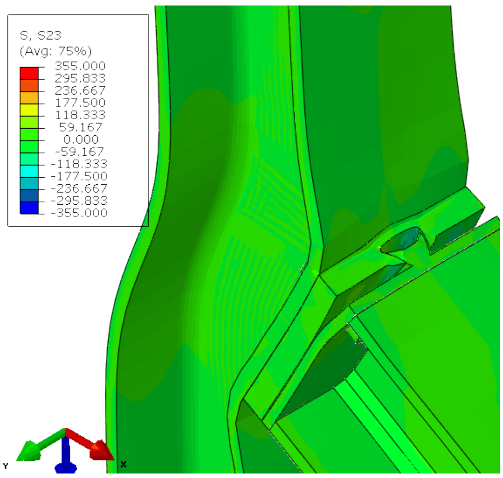

(e) σ_{yz}

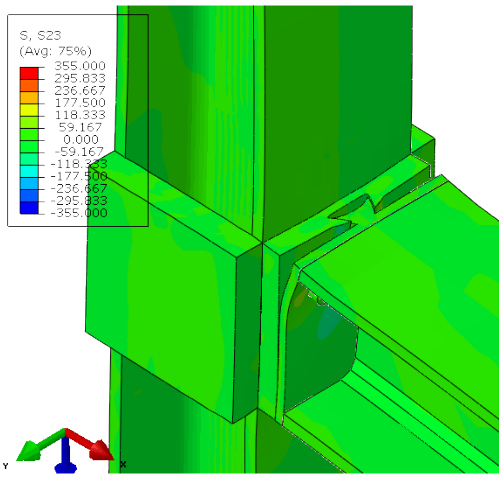

(f) σ_{yz}

Figure 7.28: Shear stress (scale factor 20)

Out-of-plane displacement

Due to the wind loads the joints are subjected to out-of-plane bending, therefor the joint is also investigated for out-of-plane bending. The test is run for both the model with and without connections on the sides, to see what the effect is of the connections on the sides. The out-of-plane bending moments are low compared to the in-plane bending moments, the maximum possible out-of-plane bending moment is 11 kNm. Both test are run for a maximum out-of-plane displacement of 50mm. The joint is symmetric so the results are fot both a positive or negative out-of-plane bending moment.

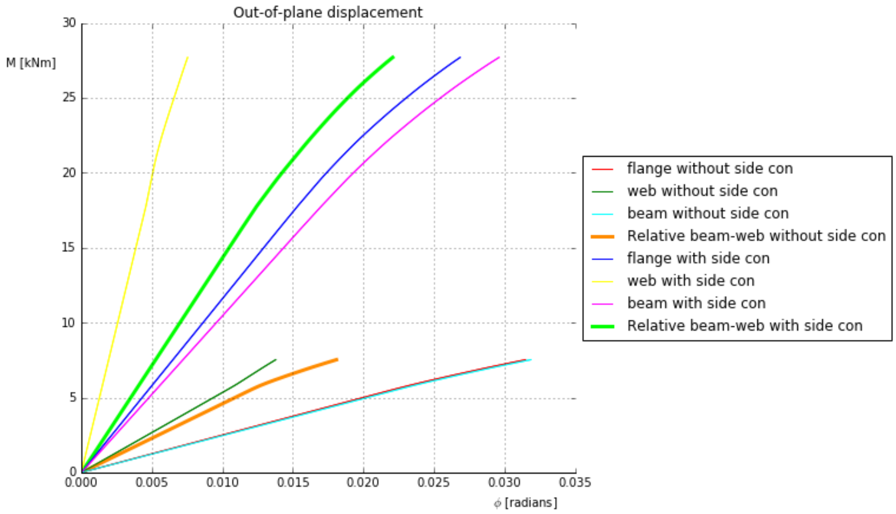

Figure 7.29: $M - \phi$ curve for out-of-plane displacement

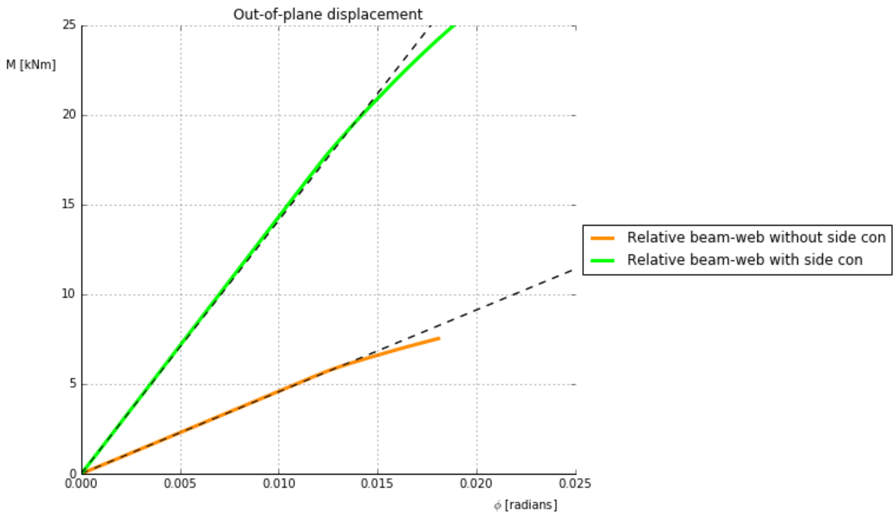

Figure 7.30: $M - \phi$ curve for relative rotation

The initial stiffness for the joint without connections on the sides is 455 kNm/rad and for the joint with connections on the side the initial stiffness is 1410 kNm/rad. The side connections increase the out-of-plane stiffness of the joint with 210%. The code provide no information for the stiffness classification of out-of-plane loaded joints, therefor the actual stiffness of the joint will be used. The elastic moment capacity is 21 kNm. The maximum out-of-plane moment falls in the elastic range so for all joints the initial stiffness can be used.

Figure 7.29 shows that the connection on the sides decrease the rotations of the joint. For the model without the connections on the sides the rotation of the flange is almost equal to the rotation of the beam. Taking into account the connections on the sides increases the relative rotation between the flange and beam. The small difference between the curve of the column flange and the curve of the beam shows that the rotation in the plug & play connection is small. Most of the beam rotation is due to the rotation of the flange.

In figure 7.31 the Von Mises stresses in the joint are shown. The subfigures 7.31a and 7.31b show a topview of the deformed joint. The limit of the legend in these subfigures is set at 235MPa which is the yield stress of the section material, these subfigures show that the yielding will occur in the web of the section. If there are no connections on the side only the part of the web closest to the beam will yield. When the side connections are taken into account also higher stress will develop in the other flange. The the web will yield then at both ends. The subfigures 7.31c and 7.31d show the Von Mises stress in which the limit of the legend is set at 355MPa, this is to show the stress in the plug & play connection, it can be seen that the inclination angle of the plug & play connection in tension is close to yielding. The figure 7.32 shows the plastic strains. The subfigure with the side connections shows that only a small part of the inclination angle in tension will yield. In both cases the columnweb will yield in the zones where the yield stress is reached.

In the figures 7.33 and 7.34 the normal and shear stress in the global directions is shown. Local stress concentrations develop in the inclination and around the bolt in tension. The plug plate will yield around the bolt in tension. The σ_{zz} in the top of the column is a consequence of the boundary conditions which do not allow the column to rotate along its axis.

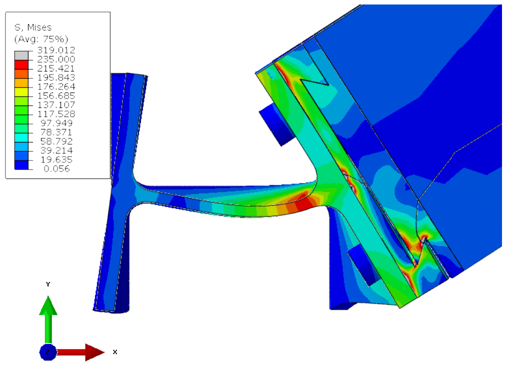

(a) Von Mises (limit legend 235MPa)

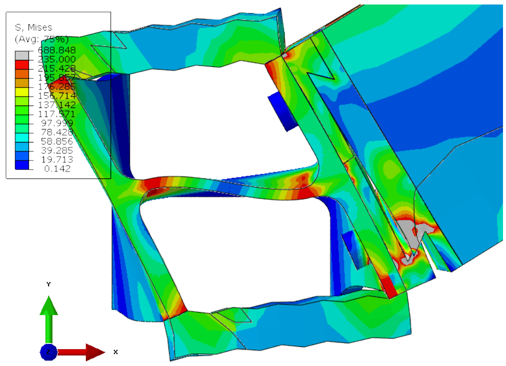

(b) Von Mises (limit legend 235MPa)

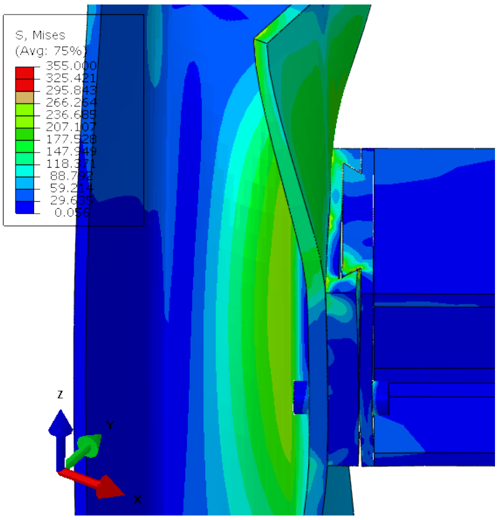

(c) Von Mises (limit legend 355MPa)

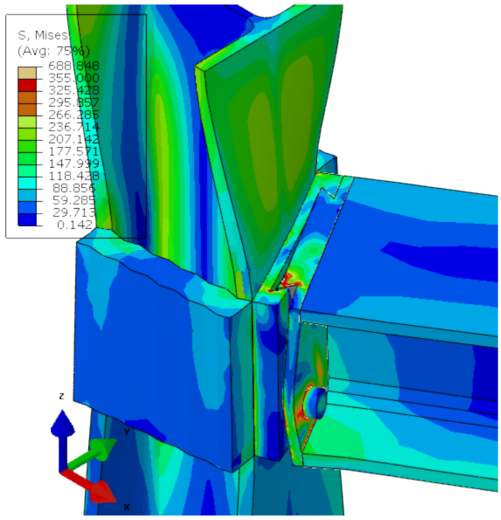

(d) Von Mises (limit legend 355MPa)

Figure 7.31: Von Mises stress (scale factor 20)

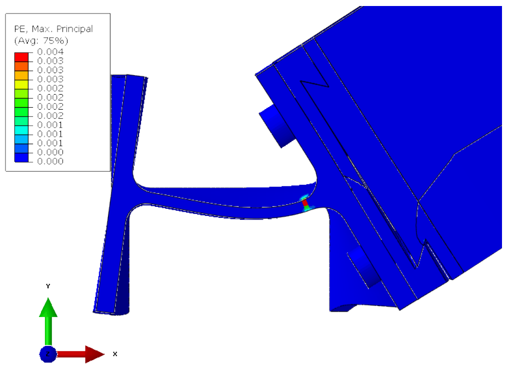

(a) Plastic strain

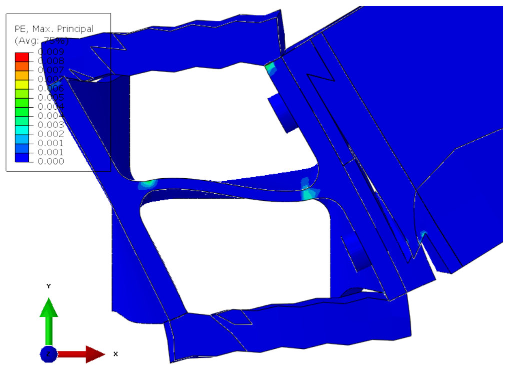

(b) Plastic strain

Figure 7.32: Plastic strain (scale factor 20)

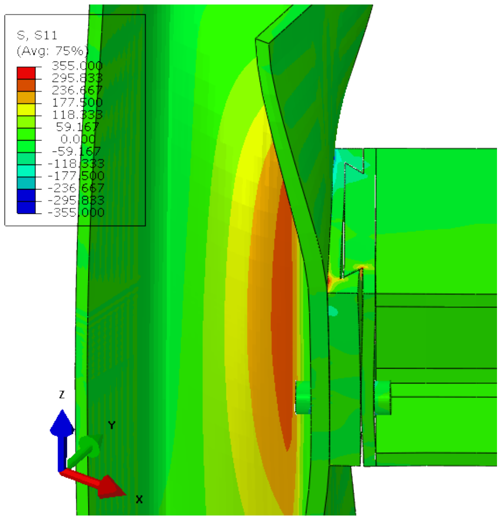

(a) σ_{xx}

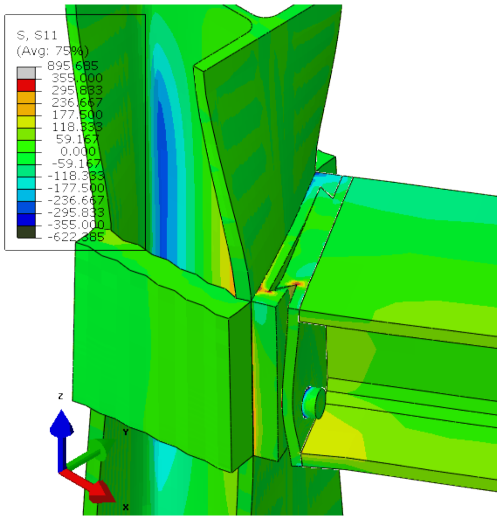

(b) σ_{xx}

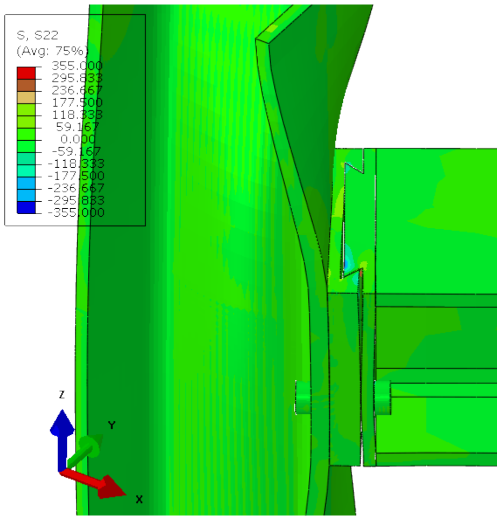

(c) σ_{yy}

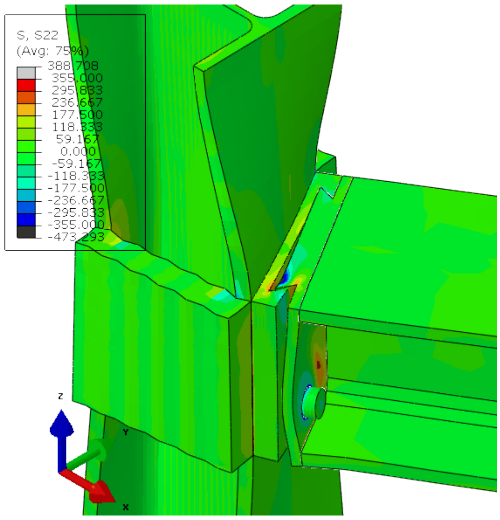

(d) σ_{yy}

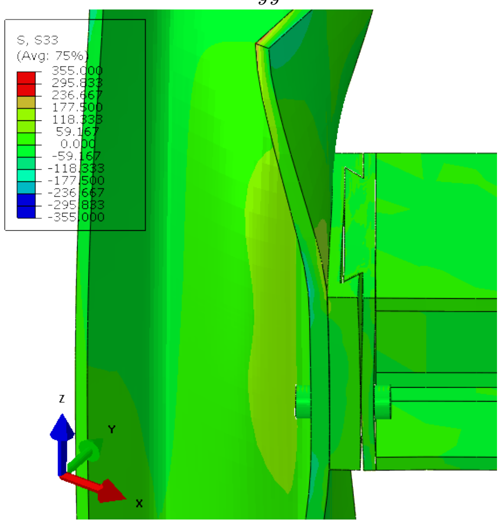

(e) σ_{zz}

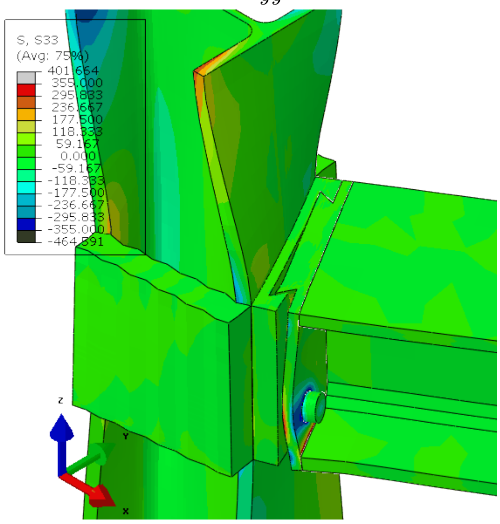

(f) σ_{zz}

Figure 7.33: Normal stress (scale factor 20)

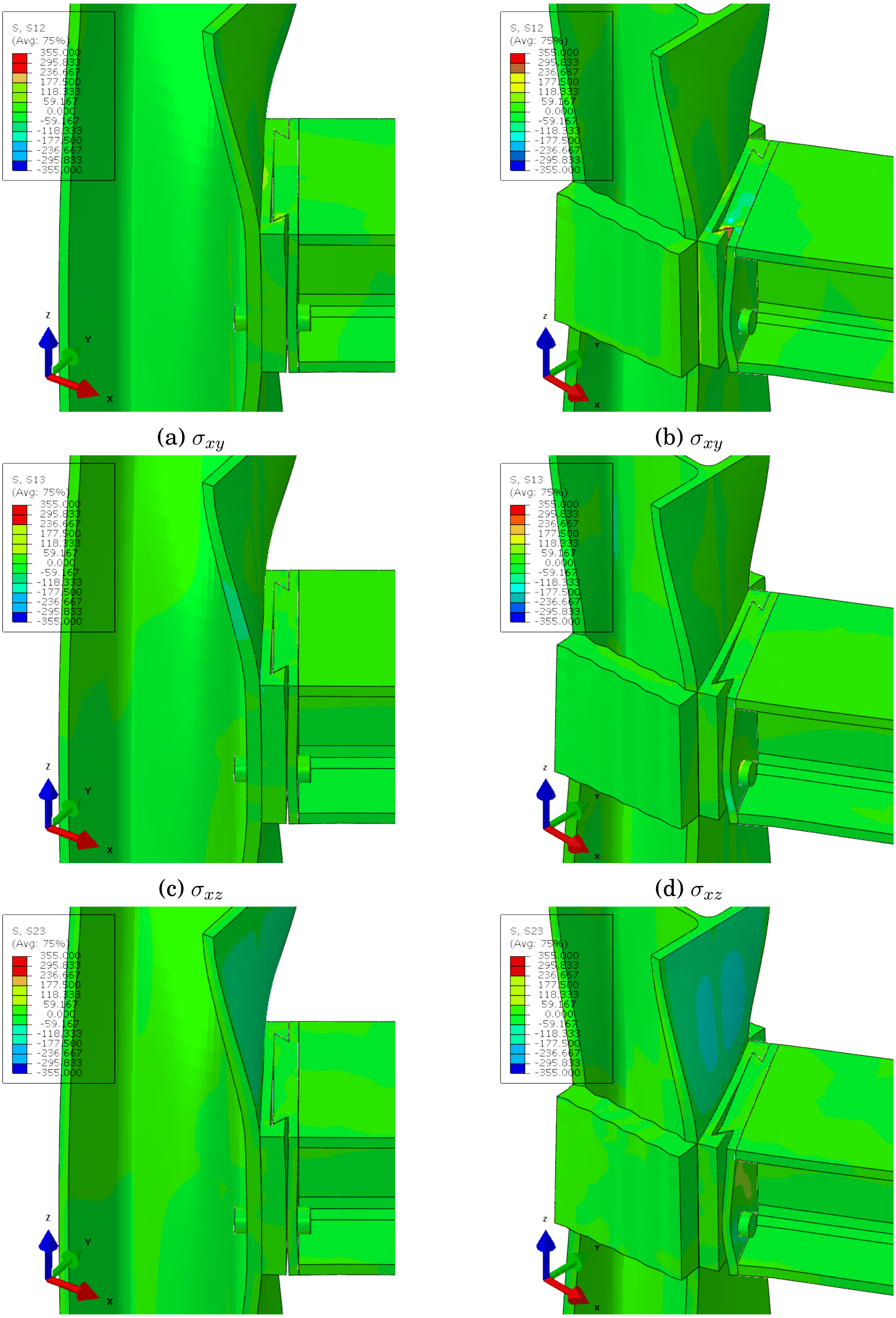

(a) σ_{xy} (b) σ_{xy}

(c) σ_{xz} (d) σ_{xz}

(e) σ_{yz} (f) σ_{yz}

Figure 7.34: Shear stress (scale factor 20)

7.5.3 Column minor axis analysis

The connection is attached to both the major and minor axis of the column. This section shows the results for the minor axis models.

For the minor axis case only one model is analysed. The model used to derive the $M - \phi$ curves is shown in figure 7.35.

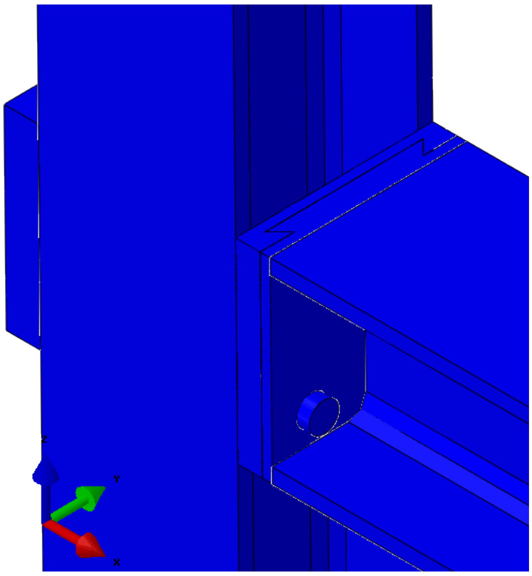

Figure 7.35: Numerical model

The model consist of one plug & play connection attached to both flanges and beam. The plug & play model on the side without beam is simplified as a solid plate. A static analysis was used to check the minor axis models.

Downwards displacement

The moment rotation curves for the minor case are obtained in the same way as for the major case. Two rotations of the beam are measured, above and below the intersection point. The moment rotation curve for a downwards displacement around the minor axis is shown in figure 7.36 and figure 7.37 zoomed in on the elastic part of the curve. The stiffness of the minor axis is 11260 kNm/rad for the top part and 9780 kNm/rad for the bottom part. The stiffness of the minor axis is for the top and bottom part respectively: 54% and 49% lower then the stiffness of the major axis case with connections on the sides, for downwards displacement. For the stiffness classification boundary the column has no the lowest stiffness as it is loaded along its weak axis. The beam stiffness of the column along its weak axis is $\frac{EI_c}{L_c} = 1315kNm/rad$ for a HEB200 and a column length of 3200mm. The rigid boundary is 25 times the beam stiffness and is drawn in figure 7.37. The pinned stiffness classification boundary of the joint is 0.5 the stiffness of the beam, the stiffness of the joint is above this value. The elastic capacity is 23 kNm, for moments above the elastic capacity the secant stiffness needs to be taken into account in the global analysis.

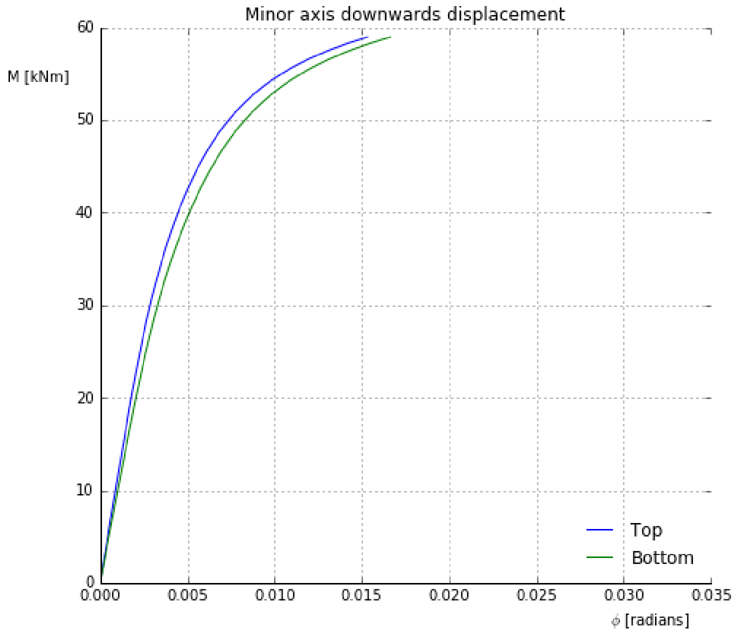

Figure 7.36: $M - \phi$ curve for minor axis downwards displacement

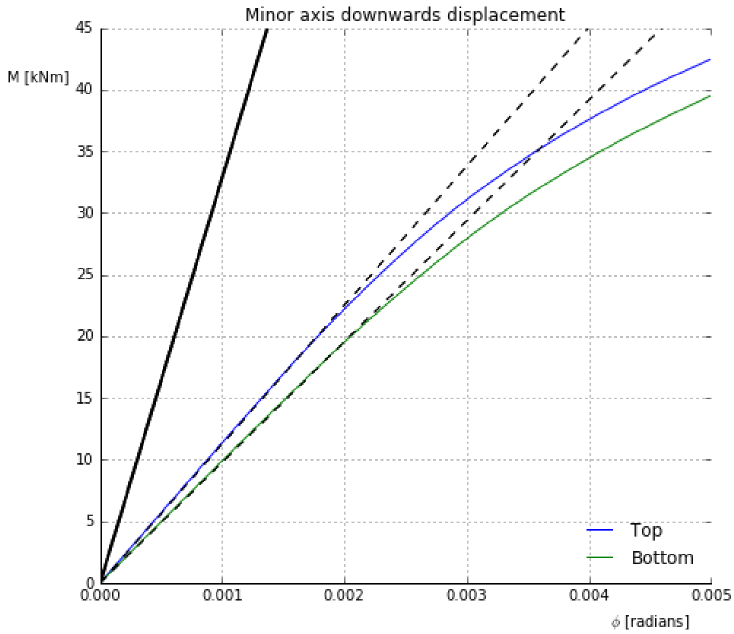

Figure 7.37: ZOOM of the $M - \phi$ curve for minor axis downwards displacement

In figure 7.38 the deformed model is shown at the final displacement of 50mm. The deformation is similar to the deformation model of the major axis case with side connections of figure 7.17. In figure 7.39 the Von Mises stress and plastic strain of the joint are shown. The joint shows plastic strain in the same parts of the connection as the major case, namely in the corners of the inclined parts of the plug and socket. Plastic strains will also develop in the socket where they are attached to the column. For the major axis case the surface of the socket is in full contact with the the column flange, for the minor axis case only a small part of the socket is in contact with the column flanges. As a consequence of this small contact part the socket will behave as a beam which is pinned supported. The inclined parts of the socket lead to moments in the sockets which causes bending of the socket. This can clearly be observed in the figures 7.39 and 7.40. In figure 7.40 the σ_{yy}, in the middle part of the socket, is the same as for a pinned beam subjected to a bending moment at both sides. The minor axis bending does not cause significant stress in web of the column. The σ_{xz}, in the socket, is a consequence of the torsional rotation of the socket. The tension part of the socket will rotate due to the bending behaviour while the compressive part of the socket is not subjected to bending.

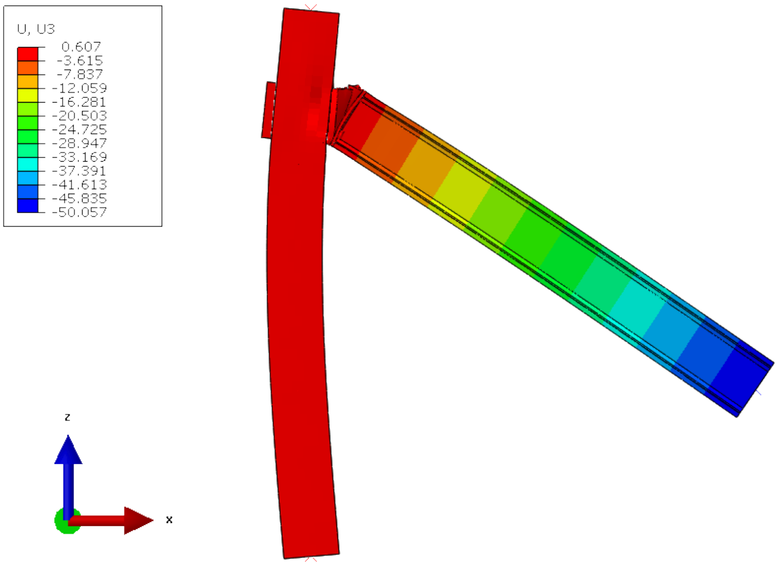

Figure 7.38: Deformed model (scale factor 20) downwards displacement

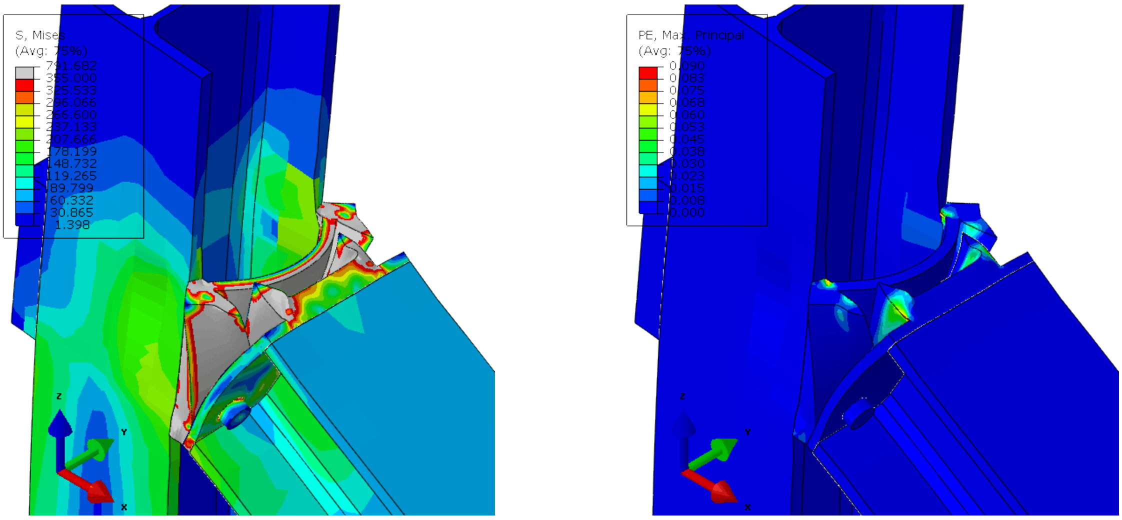

(a) Von Mises stress

(b) Plastic strain

Figure 7.39: Von Mises stress and plastic strain (scale factor 20)

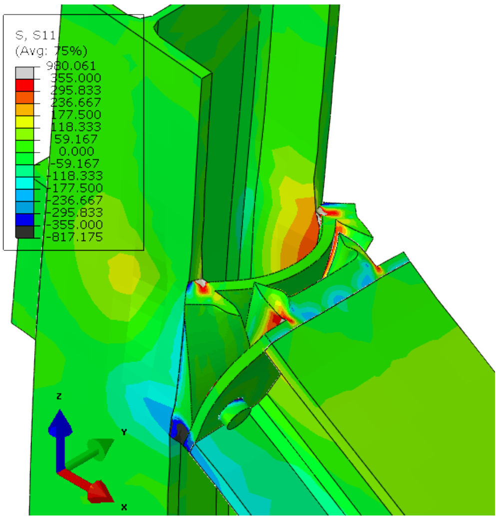

(a) σ_{xx}

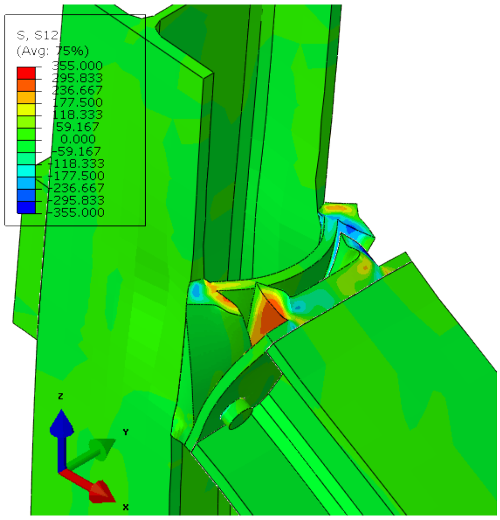

(b) σ_{xy}

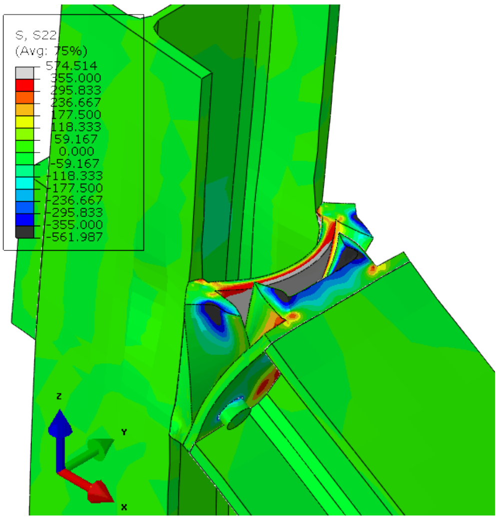

(c) σ_{yy}

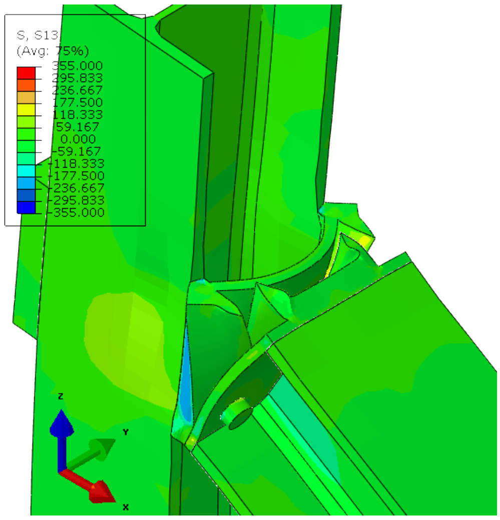

(d) σ_{xz}

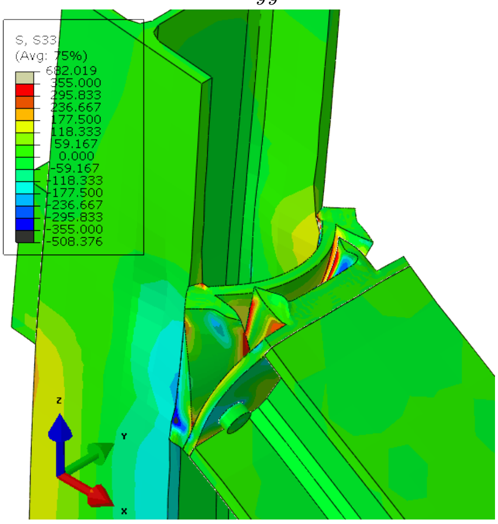

(e) σ_{zz}

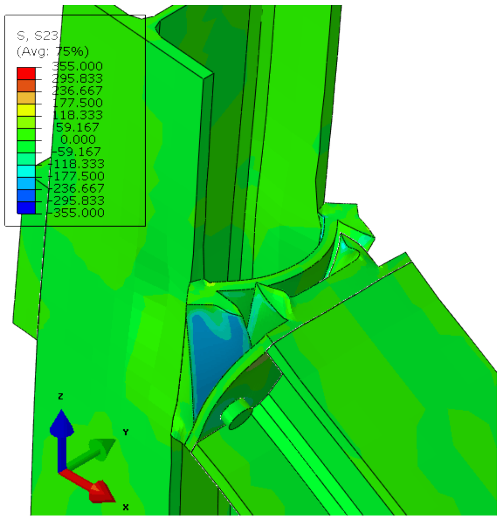

(f) σ_{yz}

Figure 7.40: Normal and shear stress (scale factor 20)

Upwards displacement

The model for upwards displacement stopped at a maximum displacement of 29mm of a total maximum applied displacement of 50mm. The results presented are the results at the final displacement of 29mm. The $M-\phi$ of the joint is given in figure 7.41 and in figure 7.42 is zoomed in on the elastic part of the $M-\phi$ curve. The stiffness is 8367 kNm/rad for the top part and 8786 kNm/rad for the bottom part. This is respectively 70% and 66% lower compared to the stiffness of the major axis case with connections on the sides, for upwards displacement. The stiffness classification boundary is also shown in figure 7.42 and it shows that the joint can be classified as semi-rigid. The elastic capacity is 32 kNm, for moments beyond this value the secant stiffness needs to be taken into account.

Figure 7.43 shows the deformation at the last increment. The displacement is similar to the major axis case with connections on the sides. The connection has the largest displacement and no local rotation occurs in the column.

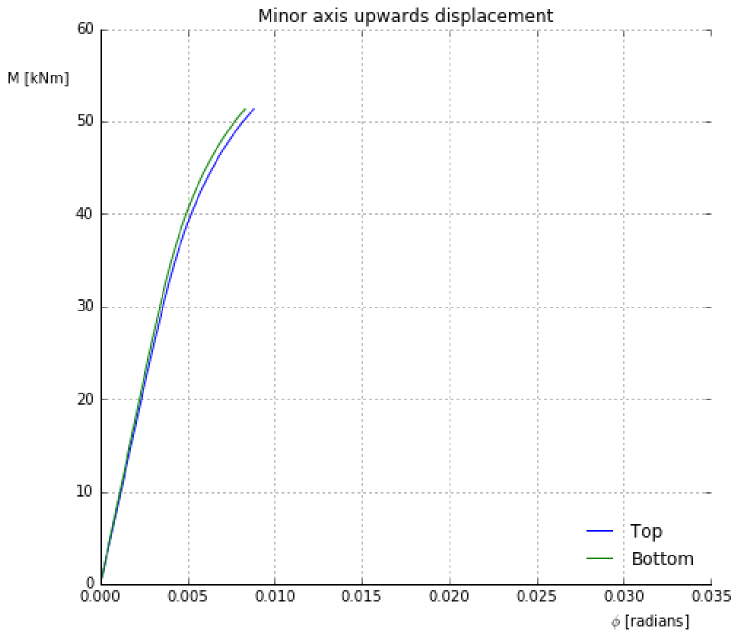

Figure 7.41: $M-\phi$ curve for minor axis upwards displacement

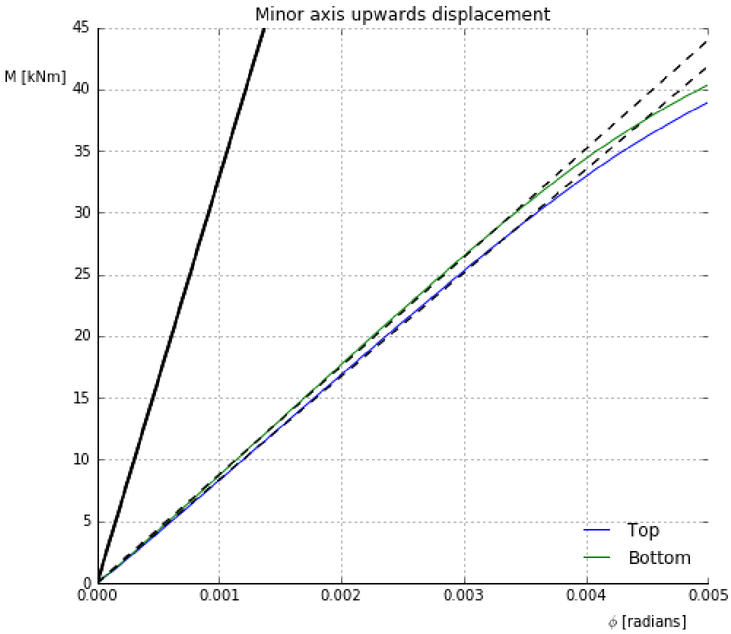

Figure 7.42: ZOOM $M - \phi$ curve for minor upwards displacement

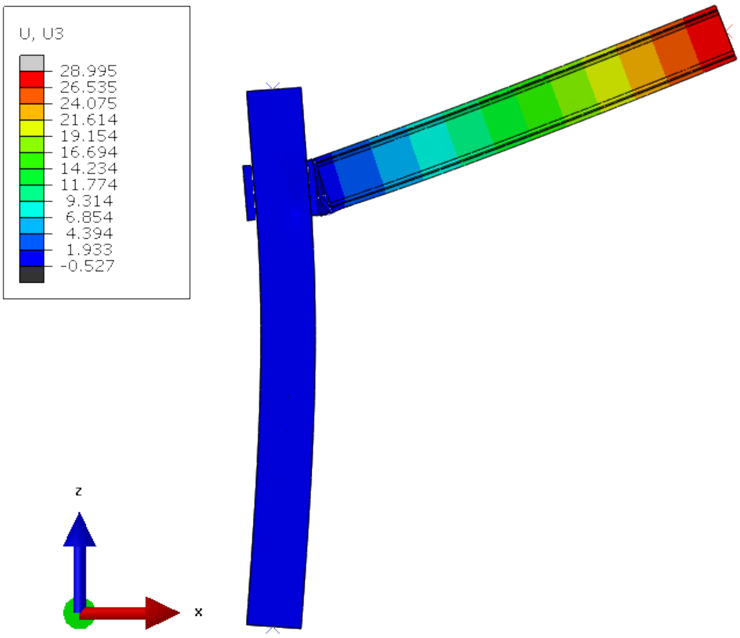

Figure 7.43: Deformed model (scale factor 20) upwards displacement

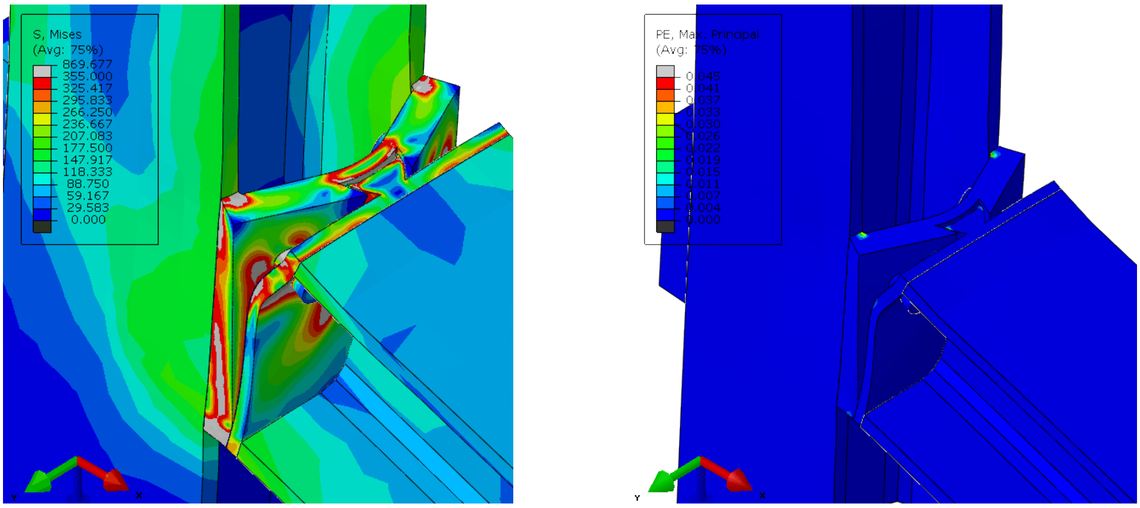

(a) Von Mises stress (b) Plastic strain

Figure 7.44: Von Mises stress and plastic strain (scale factor 20)

The figures 7.44, 7.45 and 7.46 the model is rotated to show the tension side of the connection. In figure 7.44 is shown that the connection is yielding the area around the bolts and the inclination also the tension and compression point of the socket with the column flanges are yielding. At the tension side the plug has only contact with the socket at the inclined area and at the bolts. The bolts prevent that the plug loses contact with the socket. For the minor axis case the bolts are yielding at the tension side. For the major axis case also higher bolt stress develops at the tension side, the bolt is only yielding just below the bolt head at the plug side. The bending of the socket makes that the inclination will open. This opening cause that it is easier to pull the plug out of the socket easier. The pull out behaviour of the plug in the minor axis case cause an increased stress in the bolts compared with the major axis case. See figure 7.45.

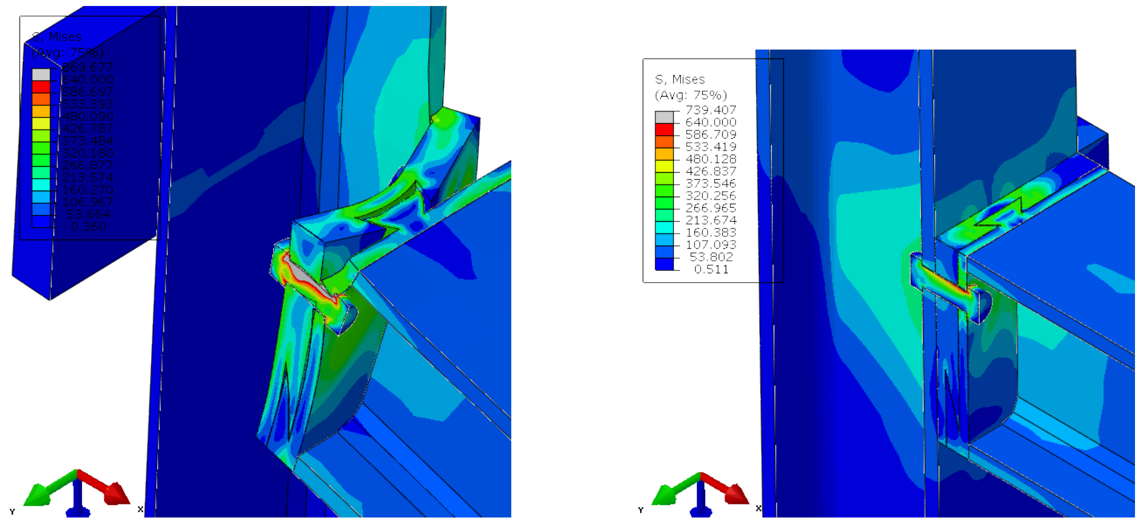

(a) Bolt stress minor axis case (scale factor 20) (b) Bolt stress major axis case (not scaled)

Figure 7.45: Bolt stress for upwards displacement

Figure 7.46 shows the decomposition of the Von Mises stress in the global directions. Similar to the minor downwards case the socket is bending as well. For the minor downwards case the moments introduced due to the inclined parts are closer to the flanges, will for the minor upwards case the inclined parts are closer to the middle of the socket. The plug bends like a pinned supported beam with moments acting close to the middle of the beam. The main contribution for the yielding of the socket at the location of the flanges is the σ_{xx}. The socket is yielding both in compression and tension at the contact with the flange. The yielding in the tension side of the socket is a combination of compression stress introduced by the bending of the socket and tension stress caused by the global bending, introduced by the beam on the connection. The compression at the bottom is caused by the global bending. That the bending moments are at the location of the inclination can be clearly observed from the σ_{yy}, the stress in y direction is the same as for a pinned beam in bending where only a bending moment is in the middle part of the beam. Similar to the previous cases, the plug plate will bend around the bolts. This results in a high stress in both the Y and Z direction in the plug. The high σ_{xz} in the outside part of the socket is a result of the torsional rotation of the socket. The tension side of the socket will bend but the compression side will not bend, this causes a torsional rotation in the socket.

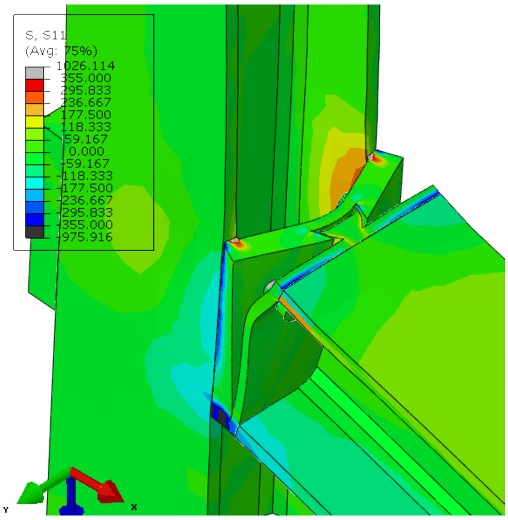

(a) σ_{xx}

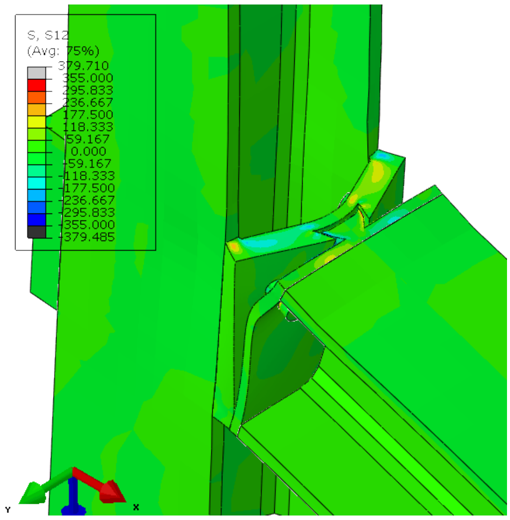

(b) σ_{xy}

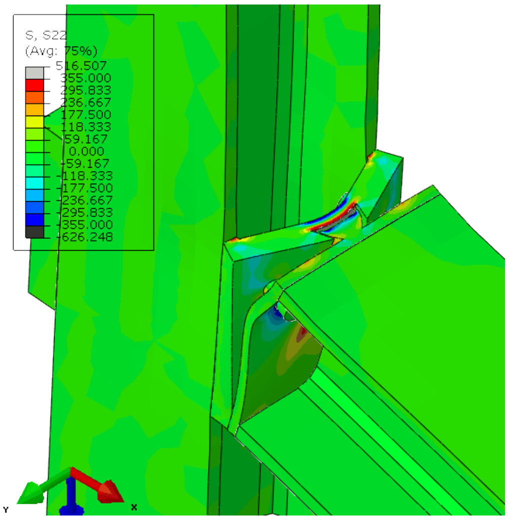

(c) σ_{yy}

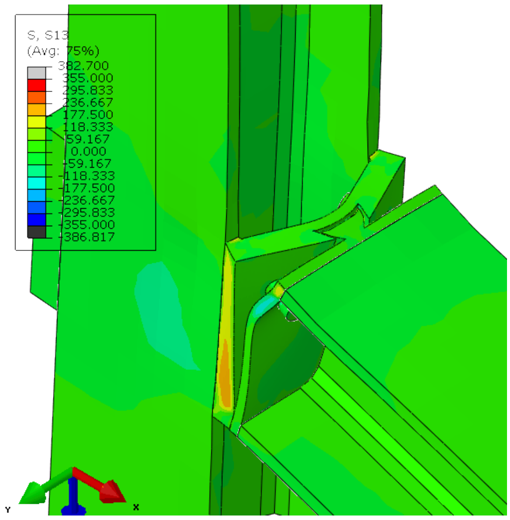

(d) σ_{xz}

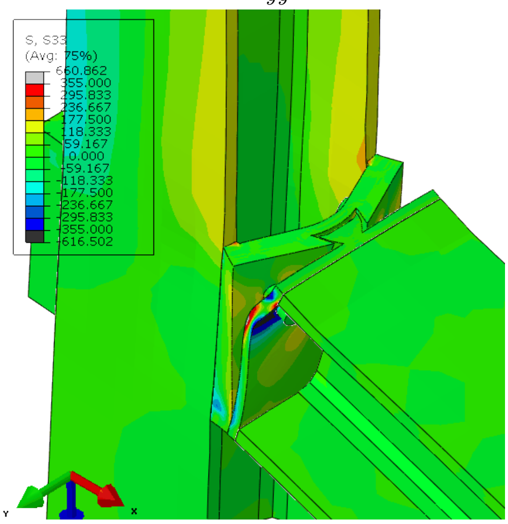

(e) σ_{zz}

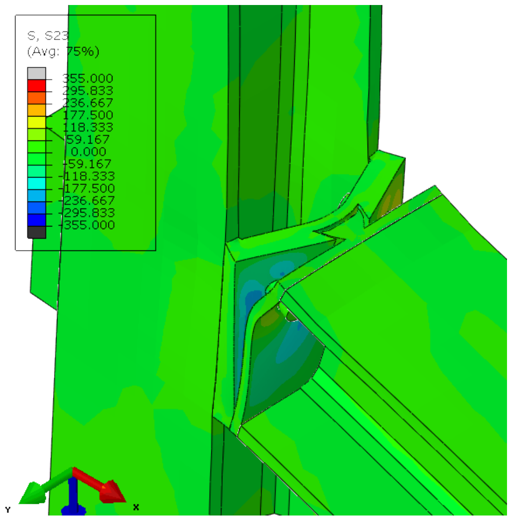

(f) σ_{yz}

Figure 7.46: Normal and shear stress (scale factor 20)

Out-of-plane displacement

Similar to the major axis joint the minor axis joint is also subjected to out-of-plane bending moments. For the analysis of the out-of-plane displacement around the minor axis of the column different data points are used compared to the major axis case. Gil, Goñi and Bayo performed also tests on a minor axis joint subjected to out-of-plane bending. The used test setup is shown in figure 7.47. The joint is symmetric so the results is for positive and negative out-of-plane bending moments the same.

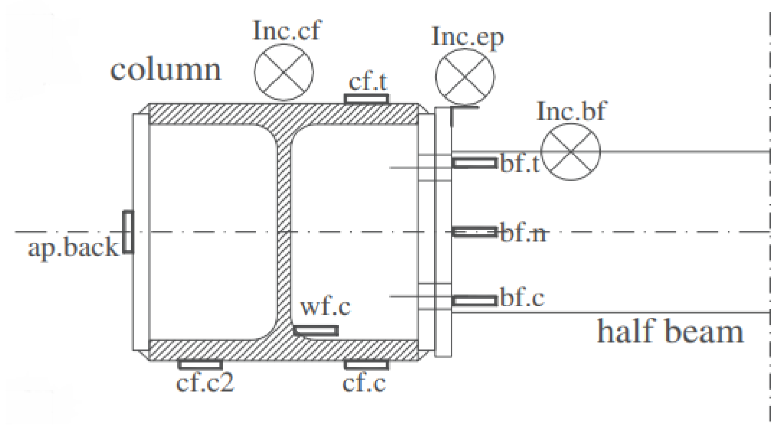

Figure 7.47: Test setup out-of-plane bending for column minor axis [11]

The figure 7.48 the used data points are shown. These data points are used to calculate the rotations of the inclinometers as shown in figure 7.47.

- **Rotation flange:** is calculated between points 1 and 2
- **Rotation connection:** is calculated between points 2 and 3
- **Rotation beam:** is calculated between points 3 and 4

The relative rotation is the rotation of the beam minus the rotation of the flange

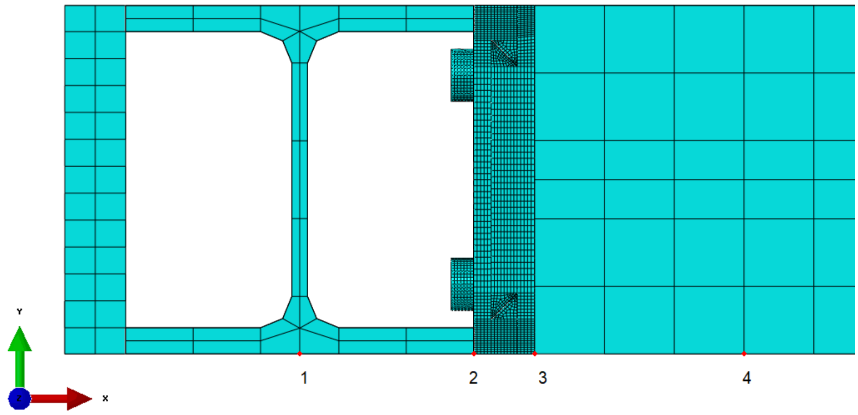

Figure 7.48: Data points for minor axis out-of-plane bending

Figure 7.50 shows the elastic part of the joint. The $S_{j,ini}$ of the joint is 5820 kNm/rad, this is 312% stiffer than the stiffness of the major axis out-of-plane stiffness including connections on the sides. The code provide no information of the classification of out-of-plane loaded joints, so the actual stiffness will be used. The elastic moment capacity of the joint is 17 kNm, for moments above this value the secant stiffness need to be used.

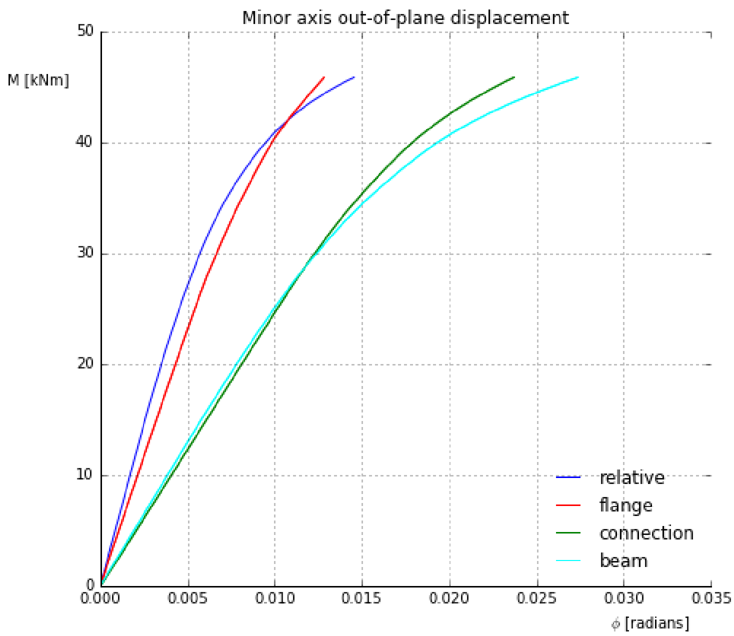

Figure 7.49: $M - \phi$ curve minor axis out-of-plane displacement

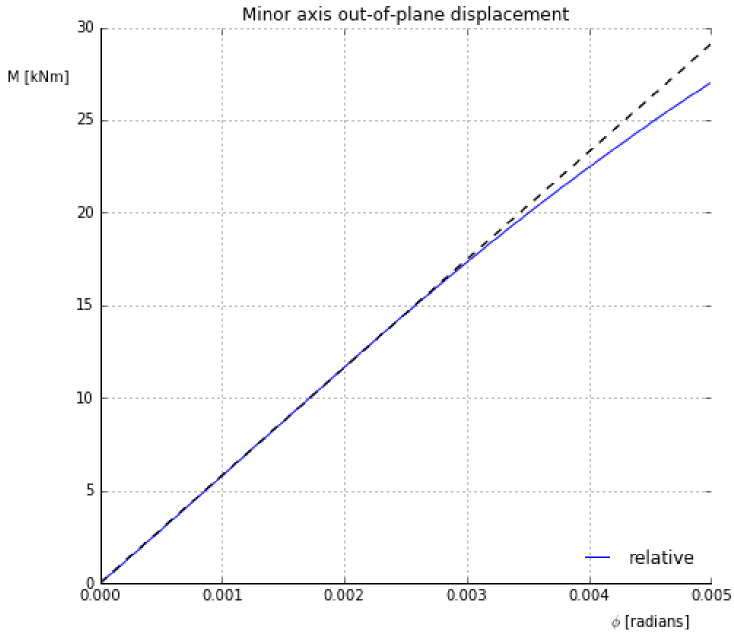

Figure 7.50: ZOOM of the $M-\phi$ curve for minor axis out-of-plane displacement

The large difference in stiffness can be clarified by figures 7.51 and 7.52. Figure 7.51 shows the Von Mises stress in the joint with legend up to 235MPa, which is the yield strength of the sections. It can be seen that the point at which the section first starts to yield would be in the end of the loaded column flanges, the major axis case showed that the section would yield in its flange. The figure 7.39 shows the Von Mises stress with a legend up to 355Mpa and the plastic strain in the joint. In the major axis case there was limited yielding in the connection for the minor axis case a large part of the plug & play connection is yielding and the plug plate is bending. The figure shows that the plastic strain will only develop in the connection and not in the section. For the major axis case a the flange of the column would bend a lot, for the minor axis case the connection is attached to both flanges and a rotation of the whole column is observed instead of local flange rotation. The weakest part for the minor axis case is the connection instead of the column in the major axis case.

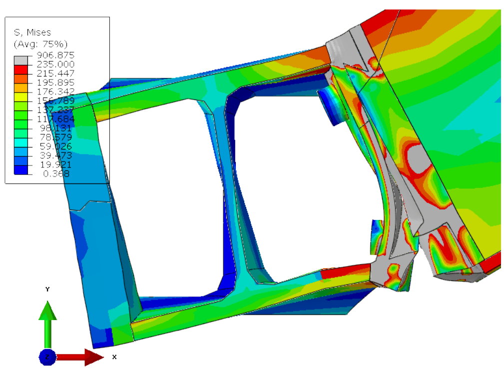

Figure 7.51: Von Mises (limit legend 235MPa and scale factor 20)

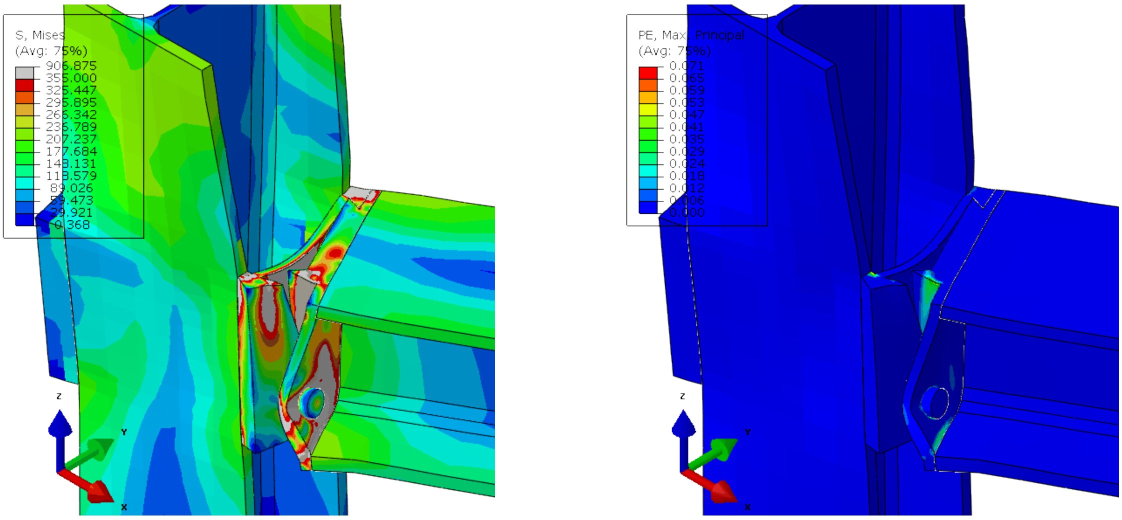

(a) Von Mises (limit legend 355MPa)

(b) Plastic strain

Figure 7.52: Von Mises and plastic strain (scale factor 20)

In figure 7.54 the stresses in the global directions is shown. Similar to the minor axis upwards displacement bending of the socket plate will occur. This can be seen in the tension stress σ_{yy} in the socket. Where for downwards displacement the whole inner part of the socket would bend more uniform, the bending of the socket due to the out-of-plane displacement is more on the tension side of the connection. This can be explained that only the tension side will cause a bending moment on the socket, the compression side will not cause a bending moment on the socket. So the socket will behave as a beam with pinned supports on which a bending moment on only one side is acting. The σ_{zz} in the top of the column is a consequence of the boundary conditions which do not allow the column to rotate alongs its axis. Besides the σ_{zz} no other significant stress will occur in the column. In the beam large axial stress (σ_{xx}) will develop, in the major axis case the column flange was the weakest part so the connection and beam could rotate without getting a large stress in the beam. In the minor axis case the column is not rotating. The displacement is causing a bending moment on the beam and connection, which cause the large σ_{xx} in the beam and connection. For the major axis case the rotation point was in the column web just below the beam flange, for the minor axis case the rotation point is at the compression flange. In figure 7.53 the stress in the bolts is shown. For the minor axis case the bolts will yield, while for the major axis case there is almost no force in the bolt. For the major axis cause the column flange will rotate and socket will not bend, for the minor axis cause the column will not rotate and the socket will bend. The bending of the socket cause that the inclination of the socket will open. The opening of the socket makes it easier for the plug to be pulled out of the socket and this leads to increasing bolts stress.

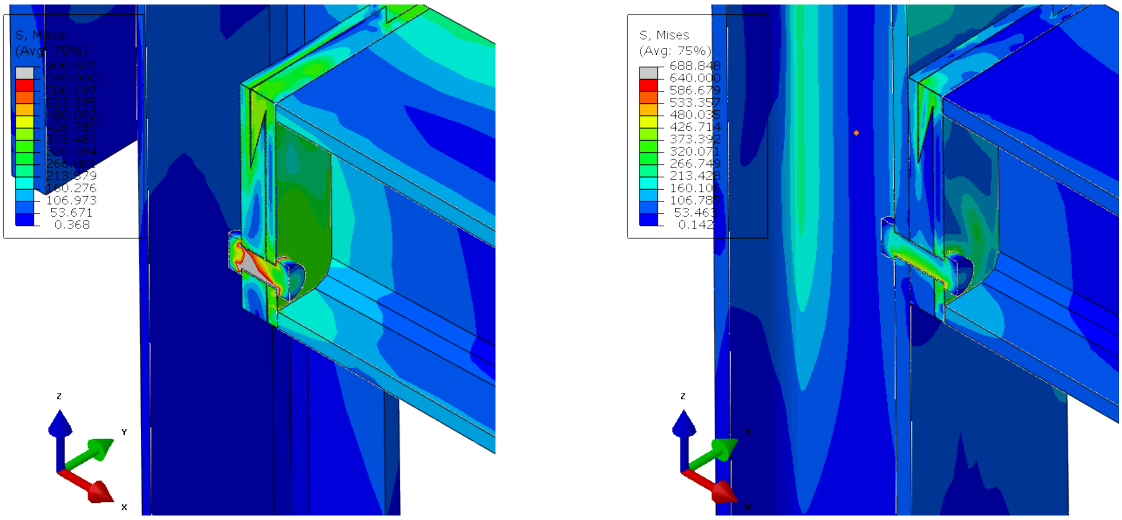

(a) Bolt stress minor axis case (scale factor 20)

(b) Bolt stress major axis case (not scaled)

Figure 7.53: Bolt stress for out-of-plane displacement

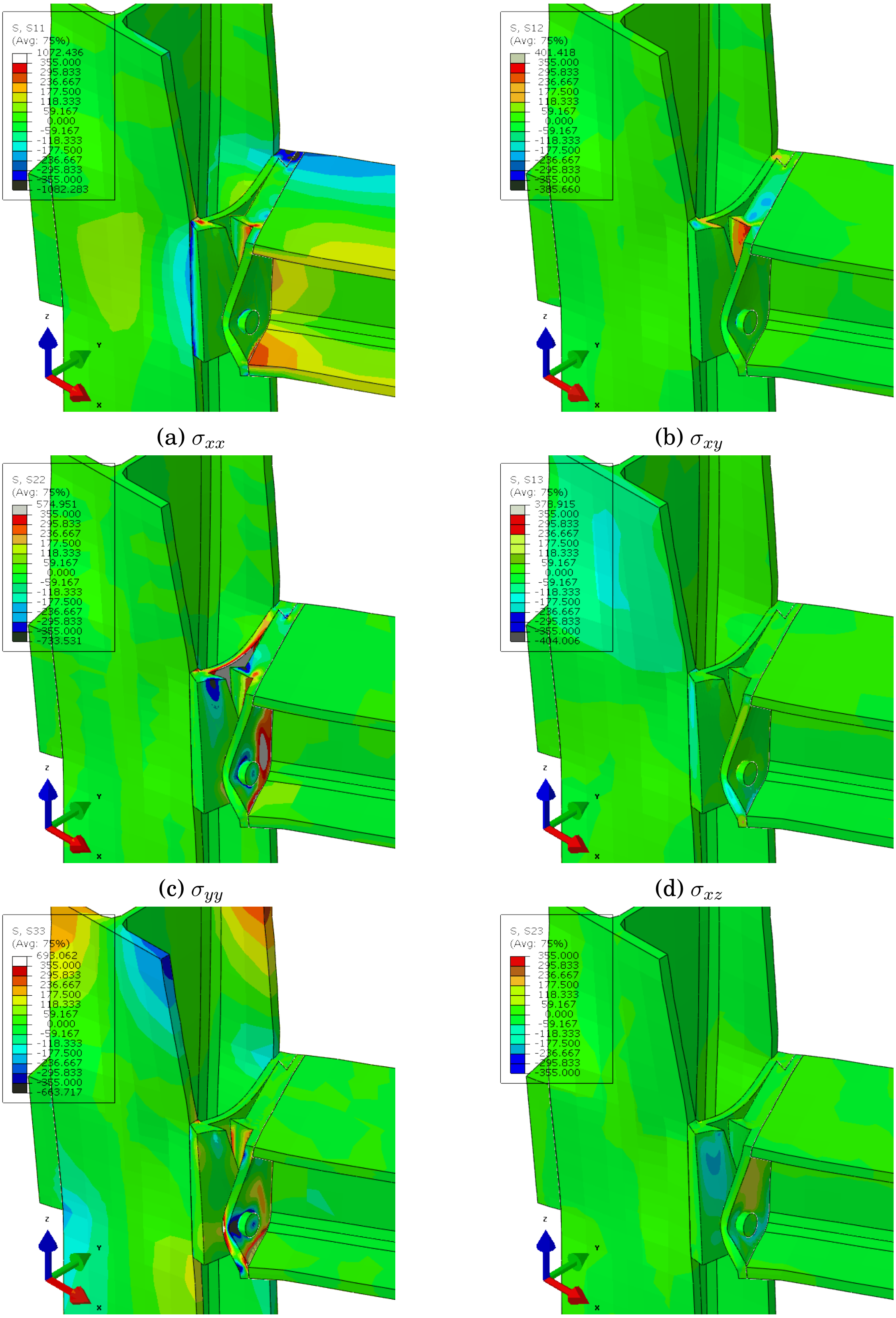

(a) σ_{xx} (b) σ_{xy}

(c) σ_{yy} (d) σ_{xz}

(e) σ_{zz} (f) σ_{yz}

Figure 7.54: Normal and shear stress (scale factor 20)

7.5.4 Summary table

This section contains a table providing the summary of the initial stiffness and elastic moment capacity for each analysis.

Table 7.4: Initial design initial stiffness and elastic moment capacity values

Column major axis		
Case	$M_{j,el,Rd}$	$S_{j,ini}$
Rigid classification boundary	-	92296 kNm/rad
Downwards displacement	30 kNm	18400 kNm/rad
Upwards displacement	50 kNm	25530 kNm/rad
Out-of-plane displacement	21 kNm	1410 kNm/rad
Column minor axis		
Case	$M_{j,el,Rd}$	$S_{j,ini}$
Rigid classification boundary	-	32862 kNm/rad
Downwards displacement	23 kNm	9780 kNm/rad
Upwards displacement	32 kNm	8786 kNm/rad
Out-of-plane displacement	17 kNm	5820 kNm/rad

7.5.5 Optimized model

In the previous sections the results of the initial connection are shown. The obtained stiffness for each combination were used in the global analysis to check the lateral displacements of the frame. The connection for the minor axis case was the most critical as the socket deformed for all load combinations.

In order to increase the stiffness of the joint a new design is made with the following design changes:

- The thickness of the socket is increased from 10mm to 40mm. For all column minor axis load cases the socket would bend due to the inclination which causes a bending moment in the socket. The thickness of the socket is increased to reduce the bending deformation of the socket.
- The thickness of the inclination is increased from 15mm to 20mm. Increasing the thickness of the inclination results in a larger contact area. Based on the results obtained from the snap-fit connection it is expected that increasing the contact area will result in a stiffer and stronger joint.
- The thickness of the plug plate is increased from 10mm to 20mm. The plug plate, which is connected to the beam, would bend at all load cases at the location of the bolts. By increasing the thickness it is expected that a higher moment is needed for yielding of the plug plate and so the stiffness and resistance would increase.
- Tolerances of 0.5mm are taken into account. For the previous analysed models a perfect fitted connection was assumed. The tolerances are taken into account by reducing the size the plug, this leads to a gap between the socket and plug as shown in figure

The new geometry is shown in figure

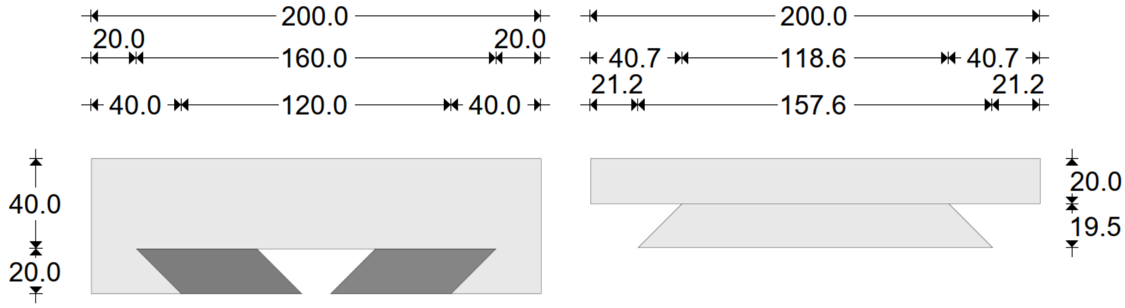

(a) Top view

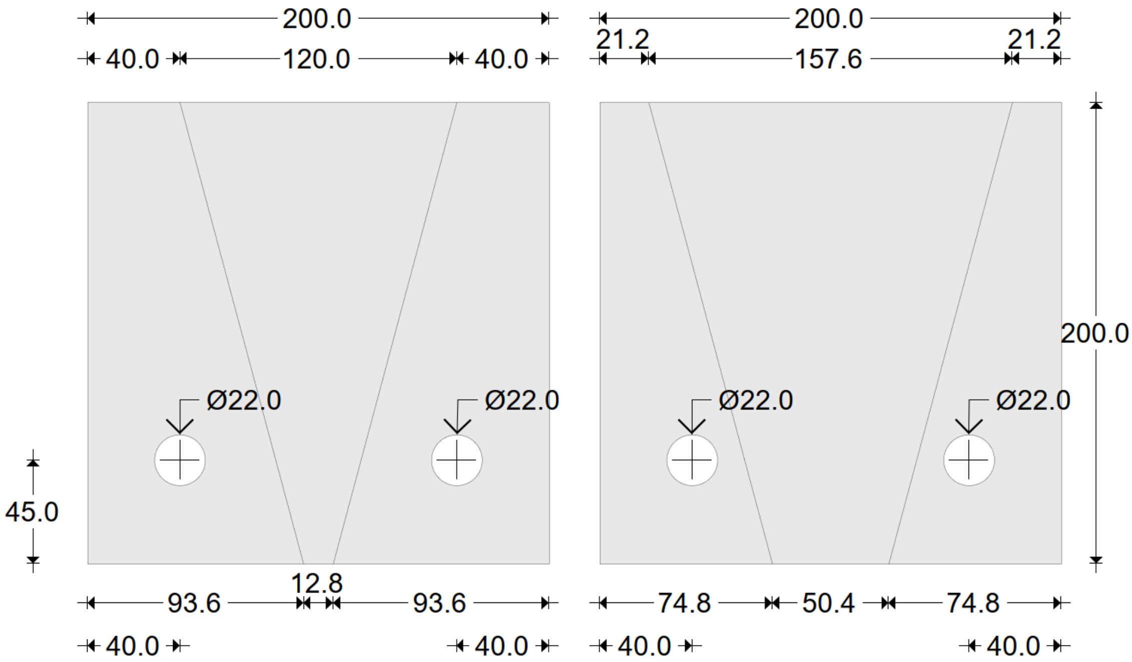

(b) Front view

Figure 7.55: Dimensions modified model

Downwards displacement

The model was loaded up to a maximum downwards displacement of 100mm. In figures 7.56 and 7.57 the $M-\phi$ curve of the optimized connection for downwards displacement is shown. Due to the tolerances there will be a gap between the socket and plug. This gap results in a low stiffness at the start, when the plug and socket are in contact the stiffness is increased. The stiffness before contact is achieved is 2360 kNm/rad for both the top and bottom part, after the parts are in contact the stiffness will be 17100 kNm/rad for the top part and 15550 kNm/rad for the bottom part. A moment of 5 kNm is necessary to initiate contact between the plug and socket. The bolts prevent the rigid body rotation of the plug within the socket, in order to achieve contact between the plug will deform at the location of the bolts. The stiffness has increased 52% for the top part and 59% for the bottom part, compared to the initial design minor axis case for downwards displacement, the stiffness for the plug and socket in contact is used. The elastic moment resistance is 55 kNm, using the non shifted curves. This is an increase of 139% compared to the initial design.

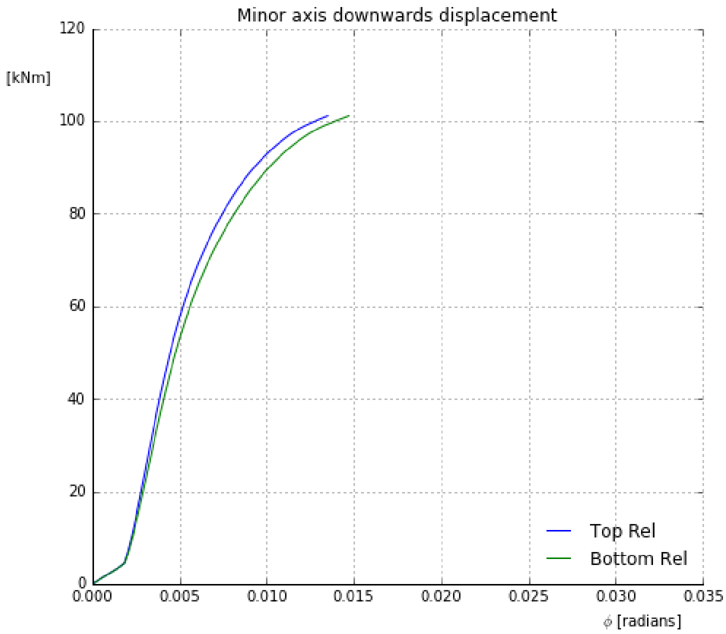

Figure 7.56: $M-\phi$ curve for optimized model

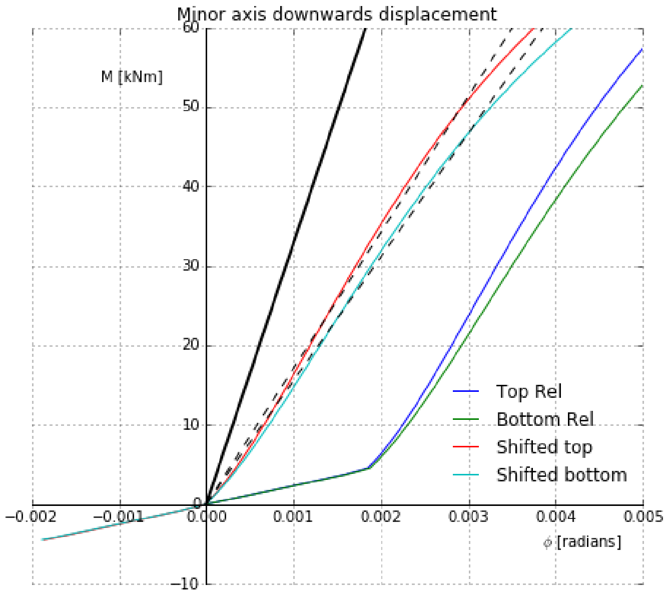

Figure 7.57: ZOOM of the $M - \phi$ curve for optimized model

The thickness of the socket has been increased to prevent the bending of the socket, it can be seen in figure 7.58 that bending of the socket is prevented. The connection still yields at the tension and compression area with the column flanges and the inclined parts of both the socket and plug. In figure 7.59 the normal and shear stress in the global coordinates is shown. The increased thickness of the socket has reduced the σ_{yy} in the socket, this stress was high as a consequence of the bending of the socket. The reduced bending deformation of the socket makes that it is harder to pull the plug out of the socket. This causes that the plug plate will deform at the location of the bolts, this results in an increased σ_{zz}. The other stress distributions has not changed significantly compared to the initial design.

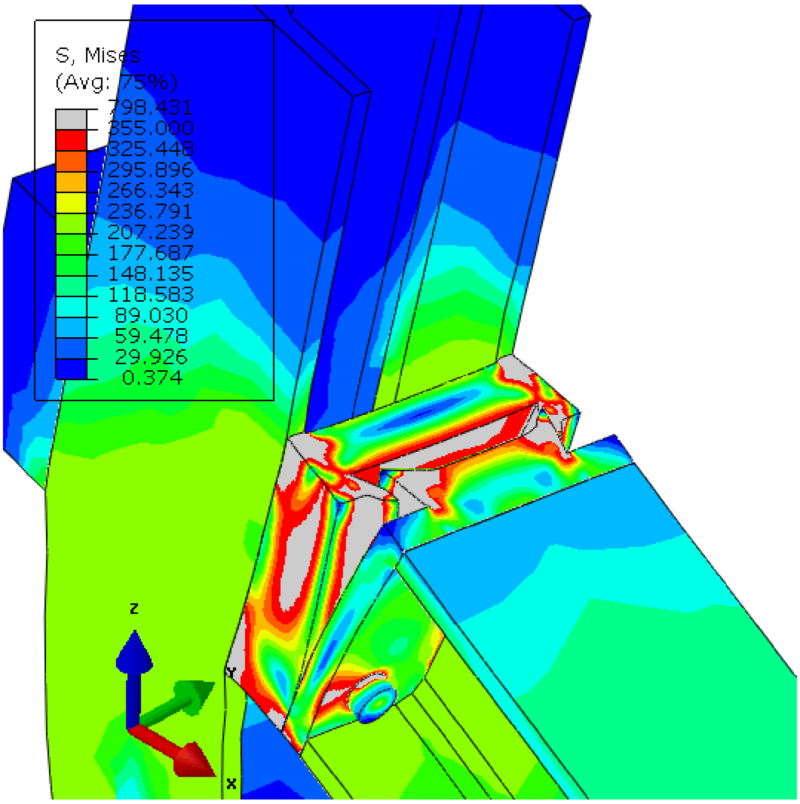

Figure 7.58: Von Mises (scale factor 10)

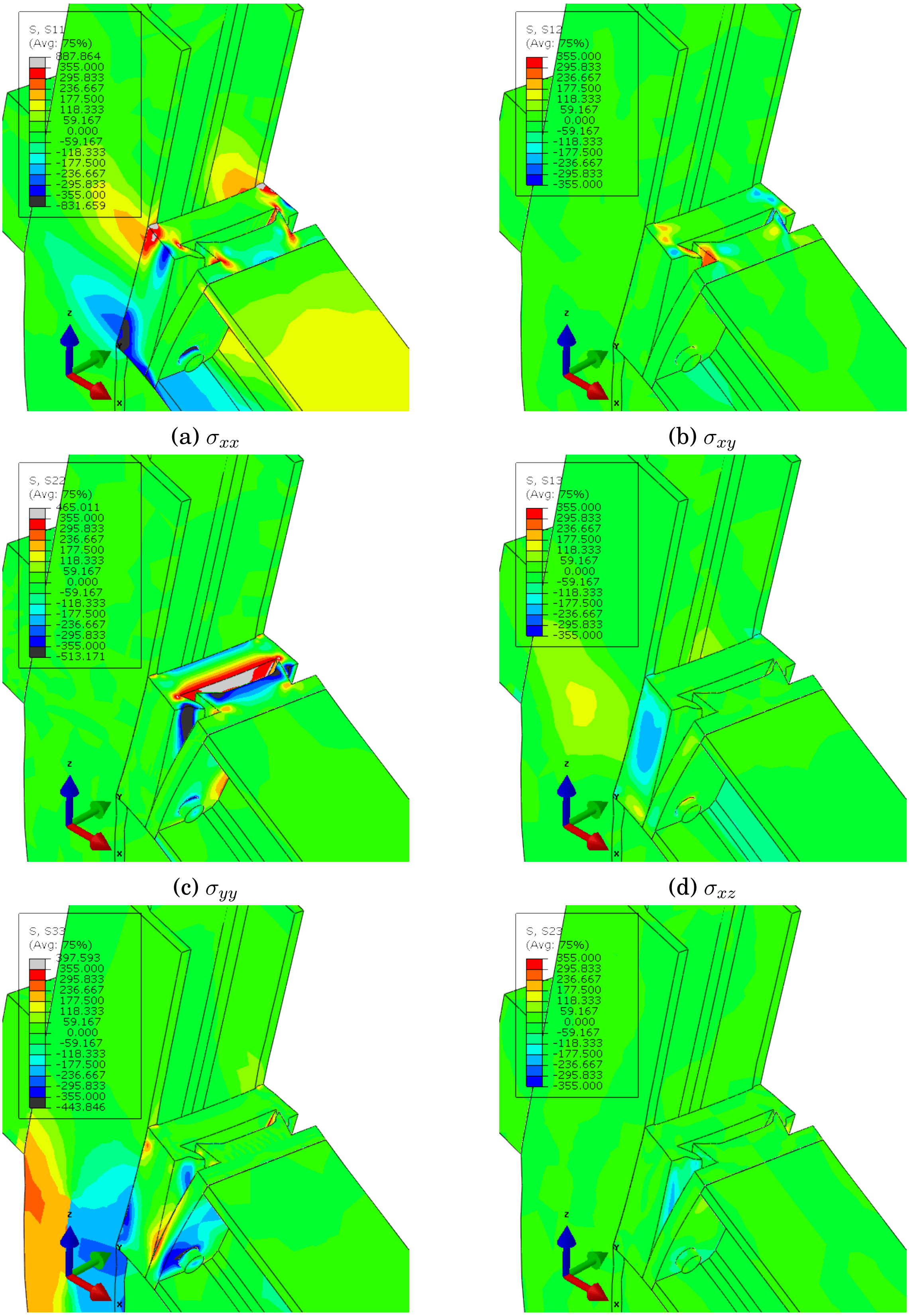

(a) σ_{xx}

(b) σ_{xy}

(c) σ_{yy}

(d) σ_{xz}

(e) σ_{zz}

(f) σ_{yz}

Figure 7.59: Normal and shear stress (scale factor 10)

Upwards displacement

The figures 7.60 and 7.61 show the $M-\phi$ curves for a maximum upwards displacement of 100mm. The upwards displacement do not show a reduced stiffness at the start, this is because the bolts are already in tension before contact between the plug and socket is initiated. The initial stiffness is 17110 kNm/rad for the top part and 16330 kNm/rad for the bottom part, this is an increase of 104% for the top part and 86% for the bottom part compared to the initial design for upwards displacement. The elastic moment resistance is 60 kNm, which is an increase of 88% compared to the initial design.

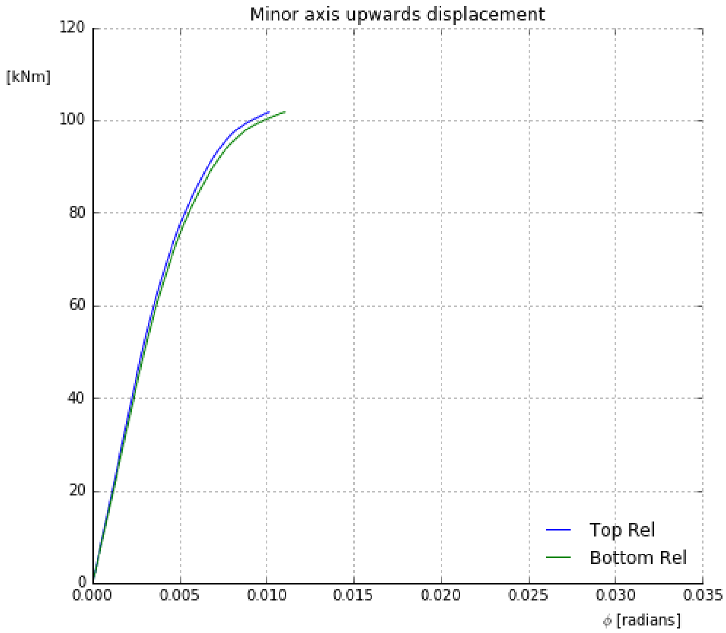

Figure 7.60: $M-\phi$ curve for optimized model

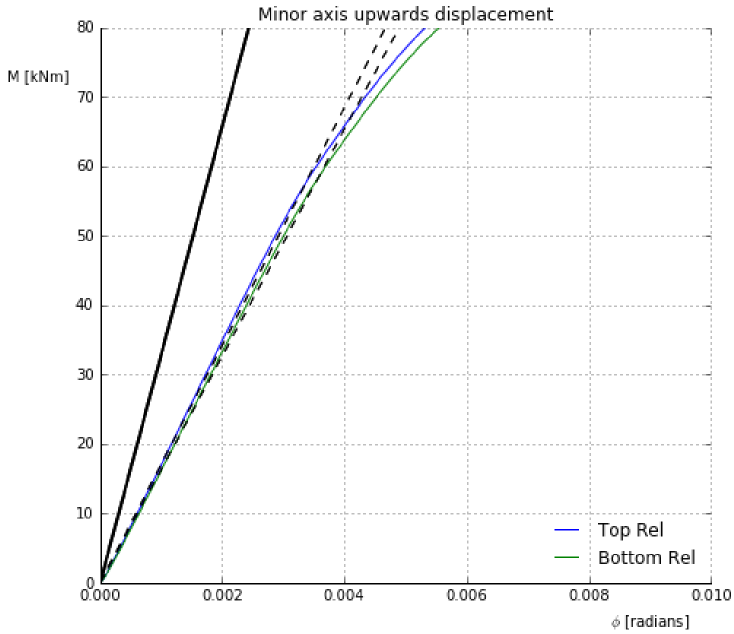

Figure 7.61: ZOOM of the $M - \phi$ curve for optimized model

In figure 7.62 the Von Mises stress is shown. The increased thickness of the socket prevents the bending deformation of the socket. Again this makes it harder to pull the plug out of the socket, as a consequence the yield stress is reach in the inclined parts of the socket, where in the initial design the inclined parts did not reach the yield stress. In the initial design a compressive σ_{xx} occurred in the top of the connection, as a consequence of the bending deformation of the socket. In the optimized the bending deformation of the socket is prevented and with that the compressive σ_{xx} in the top is eliminated. The connection will still yield at the location of the bolts.

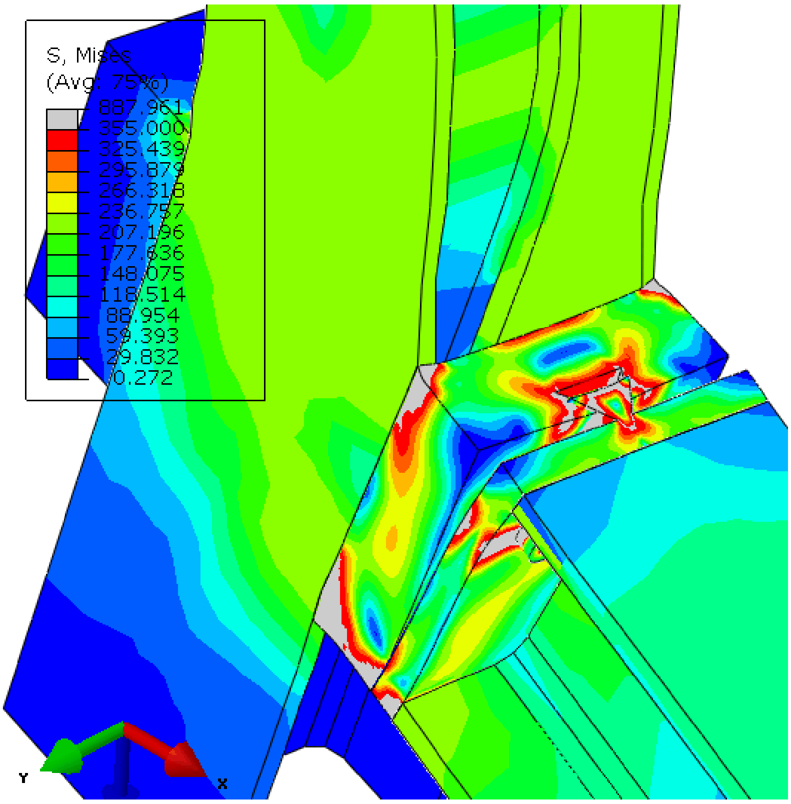

Figure 7.62: Von Mises (scale factor 10)

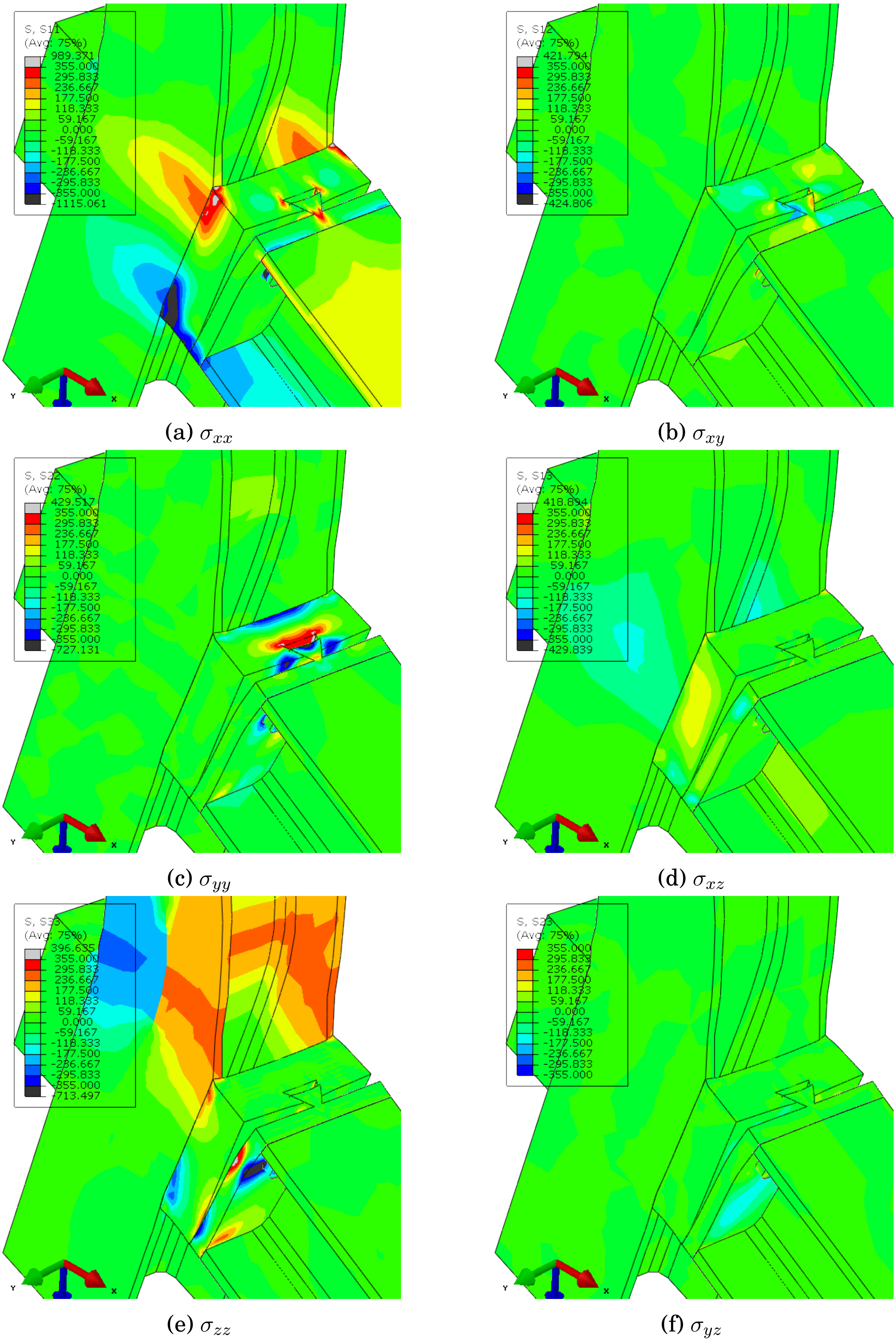

(a) σ_{xx} (b) σ_{xy}

(c) σ_{yy} (d) σ_{xz}

(e) σ_{zz} (f) σ_{yz}

Figure 7.63: Normal and shear stress (scale factor 10)

Out-of-plane displacement

In figures 7.64 and 7.65 the $M - \phi$ curve for a maximum out-of-plane displacement of 100mm is shown. The initial stiffness of the joint is 7540 kNm/rad, which is an increase of 30%. Like for the upward case there will be no slip. The bolt will be in tension before the socket and plug are in contact. So the inclination has no contribution to the initial stiffness of the joint. Point 1 in figures 7.64 and 7.65 indicates the point at which contact between the socket and plug initiates, up to point 1 the curve of the flange and the curve of connection have the same tangent, at point 1 contact between plug and socket is initiated and the plug and bolt start to yield. In figure 7.65 can be seen that after point 1 the curve will be above the elastic tangent line, this means that the contact results in an increase in stiffness. At point 2 a change in stiffness can observed, at this point the inclination of the plug starts to yield. The curve of the connection is no equal to curve of the beam and are parallel to the curve of the flange. The total rotation of the connection after point 2 is 10% more then the total rotation of the flange. So after point 2 the rotation is mainly caused by the rotation of the column instead of rotation of the connection. The elastic moment resistance is 23 kNm, which is an increase of 35%.

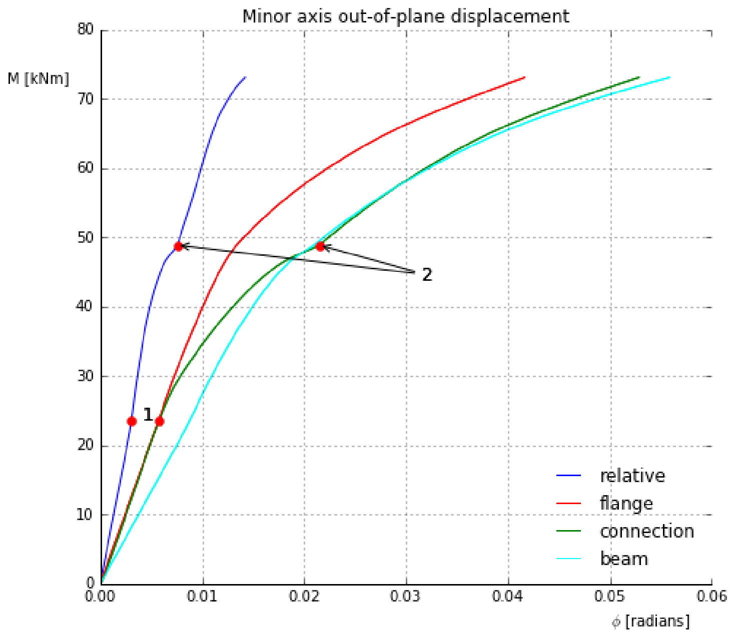

Figure 7.64: $M - \phi$ curve for optimized model

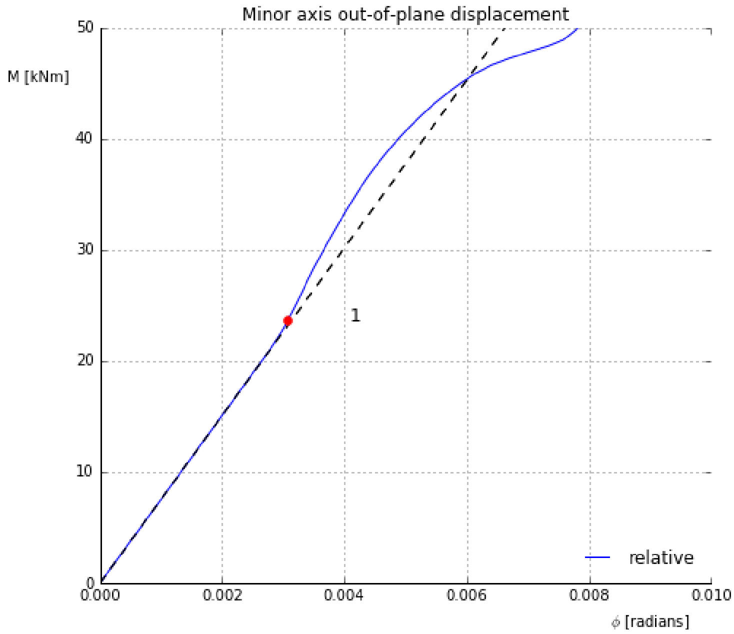

Figure 7.65: ZOOM of the $M - \phi$ curve for optimized model

Again bending deformation of the socket is prevented. Prevention of the bending deformation of the socket results in a lower σ_{yy}. From the $M - \phi$ curve was concluded that the rotation after point 2 is mainly by rotation of the column, this torsional deformation of the column leads to an increased σ_{zz}. The other stress distributions has not changed significantly compared to the initial design for minor axis out-of-plane bending

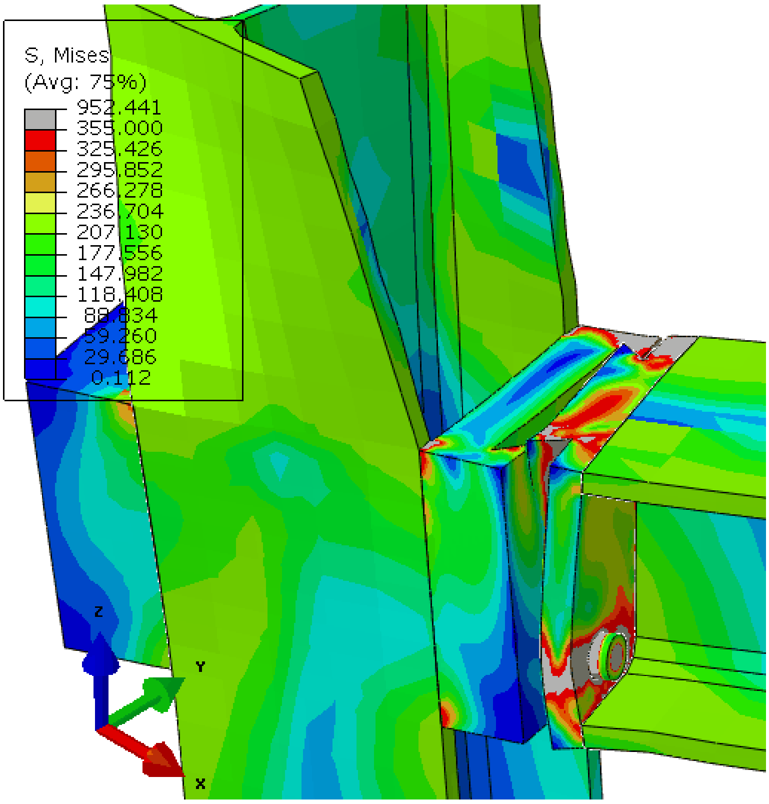

Figure 7.66: Von Mises (scale factor 10)

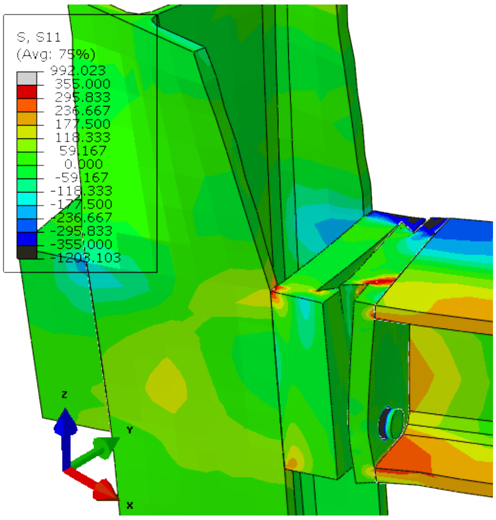

(a) σ_{xx}

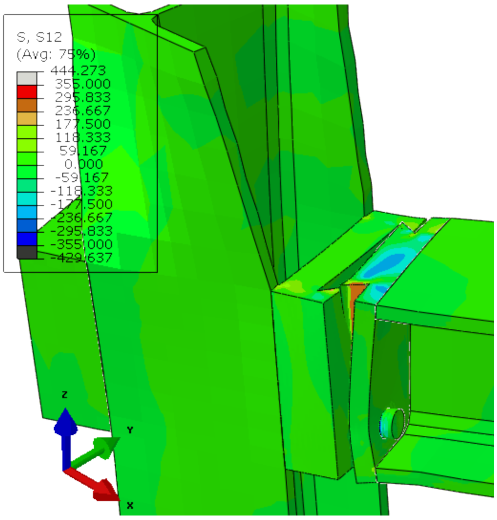

(b) σ_{xy}

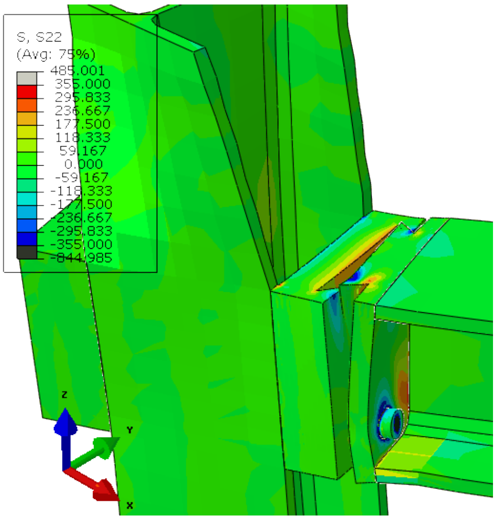

(c) σ_{yy}

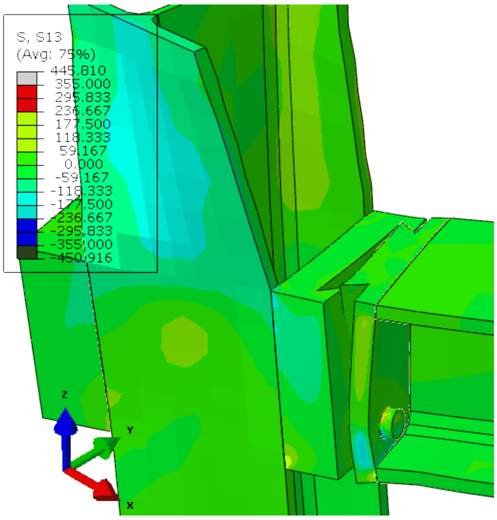

(d) σ_{xz}

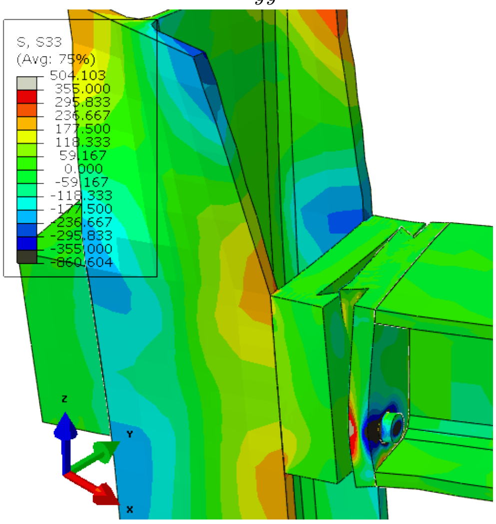

(e) σ_{zz}

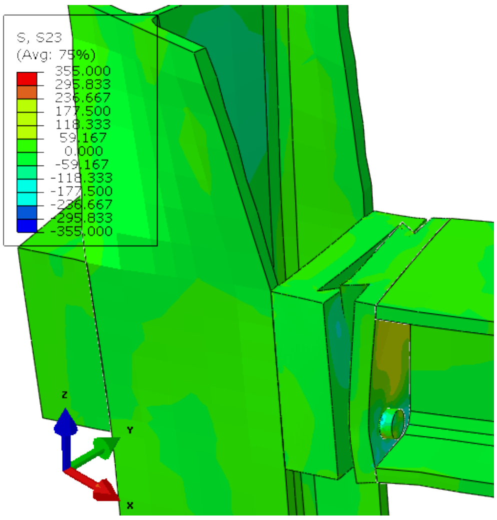

(f) σ_{yz}

Figure 7.67: Normal and shear stress (scale factor 10)

Summary table

Table 7.5 provides a summary of the results for the optimized design. The optimized design is only analysed for the minor axis case. The relative difference with the initial design is given for both the elastic moment resistance and the initial stiffness.

Table 7.5: Optimized design initial stiffness and elastic moment capacity values

	Optimized design			
Case	$M_{j,el,Rd}$	diff	$S_{j,ini}$	diff
Rigid classification boundary	-	-	32862 kNm/rad	-
Downwards displacement	55 kNm	+139 %	15550 kNm/rad	+52 %
Upwards displacement	60 kNm	+88 %	16330 kNm/rad	+86 %
Out-of-plane displacement	23 kNm	+35 %	7540 kNm/rad	+30 %

7.5.6 Evaluation of the plug & play

The plug & play connection will be evaluated with the ULS and SLS forces acting on the connection. In the SLS too large permanent deformations of the plug & play connection is not allowed and for the ULS failure of the plug & play connection is not allowed. The internal forces from the frame with all rigid connections are used.

Permanent deformations occur when the plastic strains are developed. For the SLS evaluation it is checked for each component separately whether plastic strains will develop and whether these plastic strains also cause too large permanent deformations.

Failure of the connection is when the materials cracks. A crack develops if the maximum plastic strain is reached. The maximum plastic strain of S355 is 0.262.

The plastic strains for the downwards and upwards displacement due to the SLS and ULS maximum moment is shown in the tables 7.6, 7.7, 7.8 and 7.9. The out-of-plane displacement has a low maximum moment and the maximum moment does not cause plastic strain in both SLS and ULS.

For all cases the ULS plastic strain does not reach the ultimate strain of the material. So the material would not crack in the ULS and the ULS failure criteria is satisfied. The SLS bending moments do cause some plastic strain and it should be checked whether this is accepted.

- Downwards displacement column major axis: the plastic strain occurs in the inside corner of both the plug and socket. For the plug the plastic strain is developing along the thickness of the plug.

- Upwards displacement column major axis: the plastic strain occurs in the inside corner of both plug and socket.
- Downwards displacement column minor axis: the plastic strain occurs in the inside corner of the plug and the plastic strain develops along the thickness of the plug. In the socket the plastic strain is in the contact zone between the socket and column flange, in the part of the connection in tension.
- Upwards displacement column minor axis: the plastic strain occurs in the tip of the plug and around the bolt holes. In the socket the plastic strain in the contact zone between the socket and column flange, in the part of the connection in tension.

For all cases the plastic strain in the SLS state is local and the magnitude of the plastic strain is small. A visual check should be performed to check whether the connection can be reused.

Table 7.6: Plastic strain downwards displacement column major axis

<table>
<tr><th colspan="2">SLS maximum moment of 30.98 kNm</th></tr>
<tr><td>Plug</td><td>Socket</td></tr>
<tr><td>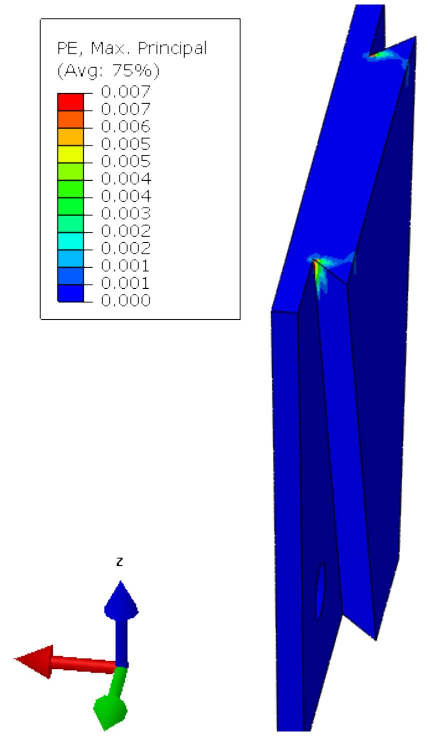
</td><td>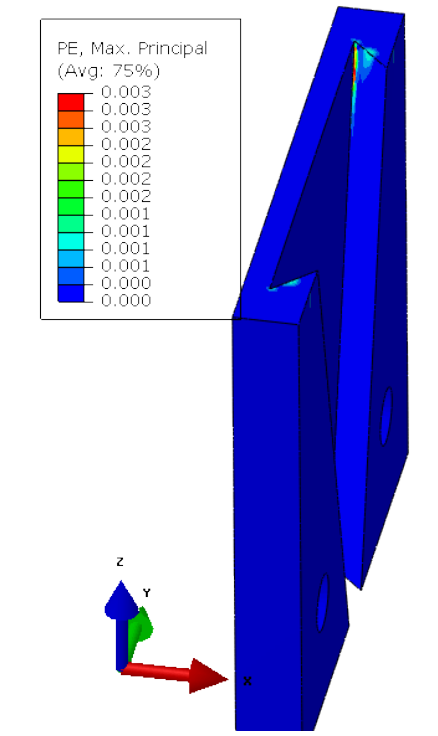
</td></tr>
<tr><th colspan="2">ULS maximum moment of 48.61 kNm</th></tr>
<tr><td>Plug</td><td>Socket</td></tr>
<tr><td>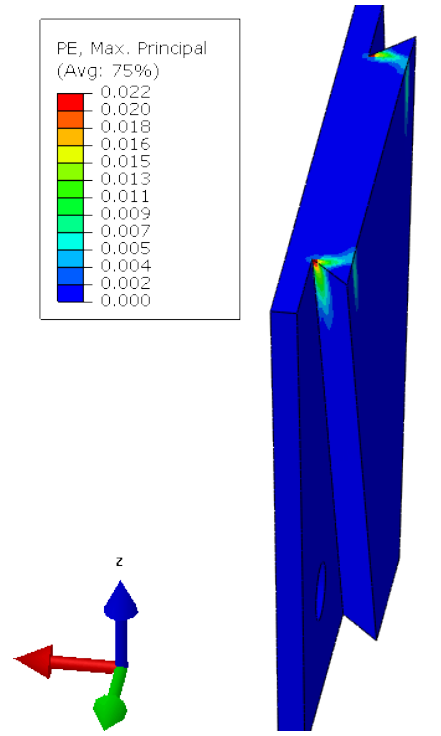
</td><td>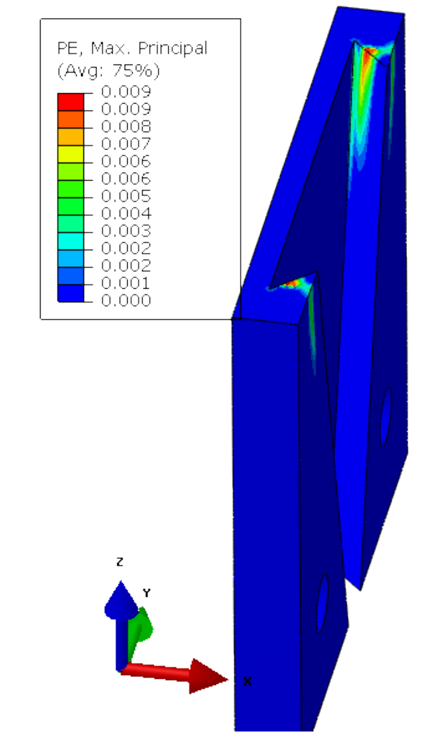
</td></tr>
</table>

Table 7.7: Plastic strain upwards displacement column major axis

<table>
<tr><td colspan="2">SLS maximum moment of 21.74 kNm</td></tr>
<tr><td>Plug</td><td>Socket</td></tr>
<tr><td>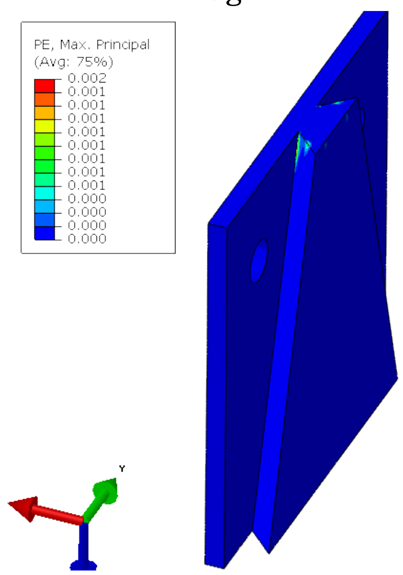
</td><td>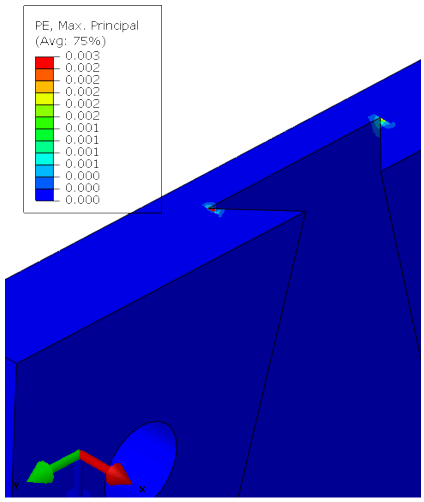
</td></tr>
<tr><td colspan="2">ULS maximum moment of 35.76 kNm</td></tr>
<tr><td>Plug</td><td>Socket</td></tr>
<tr><td>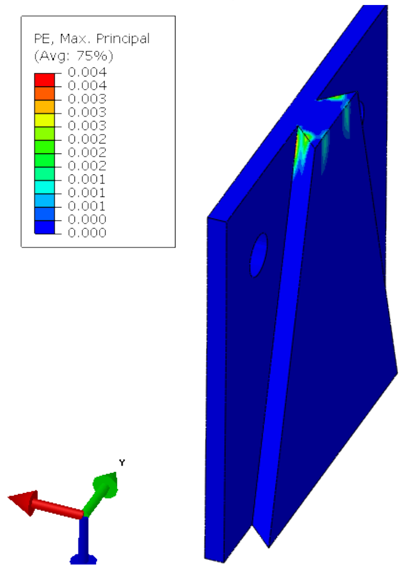
</td><td>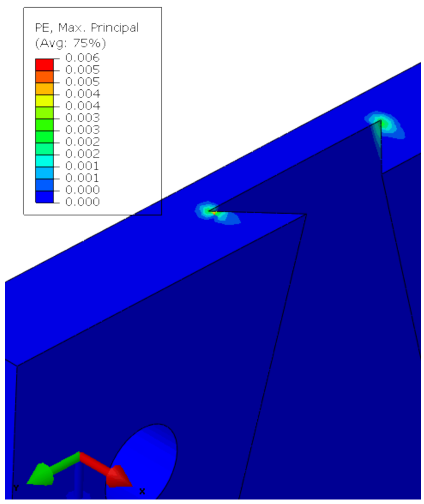
</td></tr>
</table>

Table 7.8: Plastic strain downwards displacement column minor axis

SLS maximum moment of 22.53 kNm

Plug	Socket
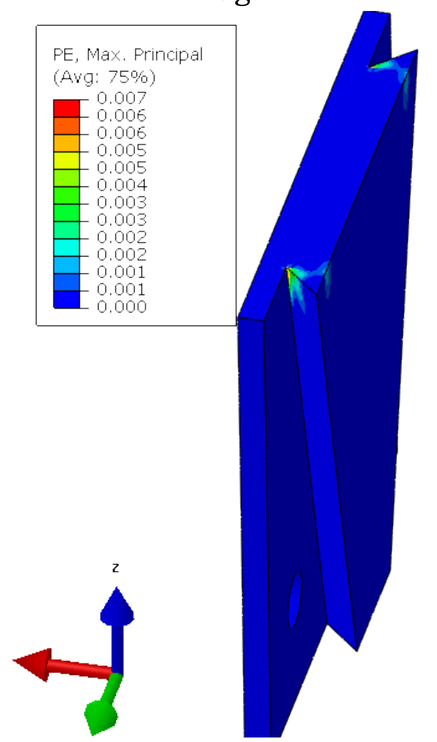	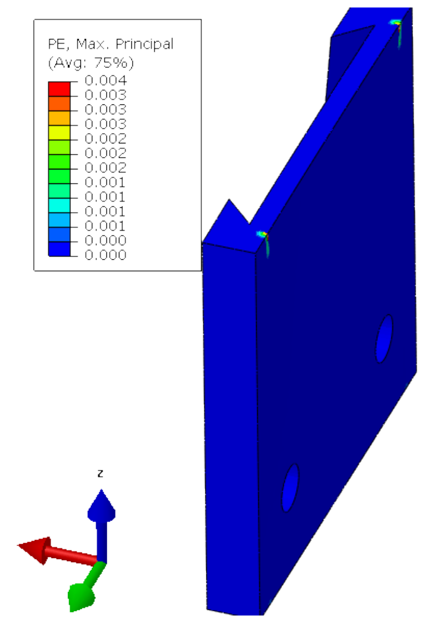

ULS maximum moment of 37.87

Plug	Socket
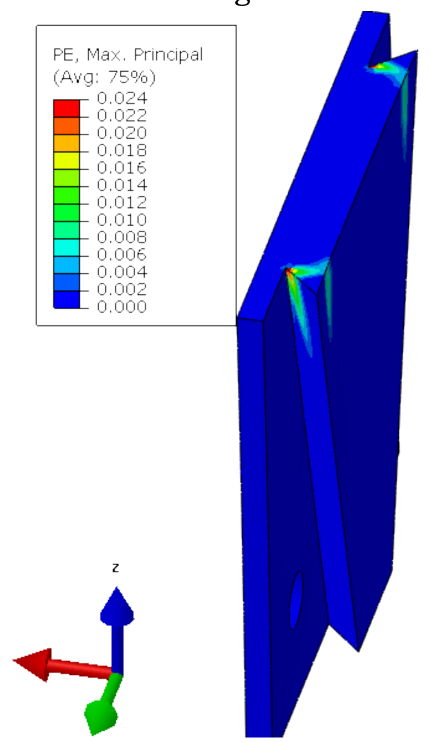	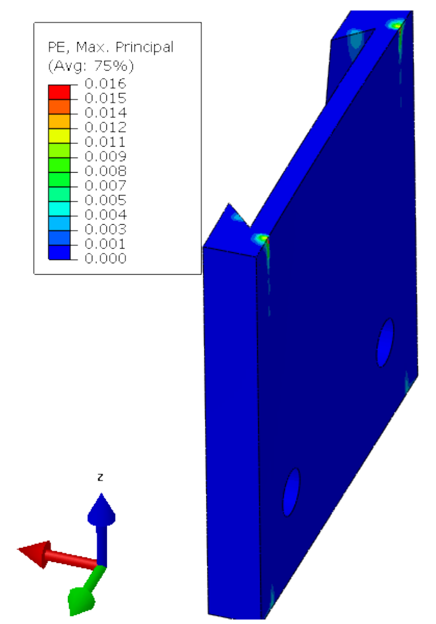

Table 7.9: Plastic strain upwards displacement column minor axis

SLS maximum moment of 21.22 kNm	
Plug	Socket
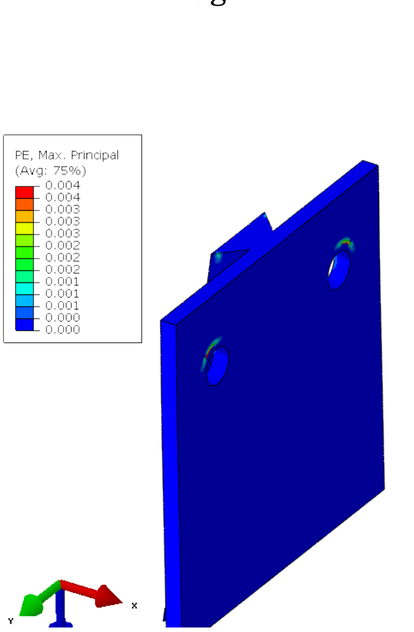	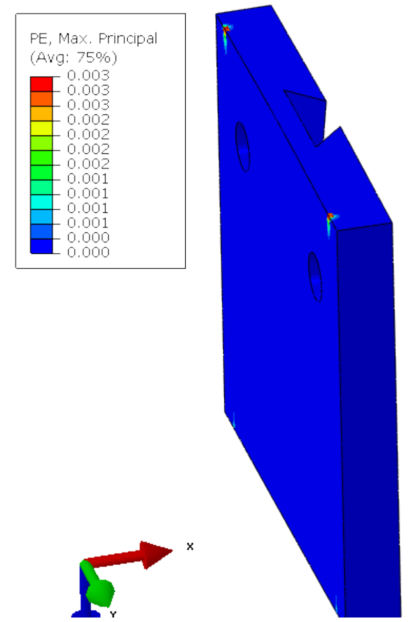
ULS maximum moment of 35.58 kNm	
Plug	Socket
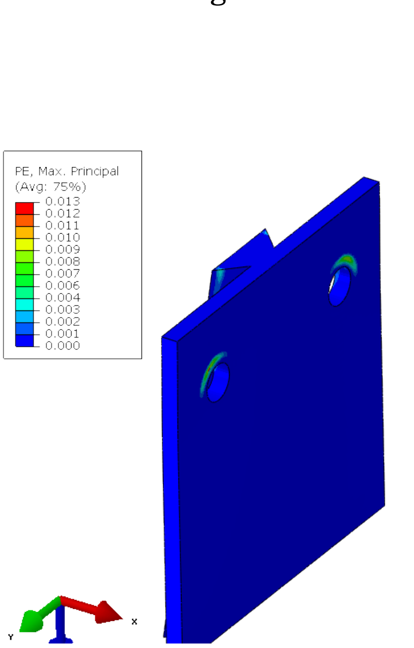	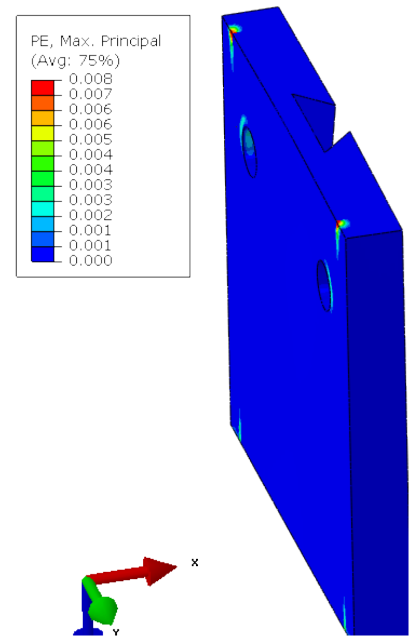

Optimized connection

For the initial design the ULS moments are above the elastic moment resistance, for the optimized design both the SLS and ULS moments are below the elastic moment resistance.

In table 7.10 the plastic strain is shown for downwards and upwards displacement, for out-of-plane displacement no plastic strain occurs. The SLS and ULS are both below the elastic moment resistance and therefore it is chosen to show the plastic strain for a moment equal to the elastic moment resistance.

For the upwards displacement the plastic strain is located at the bolt holes and the contact area between flange and socket, for both compression and tension. There is no plastic strain in the inclined parts of both socket and plug, this is because the elastic resistance is only provided by the bolts in tension. Moments above the elastic moment resistance are needed to provide contact between the socket and plug and then plastic strains will develop in the inclined parts of the socket and plug. For the downwards displacements contact between the socket and plug is initiated for moments above 5 kNm, so plastic strains no will occur in the inclined parts of the connection. The distribution of the plastic strain, for downwards displacement, is for both the initial design and the optimized design the same. The maximum values of the plastic strain in the optimized design are reduced compared with the plastic strain in ULS, while the moment has been increased from 37.87 kNm to 55 kNm. Increasing the thickness of the inclined parts did not remove the plastic strain, but it did lead to reduction of the maximum plastic strain.

In order to reuse the connection the plastic deformation should be limited and then especially in the inclined parts of the connection, as permanent deformation in the inclined parts can make it impossible to fit the plug in the socket. So for the upwards and out-of-plane case the maximum moment in SLS should be below the elastic moment resistance. When the moments are below the elastic moment resistance no plastic strain will occur in the inclined parts of the connection, as elastic moment resistance is provided only by the bolts and not by the inclined parts. For downwards displacement there will occur plastic deformation in the inclined parts. The tolerances allows for some plastic deformation of the connection and it should be checked whether it is possible to reuse the connection when the moments are kept below the elastic moment resistance.

Table 7.10: Plastic strain for optimized design

<table>
<tr><td colspan="2">Downwards displacement: elastic moment resistance of 55 kNm</td></tr>
<tr><td>Plug</td><td>Socket</td></tr>
<tr><td>
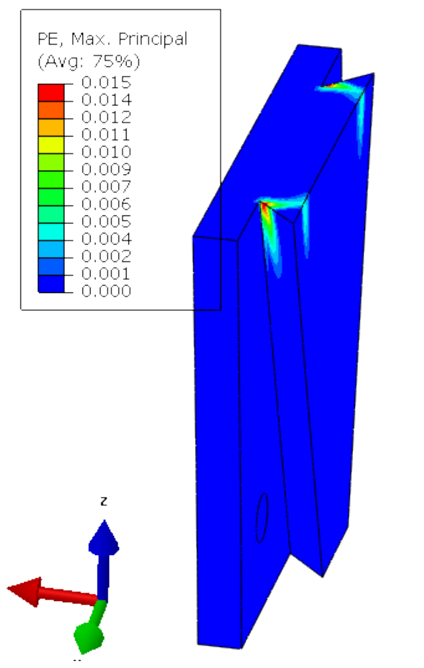

</td><td>
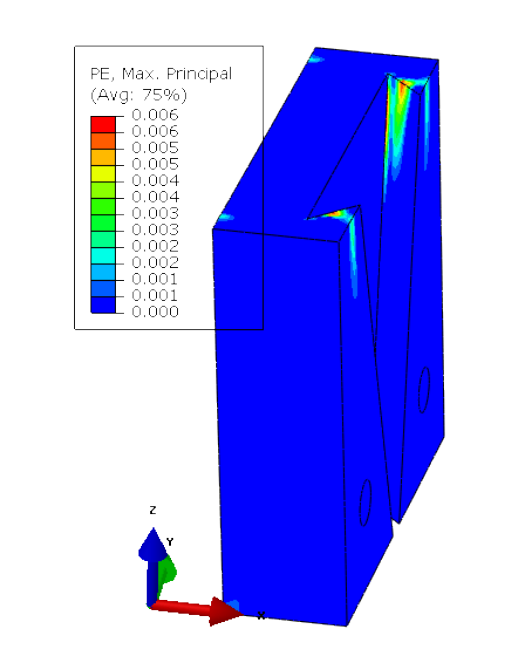

</td></tr>
<tr><td colspan="2">Upwards displacement: elastic moment resistance of 60 kNm</td></tr>
<tr><td>Plug</td><td>Socket</td></tr>
<tr><td>
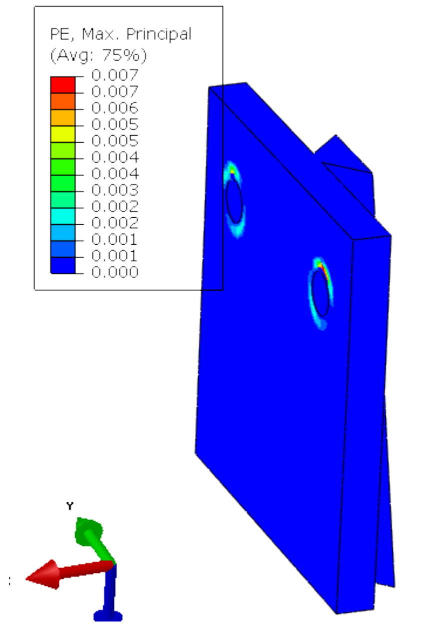

</td><td>
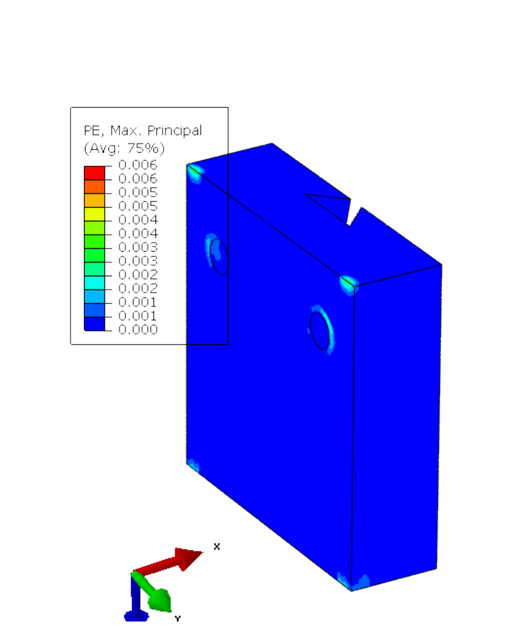

</td></tr>
</table>

7.5.7 Conclusion

The research questions for this chapter are:

- What is the design of the plug & play connection and what design considerations need to be taken into account?
- What is the structural performance of the joint for a column major and minor axis joint?
- What is the effect of a connection on all sides compared to only on one side?
- Which is the critical part of the connection?
- How can the stiffness and resistance of the joint be increased?
- Which are the criteria for re-usability of the connection?

An initial design is made which is shown in figure 7.1. For the initial design a perfect fitted connections is assumed.
The following can be concluded, regarding the initial design:

- The connections on the sides do increase the stiffness of the joint and also prevent bending of the column flange.
- The critical part of the connection is the inclined part in tension, the inclined tension part of both socket and plug will yield causing that the Plug eventually will be pulled out of the socket.
- For all load cases the plug plate will yield at the location of the bolt hole(s).
- For the column major axis case subjected to an out-of-plane displacement the column under torsion is the critical part of the joint, the column will yield in the web just below the flanges. The connections on the flanges do increase the torsional resistance of the column; however, the column is still the critical part of the joint for this load case. For the column minor axis case subjected to an out-of-plane displacement the plug & play connection is the critical part of the joint instead of the column. In this case no yielding of the column web will occur.
- For all minor axis displacement cases the socket will bend. The inclined parts of the connection which is/are in tension cause bending moments in the socket. For the minor axis case the socket is not supported between the flanges, which makes that the socket deforms like a pinned beam subjected to bending moments.
- The bending of the socket in the minor axis case, makes that the stress in the bolts will increase compared with the major axis case.

- The SLS forces will not lead to a too large permanent deformation of the connection and in the ULS the connection will not crack. The plug & play connection could therefor be reused. However, visual inspection needs to be performed to check whether the plug still fits in the socket.

After the results an optimized design is made. From the global analysis is concluded that the minor axis joints provide not sufficient stiffness, and from the analysis of the connection followed that the socket bends for all minor axis displacement cases. So the optimized connection is only checked for the minor axis cases. This optimized design also takes into account tolerances in the connection, as in reality the connection would not be a perfect fit connection. The geometry of the optimized design can be seen in figure 7.55. The thickness of the base plate material of the socket is increased to prevent the bending deformation and the thickness of the plug is increased in order to increase the stiffness of the connection.

For the optimized design the following can be concluded:

- The stiffness of the joint is increased compared to the initial design, for the downwards case the stiffness is increased with 50%, for the upwards case with 90% and for the out-of-plane case with 30%.
- The increased thickness of the socket eliminated the bending of the socket.
- Due to the tolerances a gap occurs in the connection, this gaps makes that the connection first slips before contact between the plug and socket initiates. This slip only occurs for the downwards case, for the upwards and sideways case no slip occurs as the bolt will immediately in tension.
- As for the upwards and out-of-plane case the bolts are immediately in tension the initial stiffness of the joint is only provided by the bolts, while for the downwards case the initial stiffness is provided by the inclination.
- For the out-of-plane case the column is still the critical part of the joint.
- For the upwards and out-of-plane case no plastic strains develop in the inclination, as the plug and socket are not in contact below the elastic moment resistance. For the downwards case there is some plastic strain in the inclination; however, the maximum strain is reduced compared to the initial design.
- Increasing the bolt size could increase the initial stiffness for the upwards and out-of-plane case as their initial stiffness is provided by the bolts.

Conclusion & Recommendations 8

A steel frame which should be expandable and reducible at any time wants to use plug & play connections for the beam-to-column connections as these connection could lead to to quicker and safer assembly and disassembly of steel frames. However, the stiffness and resistance of the joint cannot be calculated with the current design codes. In this thesis the focus is on the structural performance of the connection and the following objective is answered in this thesis:

To investigate if a plug & play connection can be used as a beam-to-column connection in a steel frame, by investigating the structural performance and evaluate the re-usability of the connection.

In a case study the dimensions of the used units is given together with a frame configuration used for further analysis. The steel frame has no bracing system so the stability needs to be provided by the joints. The case study is used to investigated what the possible forces are on the connection and the sections following from the global analysis limit the dimensions of the connection. It is chosen to use HEB section for both the beams and columns, as the width and height of HEB sections is equal, this makes that the same plug & play connection can be used for both the major and minor axis joints.

Other plug & play connections are investigated to see the possibilities and problems for the plug & play connection. The conclusions from the literature study are:

- A large contact area is needed for load transfer by bearing.
- Tolerances need to be taken into consideration as these would lower the stiffness of the joint.
- A self alignment feature aligns the beams to the correct position which would decrease the installation time.

Based on the results obtained in the state of art in chapter 3. An initial design is made which is shown in figure 7.1 and it assumes a perfect fitted connection. For this initial design the stiffness is investigated for downwards, upwards and out-of-plane displacement. The plug & play connection is only investigated for bending moments, assumed is that the bolts will carry the shear and normal forces.

Conclusions

The following can be concluded with regard to the initial design of the plug & play connection:

- In the analysis the assumption of rigid joints is done as the stiffness of the plug & play connection was unknown in the beginning. From the analysis follows that the plug & play connection is classified as semi-rigid instead of rigid.
- For the column major axis cases the inclined parts of the socket and plug, and the plug plate at the bolt holes are the parts of the connection which will yield. For the column minor axis cases besides the inclined parts of socket and plug, and the plug plate at the bolt holes also the socket at the contact zone with the column flanges will yield.
- One of the principles of the plug & play connection is that it should be reusable. The re-usability is evaluated as that the permanent deformations may not be too large due to the SLS forces. With the forces from the case study the plastic strain is checked and the plastic strain due to the maximum SLS moments is limited to a very small localized plastic strain in the corner of the inclined parts of both the socket and plug. For the ULS case it is not allowed that the connection would crack, the ultimate plastic strain is not reached when the ULS forces are applied. So the connection will not crack.
- For the plug & play connection subjected to an out-of-plane displacement the stiffness of the plug & play connection in the major axis case (attached fully to one flange) is lower then when the connection is in the minor axis case (attached to both flanges). The out-of-plane displacement cause a torsional moment on the column. For the major axis case the torsional resistance of the column is the critical part, while for the minor axis case the plug & play connection is the critical part which is yielding.
- The socket attached to the column minor axis behaves as a pinned beam subjected to bending moments. The bending moments are caused by the inclination which is in tensile loading. The socket will bend which cause that the inclined part of the socket will open. This opening makes it easier to pull the plug out of the socket and it leads to an stress increase in the bolts.

Based on the results obtained from the initial design an optimized design is made. From both the global analysis and the analysis of the plug & play connection followed that the minor axis joints are the most critical. An optimized design is therefore only checked for the minor axis joints. The following has been changed for the optimized design:

- First the tolerances are taken into account. Instead of a perfect fit connection there is a gap between the plug and socket.
- The thickness of the base plate of the socket is increased from 10mm to 40mm in order to prevent the bending of the socket.
- The thickness of the base plate of the plug is increased from 10mm to 20mm and the thickness of the plug is increased from 10mm to 20mm as well in order to increase the stiffness of the joint.

From the results of the optimized design the following can be concluded:

- The increased thickness of the socket does prevent the bending deformation of the socket and reduces the stress in the socket.
- The inclination still yields for all optimized cases.
- Due to the gap between the plug & socket a slip occurs for the downwards displacement case. The bolts prevent free rigid body rotation of the plug and the plug there needs to deform at the location of the bolts before contact is initiated. This results in a moment of 5 kNm required to initiate contact.
- No slip does not occur for the upwards and out-of-plane case as the bolts will be in tension immediately.
- The initial stiffness and elastic moment resistance capacity for the upwards and out-of-plane case is only provided by the bolts while for downwards case the initial stiffness and elastic moment resistance capacity is provided by the inclination.
- For the out-of-plane case the inclination increases the stiffness beyond the initial stiffness when contact between the plug and socket is initiated.
- For the upwards and out-of-plane case there is no contact between the plug and socket below the elastic moment resistance capacity, this makes that no plastic strain develops in the inclination for moments below this value.
- For the downwards case there will occur plastic strains in the inclination. The maximum value of the plastic strain is decreased for a higher moment compared to the initial design.
- For the out-of-plane case the column is still the critical part of the connection.

The connection seems to be reusable if the moments are below the elastic moment resistance capacity. Visual inspection should prove whether the plug still fits in the socket.

Answer to main objective

In order to use the plug & play connection the following criteria need to be taken into account when the plug & play connection will be used:

The re-usability of the plug & play connection limits the moment resistance of the connection to the elastic moment resistance of the joint. This in order to prevent plastic strains in the inclined parts of the connection. Due to tolerances a little plastic deformation of the inclined parts is allowed; however, these deformations may not cause that the plug will not fit the socket anymore.

The second thing that need to be taken into account is that the joint is classified as semi-rigid. In order to increase the stiffness of the connection, the thickness of the plug is increased and also the base plate thickness of both the socket and plug has been increased to increase the stiffness of the connection. Tolerances have a positive effect for the cases in which the bolts are immediately in tension, the initial stiffness is provided by the bolts only and no plastic strain develops in the inclined parts.

These two criteria limit the use of the plug & play connection. However, the purpose of the plug & play connection is to reduce the assembly and disassembly time of a steel frame. A real test should prove whether the plug & play connection would lead to this reduction and if it does the plug & play connection could be an useful connection.

References

[1] Jaspart. *Design of joints in steel and composite structures : Eurocode 3: design of steel structures, part 1-8–Design of joints, Eurocode 4: design of composite steel and concrete structures, part 1-1–General rules and rules for buildings*. ECCS - European Convention for Constructional Steelwork Ernst & Sohn, a Wiley brand, Brussels, Belgium, 2016.

[2] European Committee for Standardization. *NEN-EN 1993-1-8+C2 - Eurocode 3: Design of steel structures - Part 1-8: Design of joints*. Brussels, 2011.

[3] Jerzy K. Szlendak and Adrian Szpyrka. Resistance of plug & play n type RHS truss connections. *Open Engineering*, 10(1):563–570, July 2020.

[4] ConXTech. `https://www.conxtech.com/`.

[5] Salam Al-Sabah, Debra F. Laefer, Linh Truong Hong, Minh Phuoc Huynh, Jia-Liang Le, Tony Martin, Pantelis Matis, Patrick McGetrick, Arturo Schultz, Mohammad E. Shemshadian, and Roseanne Dizon. Introduction of the intermeshed steel connection—a new universal steel connection. *Buildings*, 10(3):37, February 2020.

[6] S Moriche Quesada. Optimization of a snap-fit connection: a steel connection for the built environment. Master's thesis, TU Eindhoven, 2016.

[7] Robert Cook, David Malkus, Plesha Michael, and Robert Witt. *Concepts and applications of finite element analysis*. Wiley, New York, NY, 4 edition, 2001.

[8] SCIA Engineer. *Basic concept training - steel code check*, 2018.

[9] European Committee for Standardization. *NEN-EN 1993-1-1+C2+A1 - Eurocode 3: Design of steel structures - Part 1-1: General rules and rules for buildings*. Brussels, 2016.

[10] Beatriz Gil and Rufino Goñi. T-stub behaviour under out-of-plane bending. i: Experimental research and finite element modelling. *Engineering Structures*, 98:230–240, September 2015.

[11] Beatriz Gil, Rufino Goñi, and Eduardo Bayo. Initial stiffness and strength characterization of minor axis t-stub under out-of-plane bending. *Journal of Constructional Steel Research*, 140:208–221, January 2018.

[12] Arash Poursadrollah, Attilio De Martino, Mario D'Aniello, and Raffaele Landolfo. Preliminary study on the seismic performance of hybrid steel structures with truss lightweight girders and plug-and-play connections. *Ingegneria Sismica*, March 2020.

[13] Luís Simões da Silva, Luís Carlos Silva, Trayana Tankova, Hélder David Craveiro, Rui Simões, Ricardo Costa, Mario D'Aniello, and Raffaele Landolfo. Performance of modular hybrid cold-formed/tubular structural system. *Structures*, 30:1006–1019, April 2021.

[14] Fleischman Robert B, Viscomi B.Vincent, and Lu Le-Wu. Atlss connections – concept, development and experimental investigation. 1990.

[15] Perreira N. D., Fleischman R. B., Viscomi B. B., and Lu Le-Wu. Automated construction and atlss connections; development, analysis, experimentation, and implementation of atlss connections for automated construction. 1993.

[16] Ministerie van Binnenlandse Zaken en Koninkrijksrelaties. Bouwbesluit 2012. https://rijksoverheid.bouwbesluit.com/Inhoud/docs/wet/bb2012, 2021.

[17] European Committee for Standardization. *NEN-EN 1991-1-1+C1+C11/NB - National Annex to NEN-EN 1991-1-1+C1+C11: Eurocode 1: Actions on structures - Part 1-1: General actions - Densities, self-weight, imposed loads for buildings*. Brussels, 2019.

[18] European Committee for Standardization. *NEN-EN 1991-1-1+C1+C11 - Eurocode 1: Actions on structures - Part 1-1: General actions - Densities, self-weight, imposed loads for buildings*. Brussels, 2019.

[19] European Committee for Standardization. *NEN-EN 1991-1-3+C1+A1 - Eurocode 1: Actions on structures - Part 1-3: General actions - Snow loads*. Brussels, 2019.

[20] European Committee for Standardization. *NEN-EN 1991-1-4+A1+C2/NB+C1 - National annex to NEN-EN 1991-1-4+A1+C2: Eurocode 1: Actions on structures - Part 1-4: General actions - Wind actions*. Brussels, 2020.

[21] European Committee for Standardization. *NEN-EN 1990+A1+A1/C2/NB - National Annex to NEN-EN 1990+A1+A1/C2: Eurocode: Basis of structural design*. Brussels, 2019.

[22] European Committee for Standardization. *NEN-EN 1090-2 - execution of steel structures and aluminium structures - Part 2: Technical requirements for steel structures*. Brussels, 2018.

Cross Section Resistance Check A

SCIA provides the cross sectional unity check for all sections. For the section with the maximum unity check the calculation is given in this appendix.

The maximum unity check occurs for an inner column at bottom level, in the table below the internal forces in the critical cross section are given:

Table A.1: Internal forces in section

N_{Ed} (kN)	$V_{y,Ed}$ (kN)	$V_{z,Ed}$ (kN)	$M_{x,Ed}$ (kNM)	$M_{y,Ed}$ (kNM)	$M_{z,Ed}$ (kNM)
-221.47	-17.03	0.11	-0.01	1.23	-33.11

Axial Force

$$N_{c,Rd} = \frac{A \cdot f_y}{\gamma_{M0}} = \frac{4.2986 \cdot 10^{-3}\ [m^2] \cdot 355\ [MPa]}{1.0} = 1525.08kN$$

$$U.C. = \frac{|N_{Ed}|}{N_{c,Rd}} = \frac{|-221.47|[kN]}{1525.08[kN]} = \mathbf{0.15}$$

Bending Moments

Cross section is class 1

$$M_{pl,y,rd} = \frac{W_{pl,y} \cdot f_y}{\gamma_{M0}} = \frac{2.4540 \cdot 10^{-4}\ [m^3] \cdot 355\ [MPa]}{1.0} = 87.12kNm$$

$$U.C. = \frac{|M_{y,Ed}|}{M_{pl,y,rd}} = \frac{|1.23|[kNm]}{87.12[kNm]} = \mathbf{0.01}$$

$$M_{pl,z,rd} = \frac{W_{pl,z} \cdot f_y}{\gamma_{M0}} = \frac{1.1980 \cdot 10^{-4}\ [m^3] \cdot 355\ [mPa]}{1.0} = 42.53kNm$$

$$U.C. = \frac{|M_{z,Ed}|}{M_{pl,z,rd}} = \frac{|-33.11|[kNm]}{42.53[kNm]} = \mathbf{0.78}$$

Shear Forces

$$V_{pl,y,Rd} = \frac{A_V \cdot \frac{f_y}{\sqrt{3}}}{\gamma_{M0}} = \frac{3.4930 \cdot 10^{-3}\ [m^2] \cdot \frac{355[mPa]}{\sqrt{3}}}{1.0} = 715.92kN$$

$$U.C. = \frac{|V_{y,Ed}}{V_{c,y,Rd}} = \frac{|-17.03|[kN]}{715.92[kN]} = \mathbf{0.02}$$

$$V_{pl,z,Rd} = \frac{A_V \cdot \frac{f_y}{\sqrt{3}}}{\gamma_{M0}} = \frac{1.3080 \cdot 10^{-3}\ [m^2] \cdot \frac{355[mPa]}{\sqrt{3}}}{1.0} = 268.09kN$$

$$U.C. = \frac{|V_{z,Ed}|}{V_{c,z,Rd}} = \frac{|0.11|[kN]}{268.09[kN]} = \mathbf{0.00}$$

Torsion

Torsion in the cross section can be neglected.

Combined Bending and Axial Force

The shear force is less then 50% of the plastic shear capacity and therefor its influence can be neglected in the combined bending and axial force check.

$$\left(\frac{|M_{y,Ed}}{M_{N,y,Rd}}\right)^{\alpha} + \left(\frac{|M_{z,Ed}}{M_{N,z,Rd}}\right)^{\beta} \leq 1$$

$$\begin{aligned} M_{N,y,Rd} &= min\left[\frac{M_{pl,y,Rd} \cdot (1-n)}{-0.5 \cdot a_w}, M_{pl,y,Rd}\right] \\ &= min\left[\frac{87.12[kNm] \cdot (1-0.15)}{1-0.5 \cdot 0.22}, 87.12[kNm]\right] \\ &= min[83.57[kNm], 87.12[kNm]] = 83.57kNm \end{aligned}$$

$$\begin{aligned} a &= (A - 2bt_f)/A = (4296 - 2 * 140 * 12)/4296 = 0.22 \\ n &\leq a\ OK \\ M_{N,z,Rd} &= M_{pl,z,Rd} \\ &= 42.53[kNm] \end{aligned}$$

$$\alpha = 2, \beta = 5n \text{ but } \beta \geq 1 \text{ so } \beta = 1$$

$$\left[\frac{|1.23|[kNm]}{83.57[kNm]}\right]^{2.00} + \left[\frac{|-33.11|[kNm]}{42.53[kNm]}\right]^{1.0} = \mathbf{0.78}$$

Lateral Torsional Buckling Check B

The beams are not lateral restrained and therefor a check must be done whether lateral torsional buckling will occur. The load is applied on the top flange of the beam.

$$
\begin{aligned}
S &= \sqrt{\frac{E \cdot I_w}{G \cdot It}} \\
&= \sqrt{\frac{210000\ [MPa] \cdot 2.2479 \cdot 10^{-8}\ [m^6]}{80769.2\ [MPa] \cdot 2.0060 \cdot 10^{-7}\ [m^4]}} \\
&= 540mm
\end{aligned}
$$

$$
\begin{aligned}
C &= \frac{\pi \cdot C_1 \cdot L_g}{L_{kip}} \cdot \left[\sqrt{1 + \frac{\pi^2 \cdot S^2}{L_{kip}^2 \cdot (C_2^2 + 1)}} + \frac{\pi \cdot C_2 \cdot S}{L_{kip}} \right] \\
&= \frac{\pi \cdot 2.29 \cdot 3.24}{3.24} \cdot \left[\sqrt{1 + \frac{\pi^2 \cdot 540^2}{3.24^2 \cdot (-0.41^2 + 1)}} + \frac{\pi \cdot -0.41 \cdot 540}{3.24} \right] \\
&= 6.73
\end{aligned}
$$

Values of C_1 and C_2 are derived by SCIA according to ECCS 119/Galea method.

$$
\begin{aligned}
M_{cr} &= k_{red} \cdot \frac{C}{L_g} \cdot \sqrt{E \cdot I_z \cdot G \cdot I_t} \\
&= 1.00 \cdot \frac{6.73}{3.240[m]} \cdot \sqrt{210000[MPa] \cdot 5.4970 \cdot 10^{-6}[m^4] \cdot 80769.2[MPa] \cdot 2.0060 \cdot 10^{-7}[m^4]} \\
&= 283.91kNm
\end{aligned}
$$

$$
\begin{aligned}
\bar{\lambda}_{LT} &= \sqrt{\frac{W_{pl,y} \cdot f_y}{M_{cr}}} \\
&= \sqrt{\frac{2.4540 \cdot 10^{-4}[m^3] \cdot 355[MPa]}{283.91[kNm]}} \\
&= 0.55
\end{aligned}
$$

χ factor determined according to EN1993-1-1 6.3.2.3 equation (6.57).

$$\begin{aligned}
\Phi_{LT} &= 0.5[1 + \alpha_{LT}(\bar{\lambda}_{LT} - \bar{\lambda}_{LT,0} + \beta\bar{\lambda}_{LT}^2] \\
&= 0.5[1 + 0.34(0.55 - 0.4) + 0.75 \cdot 0.55^2] \\
&= 0.64 \\
\chi_{LT} &= min\left(\frac{1}{\Phi_{LT} + \sqrt{\Phi_{LT}^2 - \beta\bar{\lambda}_{LT}^2}}, \frac{1}{\bar{\lambda}_{LT}^2}, 1\right) \\
&= min\left(\frac{1}{0.64 + \sqrt{0.64^2 - 0.75 \cdot 0.55^2}}, \frac{1}{0.55^2}, 1\right) \\
&= 0.94 \\
f &= 1 - 0.5(1 - k_c)[1 - 2.0(\bar{\lambda}_L T - 0.8)^2]\mathbf{but} f \leq 1 \\
&= 1 - 0.5(1 - 0.9)[1 - 2.0(0.55 - 0.8)^2] \\
&= 0.96 \\
\chi_{LT,mod} &= \frac{\chi_{LT}}{f} = \frac{0.94}{0.96} = 0.98 \\
M_{b,Rd} &= \chi_{LT,mod} \cdot W_{pl,y} \cdot \frac{f_y}{\gamma_{M1}} \\
&= 0.98 \cdot 2.4540 \cdot 10^{-4}[m^3] \cdot \frac{355[MPa]}{1.00} \\
&= 85.42kNm \\
U.C. &= \frac{|M_{y,Ed}|}{M_{b,Rd}} = \frac{|-50.53|[kNm]}{85.42[kNm]} = \mathbf{0.59}
\end{aligned}$$

So no risk of lateral torsional buckling.

Column Splice Design

C

An estimation of the resistance and stiffness of the column splice is made based on the component method given in EC 1993-1-8.

C.1 Resistance (major axis)

Regarding the resistance the following components are taken into account:

- Bolts in tension
- Endplate in bending
- Column flange in compression

Bolts in tension

The tension resistance of an individual bolt is:

$$\begin{aligned} F_{t,Rd} &= \frac{k_2 f_{ub} A_s}{\gamma_{M2}} \\ &= \frac{0.9 \cdot 800[MPa] \cdot 459[mm^2]}{1.25} \\ &= 264.38kN \end{aligned}$$

Endplate in bending

The resistance of an endplate is determined by the resistance of an equivalent T-stub. In table C.1 the relevant parameters for a equivalent T-stub are given.

Table C.1: Parameters equivalent T-stub

e	p	m	m2	n	α	Lb
50[mm]	90[mm]	39.84[mm]	32.08[mm]	49.80[mm]	6.47	67.5[mm]

The table below gives the effective lengths for an endplate in bending and the resistance for each failure mode.

Table C.2: Effective lengths endplate in bending

Row	leff,cp	leff,np	Lb*	prying forces
1	250.34[mm]	257.78[mm]	127.57[mm]	yes
2	250.34[mm]	257.78[mm]	127.57[mm]	yes
1-2	383.69[mm]	383.69[mm]	166.46[mm]	yes

Table C.3: Equivalent T-stub resistances

FT,1,Rd	FT,2,Rd	FT,3,Rd	failure mode
590.62[kN]	428.91[kN]	528.77[kN]	Mode 2
590.62[kN]	428.91[kN]	528.77[kN]	Mode 2
905.23[kN]	788.68[kN]	1057.54[kN]	Mode 2

Check whether the resistance column web in tension (according to EN 1993-1-8 (6.2.6.8)) is not critical.

$$\begin{aligned}
F_{t,wb,Rd} &= b_{eff,t,wb} t_{wb} f_{y,wb} / \gamma_M 0 \\
&= 257.78[mm] \cdot 9[mm] \cdot 235[MPa]/1.0 \\
&= 545.21kN\ (individual) \\
&= 383.69[mm] \cdot 9[mm] \cdot 235[MPa]/1.0 \\
&= 811.51kN\ (group)
\end{aligned}$$

The tension resistance of the web is larger than the equivalent T-stub resistance of the group, so the web is not critical. The sum of resistances of individual bolts in the same bolt group may not be larger than the resistance of the bolts in group, otherwise a reduction of the individual resistance needs to be made.

As $2 \cdot 428.91 = 857.82 \geq 788.68$ so the resistance of the individual bolt row closest to the compression point needs to be reduced to 359.77.

Column flange in compression

The resistance of a column flange in compression is determined according to EN1993-1-8 (6.2.6.7).

$$\begin{aligned}
F_{c,fb,Rd} &= M_{c,Rd}/(h - t_{fb}) \\
&= 643000[mm^3] \cdot 235[MPa]/(200[mm] - 15[mm]) \\
&= 816.15kN
\end{aligned}$$

Moment resistance of connection

The end plate is smaller than the flange and the rotation point is therefor taken at the end of the endplate instead of the center of the flange.

Table C.4: Moment resistance around strong axis

row	h_r	$F_{t,r,Rd}$	$M_{j,y,Rd}$
1	135[mm]	428.91[kN]	57.90[kNm]
2	45[mm]	359.77[kN]	16.19[kNm]
total			74.09[kNm]

C.2 Stiffness (major axis)

Regarding the stiffness the following components are taken into account:

- k5 - Endplate in bending
- k10 - Bolts in tension

k5 - Endplate in bending

$$\begin{aligned} k_5 &= \frac{0.9 l_{\text{eff}} {t_{\text{p}}}^3}{m^3} \\ &= \frac{0.9 \cdot \frac{383.69[mm]}{2} \cdot 20[mm]^3}{39.84[mm]^3} \\ &= 21.84mm \end{aligned}$$

Stiffness for both bolt rows.

k10 - Bolts in tension

$$\begin{aligned} k_1 0 &= 1.6 A_s / L_b \\ &= 1.6 \cdot 459[mm^2]/67.5[mm] \\ &= 10.88mm \end{aligned}$$

Rotational stiffness connection

The stiffness boundaries for an unbraced frame are:

$$S_{j,rigid} = \frac{k_b E I_b}{L_b} = \frac{25 \cdot 210000[MPa] \cdot 56960000[mm^4]}{3200} = 93.45[MNm/rad]$$

$$S_{j,pinned} = \frac{k_b E I_b}{L_b} = \frac{0.5 \cdot 210000[MPa] \cdot 56960000[mm^4]}{3200} = 1.87[MNm/rad]$$

The effective stiffness per bolt row is:

$$\begin{aligned} k_{eff} &= \frac{1}{\Sigma \frac{1}{k_i}} \\ &= \frac{1}{\frac{1}{21.84[mm]} + \frac{1}{21.84[mm]} + \frac{1}{10.88[mm]}} \\ &= 5.45mm \end{aligned}$$

The equivalent lever arm is:

$$
\begin{aligned}
z_{eq} &= \frac{\Sigma k_{eff} \cdot h^2}{\Sigma k_{eff} \cdot h} \\
&= \frac{5.45[mm] \cdot 45[mm]^2 + 5.45[mm] \cdot 135[mm]^2}{5.45[mm] \cdot 45[mm] + 5.45[mm] \cdot 135[mm]} \\
&= 112.5mm
\end{aligned}
$$

The equivalent stiffness is:

$$
\begin{aligned}
k_{eq} &= \frac{\Sigma k_{eff} * h}{z_{eq}} \\
&= \frac{5.45[mm] \cdot 135[mm] + 5.45[mm] \cdot 45[mm]}{112.5[mm]} \\
&= 8.72mm
\end{aligned}
$$

The initial stiffness is:

$$
\begin{aligned}
S_{j,ini} &= \frac{E z_{eq}^2}{\frac{1}{k_{eq}}} \\
&= \frac{210000 \cdot 112.5^2}{\frac{1}{8.72}} \\
&= 23.18 MNm/rad
\end{aligned}
$$

The connection is regarded as semi-rigid.

C.3 Resistance (minor axis)

Like for the strong axis the following components are regarded for the stiffness calculation of the connection:

- Bolts in tension
- Endplate in bending
- Column flange in compression

Bolts in tension

The resistance for bolts in tension is the same as for the in the case of the strong axis.

Endplate in bending

The Eurocode do not specifically specify rules for bending around the minor axis. An estimation of the stiffness around the minor axis is done by applying the rules which are in the Eurocode.

The effective length of the boltrow between the flanges is calculated with the assumption that it behaves the same as an extended endplate. This assumption neglects the effect of the column flanges on the effective length. Figure C.1 shows the variables needed to calculate the effective lengths. In figure C.2 the values for effective lengths regarding an extended endplate are shown.

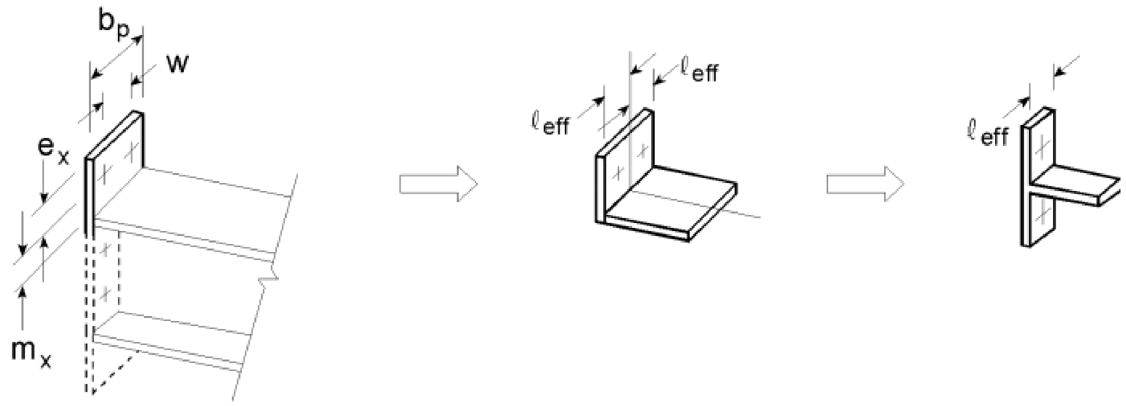

Figure C.1: Effective length extended endplate [2]

Table C.5: Parameters effective length

e_x	m_x	w	b_p
50[mm]	39.84[mm]	90[mm]	180[mm]

With these values the effective lengths are calculated using the following equations

$$\begin{aligned}
&\underline{Circular}\\
2\pi m_{\mathrm{x}} &= 250.1mm\\
\pi m_{\mathrm{x}} + w &= 215.0mm\\
\pi m_{\mathrm{x}} + 2e_{\mathrm{x}} &= 225.0mm\\
&\underline{Non\ Circular}\\
4m_{\mathrm{x}} + 1.25e_{\mathrm{x}} &= 221.7mm\\
e + 2m_{\mathrm{x}} + 0.625e_{\mathrm{x}} &= 160.85mm\\
0.5b_{\mathrm{p}} &= 90mm\\
0.5w + 2m_{\mathrm{x}} = 0.625e_{\mathrm{x}} &= 155.85mm
\end{aligned}$$

So the minimum effective length is 90mm, in the previous section is shown that prying forces are developed. There is only on row of bolts, so the equivalent T-stub resistances are:

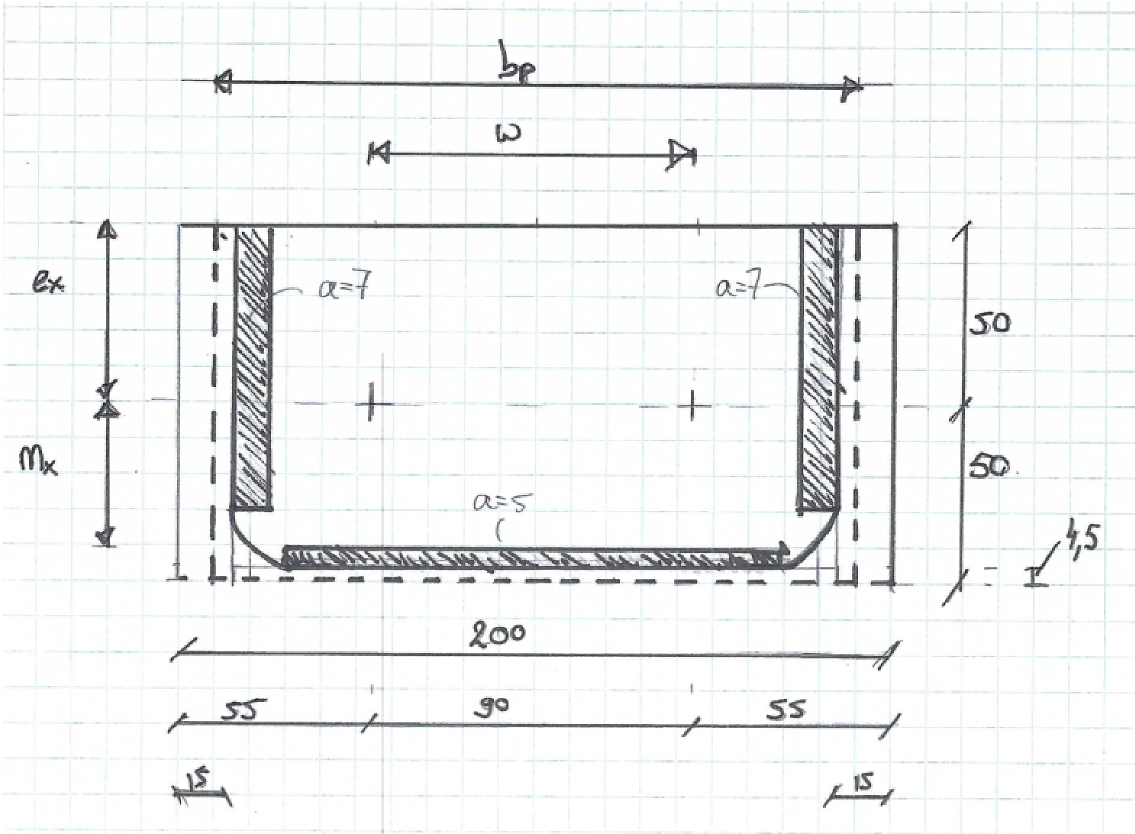

Figure C.2: Effective lengths

Table C.6: Equivalent T-stub resistances

FT,1,Rd	FT,2,Rd	FT,3,Rd	failure mode
425.13[kN]	388.62[kN]	528.77[kN]	Mode 2

All values in table C.6 are multiplied by 2 to take into account the resistance of both bolts.

Column flange in compression

The section is considered as a class 1 section. This means that full plasticity can develop in the sections. So when bending is around the minor axis half of each flange will reach full plasticity in compression and the other half will reach full plasticity in compression. This results in the following compressive force:

$$\begin{aligned} F_{\text{c,fb,Rd}} &= 2b_{\text{eff}}\, t_{\text{fc}}\, f_{\text{y,c}} \\ &= 2 \cdot 100[mm] \cdot 15[mm] \cdot 235[N/mm^2] \\ &= 705kN \end{aligned}$$

The factor 2 takes into account both flanges and the b_{eff} is equal to half the width of the flange. The contribution of the web is neglected.

Moment resistance of connection

The compression point is taken at the center of the compression forces which is at a quarter of the web, so 50mm from the edge of the plate (same height as the bolt row). The internal lever arm is the distance between the bolts and the compression point, which is 100mm.

$$\begin{aligned} M_{\text{j,y,Rd}} &= h_{\text{r}}\ F_{\text{t,r,Rd}} \\ &= 0.1[m] \cdot 366.62[kN] \\ &= 36.66kNm \end{aligned}$$

C.4 Stiffness (minor axis)

Like for the strong axis the following components are regarded for the stiffness calculation of the connection:

- k5 - Endplate in bending
- k10 - Bolts in tension

k5 - Endplate in bending

$$k5 = \frac{0.9 l_{\text{eff}} {t_{\text{p}}}^3}{m^3} \tag{C.1}$$

$$= \frac{0.9 \cdot 90 \cdot 20^3}{39.84^3} \tag{C.2}$$

$$= 10.28mm \tag{C.3}$$

k10 - Bolts in tension

The stiffness of a bolt in tension remains the same as for major axis bending.

Rotational stiffness connection

There is only one boltrow so the initial stiffness can be calculated directly.

$$\begin{aligned} S_{\text{j,ini}} &= \frac{Ez^2}{\Sigma \frac{1}{k}} \\ &= \frac{210000[N/mm^2] \cdot 100[mm]^2}{\frac{1}{10.28} + \frac{1}{10.28} + \frac{1}{10.88}} \\ &= 7.33MNm/rad \end{aligned}$$

Internal Forces D

The Plug & Play connection needs to be evaluated by the internal forces from both the ULS and SLS. The maximum major and minor axis bending moments on both the major and minor axis joints are given in this appendix.

Internal Forces in ULS

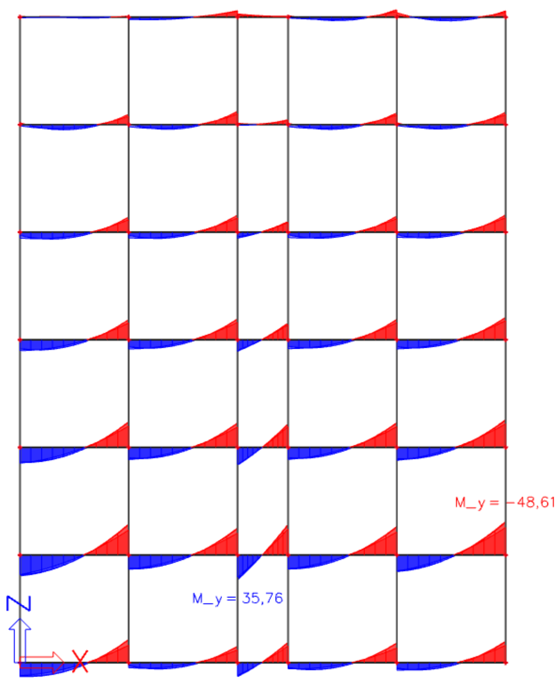

Figure D.1: Beam major axis bending moment wind in X direction

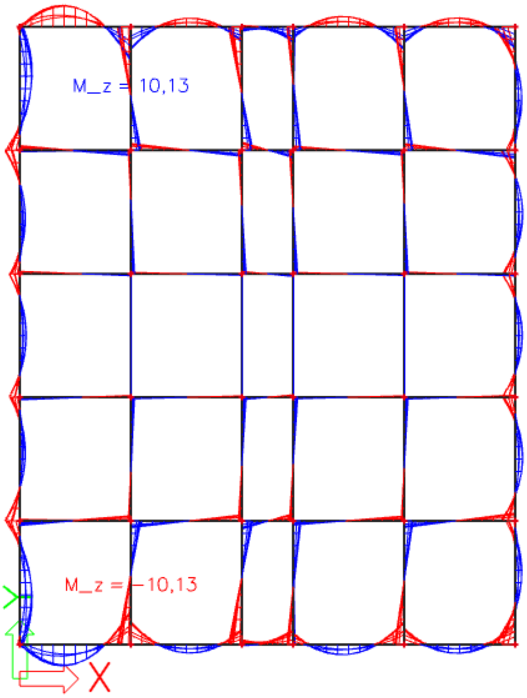

Figure D.2: Beam minor axis bending moment wind in X direction

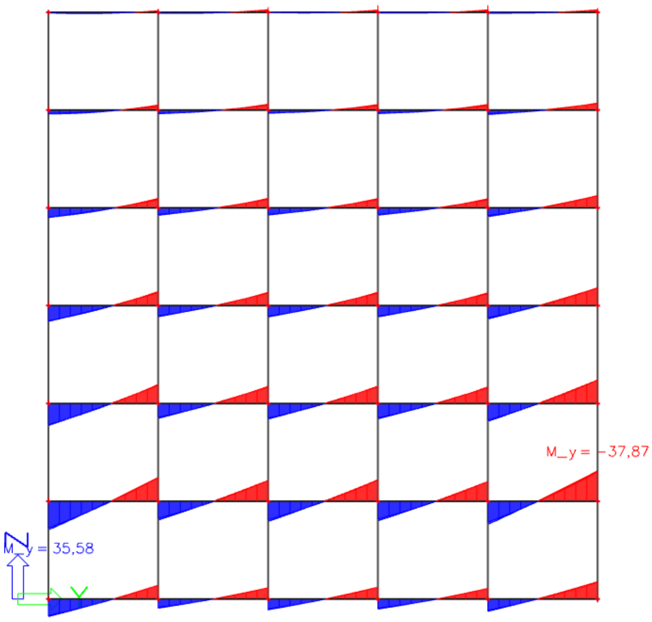

Figure D.3: Beam major axis bending moment wind in Y direction

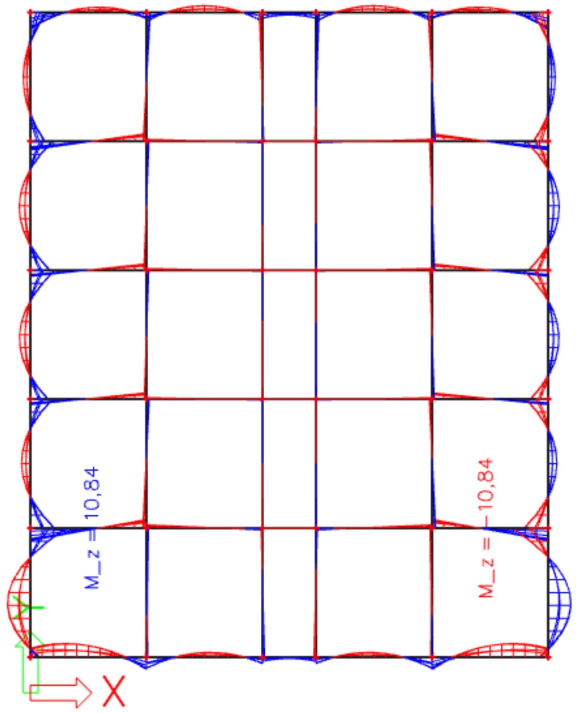

Figure D.4: Beam minor axis bending moment wind in Y direction

Internal Forces in SLS

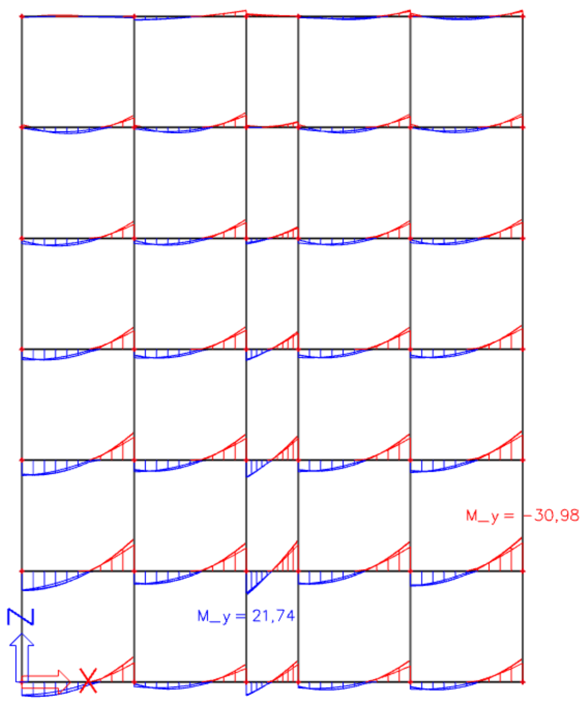

Figure D.5: Beam major axis bending moment wind in X direction

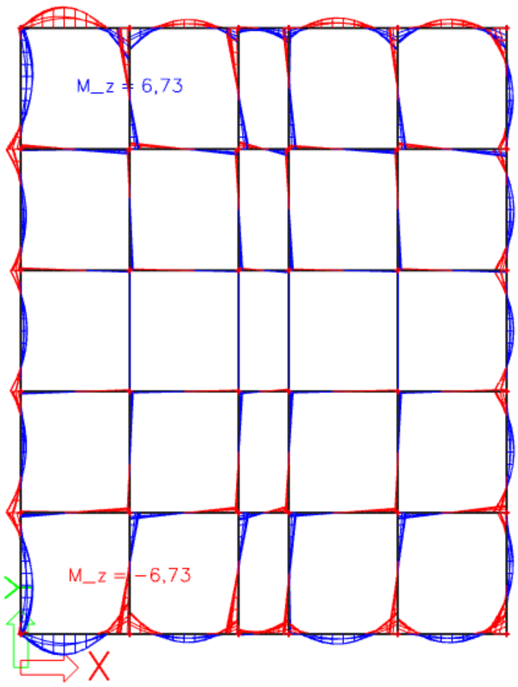

Figure D.6: Beam minor axis bending moment wind in X direction

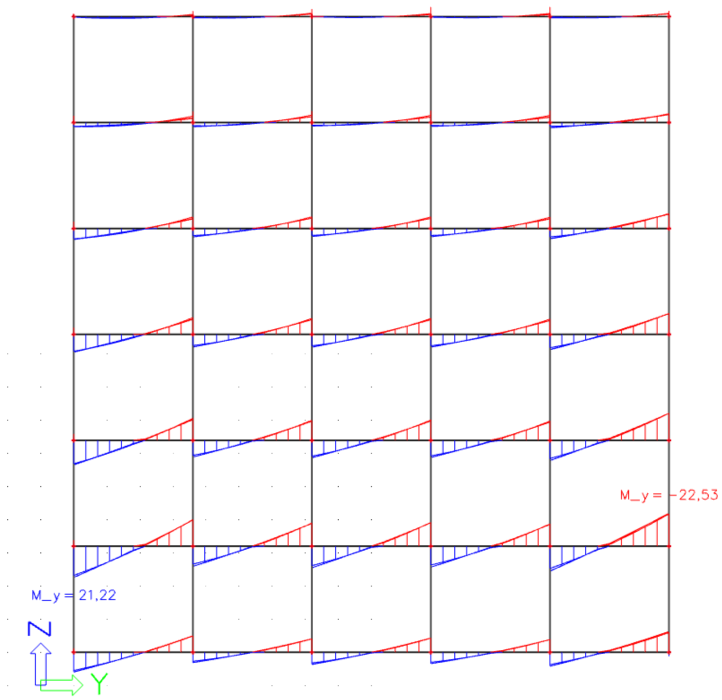

Figure D.7: Beam major axis bending moment wind in Y direction

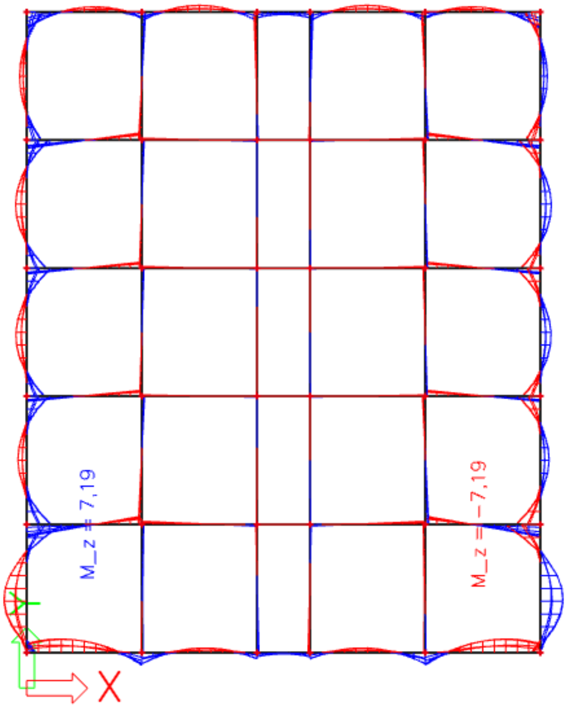

Figure D.8: Beam minor axis bending moment wind in Y direction

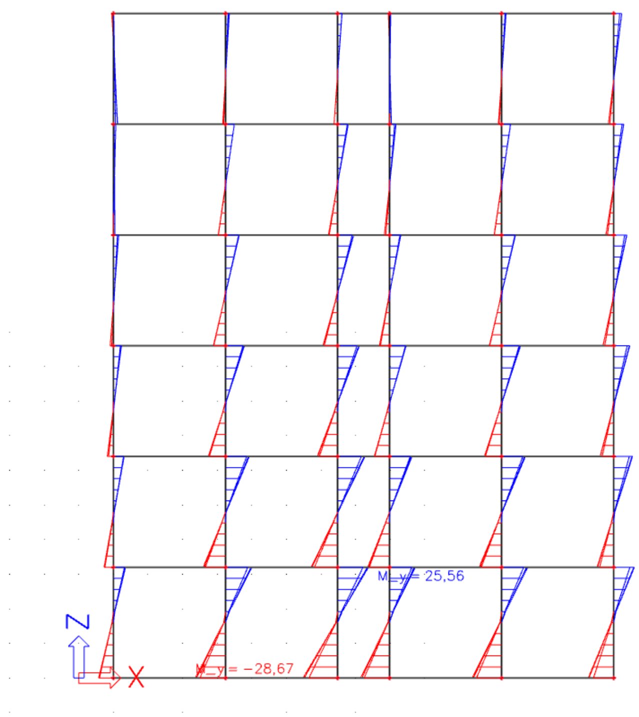

Figure D.9: Column major axis bending moment wind in X direction

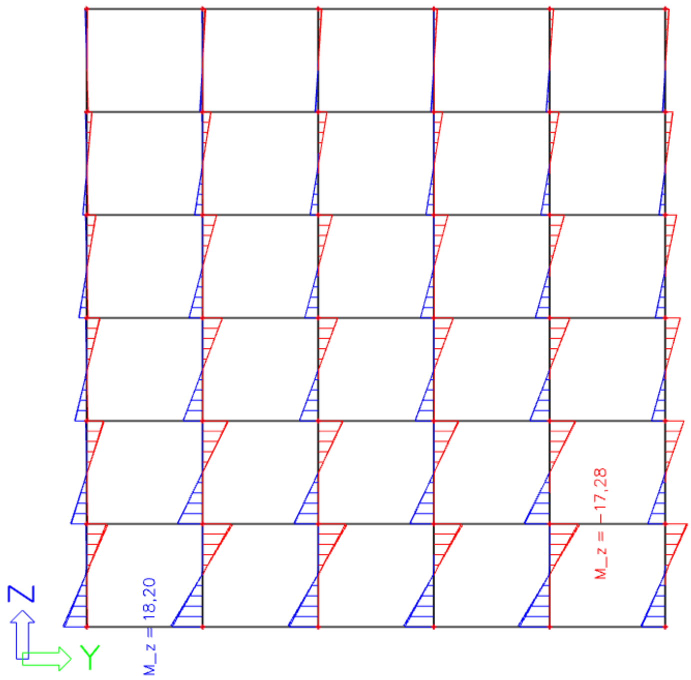

Figure D.10: Column minor axis bending moment wind in Y direction

Internal Forces in SLS with real joint stiffness

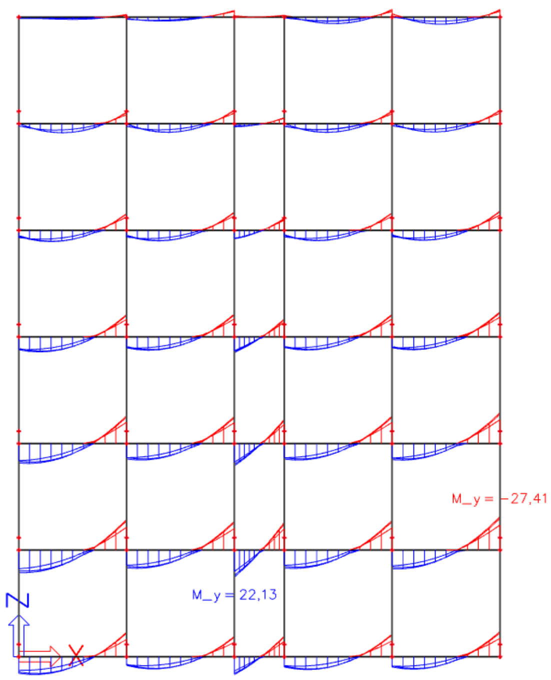

Figure D.11: Beam major axis bending moment wind in X direction

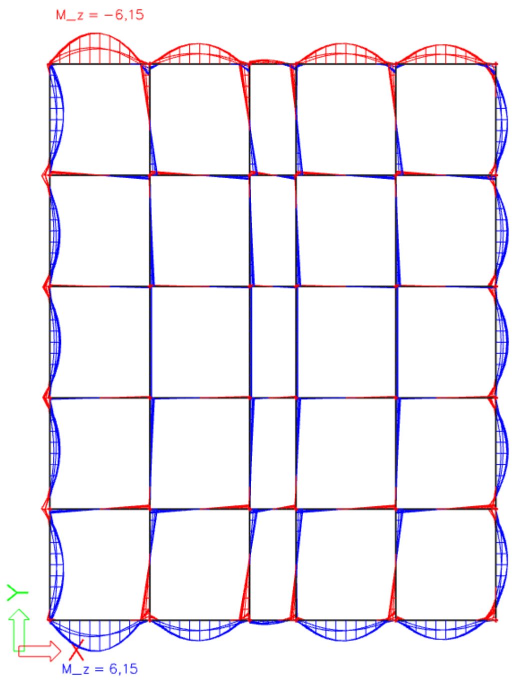

Figure D.12: Beam minor axis bending moment wind in X direction

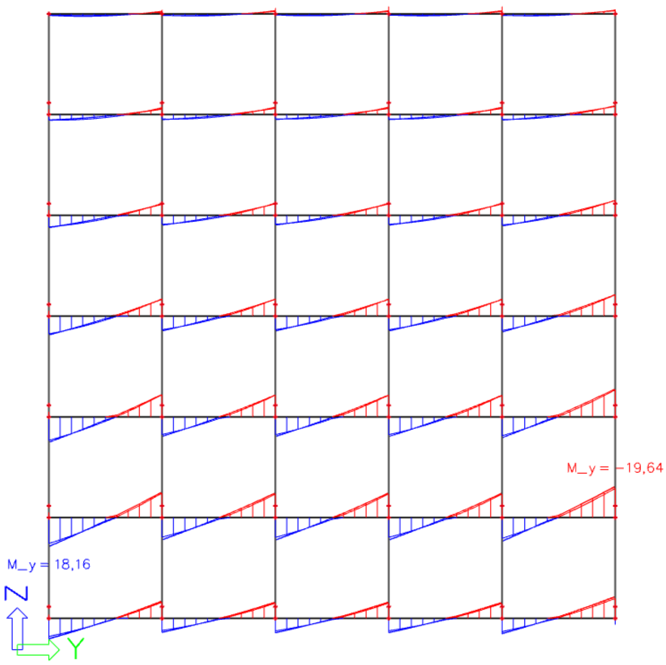

Figure D.13: Beam major axis bending moment wind in Y direction

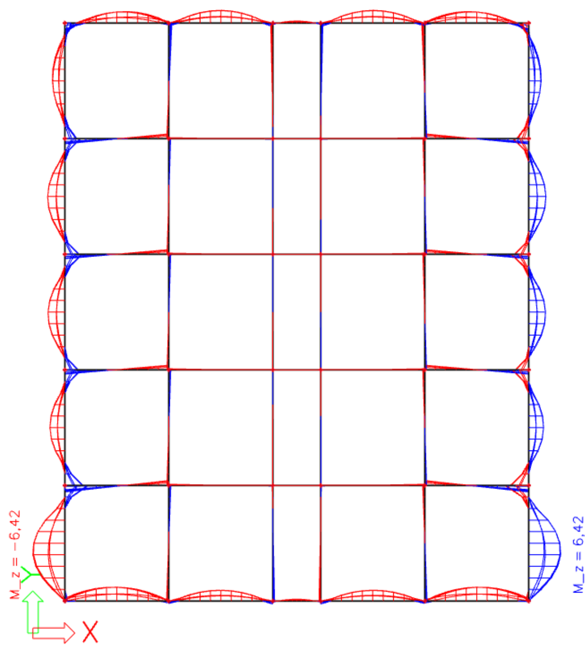

Figure D.14: Beam minor axis bending moment wind in Y direction

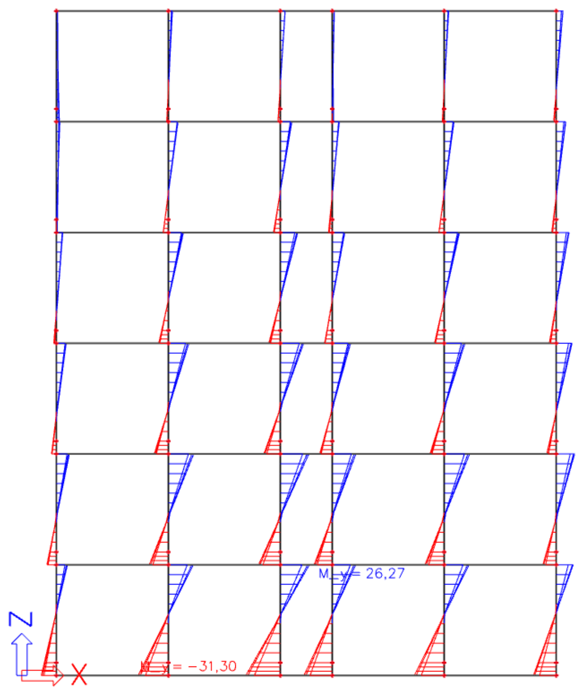

Figure D.15: Column major axis bending moment wind in X direction

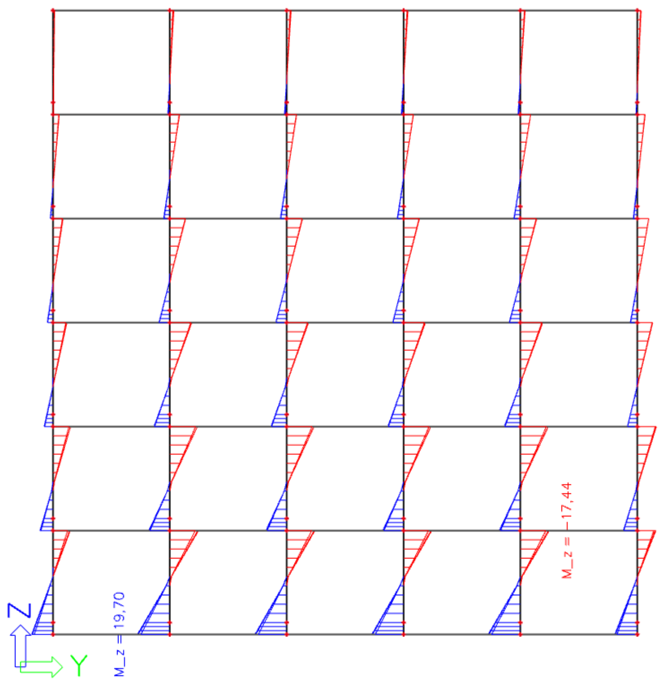

Figure D.16: Column minor axis bending moment wind in Y direction